

Investigating LXR as a therapeutic target in triple negative breast cancer.

Volume 1

Samantha Alex Hutchinson

Submitted in accordance with the requirements for the degree of
Doctor of Philosophy

The University of Leeds
School of Food Science and Nutrition

January, 2020

Supervised by Dr James L. Thorne¹, Associate Professor Thomas A. Hughes² and
Professor Janet E. Cade¹.

School of Food Science and Nutrition¹ and School of Medicine², University of Leeds,
Leeds.

Declaration

The candidate confirms that the work submitted is her own and that appropriate credit has been given where reference has been made to the work of others.

.....

S. A Hutchinson

January 2020

This copy has been supplied on the understanding that it is copyright material and that no quotation from the thesis may be published without proper acknowledgement.

Acknowledgements

Firstly, I would like to acknowledge funding for my PhD from the Leeds Doctoral Scholarship programme and the School of Food Science and Nutrition, making this work possible.

I would like to acknowledge my supervisors, Dr James Thorne, Dr Thomas Hughes and Professor Janet Cade and thank them for their guidance and mentorship throughout my PhD. Their expertise and intellect has been essential to this work, in particular the knowledge of LXR and co-factor expression offered by James, and the expertise in breast cancer and the tumour microenvironment provided by Tom. Furthermore, their dedication to not only my project but also my personal development has made it a pleasure to work alongside them.

I would like to thank Dr Hanne Roberg-Larsen (Oslo) for her support, hard work and collaborations measuring intratumoural variations in oxysterol content by LCMS/MS. And special thanks to Dr Erik Nelson (Chicago) for his invaluable collaboration on the *in vivo* mouse study. I would also like to thank Priscilia Lianto for sharing her MTT assay data supporting both my peer-reviewed articles and thesis. I would also like to further acknowledge my colleagues in the Thorne/Moore labs who have made my final year more enjoyable, in particular Dr Bernadette Moore who has been an unofficial mentor throughout my time in Leeds, and has provided support, advice and friendship. And a special mention goes to Dr Denise Ngai Li who became a close friend early on in my PhD and whose advice and friendship has been greatly appreciated.

Finally, I would like to thank my parents, brothers, and grandparents for their support throughout my PhD, I could not have done this without you all. Special thanks go to my partner Abby for her patience, understanding and encouragement, particularly during the last 6 months of experiments.

Abstract

The development of hormone therapies, such as tamoxifen, have substantially improved breast cancer outcomes for hormone receptor positive breast cancers. A subtype of breast cancers known as the triple negative breast cancers (TNBC) however, cannot benefit from these therapies due to their lack of receptors or overexpression of HER2 (ER-/PR-/HER2-). The triple negative subtype is associated with poorer prognosis and earlier relapse; novel therapies are urgently required for this cancer of unmet clinical need.

The liver X receptor (LXR) is a ligand induced transcription factor with essential roles in cholesterol metabolism. LXR α and its binding partner RXR β were found to be expressed at significantly higher levels in triple negative breast cancers relative to ER-positive breast cancers. I hypothesised that LXR α activity was altered between breast cancer subtypes and may influence chemotherapy efficacy.

Enhanced LXR α response to ligand was identified in the TNBC subtype relative to the Luminal A subtype. Furthermore, LXR α was identified as a mediator of chemotherapy resistance through the control of the p-glycoprotein/ABCB1 in TNBC. I further hypothesised that the p-glycoprotein/ABCB1 may be targetable through phytosterol treatments which were shown to antagonise oxysterol-induced LXR α activity and expression of its targets which, we have been shown to include p-gp/ABCB1.

In summary, I have identified a novel LXR α target gene (p-gp/ABCB1) in TNBC which confers chemotherapy resistance through enhanced export of the chemotherapy drug epirubicin. I have also established a mechanism to impair the oxysterol:LXR α axis through phytosterol treatment. The data presented here may have important implications to aid better treatment plans for patients undergoing chemotherapy treatment. It may also help identify individuals at risk of therapy failure.

Table of Contents

Contents

Acknowledgements	3
Abstract	4
Table of Contents	5
List of Abbreviations	11
List of Tables	14
List of Figures	15
Chapter 1 Introduction	19
1.1 Breast Cancer	19
1.1.1 Classification	19
1.1.1.1 Grade/Stage	20
1.1.1.2 Molecular Receptors.....	20
1.1.2 Breast Cancer survival rates.....	21
1.1.3 Treatments	22
1.1.3.1 Tamoxifen, herceptin and aromatase inhibitors	22
1.1.3.2 Systemic Chemotherapy	24
1.1.3.3 Radiotherapy and Surgery.....	24
1.1.4 Risk Factors	25
1.1.4.1 Prognostic factors.....	25
1.1.4.2 Non-modifiable prognostic factors	26
1.1.4.3 Modifiable prognostic factors	26
1.1.4.4 Secondary prevention.....	27
1.1.5 Chemotherapy resistance.....	29
1.2 The Liver X Receptor	31
1.2.1 LXR form and function.....	33
1.2.2 Cofactors.....	35
1.2.3 Nuclear receptor de-regulation in cancer	37
1.3 Cholesterol, LXR and Cancer	38
1.3.1 Cholesterol, obesity and statins.....	40
1.3.2 Oxysterols and the cholesterol pathway	42
1.3.3 Oxysterols from support cells	44
1.3.3.1 Fibroblasts.....	45
1.3.3.2 Macrophages.....	46
1.3.3.3 Adipocytes.....	47

1.3.4 Cholesterol in Cancer	48
1.3.5 Oxysterol regulation of LXR.....	49
1.3.5.1 In Prostate Cancer	50
1.3.5.2 In Breast Cancer	50
1.3.6 Dietary ligands	51
1.3.6.1 Plant sterol biology	52
1.3.6.2 Phytosterol/phytostanol regulation of LXR.....	53
1.3.6.3 Breast cancer risk and cholesterol status	55
1.3.7 Chemoresistance and LXR through the p-glycoprotein.....	56
Chapter 2	59
Hypothesis:	59
Aims:	59
Chapter 3 Materials and Methods	60
3.1 Cell culture	60
3.1.2 Drugs and reagents.....	60
3.2 Generation of LXR-reporter cell lines	64
3.2.1 Puromycin titration curve	66
3.2.2 Transduction with lentiviral particles	66
3.2.3 Luciferase assay	67
3.2.4 Clone selection, storage and copy number analysis	68
3.2.4.1 Clone selection.....	68
3.2.4.2 Storage/freezing down cells.....	68
3.2.4.3 Copy number analysis	68
3.3 Time course assays	70
3.4 RNA extraction and quantification	71
3.5 Reverse transcription	71
3.6 Gene expression analysis	72
3.6.1 Taqman.....	72
3.7 Colony forming assay.....	72
3.8 Chemotherapy efflux assay	73
3.9 siRNA knockdowns	74
3.10 TCGA Dataset analysis	74
3.11 Volcano plots.....	75
3.11.1 LXR α target gene plot	75
3.11.2 Systematic literature search for chemotherapy resistance genes	76

3.11.3 Evaluation of LXR α binding	77
3.12 Primary breast tumour analysis	78
3.12.1 Tumour characteristics	78
3.12.2 LCMS	79
3.12.3 Tissue RNA extraction.....	82
3.12.4 Reverse transcription and qPCR	83
3.12.5 Correlations with LXR expression.....	83
3.13 <i>in vivo</i> Mouse study.....	83
3.13.1 Treatment Plan.....	84
3.13.4 Tumour analysis	84
3.14 MTT assay	84
Chapter 4 LXRα activity and function is enhanced in triple negative breast cancer relative to Luminal A BCa.....	85
4.1 Introduction	85
4.2 Hypothesis and Aims.....	88
4.3 Results	89
4.3.1 Expression of LXR α and its regulatory factors, but not ligand concentration, is different between breast cancer subtypes.....	89
4.3.2 LXR cofactor expression is skewed towards transcriptional activation in TNBC and towards repression in ER-positive disease.	97
4.3.3 Triple negative breast cancer is transcriptionally responsive to LXR ligands and Luminal A BCa is resistant.	98
4.3.4 Corepressors control LXR α transcriptional responsiveness in breast cancer.	113
4.3.5 Enhanced LXR α activity and function increases the risk of patient relapse.	120
4.4 Discussion.....	123
4.5 Summary.....	126
Chapter 5 LXR links cholesterol hydroxylation to chemotherapy resistance in breast cancer.	127
5.1 Introduction	127
5.2 Hypothesis and Aims.....	129
5.3 Results	131
5.3.1 LXR activation protects breast cancer cells from chemotherapy assault.	131

5.3.2	The oxysterol-LXR axis regulates genes which promote chemotherapy resistance in triple negative breast cancer.	135
5.3.3	LXR regulates chemotherapy drug efflux from breast cancer cells.	142
5.3.4	P-gp/ABCB1 dependent chemoresistance is partially dependant on LXR α in breast cancer.	145
5.3.5	Enhanced p-gp/ABCB1 expression correlates with LXR α expression in breast cancer patient tumours.	150
5.3.6	LXR ligands reduce the efficacy of the chemotherapy agent epirubicin <i>in vivo</i>	154
5.4	Discussion.....	156
5.4.1	Enhanced p-gp/ABCB1 expression predicts reduced survival in triple negative breast cancer patients	158
5.4.2	Oxysterols regulate the p-glycoprotein via LXR α in the blood brain barrier	159
5.4.3	P-gp/ABCB1 is regulated in triple negative breast cancer and BCRP in ER-positive breast cancer cells	159
5.4.4	Oxysterols promote <i>in vivo</i> tumour growth and LXR-dependent metastasis	160
5.5	Summary.....	161
Chapter 6 Fibroblasts activate LXRα in adjacent triple negative breast cancer epithelial cells.....		162
6.1	Introduction	162
6.2	Hypothesis and Aims.....	163
6.3	Results.....	164
6.3.1	Cancer-associated fibroblasts have high concentrations of oxysterols.....	164
6.3.2	Fibroblasts activate adjacent LXR α epithelial triple negative breast cancer cells	165
6.4	Discussion.....	170
6.5	Summary.....	174
Chapter 7 Phytosterols antagonise oxysterol-mediated LXRα activation and chemosensitize triple negative breast cancer cells.....		175
7.1	Introduction	175
7.2	Hypothesis and Aims.....	180
7.3	Results.....	181
7.3.1	Phytosterols weakly modulate LXR.	181
7.3.2	Phytosterols antagonise oxysterol-LXR α activation.	184

7.3.3 Phytosterols attenuate the oxysterol-LXR driven expression of the p-glycoprotein/ABCB1.	195
7.4 Discussion.....	202
7.5 Summary.....	206
Chapter 8	207
8.0 Discussion.....	207
8.1 LXR α activity is enhanced in triple negative breast cancer ..	207
8.2 Fibroblasts can activate LXR α in BCa cells.	208
8.3 Enhanced LXR activity predicts poorer patient outcome and reduced treatment efficacy	210
8.4 Phytosterols antagonise the oxysterol:LXR axis	211
8.5 Future prospective.....	212
8.6 Future work	215
Chapter 9	217
9.0 Conclusion	217
Chapter 10 Additional outcomes of this PhD.....	219
10.1 Oral Presentations.....	219
10.2 Poster Presentations	220
10.3 First author publications	220
10.3.1 Methods chapter.....	220
10.3.2 Peer-reviewed journal articles	220
10.3.3 Peer-reviewed journal articles in preparation	221
10.4 Additional contributions	221
10.4.1 Peer-reviewed journal articles	221
10.4.2 BSc/MSc student projects	221
Appendix A.....	222
A.1 Table of LXR α target genes and their genomic binding scores (identified using the Cistrome database).	222
A.2 Table of genes associated with chemotherapy resistance.	228
A.3 LXR α binding in the promotor of genes associated with chemotherapy resistance.	233
Appendix B Published manuscripts	234
B.1 ER-Negative Breast Cancer Is Highly Responsive to Cholesterol Metabolite Signalling	234
B.2 Phytosterols Inhibit Side-Chain Oxysterol Mediated Activation of LXR in Breast Cancer Cells.....	256

List of References276

List of Abbreviations

22OHC	22-hydroxycholesterol
24,25-EC	24,25-epoxycholesterol
24OHC	24-hydroxycholesterol
25OHC	25-hydroxycholesterol
26OHC	25,26-hydroxycholesterol
7KETO	7-ketocholesterol
ABC	ATP-binding cassette
ACAT	Acetyl CoA acetyltransferase
ACC	Acetyl CoA carboxylase
AI	Aromatase inhibitors
AR	Androgen receptor
BBB	Blood brain barrier
BCa	Breast cancer
BCRP	Breast cancer resistance protein
BCS	Breast conserving surgery
BMI	Body mass index
BRAS	Brassicasterol
CAF	Cancer-associated fibroblast
CAMP	Campesterol
CCR7	Chemokine receptor type 7
ChIP-Seq	Chromatin immunoprecipitation sequencing
CoA	Coactivator
CoR	Corepressor
CR	Chemotherapy resistance
CSC	Cancer stem cell
CYP	Cytochrome P450
DCIS	Ductal carcinoma in situ
DMEM	Dulbecco's modified eagle medium
DNA	Deoxyribonucleic acid
ECM	Extracellular matrix
EMT	Epithelial mesenchymal transition
EPI	Epirubicin
ESR	Estrogen receptor
FAS	Fatty acid synthase
FCS	Foetal calf serum

FDR	False discovery rate
FS	Free survival
FXR	Farnesoid x receptor
GR	Glucocorticoid receptor
GW	GW3965
HER2	Human epidermal growth factor receptor 2
HR	Hazard ratio
HRE	Hormone response element
LCOR	Ligand recruited corepressor
LDL-C	Low density lipoprotein-cholesterol
LHRH	Luteinizing hormone-releasing hormone
LNCaP	Lymph node carcinoma of the prostate
LOD	Limit of detection
LXR	Liver x receptor
LXRE	LXR response element
MDRP	Multidrug resistance protein
MPMs	Mouse peritoneal macrophages
MTP	Microsomal triglyceride transfer protein
MTT	3-(4,5-Dimethylthiazol-2-yl)-2,5-diphenyltetrazolium bromide
NACT	Neoadjuvant chemotherapy
NCIN	National cancer intelligence network
NCOA1	Nuclear receptor coactivator 1
NCOA2	Nuclear receptor coactivator 2
NCOA3	Nuclear receptor coactivator 3
NCOR1	Nuclear receptor corepressor 1
NCOR2/SMRT	Nuclear receptor corepressor 2
NF2	Non-cancerous fibroblast
NFE	Nitrogen flushed ethanol
NFW	Nuclease free water
NR	Nuclear receptor
NRIP1	Nuclear receptor interacting protein 1
OHC	Oxysterol
OS	Overall survival
PBS	Phosphate buffered saline
PCa	Prostate cancer

P-gp	P-glycoprotein
PGR	Progesterone receptor
POP	Phytosterol oxidised products
PPAR	Peroxisome proliferator activated receptor
PSS	Phytosterol/phytostanol
RARs	Retinoic acid receptor
RNA	Ribonucleic acid
RR	Relative risk
RRFS	Recurrence regional free survival
RXR	Retinoid x receptor
SEM	Standard error of the mean
siRNA	Small inhibitory RNA
siSCR	Small inhibitory scrambled sequence
SITO	Sitosterol
STAN	Sitostanol
STIG	Stigmasterol
SULT2B1	Sulfotransferase
TAMs	Tumour associated macrophages
TME	Tumour microenvironment
TNBC	Triple negative breast cancer
V20	Verapamil at the concentration of 20 μm
VC	Vehicle control
VDR	Vitamin D receptor
VLDL	Very low-density lipoprotein
WCRF-CUP	World cancer research fund - continuous update project

List of Tables

Table 1 Nuclear receptor ligands.	62
Table 2 List of drugs.	63
Table 3 The Lentiviral reporter features and functions.	66
Table 4 Gene sequences.	70
Table 5 Taqman Assays.	72
Table 6 siRNA catalogue numbers.	74
Table 7 Patient tumour characteristics.	78
Table 8 Patient tumour characteristics.	79

List of Figures

Chapter 1

Figure 1. 1 Aromatase inhibitor mode of action.....	24
Figure 1. 2 LXR protein and domain structure	33
Figure 1. 3 Type I and type II nuclear receptors.	Error! Bookmark not defined.
Figure 1. 4 Oxysterols serve as signalling molecules to control cholesterol metabolism via LXR.	39
Figure 1. 5 Chemical structure of cholesterol, side-chain oxysterols and plant sterols/stanols:.....	42

Chapter 3

Figure 3. 1 Schematic diagrams of LXR reporter constructs.....	65
Figure 3. 2 LXR α target gene selection.	76
Figure 3. 3 Chemotherapy resistance gene selection.....	77

Chapter 4

Figure 4. 1 Expression of the nuclear receptor LXR α is higher in TNBC compared to Luminal A BCa.....	91
Figure 4. 2 The enzymes involved in cholesterol conversion to oxysterols, oxysterol esterification and oxysterol further modification are differentially expressed in TNBC and Luminal A BCa.....	93
Figure 4. 3 Total, esterified and free oxysterol concentrations in TNBC and Luminal A BCa.	95
Figure 4. 4 The ratio of 24OHC, 25OHC and 26OHC total to esterified oxysterol concentrations significantly correlate in the Luminal A breast tumours, but only 24OHC and 26OHC correlate in TNBC tumours.....	96
Figure 4. 5 Co-activators and co-repressors are differentially expressed in TNBC and Luminal A BCa.....	98
Figure 4. 6 LXR α is transcriptionally responsive to agonists in TNBC but not ER-positive MCF-7 cells.....	101
Figure 4. 7 Luminal A BCa cells are insensitive to oxysterol treatment.....	102
Figure 4. 8 LXRs response to ligand is enhanced in TNBC cell cultures relative to Luminal A.	104
Figure 4. 9 The LXR target genes ABCA1 and APOE significantly correlate with LXR α in TNBC patient tumours but not LXR β	106
Figure 4. 10 LXR α is recruited to canonical (A) and novel (B) target gene promoters after GW3965 treatment and correlates with the expression of novel target genes in breast tumours.	109

Figure 4. 11 LXR α expression correlates with target genes in ER-negative tumours but not ER-positive. 110

Figure 4. 12 LXR ligands drive expression of hypothesised LXR target genes in TNBC cell cultures relative to Luminal A cells. 112

Figure 4. 13 NCOR1, NCOR2 and LCOR were successfully knocked down in MDA-MB-468 and MCF-7 cells..... 114

Figure 4. 14 NCOR and LCOR knockdown restores sensitivity to ligand and de-represses basal expression of LXR target genes. 116

Figure 4. 15 NCOR1, NCOR2 and LCOR knockdown enhances expression of LXR target genes ABCA1 and APOE in TNBC and Lumina A reporter cells. ... 117

Figure 4. 16 Knockdown of corepressors increases sensitivity to ligand, and knockdown of LXR α in attenuates the expression of LXR target genes ABCA1 and APOE..... 119

Figure 4. 17 Enhanced expression of ABCA1 was observed in patient tumours who relapsed compared to those with primary disease. 122

Chapter 5

Figure 5. 1 Do LXR ligands alter the efficacy of chemotherapy drugs? 130

Figure 5. 2 Treatment of breast cancer cell cultures with synthetic LXR ligands protects against subsequent exposure to the chemotherapy agent epirubicin. 132

Figure 5. 3 Treatment of breast cancer cell cultures with endogenous LXR ligands protects against subsequent exposure to the chemotherapy agent epirubicin. 133

Figure 5. 4 Oxysterols alter the efficacy of the chemotherapy agent epirubicin. 135

Figure 5. 5 LXR α is significantly more likely to correlate with chemoresistance genes in TNBC.. 138

Figure 5. 6 Examples of the some of the strongest correlating genes with LXR α in TNBC and Luminal A BCa patient tumours. 139

Figure 5. 7 LXR ligands induce expression of the p-glycoprotein/ABCB1 in TNBC cells but downregulates its expression in Luminal A cells in an LXR dependent manner. 140

Figure 5. 8 LXR ligands also drive transcription of predicted genes involved in chemoresistance in TNBC. 141

Figure 5. 9 The synthetic LXR ligand GW3965 enhances epirubicin export via p-gp/ABCB1 in TNBC cells. 143

Figure 5. 10 Oxysterols enhance epirubicin export and is reversed by verapamil in TNBC cells..... 144

Figure 5. 11 The p-gp/ABCB1 inhibitor verapamil increases intra-cellular retention of epirubicin in TNBC cells but not MK571 and KO143 inhibitors.	145
Figure 5. 12 Knockdown of LXR α in BCa cells.	146
Figure 5. 13 Knockdown of LXR α attenuates ABCG2 and ABCC1 expression in ER-positive cells.....	146
Figure 5. 14 Knockdown of LXR α , LCOR and NCOR alters P-gp and BIRC3 expression.	147
Figure 5. 15 Knockdown of LXR α increases chemotherapy efficacy demonstrating chemoresistance is LXR dependent.	149
Figure 5. 16 Increased expression of p-gp/ABCB1 was observed in TNBC breast tumours.....	151
Figure 5. 17 LXR α and LXR β expression strongly correlates with ABCB1 in TNBC patient tumours who have relapsed.	153
Figure 5. 18 LXR agonists reduce anti-tumoural efficacy of epirubicin in TNBC cells grafted into mice.....	155
Figure 5. 19 Mice treated with LXR agonists have enhanced expression of Abca1 and Abcb1b.	156

Chapter 6

Figure 6. 1 Fibroblasts may secrete oxysterols into the tumour microenvironment.	163
Figure 6. 2 Cancer-associated fibroblasts have high concentrations of oxysterols relative to epithelial cells.....	165
Figure 6. 3 Fibroblast co-cultures with epithelial cells activate LXR α in TNBC luciferase reporters but not ER+ luciferase reporters.	166
Figure 6. 4 LaCAF conditioned media activates LXR α in TNBC and liver HepG2 cell reporters.....	168
Figure 6. 5 NF2 conditioned media activates LXR α in Luminal A, TNBC and liver HepG2 cell reporters.....	169

Chapter 7

Figure 7. 1 Phytosterols alter oxysterol signalling in several ways.....	179
Figure 7. 2 Graphical abstract.	181
Figure 7. 3 Phytosterols are anti-proliferative in breast cancer cell cultures.....	182
Figure 7. 4 LXR α is only weakly modulated by PSSs treatment in breast cancer cell lines.....	184
Figure 7. 5 Phytosterols antagonise oxysterol-LXR α activation in TNBC MDA-MB-468 cell cultures.	186

Figure 7. 6 Phytosterols antagonise oxysterol-LXR α activation in TNBC MDA-MB-231 cell cultures.	188
Figure 7. 7 Phytosterols antagonise oxysterol-LXR α activation in ER-positive MCF-7 cell cultures.....	189
Figure 7. 8 LXR α activity when treated with phytosterols at 10 μ M.	190
Figure 7. 9 Inhibition of oxysterol induced LXR α activity by PSS and cell lines.	191
Figure 7. 10 Phytosterols antagonise oxysterol-LXR activation of the canonical target genes ABCA1.	193
Figure 7. 11 Phytosterols antagonise oxysterol-LXR activation of the canonical target genes APOE.	194
Figure 7. 12 Phytosterols weakly regulate of LXR target genes.....	195
Figure 7. 13 Phytosterols antagonise oxysterol-LXR activation of ABCB1.....	197
Figure 7. 14 Phytosterols downregulate the expression of ABCB1 in Luminal A cells.....	198
Figure 7. 15 Sitosterol reverses the OHC-LXR effects of enhanced epirubicin exportation.....	199
Figure 7. 16 Sitostanol reverses the OHC-LXR effects of enhanced epirubicin exportation.....	201

Chapter 1 Introduction

1.1 Breast Cancer

Breast Cancer (BCa) is the most frequent malignancy worldwide in females and the second most common cause of cancer related death [1, 2]. Worse disease-free survival is observed with patients who are overweight or obese [3, 4], and those who have associated co-morbidities such as elevated levels of low-density lipoprotein cholesterol (LDL-C) [5], or high saturated fat intake [6] when compared to their leaner counterparts. Improvements in the treatment and early detection of breast cancers through mammography screening programs are contributing to the reduction of BCa mortality [7] however in Europe and the US combined, over 120,000 annual BCa deaths are still expected [7, 8]. Drug development time and the costs associated with development and testing of new drugs are high, as such, focus on preventing the development of metastatic breast cancer may be a more efficient use of time and resources, especially when primary breast cancer is rarely the cause of breast cancer mortality.

1.1.1 Classification

Classification of breast cancers is essential for informed treatment decisions. Molecular receptor expression in breast cancer subtypes can dictate how a patient responds to certain therapies and if treatment plans are not personalised this can result in poor treatment efficacy. Other factors, such as stage and grade of the tumour are also important for classification of breast tumours to provide the best treatment plan for that tumour subtype at that specific grade/stage.

1.1.1.1 Grade/Stage

The stage and grade of a cancer are contributing factors that will influence the treatment decision. The stage of a cancer assesses the size and spread of the cancer into surrounding tissues. The grade of a tumour assesses the proliferation and phenotype of the cancer cells compared to healthy cells. Around 60 % of women who present at clinic with stage I or stage II breast cancers undergo breast-conserving surgery (BCS), which may be either a partial mastectomy or a lumpectomy [9]. Over 35 % of women who present with stage I or stage II breast cancers will undergo mastectomy [9]. Furthermore, women who present at clinic with stage III are more likely to undergo mastectomy (72 %) compared to BCS (21 %) or radiotherapy and or chemotherapy (7 %) [9]. And over half of the women who present with stage IV BCa receive radiation therapy alone or in combination with chemotherapy (76 %). Notably, 79 % of women with hormone receptor-positive BCa receive hormone therapies regardless of stage [10] suggesting hormone-receptor status is also important in the treatment of breast cancers.

1.1.1.2 Molecular Receptors

BCa can be sub-classified based on receptor status to inform treatment decisions as well as prognosis. This characterises tumours based on the cancer cell expression of molecular receptors such as, the estrogen receptor (ER) and progesterone receptor (PR) and the overexpression of human epidermal growth factor receptor 2 (HER2) receptors combined with proliferative index through the Ki-67 status [11]. The estrogen receptor and the progesterone receptor are receptors which bind the respective hormones, estrogen and progesterone. Cancer cells that express these hormone receptors (ER/PR) require the binding of the specific hormones to grow and

metastasize. BCas are categorised into four main subtypes, Luminal A, Luminal B, HER2-positive (HER2+) and triple negative breast cancer (TNBC). Luminal A BCas are hormone receptor-positive for the ER and or the PR and HER2-negative with low ki-67 levels, Luminal B BCas are hormone receptor-positive for the ER and or the PR and either HER2-positive or HER2-negative with high ki-67 levels. HER2+ BCas are hormone receptor-negative and HER2-positive, whereas the TNBC subtype is negative for all three receptor types. As studies and research evolve, further sub-classification of breast tumours into new molecular entities is expected. This was the case for a TNBC subtype known as Claudin-low, which was identified and characterized in human and mouse tumours, and in a panel of BCa cell lines (BT549, MDA-MB-231, MDA-MB-435 and Hs578T) [12, 13]. TNBC subtypes all have poor prognosis and a higher risk of relapse which demonstrates the requirement for novel therapeutics targeting new molecular targets particularly in this subtype.

1.1.2 Breast Cancer survival rates

Luminal breast cancers are the most common breast cancer subtypes accounting for 30-70 % of all BCas. Luminal breast cancers have the highest 10-year recurrence regional free survival (RRFS) rate, (Luminal A, 96 %, and Luminal B, 88 %) when compared to other subtypes [14, 15]. The TNBC subtype accounts for 20 % of all BCas [16] but are less likely to respond to treatment. TNBCs are also more likely to become metastatic and the patients therefore have a poorer prognosis [17]. Patients with TNBC have approximately 10 % higher risk of relapse within the first 5 years post-surgical resection, which then declines to below that of other BCa subtypes after that [18-20].

Over the last few decades marked improvements in the successful treatment of breast cancers have been observed coinciding with the development of targeted therapies such as tamoxifen and herceptin. Overall, the 5-year survival rate for non-subtype specific breast cancer is 89 % and the 10-year survival rate is 83% [9]. A large proportion of these statistics however, will be representative of luminal breast cancers which have hormone therapies available, or BCAs that are HER2-positive and can be treated with monoclonal antibodies such as herceptin.

1.1.3 Treatments

Molecular differences in BCa subtypes dictate which course of systemic treatment the patient receives. Cancer cells within tumours that express the ER and/or the PR require the binding of estrogen/progesterone to grow and metastasize. Tamoxifen is a hormone therapy that inhibits the estrogen receptors which inhibits the growth and spread of the BCa. The endocrine axis is successfully targeted through inhibiting; hormone synthesis with aromatase inhibitors and hormone receptors with antagonists like tamoxifen. HER2 signalling is successfully interrupted with monoclonal antibody therapies such as herceptin [21]. Targeting of the endocrine axis has benefited patients with hormone receptor positive cancers however, treatment of the TNBC subtype remains challenging with no targeted therapies developed to date [21].

1.1.3.1 Tamoxifen, herceptin and aromatase inhibitors

Hormone therapies are systemic and therefore affect cells all over the body. They are often given as adjuvant therapy (post-surgery) to reduce the risk of recurrence or occasionally as a neoadjuvant therapy (pre-surgery). Hormone therapies, such as tamoxifen are usually taken for 5-10 years after the primary diagnosis but can also

be used to treat local secondary ER-positive tumours or ER-positive metastatic tumours. Tamoxifen is an example of a cancer chemoprevention agent which inhibits the ER. Unfortunately many of these agents have side effects, such as tamoxifen, which is an extremely successful agent used to prevent tertiary BCa development [22] however the use of tamoxifen increases the risk of other reproductive system cancers [23].

Some tumour cells have increased expression of a growth promoting protein HER2/neu (HER2) which usually display enhanced tumour growth and metastatic progression. Herceptin is a commonly used drug to treat tumours that are HER2 enriched which is a monoclonal antibody that specifically targets the HER2 receptors. Aromatase inhibitors (AI) are drugs that stop the production of estrogen by interfering with aromatase which converts androstenedione into estrone then estradiol, and/or testosterone into estradiol (as shown in **Figure 1.1**). Aromatase inhibitors are often used in post-menopausal women as small amounts of estrogen are made in fat tissue by the enzyme aromatase even after menopause. Letrozole and anastrozole are examples of aromatase inhibitors which are given daily. AIs are commonly given after surgery either alone or after tamoxifen to stop tumour recurrence. Pre-menopausal women whose tumour is ER-positive are likely to be treated with tamoxifen post-surgery with the addition of AIs later if necessary, given with luteinizing hormone-releasing hormone (LHRH) which is an ovary suppression drug [24].

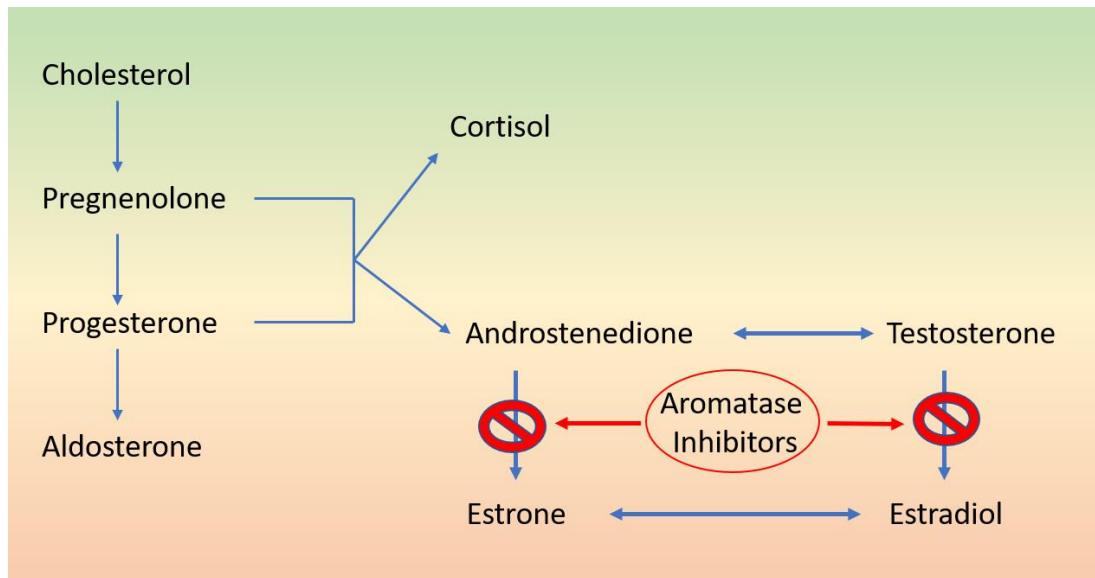


Figure 1. 1 Aromatase inhibitor mode of action.

Cholesterol is converted to pregnenolone and then progesterone, both of which can be converted to androstenedione. Androstenedione is then either converted directly to estrone by aromatase, or to testosterone then estradiol by aromatase. Aromatase inhibitors block the synthesis of estrone and estradiol.

1.1.3.2 Systemic Chemotherapy

Chemotherapy is the delivery of toxic agents into the patient's cancer cells to damage the cell and force the process of apoptosis. Chemotherapy can be given as neoadjuvant chemotherapy to reduce the tumour size and invasiveness before surgery, or as adjuvant chemotherapy to eradicate any remaining cancerous cells left after surgery. Chemotherapy may also be used to treat metastatic tumours that have colonised in other tissues. Chemotherapy is also used to reduce the risk of BCa recurrence, however high doses of anthracyclines (which are the most commonly used chemotherapy drugs) for long periods of time can result in cardiotoxicity [25].

1.1.3.3 Radiotherapy and Surgery

Surgery is commonly used to remove breast cancer tumours. Patients who present at clinic with low stage and grade tumours often receive surgery in combination with

other treatments such as tamoxifen to stop the growth of the tumour and reduce the risk of recurrence. A report completed by the National Cancer Intelligence Network (NCIN) showed out of all patients diagnosed with breast cancer in England between 2004-2006, 90 % of patients in the age groups 40-49, 50-59 and 60-69 received surgery for a major resection through the NHS [26].

Radiotherapy is often used to treat stage I-IV cancers usually in combination with other treatments such as breast conserving surgery. Radiation can be used to destroy any remaining cancer cells after surgical resection of large tumours or to target metastatic cancers where large sections cannot be removed such as in bone or the brain. Typically, two types of radiotherapy are used to treat breast cancer, external beam radiation or internal radiation.

1.1.4 Risk Factors

Cancer is a heterogenous and complex problem. Cancers from the same subtype with similar molecular markers can respond to the same treatments very differently, and this is believed to be due to individual characteristics. Understanding these characteristics that make patients more at risk for poor response to treatment may help identify targets to improve patient outcomes.

1.1.4.1 Prognostic factors

There are multiple prognostic factors associated with an increase in breast cancer occurrence and recurrence, some of which are modifiable and some that are not. The non-modifiable prognostic factors for breast cancer include; grade, stage, receptor status, heterogeneity of the tumour microenvironment, genetics [27, 28], mammographic density and pathological response to neoadjuvant chemotherapy (NACT). The modifiable risk factors for breast cancer include; waist-to-hip ratio [29],

body mass index (BMI) [30], obesity [31-34] saturated fat intake [6], physical inactivity [35], first pregnancy at later stages of life [36], and lifestyle [37].

1.1.4.2 Non-modifiable prognostic factors

One of the most widely accepted biomarkers for BCa risk is mammographic density [38], which has been associated with a 4-6-fold increase of BCa risk in women with highly dense mammographic density [38]. Mammographic density is thought to be a non-modifiable risk factor associated with an increased risk of BCa, although there are some studies that have shown changes in mammographic density caused by hormone therapies [39, 40] which have been shown to alter the risk associated with BCa [41]. As previously mentioned, stage, grade and the receptor status of the tumour all impact the level of risk associated with the particular breast cancer.

1.1.4.3 Modifiable prognostic factors

Most modifiable prognostic factors are dietary related, but there are some that are not. For example, BCa risk in women is known to double every decade before the menopause, after which risk increase slows substantially. With this in mind, it is interesting to note that BCa is more frequently diagnosed in women after menopause which suggests other factors like diets high in fat are of great importance to the development of BCa [37]. This is further supported by multiple studies showing generation of women who have migrated from low risk countries (such as Japan) to high risk countries (such as America) and have displayed the increased risk of cancer associated with the new region [42-45]. The World Cancer Research Fund Continuous Update Project (WCRF CUP) and many other studies continue to assess the many factors that contribute to the development of BCa.

One of the most modifiable risk factors for breast cancer is physical inactivity [35]. Physically active women displayed a 20-30 % reduction in breast cancer risk compared to women who were physically inactive [35], and the same study observed a 30-40 % reduction in colon cancer risk in both men and women who were physically active [35]. Furthermore, physically active lifestyles or long-term pharmacological therapies (such as statins) that reduce LDL-C [46, 47] and diets rich in phytosterols (plant-based diets) [48] are associated with reduced risk of primary breast cancer, improved patient survival and a reduction in recurrent breast cancer.

Postmenopausal women whose BMI is greater than 25 are also known to have an increased risk of developing invasive BCa compared to women with a healthier BMI [30], and an overall increased risk of 61 % (95 % CI 1.43-1.80) [49]. Furthermore, obesity is associated with hypercholesterolemia, and has been linked to a 2-fold increase in BCa risk [37, 44]. Diet has been labelled as the second most preventable cause for cancer [50] after cigarette smoking, and as such demonstrates key roles with the support of other evidence, that cholesterol is linked to BCa through obesity and high circulating LDL-C levels. Additionally, many studies ultimately highlight obesity as a BCa risk factor [31-34] and in women has been linked with an increase in cancer death [51].

1.1.4.4 Secondary prevention

The treatment of primary breast cancers is often successful particularly for those with hormone receptor positive breast cancers. The majority of breast cancer deaths occur due to failure of treatment and the formation of secondary tumours, highlighting a key area for improvement. As mentioned physically active lifestyles

that lower LDL-C [46, 47] and plant-based diets [48] are associated with a reduction in recurrent breast cancer, and high LDL-C is largely associated with an increase in BCa recurrence [51].

Secondary tumours can either be local, regional or distal/metastatic. Metastatic tumours are those that have invaded the lymphatic system or vascular systems allowing distribution via the lymph nodes or venous/arterial system. Once the cancerous cells have exploited the lymph nodes and vascular system, the tumour cells can form secondary tumours in other niche organs often resulting in the need for chemotherapy or radiotherapy. Metastatic relapse is a major cause of BCa treatment failure, however it remains unclear why some patients with similar disease succumb to relapse, but others do not [28, 52]. It is clear however, that some subtypes (particularly the TNBC) are more likely to relapse within the first 5 years post treatment. For example, the study analysed a dataset of 269 TNBC patients and showed the 5-year overall survival (OS) rate to be 74.5 % for this subtype [53], with metastasis recurrence rates for TNBC to be 2 % local and 31.5 % distal. Furthermore, out of those TNBC patients who relapsed 77.6 % of these patients did not survive, equating to 70 patient deaths out of the 90 patients who relapsed [53].

For patients who have ER-positive BCa, tamoxifen is often used to inhibit the growth of the cancer through blocking estrogen interactions with the estrogen receptor. The development of metastatic tumours are lethal and often result in death. Therefore, finding novel therapeutic targets linked to risk factors associated with LDL-C and cholesterol pathways is essential to understand the mechanisms underpinning why cholesterol and diet are associated with BCa recurrence.

1.1.5 Chemotherapy resistance

BCa is the most common malignancy in women and although treatment of primary cancer is successful, chemoresistance is still a major issue for the treatment of secondary tumours. Chemoresistance occurs when treatment of cancer is unsuccessful or fails, this could be due to a variety of mechanisms such as; the detoxification of anti-cancer therapies either by metabolising the drug into an inactive molecule [54] or by efflux of drug from the cell [55], interruption of the apoptotic signalling pathway [56]. The TNBC relapse is linked to failure of chemotherapy drug delivery and retention within the cell, linking further to drug exportation.

The definition of chemoresistance or chemotherapy resistance (CR) is the lack of or partial response by a tumour to systemic chemotherapy. Metastatic cancer or metastasis is defined as the migration of cancer cells from the primary tumour and the formation of secondary tumours in other tissues either through the lymph system or bloodstream. Proximal metastasis is cancer that has migrated to an area near the primary site and distal metastasis is cancer that has spread to other regions, usually a different organ.

BCa recurrence is particularly common in TNBC, with 35 % of TNBC patients relapsing within the first 6 years post treatment [57]. In a study of 123,780 BCa patients with stages I, II and III, the authors found the 5-year free survival (FS) rate for TNBC (75-80 %) was considerably lower than the FS rate for other BCa subtypes (90.75 %) [58], which reflects the lack of targeted treatment available for this subtype. Lower survival rates and high relapse rates in the TNBC subtype demonstrates the aggressiveness of this BC subtype. Furthermore, another study with 2394 patients

found survival rates for the TNBC patients to be 62 % which was notably lower than the rate for the Non-TNBC subtypes at 72 % [59]. Although both studies show TNBC survival rates to be lower than the non-TNBC subtypes, the rates across both studies are varied suggesting other factors other than subtype effect the survival and relapse risk in BCa patients.

Although targeted endocrine therapies have a large success in the treatment of primary tumours in the first instance, countless patients relapse with endocrine therapy resistant disease [21] and chemotherapy resistance [60]. Chemoresistance (innate or acquired), can apply to individual chemotherapy agents or a class with analogous mechanistic of actions [61]. Additionally, interruption of the apoptotic signalling pathway is often a major cause for the failure of anticancer therapies [56]. Innate chemoresistance occurs immediately after the first exposure to chemotherapy treatments, whereas acquired chemotherapy resistance usually arises when a patient has been exposed to one class of treatment for an extended period. Interestingly, the bidirectional interplay between the extracellular matrix (ECM) and tumours has recently been shown to promote resistance to endocrine and other targeted therapies [62, 63].

Active efflux of chemotherapy agents from within cancer cells is one of the key mechanisms of chemoresistance, others include; mutations or changes in mitotic checkpoint signals, modification of drug targets, detoxification of cytotoxic chemotherapy agents, drug appropriation, and improved deoxyribonucleic acid (DNA) repair mechanisms [61]. The increased expression of liver x receptor (LXR) canonical target genes belonging to the ATP-binding cassette transporters (ABC-transporters) can be associated with unsuccessful drug effect and cancer cell survival

during chemotherapy. ABCA1 is a recognised target gene of LXR with roles in cholesterol efflux, however other ABC-transporters are also thought to be regulated by LXR. ABCB1, ABCC1 and ABCG2 are ABC-transporters with roles in chemotherapy drug efflux [64]. Increased expression of ABCA1 and ABCG1 has been shown to enhance cellular cholesterol efflux in THP-1 monocytes when treated with Riccardin C via LXR α activation [65]. Furthermore, ABCA1, ABCG1 and ABCG8 were shown to be increased in the liver and small intestine via LXR activation by the synthetic LXR agonist T0901317 [66]. Cholesterol and its metabolites (including the oxysterols) are LXR ligands and as such drive LXR activity, targeting genes involved in cholesterol efflux, exportation and maybe chemotherapy resistance linking the cholesterol-LXR axis with regulation of ABC-transporters and the development of chemoresistance.

1.2 The Liver X Receptor

Metabolic processes and gene expression cascades are regulated by nuclear receptors (NRs), which are a major family of signal-stimulated transcription factors. Transcriptional interactions at target gene promoters involve ligand/signal-dependent communications of NRs with many co-regulatory proteins [67]. These NRs respond by controlling transcriptomes involved in important processes such as proliferation [68]. Type 1 NRs such as ER, androgen receptor (AR) or PR bind to ligand in the cytosol, form homodimers or heterodimers and translocate from the cytoplasm into the nucleus to bind to DNA hormone response elements (HREs). Type 2 NRs remain in the nucleus even in the absence of ligand binding as heterodimers to DNA. In the absence of ligand, the type 2 NRs such as LXR or retinoid x receptor (RXR) will associate with co-repressor proteins and when ligand binding occurs the

co-repressors dissociate, and the NRs recruit co-activator proteins along with ribonucleic acid (RNA) polymerase to facilitate transcription.

The liver x receptor (LXR) is a member of the nuclear receptor superfamily and is a ligand activated transcription factor [69]. Two forms of LXR are known to exist LXR α (NR1H3) and LXR β (NR1H2), both of which were identified in cDNA libraries [70-72] and originally believed to be orphan nuclear receptors. The human LXR α gene is located on chromosome 11p11.2, has 11 exons and is predominantly expressed expressed in metabolically active tissues and cells such as the liver, macrophages and small intestine [70, 73]. The human LXR β gene is located on chromosome 19q13.3, has 8 exons [74] and is ubiquitously expressed [75]. Both LXR isoforms form heterodimers with the retinoid X receptor (RXR) and initiate transcription through binding to response elements in target gene promoters [73]. Nuclear receptors such as LXR α , can have multiple isoforms [76] and often have alterations in their domain structures as shown in **Figure 1.2**.

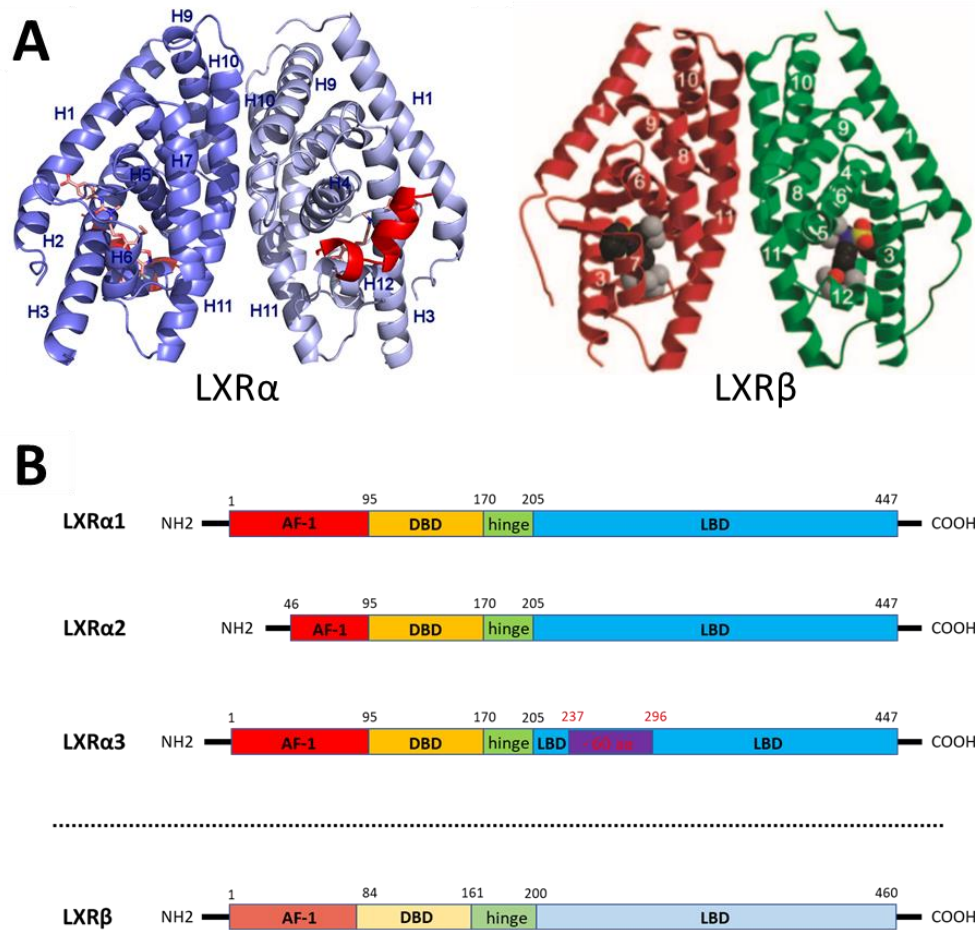


Figure 1. 2 LXR protein and domain structure.

The protein structures of LXR α [77] and LXR β [78] are shown (A) with a synthetic ligand bound to each from the front view (left) and from the back view (right). The helices are numbered 1-12. The protein structure of LXR α also shows the coactivator (SRC-1) bound (red spiral). B) Shows a schematic representation of the known three LXR α isoforms (originally published by Chen *et al*, 2005 [76] and LXR β genomic structure. All three LXR α variants (LXR α 1, LXR α 2, and LXR α 3) and LXR β have; a ligand-independent transcriptional activation function (AF-1) domain which is located at the N-terminus [red], a DNA binding domain (DBD) [yellow], a hinge region which is involved in conformational changes between active and inactive states [green], and a ligand binding domain (LBD) [blue] ending with a carboxyl terminus. The LXR α variants LXR α 2 and LXR α 3 each have alterations in their structure. LXR α 2 has a shorter AF-1 region than LXR α 1 and LXR α 3. LXR α 3 has a region within the LBD that is missing amino acids (aa) [purple box, red annotation].

1.2.1 LXR form and function

NRs are categorized based on affinity, and steroid receptors such as the ER or the AR or seco-steroid receptors such as the vitamin d receptor (VDR) and retinoic acid receptor (RARs) belong to the NR group with high affinity for ligand which respond to dietary factors in the low nanomolar range. Low binding affinity NRs such as LXRs,

farnesoid x receptors (FXRs) and peroxisome proliferator activated receptor (PPARs) respond to a much wider range of lipophilic molecules at the micromolar range. The remaining group of NRs are the orphan NRs, which have no known endogenous ligands or ligand binding domains identified yet, such as NR4A1 or Nur77 and utilize cofactors instead of ligands to regulate through changes in protein bioavailability. High and low affinity NRs are stimulated by ligand interaction with the binding domain, and these ligands are typically dietary derived compounds often involved in processes like glycolysis and oxidative phosphorylation [79]. LXR α and LXR β are important NRs that interact with dietary ligands regulating the expression of genes involved in cholesterol storage, efflux and eradication.

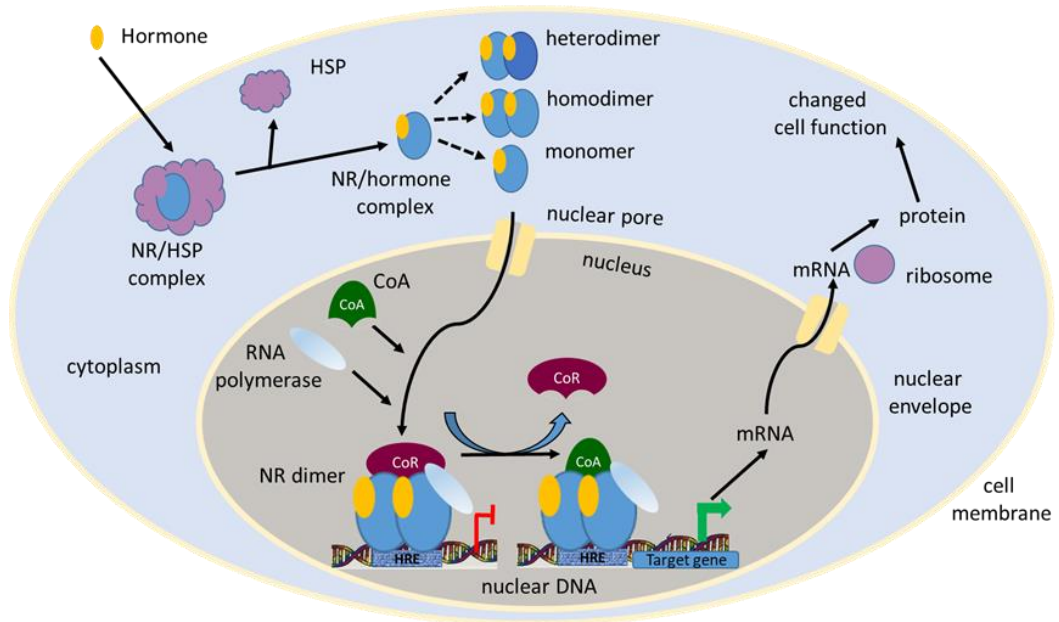
The two LXR α and LXR β isotypes share 75 % sequence homology in their ligand-binding and DNA-binding domains and function. The LXR-RXR heterodimer binds to the DNA within gene regulatory regions favorably identifying LXR response elements (LXRE). Both LXR α and LXR β and can be activated either by an LXR agonist (such as T0901317/GW3965) or an RXR agonist (*9-cis* retinoic acid) [80]. LXR is phosphorylated at Ser198 and ligand-induced LXR phosphorylation at this site changes its activity in a gene-specific fashion [67, 81]. Interestingly, T0901317 has been shown to promote LXR α phosphorylation at serine 198, however the RXR ligand *9-cis* retinoic acid (*9-cis*) inhibits LXR α phosphorylation [67, 81]. Furthermore, LXR α serine 198 (S198) phosphorylation has been shown to regulate the chemokine receptor type 7 (CCR7), which is not expressed in all cell types however in those cells that do, an open chromatin configuration is observed [81].

1.2.2 Cofactors

Nuclear receptors are controlled through interactions with ligands, and in the absence of ligand the nuclear receptor LXR recruits co-repressors to constitutively associate with and bind to the promoter of the LXR target genes. The first corepressors, nuclear receptor interacting protein 1 (NCOR1) [82] and nuclear receptor interacting protein 2 (NCOR2/SMRT) [83] were discovered in 1995, and the ligand recruited corepressor (LCOR) [84] in 2003. Corepressors such as NCOR1 and NCOR2/SMRT are large proteins which possess independent repression domains and bind to nuclear receptors in the absence of ligand [85]. Their nuclear receptor binding and repression functions are facilitated through the carboxyl and amino terminal halves of the molecules and upon binding, changes the positioning of the helix 12 (H12) in the ligand binding domain of the NR. The H12 positioning has been shown to be critical for the binding of coactivators [86] and interestingly, loss of H12 enhances repression and corepressor binding of nuclear receptors such as RXR [87, 88] and PPAR [89]. A corepressors role is to downregulate the expression of genes under the control of transcription factors by binding to specific transcription factor binding sites.

Coactivators such as nuclear receptor coactivator 1 (NCOA1) and nuclear receptor coactivator 3 (NCOA3) are recruited to the transcription factor binding site by nuclear receptors in the presence of ligand to increase the rate of transcription for genes under the control of the nuclear receptor (see **Figure 1.3**). However, corepressors and coactivators both bind to the same binding sites, but cannot be bound simultaneously, they must compete for binding.

Type I NR: high affinity for ligand



Type II NR: low affinity for ligand

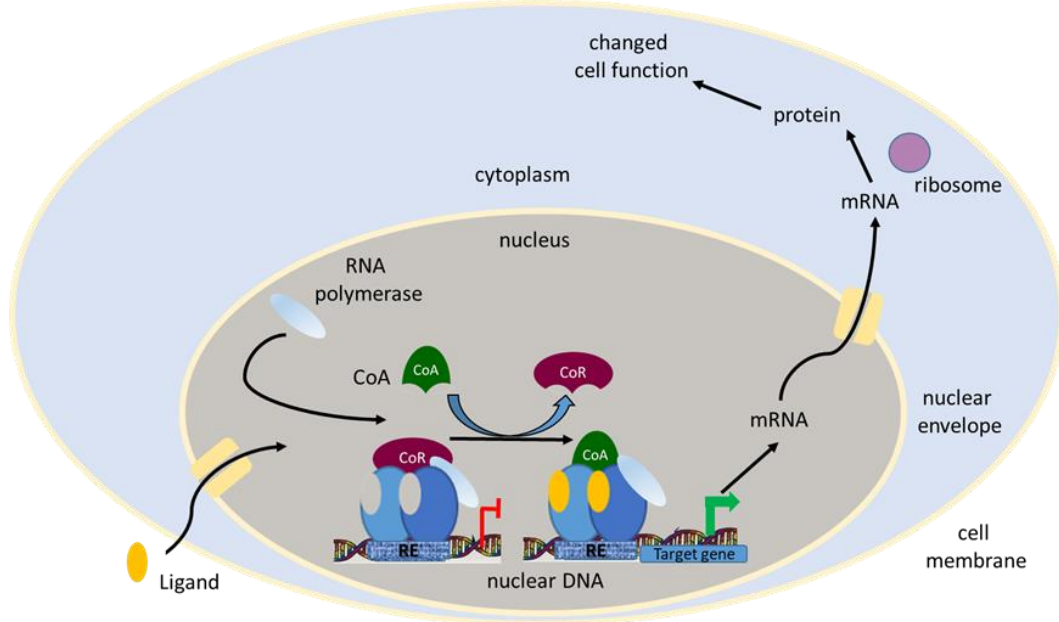


Figure 1. 3 Type I and type II nuclear receptors.

Nuclear receptors (NRs) are categorized based on affinity. High affinity NRs are shown in the top diagram: a hormone (yellow oval) enters the cytoplasm of a cell. The NR dissociates the heat shock protein (HSP) and the hormone binds creating a NR/hormone complex. The NR either remains as a monomer or forms a homodimer or heterodimer and translocates into the nucleus (grey oval) binding to a hormone response element (HRE) in the DNA. The NR dimer recruits coregulators such as a corepressor or coactivator and RNA polymerase (light blue oval). The mRNA is translated to protein and cell function is changed. Low affinity NRs are shown in the bottom diagram: a ligand (yellow oval) enters the nucleus (grey oval) of a cell. The NR heterodimer remains in the nucleus bound to the response element (RE) in the DNA. In basal conditions corepressors (red shape) are associated with the NR complexes. In the presence of ligand the NR heterodimer recruits a coactivator (green shape) and RNA polymerase (light blue oval) causing the corepressor to dissociate and initiating transcription. The mRNA is translated to protein and cell function is changed.

1.2.3 Nuclear receptor de-regulation in cancer

The three main co-activators associated with expression and regulation in BCa are NCOA1, nuclear receptor coactivator 2 (NCOA2) and NCOA3, and interestingly NCOA3 expression has been shown to be more highly expressed than NCOA1 and NCOA2 in MCF-7 (ER-positive BCa) cells compared to SK-BR-3 (HER2+) cells [90]. However, NCOA1 is known for its role in supporting BCa metastasis through activation of the matrix metalloproteinase and Twist1 genes [91, 92]. Furthermore, NCOA1 was more responsive to changes in nutrient status in aggressive metastatic cancers such as MDA-MB-231 (ER-negative BCa) and PC-3 (prostate cancer) than the less aggressive cells such as MCF-7 (ER-positive BCa) and lymph node carcinoma of the prostate (LNCaP) [93].

The three main co-repressors of LXR are NCOR1, NCOR2 and nuclear receptor interacting protein 1 (NRIP1) and enhanced expression of these co-repressors has been observed in cancer [94, 95]. LXR α conformation and serine 198 phosphorylation have been linked to the influenced recruitment of cofactors, such as NCOR [67, 81]. NCOR1 and NCOR2 skew the transcriptome selectively through restriction of NR signalling, which has been linked to further facilitating the Warburg effect [79]. Additionally, basal mRNA levels in tumour cells are also frequently enhanced in cancer relative to non-cancerous cells, and decreased LXR-ligand sensitivity is often observed [79]. Additionally, loss of function in NCOR1 and NCOR2 mutations has been found to aid BCa development [96], underlining the complexity of NRs, cofactors and their interactions with ligands.

1.3 Cholesterol, LXR and Cancer

Cholesterol is the primary sterol component of mammalian cells and is of key importance for cell function and viability [97]. Large amounts of energy expenditure are required to regulate cholesterol levels through mechanisms such as; de novo synthesis, storage and elimination of cholesterol via efflux (see **Figure 1.4**), intracellular transfer and metabolic pathways [98, 99]. Cholesterol also serves as a structural constituent of the cellular membrane and when incorporated into a phospholipid bilayer it organises itself, so the hydrophobic tail is in the bilayer and the polar hydroxyl group (head) of the compound is close to the surface, allowing the polar group interactions with neighbouring phospholipids altering the membrane structure [100].

Cholesterol is an important component of cell membranes and because of this, cells have evolved intricate mechanisms to regulate distribution of sterols and their abundance [101]. Cholesterol is synthesised in the endoplasmic reticulum, travels to the golgi, combines with sphingolipids and is then transported to the plasma membrane in lipid rafts [102]. Lipid rafts are made up of lipids arranged in an ordered phase [103], and its these rafts that are responsible for the molecular sorting of membrane proteins into select areas of the membrane.

LXR is stimulated by the interaction with oxidized cholesterol or oxysterols. The synthetic LXR agonists T0901317 and GW3965 and the antagonist GSK2033 have been the focus for many studies, which have demonstrated their efficacious regulation of LXR. Sabol *et al*, established the up-regulation of the ATP-binding cassette G1 (ABCG1) through treatment of 1 μ M T0901317 in Raw264.7 cells transfected with an ABCG1 promoter and (LXRE), and further demonstrated the

same in the HepG2 liver cell line [104]. Nelson *et al*, established the activation of LXR in the development of breast tumours in the ER-positive MCF-7 cell line by the synthetic LXR agonist GW3965 [105], demonstrating cholesterol synthesis and LXR have a role in BCa development. LXR ligands have been linked to cancer in many studies [66, 73, 106-108] via their LXR-driven luciferase activity or increased expression of LXR target genes involved in cholesterol efflux. LXR has several endogenous ligands that have been established in a series of different cell lines and tumours [66, 73, 104-112].

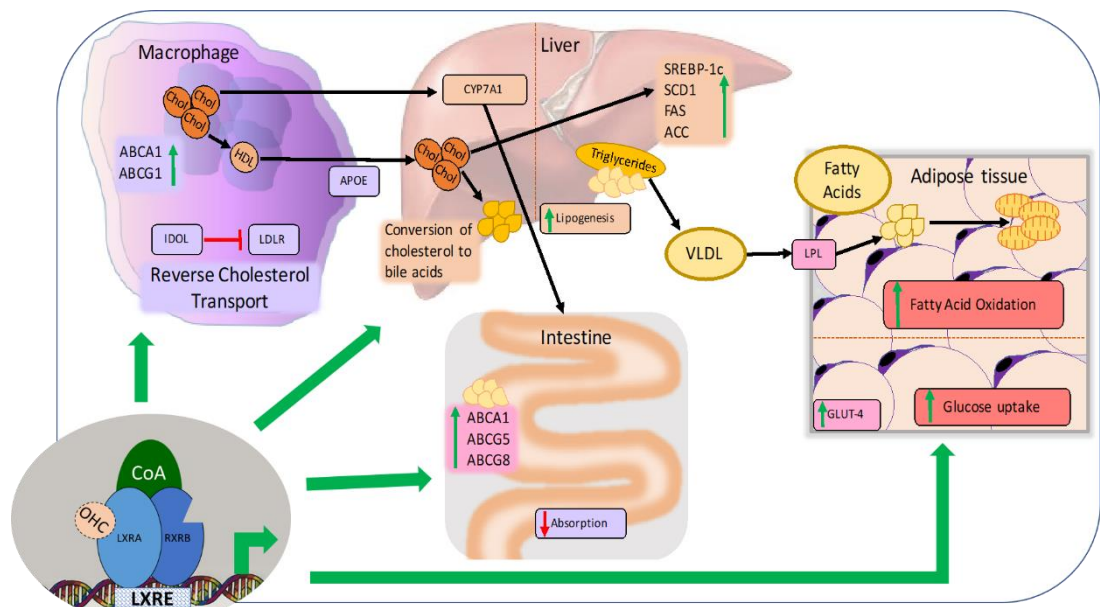


Figure 1. 4 Oxysterols serve as signalling molecules to control cholesterol metabolism via LXR.

LXR is regulated by oxysterols/ligands binding which controls reverse cholesterol transport in macrophages through inhibition of the low density lipoprotein receptor (LDLR) by LXR activation of the inducible degrader of the LDL receptor (IDOL). LXR activation upregulates expression of ABCA1 and ABCG1 which efflux cholesterol out of the macrophages and into the liver. In the liver cholesterol either regulates genes involved in lipogenesis such as fatty acid synthase (FAS) and acetyl CoA carboxylase (ACC) to convert acetyl-CoA into triglycerides for storage in fat tissue or is converted to bile acids. In the intestine, upregulation of ABCA1, ABCG5 and ABCG8 lower triglyceride absorption to maintain cholesterol levels.

1.3.1 Cholesterol, obesity and statins

In high-income countries such as the UK [113] and USA [114], obesity prevalence is high, in comparison to low-income countries such as Brazil [115]. Furthermore, altered cholesterol metabolism, which is considered a co-morbidity of obesity, has recently emerged as an independent risk factor of BCa in post-menopausal women [116]. High dietary cholesterol intake in a cohort of women increased risk of BCa cancer by 48 % [117] demonstrating the impact of altered cholesterol signalling and obesity in BCa development.

Statins are routinely used in high risk patients to lower circulating LDL-C levels. Statins have been shown to induce cell cycle arrest in the G1 phase *in vitro* reducing cell proliferation in BCa cell cultures [118, 119] and a variety of other cell types [120]. Importantly, statins reduce the relative risk (RR) of several diseases, such as vascular events regardless of age, baseline LDL-C, and sex RR=0.79 (95% CI 0.77-0.81, per 1.0 mmol/L reduction) [121]. Several epidemiologic studies have been conducted assessing the effects of statins on BCa, whilst most studies have shown reductions in BCa occurrence [122] there are studies who have not observed this same effect [123, 124].

These differences in epidemiologic study outcomes may be explained by the use of different statin types. There are two main types of statins, lipophilic and lipophobic statins. Lipophilic statins interrupt mevalonate synthesis in peripheral and liver tissues due to their ability to diffuse across membranes, showing possibilities of cholesterol dependent and independent effects [125]. Lipophobic statins affect hepatocytes that express transporter molecules due to active transport being their only mode of uptake [125]. Kumar *et al*, conducted one of the largest retrospective

ER-negative tumour studies during which they analysed data from 2,141 female participants who had a BCa incident. The study assessed statin use among the women previous to the BCa incidence and identified women taking lipophilic statins for more than a year had proportionally fewer ER/PR-negative tumours OR=0.63 (95% CI 0.43-0.92: p=0.02) relative to women who did not use statins or had been for less than a year [122], which supports the need for larger meta-analysis to analyse the effects of lipophilic and lipophobic statin use separately.

Evidence signifying statins as a pharmacological compound to reduce BCa reoccurrence by inhibiting cholesterol absorption has been shown [121, 125-129]. A meta-analysis showed a safe decrease of the 5-year cardio-vascular incidence by 21 % with each 1.0 mmol/L reduction of cholesterol in patients when treated with statins [121]. Furthermore, Garwood *et al*, presented a pilot study of 40 women with stage I BCa or had a confirmed diagnosis of ductal carcinoma in situ (DCIS) who were treated with fluvastatin which is a lipophilic statin [125]. Ahern *et al*, reviewed these studies and concluded that a clinical trial of BCa therapy with statins, particularly simvastatin would develop existing data demonstrating statins as a prevention of BCa recurrence [126].

Cholesterol is modified by members of the cytochrome P450 family to produce a pool of signalling molecules termed oxysterols (as shown as **Figure 1.5**). Oxysterols allow local and systemic homeostatic control of cholesterol metabolism via their binding affinity for LXR. The different oxysterols converted from cholesterol have varying capacities to drive LXR-mediated transcription suggesting an element of selective modulation. Furthermore, there appears to be little variation between

oxysterol concentrations in BCa subtypes [130] suggesting LXR activity or response to ligand may be altered in different subtypes.

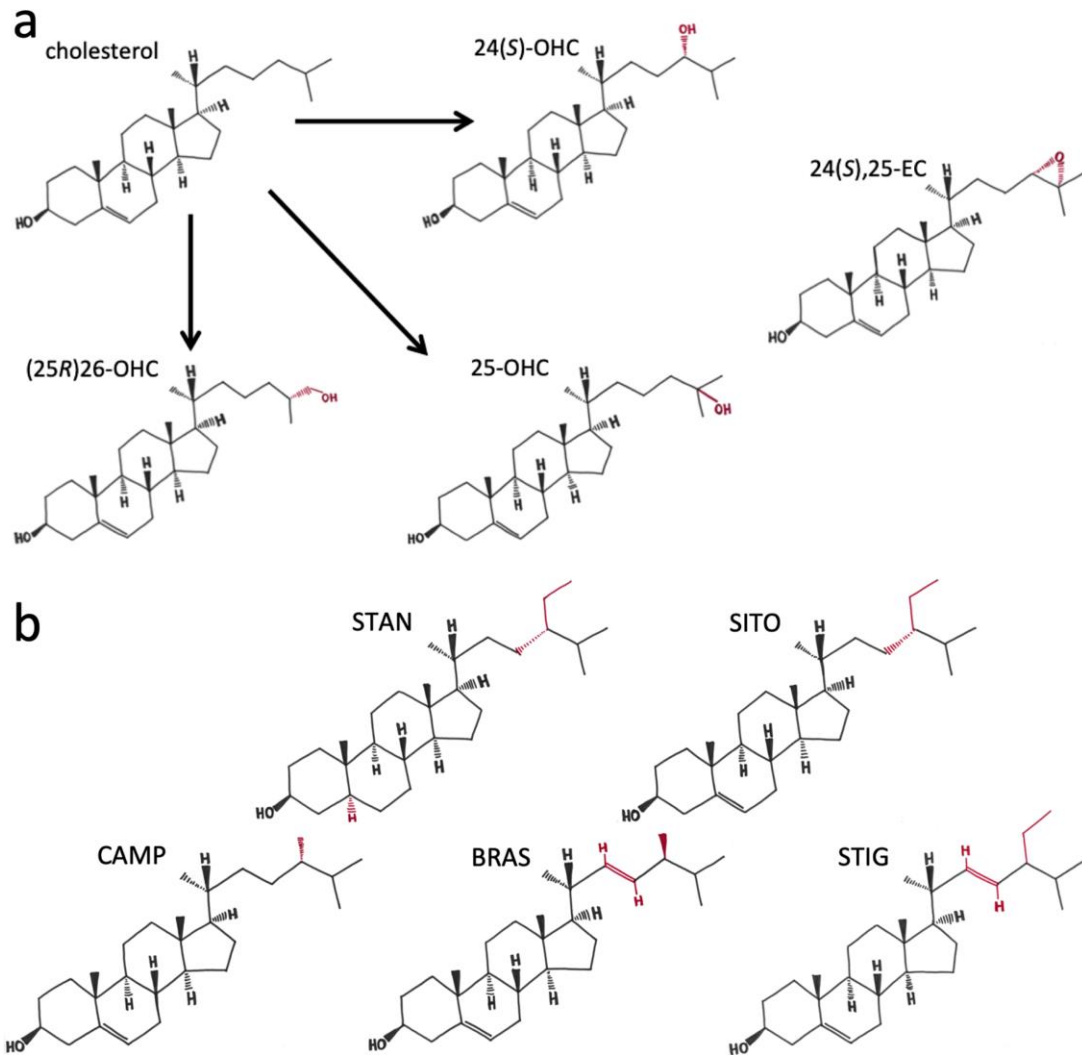


Figure 1. 5 Chemical structure of cholesterol, side-chain oxysterols and plant sterols/stanols:

(a) cholesterol differences from oxysterols 24(S)-OHC, 25-OHC, (25R)26-OHC and 24(S),25-EC are highlighted; (b) structures of phytostanol (sitostanol (STAN)) and phytosterols (β -sitosterol (SITO); campesterol (CAMP); brassicasterol (BRAS); stigmasterol (STIG) used in this study. Differences in structure with cholesterol are shown in red. Image previously published by Hutchinson *et al* [131].

1.3.2 Oxysterols and the cholesterol pathway

Oxysterols were first acknowledged as the main endogenous ligands for LXR α in 1996 and confirmed shortly after in 1997 [111, 112, 132]. A variety of oxysterols are known

to exist, some of which include: 7-ketocholesterol (7KETO), 22-hydroxycholesterol (22OHC), 24-hydroxycholesterol (24OHC), 25-hydroxycholesterol (25OHC), 25,26-hydroxycholesterol (26OHC) and 24,25-epoxycholesterol (24,25-EC) [73]. Oxysterols bind to and activate LXR α inducing expression of LXR α target genes. Janowski *et al*, were the first to show enhanced LXR α activation in CV-1 cells after treatment with 22OHC, 24OHC, 25OHC and 26OHC (previously referred to as 27OHC) at 10 μ M [111], followed by Forman *et al*, who also showed increased LXR α activation by 22OHC, 25OHC and 26OHC in CV-1 cells at 10 μ M [132]. Furthermore, activation of both LXR α and LXR β in CV-1 cells was observed when treated with 22OHC and 24OHC [112], and in Raw264.7 cells when treated with 22OHC [133]. The canonical LXR target genes HMGCR, NPC1L1, SR-BI and LDLR were repressed by 25OHC in HepG2 cells [109], however in HEK293 cells, 24,25-EC successfully stimulated LXR α driven luciferase activity by 9-fold [66]. Interestingly, 25OHC and 26OHC failed to activate LXR α in luciferase driven CV-1 cells [112], suggesting LXR α response to oxysterols is cell type and oxysterol conformation dependant.

Oxysterols are anti-proliferative when bound to LXR α , but when bound to estrogen they are pro-proliferative [110, 134]. Hydroxylation of the cholesterol side-chain is the initial stage in the bile acid synthesis pathway and results in hydroxycholesterols (OHCs) with reactive –OH groups. They can damage DNA and proteins but are also signalling molecules for regulators of cholesterol biosynthesis and lipid homeostasis pathway (e.g. LXR α/β , ROR γ). Of all the oxysterols, 26OHC is the most researched oxysterol, possibly due to its abundance rather than efficacy as a ligand. 26OHC has been shown to be elevated in ER-positive breast tumours [110] when compared to healthy tissue and is able to encourage epithelial-mesenchymal transition (EMT) in

ER-positive BCa [135] and TNBC [105] cells (if applied at supra-physiological concentrations, although without a carrier the hydrophobicity of oxysterols makes assessing their solubility *in vitro* challenging). Furthermore, circulating levels of 25OHC have been found elevated in patients treated for metastatic relapse compared to patients receiving treatment in the adjuvant setting [136], linking elevated oxysterol concentrations with BCa progression and relapse.

In normal cell biology, nuclear receptors such as LXR α act as sensors to control intracellular cholesterol levels. In high cholesterol conditions, LXR activity is enhanced to transcriptionally control the export and trafficking of excess cholesterol. LXR controls the expression of efflux pumps such as ABCA1 for export of excess cholesterol or APOE for transport of cholesterol. In cancer biology, these essential cholesterol signalling pathways are often altered and cross-talk between cancer epithelial cells and support cells have been linked to cancer progression [137], metastatic relapse [138], and cancer stem cell (CSC) self-renewal [139]. Furthermore, patients who have tumours that are heterogenous with enhanced support networks (supported by fibroblasts, macrophages, adipocytes) tend to have poor prognosis.

1.3.3 Oxysterols from support cells

Breast cancer tumours are heterogeneous supported by a tumour microenvironment (TME) composed of multiple non-cancer cell types [140]. The TME is made up of support cells, immune cells and adipose cells which store and secrete factors into the TME, aiding and influencing cancer epithelial cell signalling pathways [141]. Macrophages, adipocytes and fibroblasts regulate expression of cytochrome P450 (CYP) enzymes to synthesise oxysterols and secrete them into the

TME supporting cancer epithelial cells [142]. Patients who have tumours with enhanced support cell microenvironments tend to have a poor prognosis, allowing the cancer cells to employ TME-driven metastatic and proliferative behaviours via paracrine signalling [143-145].

1.3.3.1 Fibroblasts

Fibroblasts are support cells which provide collagen and ECM to the surrounding cells. They have migratory capacities and often exhibit an asymmetrical forked cytoplasm. Fibroblasts have been shown to not only produce 24OHC, 26OHC [146] and 25OHC [147], but also further modify oxysterols through CYP7B1 regulation [147]. Additionally, fibroblasts have been shown to regulate HMG-CoA reductase activity through 24,25-EC production [148].

There is evidence suggesting patients with breast tumours supported by fibroblasts tend to have poorer prognosis [144, 149] and tumour-stroma may have prognostic value [150]. Fibroblasts in the TME are often referred to as cancer associated fibroblasts (CAFs). One miRNA in particular has been linked to the progression of fibroblasts into CAFs, mir-21, which has been shown to inhibit smad7 translation (an inhibitor of TGF- β) which resulted in the transformation of resident fibroblasts (or non-cancerous fibroblasts) into CAFs [151], and has been shown to support cancer progression [152]. CAFs have also been shown to promote breast cancer tumour growth and metastasis in 4T1 orthotopically injected Balb/c mice [153]. Furthermore, fibroblasts derived from malignant breast tissue of women with invasive breast cancer were found to have different gene expression profiles when compared to fibroblasts from women with non-cancerous breast tissue [154].

Additionally, another study by Bauer *et al*, compared the gene expression profiles in matched breast CAFs and non-cancerous fibroblasts from six primary human breast carcinoma and also found a panel of up-regulated genes in the CAFs relative to the non-cancerous fibroblasts but also found high variance in non-cancerous fibroblasts suggesting heterogeneity may originate from the non-cancerous fibroblasts.

1.3.3.2 Macrophages

Macrophages are immune cells which are known for their fundamental role of phagocytosis and secondary roles as antigen presenting cells stimulating T lymphocytes. Macrophages are not specifically associated with a region of the body, but are signalled or recruited to a site by chemokine receptors such as chemokine receptor 2 (CCR2) [155], or growth factors such as colony stimulating factor 1 (CSF1) secreted by BCa cells [156]. Monocytes are undifferentiated macrophages prior to recruitment and once stimulated they differentiate, mature and become macrophages. There are two subtypes of macrophages: M1 and M2 macrophages. M1 macrophages are classically activated macrophages which typically display anti-tumorigenic properties and have roles in the pathogenic defence [156]. M2 macrophages are alternatively activated macrophages and these are pro-tumorigenic which express anti-inflammatory cytokines (IL-4, IL-10 and IL-13) [156] and angiogenic factors (EGF and VEGF) [157, 158]. Interestingly, macrophages originally located in the tissue prior to tumour formation contribute little numbers to the TME [159]. Tumour associated macrophages (TAMs) are recruited to the tumour formation site as monocytes and differentiate into macrophages [160]. Macrophages are recruited by chemokines and the most commonly formed

chemokine is the chemokine ligand 2 (CCL2), which has been shown to positively correlate with macrophage accumulation in human breast tumours [161].

In normal cell biology oxysterol levels in macrophages are low [162], but outside their normal role as immune cells, macrophages have been shown to produce high levels of oxysterols to increase cholesterol elimination to inhibit foam cell formation [163] signifying they may have a central role in the cross-talk between lipid metabolism and immune regulation in disease. CYP27A1 is highly expressed in both macrophage subtypes [163], resulting in 26OHC production and delivery to cancer cells. In monocytes (early stage unstimulated macrophage cells) however, 26OHC production is low and only increases after maturation [162]. Interestingly, CH25H (the enzyme responsible for the conversion of cholesterol to 25OHC) is abundantly expressed in M1 macrophages, whereas CH25H expression in the M2 macrophage remains relatively low similar to the expression levels in monocytes [164]. Production of 24,25-EC has also been shown to enhance expression of ABCA1 and ABCG1 in macrophages promoting cholesterol efflux and inhibiting foam cell formation [165] linking these immune cells and their oxysterol production with enhanced LXR signalling in tumours supported by the TME.

1.3.3.3 Adipocytes

Adipocytes are non-cancerous cells which vary in size, storing fat in the forms of cholesterol or triglycerides. Their roles typically include energy expenditure and the secretion of adipokines which are signalling proteins. Adipocytes, like macrophages express high levels of CYP27A1 however adipocytes express low levels of the enzyme CYP7A1 which suggests adipocytes produce 26OHC without further modification of

the molecule [166]. CYP11A1 is also upregulated in mature adipocytes relative to adipocytes prior to maturation, demonstrating their ability to synthesise 22OHC [166]. Furthermore, synthesis of 25OHC was demonstrated in adipocytes prior to differentiation (pre-adipocytes) through enhanced expression of CH25H [167], and regulation of CYP46A1 by calorie consumption in adipocytes [168].

1.3.4 Cholesterol in Cancer

Cholesterol is a crucial compound with vital roles in the membrane structure and the synthesis of bile acids, vitamin D and steroid hormones [169]. Cholesterol in cancer is also a key requirement for the fast rate of uncontrollable cancer cell proliferation as shown by Shimizu *et al*, demonstrating increased plasma cholesterol enhanced tumour formation and increased tumour burden [170]. Cholesterol is tightly regulated within healthy individuals preventing over accumulation within the body, where this fails the development of atherosclerosis can happen due to the build-up of cholesterol plaques in the arteries [109]. Cholesterol homeostasis is regulated by several pathways with vital roles in the generation of endogenous cholesterol, the absorption of dietary sterols and its eradication and the production of bile acids. Prevention of cholesterol accumulation is controlled by the LXRs regulation of target genes involved in cholesterol catabolism, storage, efflux and elimination [169]. Cholesterol homeostasis is important for the body to generate and reutilize metabolites for energy production.

Cholesterol absorption is regulated by the NRs LXR α and LXR β which are known to respond to elevated cholesterol levels via transactivation of LXR target genes (ABCA1, ABCG1, ABCG5 and ABCG8) involved in sterol transport [169]. LXR has been

shown to control lipogenesis, including fatty acid synthesis (FAS) and export of very low-density lipoprotein (VLDL) showing links to hyperglyceridaemia induced by high carbohydrate/low-fat diets, atherosclerosis and hyperglycaemia [171]. Furthermore, treatments of plant sterols disrupted cholesterol homeostasis through decreased cholesterol synthesis inhibited SREBP-2 processing in mice and via LXR α -mediated luciferase activity in CHO-7 cells [172]. These alterations in cholesterol homeostasis and cancer metabolism indicate a role for cholesterol in cancer progression. Enhanced circulating LDL-cholesterol (hypercholesterolemia) and surplus glucose from diet are therefore linked as contributing factors in cancer development as such, targeting members of the nuclear receptor family, LXR α in particular [105, 106, 110, 134] has become of particular interest in BCa research.

1.3.5 Oxysterol regulation of LXR

Cholesterol and its role in cancer progression was suggested as early as 1913, when Robertson and Burnett, demonstrated tumour growth was accelerated following injections of cholesterol into xenographs [173]. Multiple studies have compared cholesterol levels in cancer tumours and healthy tissue, many of which have shown increased cholesterol levels in a range of different tumours, for example oral [174], gastrointestinal [175], thyroid [176], colon [177], prostate [178] and breast [110, 136]. Interestingly, low serum cholesterol levels have been observed in patients with cancer [179, 180] which suggests cholesterol may accumulate within tumours. Many have looked at mechanisms that increase intracellular cholesterol in cancer cells, including the rate limiting HMG-CoA activity in the cholesterol synthesis pathway [181] and its loss of feedback inhibition by cholesterol [182]. The LDLR was also

shown to increase uptake of extracellular cholesterol [183, 184] and reduce the expression of the canonical LXR target gene ABCA1 a well-known cholesterol efflux pump [184, 185]. Thus, demonstrating the complexity of the interconnected mechanisms of cholesterol acquisition by cancer cells and tumours.

1.3.5.1 In Prostate Cancer

Evidence of oxysterol roles in prostate cancer have also been explored given that hypercholesterolemia leads to the increased risk of prostate cancer [186]. Prostate cancer development is dependent on the hormone androgen, mediated by the AR. Proliferation of prostate cancer cells is triggered by the AR and is associated with poor disease free survival in patients [187]. The LXR synthetic ligand T0901317, was shown to inhibit cell proliferation and tumour formation in tumour xenografts of LNCaPs prostate cells in athymic nude mice, showing a significant reduction in the growth of the tumours. Furthermore, LXR α signalling was determined by mRNA analysis showing a 3.5-fold increase of ABCA1 induction [188]. LXR α appears to have a protective role in the repression of prostate cancer [189] which is also supported by Chuu *et al*, who also showed a reduction in tumour growth and progression of LNCaP prostate xenografts in athymic nude mice when treated with T0901317 [190], and further showed LXR agonists stimulate cell cycle arrest via the up-regulation of p27 [191]. Therefore, demonstrating LXR regulation by its ligands has a beneficial effect on prostate cancer.

1.3.5.2 In Breast Cancer

In the last 5 years new roles for oxysterol signalling in BCa have been identified, with most studies focusing on 26OHC, largely due to abundance. 26OHC is however, a

weak ER and LXR ligand in BCa [105]. Nevertheless, elevated levels of 26OHC were found in breast tumour relative to normal breast tissue [110]. And treatment of 26OHC was shown to drive ER-positive BCa growth via the ER and LXR α -dependent EMT [105]. Furthermore, Nelson *et al*, established that knockdown of the CYP27A1 enzyme accountable for the conversion of cholesterol into 26OHC resulted in the reduction of hypercholesterolemia-promoted tumour growth in mice [105]. Additionally, in MCF-7 cells, ABCG1 relative mRNA expression was significantly increased by 20 μ M T0901317 as well as 22OHC [106], whereas Wu *et al* demonstrated treatment of 26OHC promoted ER-positive BC growth via diminished CYP7B1 expression [110]. More recently, 26OHC was also shown to drive metastasis of breast tumours via $\gamma\delta$ T cells [21]. In addition to this, larger tumours derived from ER-negative MDA-MB-231 cells were observed in mice with high circulating LDL-C concentrations compared to mice with low LDL-C [51]. Finally, studies have reported that high total cholesterol is associated with an increase in BCa recurrence [192] and reduced disease free survival with high serum LDL-C [5]. Thus, showing that oxysterol signaling via LXR α has clear roles in the progression of BCa.

1.3.6 Dietary ligands

Phytosterols are similar in structure to several well-known LXR ligands, notably the oxysterols (**Figure 1.5**). The most abundant phytosterol in the human diet is β -sitosterol, and phytosterol mixtures commonly include other sterols such as campesterol, stigmasterol and dihydrobrassicasterol [193]. Phytosterols and phytostanols are consumed either as whole foods as part of the human diet or as

components added to margarines or yoghurt drinks to reduce LDL-C. Another way to lower LDL-C is through pharmacological intake of statins.

1.3.6.1 Plant sterol biology

Phytosterols are natural plant constituents and by the early 1970s, over 40 different sterols had been identified from 7 different plant classes [194]. By the 2000s more than 100 sterols had been identified [195], and over 250 sterols are now known to exist [196]. Phytosterols and phytostanols (PSSs) are essential components of plant cell membranes [197] which lower the intestinal absorption of dietary cholesterol [198-200]. Lowering LDL-C significantly reduces the risk of cardiovascular disease, which can be achieved through the means of pharmacological statins [121] or by as high as 15 % through the consumption of a phytosterol rich diet (approx. 2-3 g/d) [201-203]. A reduction in cholesterol absorption by phytosterol intake has been linked to phytosterol/cholesterol competition for micelle incorporation, due to the displacement of cholesterol by phytosterols which have a higher affinity for intestinal micelles [202]. Phytosterols have been shown to be in the low micromolar range in the serum of the general population [204], however phytosterols are not easily absorbed, as such a moderate daily intake (approx. 2-3 g/d) is recommended for phytosterol consumption.

Plant sterols or phytosterols are essential components of plant cell membranes [197] and have equivalent cellular functions in plants to those of cholesterol in mammals. Phytostanols are saturated sterols (**shown in Figure 1.5**) lacking a double bond in the ring structure and are hydrolysed in the upper small gut [205]. Phytosterols have similar structures to that of the oxysterols which allows them to be considered as selective modulators of LXR α and act as inhibitors of other nuclear receptors such as

FXR as shown by Carter *et al* [206]. Selective modulator is a term used to describe compounds that act in a tissue specific manner, for example, Tamoxifen is an antagonist of the estrogen receptor in breast tissue but is an agonist in other regions such as bone [207]. A full agonist is a compound that activates a receptor in all tissue types. It is unclear why there are so many variants of plant sterols but the range of structural forms, some of which mimic mammalian cholesterol modifications [208], provide exploitable biophysical properties (such as side chain branching and saturation) [209] for use in prevention and/or treatment of human cholesterol-related diseases.

1.3.6.2 Phytosterol/phytostanol regulation of LXR

Given the structural similarities of PSSs and oxysterols it is not surprising there is a range of molecular evidence to suggest that PSSs are LXR ligands. If PSSs are accumulated in adequate amounts they integrate into the plasma membrane altering membrane fluidity, signalling cascades and lateral pressure on protein complexes [209]. Systemically, PSSs can alter cholesterol metabolism through; impairing cholesterol uptake from the diet [210], inhibiting enzymatic conversion of cholesterol to oxysterols [211] and inhibiting enzymes involved in cholesterol metabolism [172].

In vitro PSSs have been shown to be LXR α ligands in HEK293 LXR α luciferase reporters, which were responsive to treatments of sitosterol, brassicasterol, campesterol and stigmasterol at 10 μ M [66]. Down regulation of the canonical LXR target genes NPC1L1, HMGCR, SR-BI and LDLR was observed in HepG2 cell cultures treated with sitosterol and stigmasterol, and interestingly to a similar suppression level as that of 25OHC [109]. Other canonical LXR genes have also been shown to be

regulated by phytosterols as demonstrated by Plat, Nichols and Mensink who showed ABCA1 up-regulation by sitosterol, sitostanol and campesterol in Caco2 cell cultures [212]. Evidence of phytosterol regulation of LXR has also been demonstrated in hamsters when fed phytosterol diets. Plasma levels of LDL-C, cholesterol absorption and triglycerides were reduced in the hamster group which were fed phytosterols, but not in those which were fed phytosterol oxidised products (POP) [213]. Furthermore, the expression of the ABC-transporter ABCG5, microsomal triglyceride protein (MTP) and the esterification enzyme acetyl CoA acetyltransferase (ACAT) were also reduced [213].

Interestingly Alemany *et al*, saw a decrease in the expression of ABCG5 in Caco2 cells when incubated with 7-ketostigmasterol at 60 μ M, as well as a decrease in ABCG8 expression. NPC1L1 however, was not altered by POP treatments but there was an increase in HMG CoA in the Caco2 cell cultures resulting in an increase in cholesterol synthesis [214]. In a co-activator peptide recruitment assay phytosterols from the 4-desmethylsterol family were shown to be effective LXR α agonists, with campesterol and sitosterol inducing ABCA1 expression in Caco2 [212]. ABCA1 and ABCG1 expression was also increased in mouse peritoneal macrophages (MPMs) when treated with stigmasterol (10 μ M), 25OHC (10 μ M) or T0901317 (1 μ M), however 25OHC significantly decreased expression of HMGCR and LDLR [215]. PSSs can bind and may activate LXR in a cell type dependent manner and has been suggested by O'Callaghan, that phytosterols control cholesterol absorption by reducing esterification within the enterocyte which reduces the packaging of cholesterol into chylomicrons via MTP [216]. Additionally, Brauner *et al*, demonstrated an increase in ABCA1 expression by cholesterol treatment in Caco2 cell cultures, however co-

treatment of cholesterol with either campesterol or sitosterol attenuated transcriptional output of the LXR target gene [211], suggesting phytosterols are selective modulators of LXR and actively compete for binding.

1.3.6.3 Breast cancer risk and cholesterol status

Other than how PSSs can lower LDL-C, very little is known about their functions at the molecular level in healthy tissue or in cancer biology. There is however circumstantial evidence (where dietary intake of plants and therefore PSS are assessed for BCa risk) which suggest anti-cancer properties of phytosterols.

There have been numerous studies exploring the consumption of phytosterols and their effects on lower circulating cholesterol. For example, a study by Miettinen *et al*, showed patients who were fed sitosterol-containing margarine had a reduction in serum cholesterol levels (1 year mean reduction 10.2 %) when compared to a control group which had a mean increase of 0.1 % [199]. Furthermore, a meta-analysis of 217 epidemiologic studies found a strong association between fruit and vegetable consumption and the incidence of cancer [217]. Additionally, other analyses have shown a reduction in the risk of developing common cancers by 50 % when at least 5 servings per day of fruit and vegetables are consumed (when compared to those who ate less than 2 servings per day) [218]. Reduced cancer risk was also shown in observational studies where healthy dietary patterns linked to high PSS intake [219] and the consumption of plant-rich diets [220] have shown improved survival and reduced cancer incidence. Furthermore, clinical intervention trials demonstrated reduced rates of BCa and/or an increase in survival when saturated fat intake was lowered [48, 221].

Pharmacological intake of statins is used to help reduce circulating LDL-C in high risk patients. Statins have been shown to reduce LDL-C in multiple studies, one of which also reduced the risk of major vascular events RR=0.79 (95 % CI 0.77-0.81, per 1.0 mmol/L) irrespective of previous vascular events, age, sex and baseline LDL-C [222]. There are many studies that have looked at the effects of statin use, and some of these have specifically looked at the effects on BCa risk. One of the largest published cohorts who were looking specifically at the impact of statin use on overall risk (OR) in ER-negative BCa tumours, demonstrated a reduction in ER-negative BCa OR=0.63 (95 % CI 0.43-0.92: p=0.02) in women taking lipophilic statins for more than a year [122]. In human BCa cell line models, research has shown interesting anti-cancer effects of statins when used in combination with the chemotherapy drug doxorubicin or cisplatin [119]. Statins have also been shown to reduce cell proliferation *in vitro* by inducing cell cycle arrest in the G1 phase [119] and induce apoptosis [129] in multiple BCa cell lines. Furthermore, fluvastatin (a lipophilic statin) was shown to reduce proliferation and increase apoptosis in women with high grade BCa [125]. However, not all studies have shown favourable effects for all statin types. Pocobelli *et al*, reported they found no change in BCa risk in patients who used hydrophilic statins, but they did observe a reduction in BCa risk in women who had taken fluvastatin OR=0.5 (95 % CI 0.3-0.8) for less than 5 years [124].

1.3.7 Chemoresistance and LXR through the p-glycoprotein

The ABC-transporters are a superfamily of essential efflux pumps responsible for the ATP powered translocation of substrates such as cholesterol or chemotherapy drugs across cell membranes. The canonical LXR target gene ABCA1 for instance, is an ABC-

transporter that controls intracellular cholesterol efflux. Others such as ABCG1, ABCG5 and ABCG8 are known sterol efflux pumps also under the control of LXR, but LXRs control of other ABC-transporters such as ABCB1 (p-glycoprotein) in breast tissue remains unidentified. P-gp/ABCB1 is an important protein, with its roles in chemotherapy drug efflux established in cancer [223]. Chemotherapy efflux pumps can reduce the efficacy of chemotherapy treatment by exporting toxic drugs out of the cancer cells which stops the drug intercalating with DNA and minimalizes the drug effects. This is a common cause of chemotherapy resistance and is associated with the over expression of chemotherapy drug pumps, such as the p-gp/ABCB1 [224], multidrug resistance protein (MDRP) [225] and the breast cancer resistance protein (BCRP) [226]. LXR α is not commonly associated with regulated expression of the p-glycoprotein/ABCB1 (p-gp/ABCB1). One study however, showed 24OHC, 26OHC and T0901317 increased the expression of p-gp/ABCB1 in the blood brain barrier (BBB) which resulted in the efflux of oxysterols across the membrane and restriction of amyloid- β peptide A β peptide efflux [227]. This suggests a therapeutic role for LXR α regulation of p-gp/ABCB1 in the brain, but also in regions where LXR α activity is enhanced.

Overall links between breast risk and cholesterol status have been discussed, whether it be through plant-based diets improving survival and lowering cancer incidence [219, 220], reduced risk of major vascular events by statin-associated LDL-C reduction [222] or reduced rates of BCa incidence by decreasing saturated fat intake [48, 221]. Furthermore, cholesterol metabolites have been shown to promote BCa growth [105, 110] and metastasis [21], induce EMT [105] and has been found elevated in patient serum at relapse [136]. Finally, the LXR ligands 24OHC and 26OHC

were shown to regulate the chemotherapy efflux pump p-gp/ABCB1 [228] which is often linked to the development of chemotherapy resistance [223]. Therefore, suggesting roles for; altered oxysterol signalling in breast cancer with cross-talk from support cells, oxysterols-LXR dependent chemotherapy resistance through the p-gp/ABCB1, and phytosterol-LXR impairment of the oxysterol-LXR signalling pathways.

Chapter 2

Hypothesis:

Regulation of the oxysterol-LXR α -axis leads to the development of chemoresistance in TNBCs. PSSs antagonise LXR α activation and therefore counteract chemotherapy resistance effects.

Aims:

- a) Establish whether LXR α activity and function is enhanced in TNBC relative to Luminal A/ER-positive disease.
- b) Determine if enhanced LXR α activity leads to chemoresistance in TNBCs.
- c) Establish if fibroblasts can activate LXR α in TNBC and Luminal A breast cancer epithelial cells.
- d) Determine if phytosterols antagonise LXR α activation in TNBC.

Chapter 3

Materials and Methods

3.1 Cell culture

The BCa cell lines MDA-MB-468, MDA-MB-231 and MCF-7 and the breast fibroblasts NF2 and LaCAF were provided by Dr Thomas Hughes (St. James University Hospital, Leeds). BCa cells were cultured in Dulbecco's modified eagle medium (DMEM, Thermo Fisher, Cat: 31966047) supplemented with 10 % foetal calf serum (FCS) (Thermo Fisher, UK, Cat: 11560636) and maintained at 37 °C with 5 % CO₂ in a humidified incubator (Panasonic, MCO-170A1CUV-PE, UK). Cells were seeded to 1 x 10⁶ cells in a T75 tissue culture treated flask (Nunc, Thermo Fisher, UK, Cat: 10364131) for routine passaging every 3-4 days to ensure confluency remained between 20-80 % which was determined using an inverted microscope (Ceti, Medline, UK, X20 lens). Routine passaging of cells was completed as follows. Cells were washed with 5 mL phosphate buffered saline (PBS; Thermo Fisher, UK, Cat: 10209252) and detached with 3 mL 1X trypsin (Thermo Fisher, UK, Cat: 10779413). Trypsin was deactivated after 3-5 minutes with 7 mL DMEM containing FCS. Cells were resuspended using a sterile stripette and pipette to ensure a single cell suspension, before 10 µL was used to count cells using a haemocytometer with trypan blue (Thermo Fisher, UK, Cat: 15250061) to distinguish between live and dead cells.

3.1.2 Drugs and reagents

Drugs stocks were stored at -20 °C and diluted or dissolved as stated in the table below. Oxysterols were prepared in a sterile unit and diluted in nitrogen flushed ethanol (NFE) to prevent auto-oxidation. The following phytosterols were provided

by E. Trautwein (Unilever, Vlaardingen, Holland) or later purchased from Avanti and stored in NFE at 5 mM or 20 mM stocks at -20 °C. Epirubicin was protected from light in aluminium foil.

Table 1 Nuclear receptor ligands.

The ligand name is included in the first column followed by its acronym in the second column. The third column provides details of the company the ligand was purchased from and the fourth column for the catalogue or identifier code. The diluent is shown in the fifth column and the stock concentration in the sixth. The seventh column provides the ligand EC50 or IC50 followed by the model details in the eighth column. The ninth column provides details of known target receptors the ligand interacts with.

Ligand	Acronym	Company	Identifier	Diluted	Stock	EC50/IC50	Model	Target Receptors
T0901317	T090	Cayman	71810	DMSO	10 mM	50 nM	HEK293	LXR α , LXR β , FXR.
GW3965	GW	ToCris	2474	ETOH	10 mM	190 nM	Cell based	LXR α , LXR β , PXR
GSK2033	GSK	ToCris	5694	ETOH	10 mM	17 nM	HEK293	LXR α , LXR β , ER α , ER β , PR, GR, RXR, VDR, PXR, FXR, CAR, ROR α
22-hydroxycholesterol	22OHC	Avanti	700058	NFE	10 mM	5 μ M	CV-1	LXR α , LXR β
24-hydroxycholesterol	24OHC	Avanti	700071	NFE	10 mM	4 μ M	CV-1	LXR α , LXR β
25-hydroxycholesterol	25OHC	Avanti	700019	NFE	10 mM	7 μ M	CV-1	LXR α , LXR β , ER α
25,26-hydroxycholesterol	26OHC	Avanti	700021	NFE	10 mM	85 nM	HEK293	LXR α , LXR β , ER α , ER β
24,25-epoxycholesterol	24,25	Avanti	700037	NFE	10 mM	10 μ M	CV-1	LXR α , LXR β
7-ketcholesterol	7-KETO	Avanti	700015	NFE	10 mM	N/A	N/A	LXR α , LXR β
β-sitosterol	SITO	Avanti	700095	NFE	5 mM	42 nM	CoA Peptide	LXR α , LXR β
β-sitostanol	STAN	Avanti	700121	NFE	5 mM	136 nM	CoA Peptide	LXR α , LXR β
Campesterol	CAMP	Avanti	700126	NFE	5 mM	43 nM	CoA Peptide	LXR α , LXR β
Brassicasterol	BRAS	Avanti	700122	NFE	5 mM	N/A	N/A	LXR α , LXR β
Stigmasterol	STIG	Avanti	700062	NFE	2.5 mM	N/A	N/A	LXR α , LXR β

ETOH; ethanol, NFE; nitrogen flushed ethanol, DMSO; dimethyl sulfoxide, CoA Peptide; coactivator peptide assay.

Table 2 List of drugs.

The chemical or drug name is included in the first column followed by its acronym in the second column. The third column provides details of the company the item was purchased from and the fourth column for the catalogue or identifier code. The diluent is shown in the fifth column and the stock concentration in the sixth.

Chemical	Acronym	Company	Identifier	Diluted in	Stock conc.
Puromycin Hydrochloride	Puro	Santa Cruz	sc-108071	NFW	25 mg/mL
MK-571	MK	Cambridge Bioscience	10029	DMSO	10 mM
KO143	KO	Sigma	K2144	DMSO	10 mM
Verapamil	V20	Insight Biotechnology	sc-3590	NFW	10 mM
Epirubicin	EPI	Cambridge Bioscience	12091	NFW	10 mM
Thiazolyl Blue Tetrazolium	MTT	Sigma	M2128	PBS	5 mg/mL
Crystal Violet	CV	Sigma	V5265	H ₂ O, ETOH, MeOH	1 % CV solution

ETOH; ethanol, NFW; nuclease free water, DMSO; dimethyl sulfoxide, PBS; phosphate buffer solution, H₂O; water, MeOH; methanol, CV; crystal violet.

3.2 Generation of LXR-reporter cell lines

Signal lentiviral particles (LXR α) were purchased from Qiagen (Cat: CLS-7041L, LXR α TRE sequence: TGAATGACCAGCAGTAACCTCAGC) and transduced into the cells. Each vector contain at least 5 TRE repeats. Schematic diagrams of A) the LXR α Signal lentiviral particles, B) the negative control lentiviral particles and C) the constitutively active positive control lentiviral particles used to generate the reporter cell lines are shown below in **Figure 3.1**. Following the schematic is a table of the vector key features.

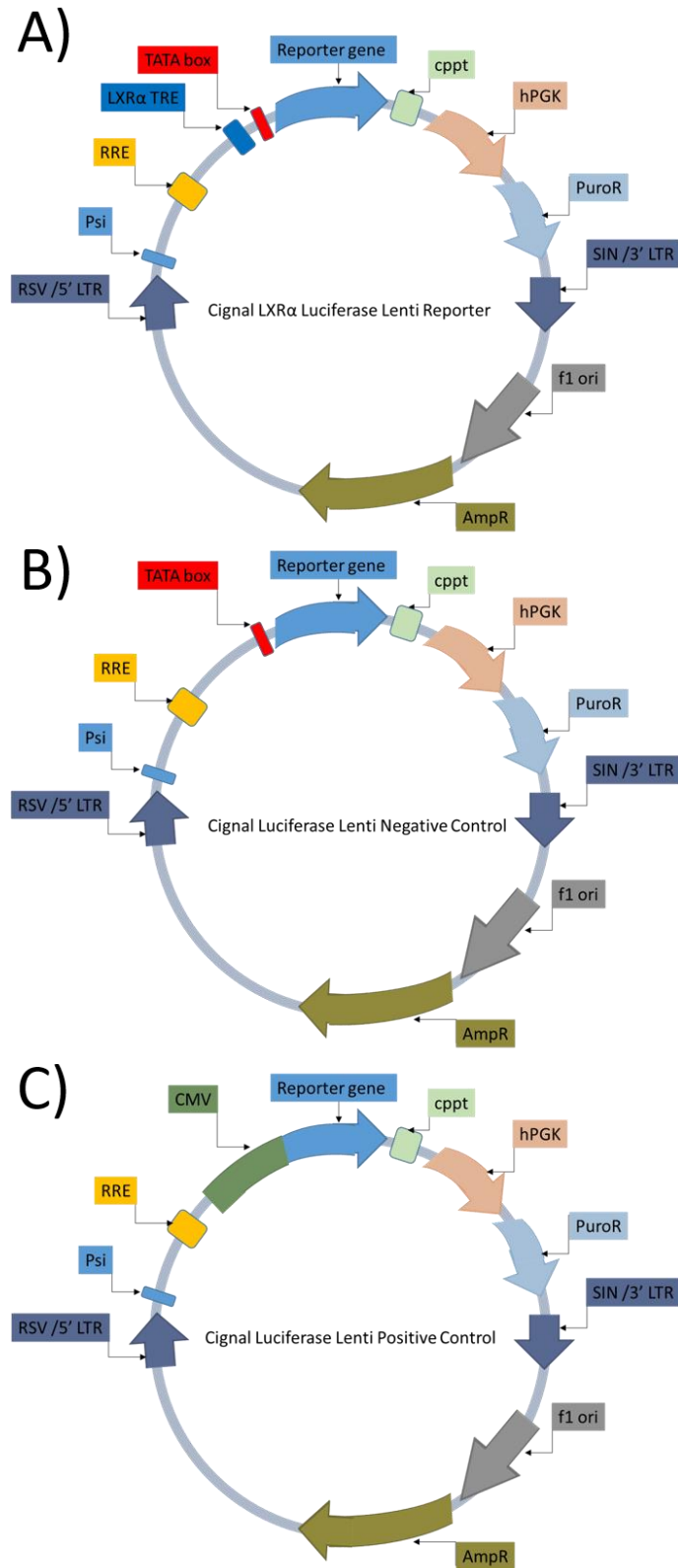


Figure 3. 1 Schematic diagrams of LXRα reporter constructs.

The Cignal lentiviral particles used to generate A) LXRα responsive B) negative control and C) constitutively active positive control reporter cell lines are shown here. Key differences include; the addition of the LXRα transcription response element (TRE) in the LXRα responsive reporter, the lack of TRE in the negative control reporter and the addition of a CMV constitutively active promoter in the positive control. Key features are shown in Table 3.

Table 3 The Lentiviral reporter features and functions.

The plasmid features from the LXR α reporter construct schematic diagrams are shown in the first column with the function described in the second column.

Feature	Function
RSV-5' LTR; Hybrid Rous sarcoma Virus (RSV) enhancer/promoter-U5 long terminal repeat	Permits reverse transcription of viral mRNA and viral packaging
Psi; Packaging signal	Allow viral packaging
RRE; Rev response element	Involved in the packaging of viral transcript
cppt; Central polypurine tract	Involved in the nuclear translocation and integration of transduced viral genome
Reporter gene (firefly luciferase)	Allow quantification of transcription
hPGK; human phosphoglycerate kinase eukaryotic promoter	Permits high-level expression of the mammalian selection marker (puromycin)
PuroR; puromycin resistance gene	Can be used for mammalian selection
SIN/3'LTR; 3' self-inactivating long terminal repeat	Modified 3'LTR that allows viral packaging but self-inactivates the 5'LTR for biosafety purpose. The element also contains a polyadenylation signal for efficient transcription termination
f1 ori; f1 origin of replication	Origin of DNA replication for bacteriophage f1
AmpR; ampicillin resistance gene	Allows selection of the plasmid in E.coli
LXRα TRE; LXRα Transcription response element	Permits regulation of reporter gene expression by a specific transcription factor - LXR α
TATA box	Act as an minimal promoter
CMV; Cytomegalovirus	Constitutively active promotor

3.2.1 Puromycin titration curve

Cells were seeded at 3×10^4 cells per well in a 96-well plate, incubated overnight and a puromycin titration applied to the plate ranging from 8 $\mu\text{g}/\text{mL}$ to 0 $\mu\text{g}/\text{mL}$. Cells were in DMEM containing puromycin for 5 days with media replaced fresh on day 3. After 5 days the wells were inspected under a microscope and the lowest concentration of puromycin that resulted in complete cell death was chosen for reporter cell isolation.

3.2.2 Transduction with lentiviral particles

Cells were seeded at 30,000 cells per well in a 24-well plate and incubated overnight. Signal lentiviral particles (LXR α) were purchased from Qiagen (Cat: CLS-7041L)

and transduced into the cells using 10,000 particles/ μL (total amount used varied dependant on cell line MOI) and 8 $\mu\text{g}/\text{mL}$ SureEntry transduction reagent. MDA-MB-468 cells had 150,000 transduction units/well, MDA-MB-231 cells had 30,000 transduction units/well and MCF-7 cells had 60,000 transduction units/well. After 18 h the particles were removed and fresh DMEM supplemented with 0.1 mM non-essential amino acids (Thermo Fisher, Cat: 12084947) and 100 U/mL penicillin and 100 $\mu\text{g}/\text{mL}$ streptomycin (Thermo Fisher, Cat: 10378016) were added to the cells. Cells were passaged to a 6-well plate after 24 h to avoid over confluency and incubated for a further 24 h. DMEM was then replaced with DMEM containing puromycin (1 $\mu\text{g}/\text{mL}$ as determined in section 3.2.1) to isolate successfully transduced cells.

3.2.3 Luciferase assay

The method for cell culture was followed, once the luciferase reporter cells were re-suspended to 1×10^6 cells/mL dilute 1/10 to achieve 10,000 cells/100 μL . 100 μL of cell suspension was plated in a 96 well white walled tissue culture (TC) plate (Greiner Bio-one, Cat: 655098) and incubated for 8 h. Cells were treated with oxysterols (Avanti: 1 pM-50 μM), phytosterols (Avanti: 1 pM-50 μM) and synthetic ligands (GSK2933, T0901317 and GW3965: 1 pM-50 μM) as positive controls /vehicle control (NFE, DMSO) as required and incubated overnight for 16 h. Cells were washed with PBS and lysed with 30 $\mu\text{L}/\text{well}$ passive lysis buffer 1X and placed on a rocker for 15 min. Injectors were used on the Tecan Spark 10M (TECAN, Spark 10M, UK) to inject 50 μL (optimised) LAR II (Promega, Uk, Cat: E1501) into the sample well and luminescence was then measured. This was completed well by well. LXR α activation was normalised to a vehicle control, error bars represent standard deviation.

3.2.4 Clone selection, storage and copy number analysis

3.2.4.1 Clone selection

Following reporter generation, cells were harvested using trypsin and cells counted. Cell suspensions were diluted to achieve 100 cells/200 μ L, and, using a p200 multichannel pipette, 200 μ L per well was plated into the first column of a 96 well plate. The rest of the plate was filled with 100 μ L of fresh media and a 2-fold serial dilution was performed moving 100 μ L of cell suspension from the first column to the second, mixed, from the second to the third and so on. The dilution series aimed to plate single cells roughly between columns 6-9. Cells were incubated for 16-24 h. Using a microscope, wells containing single cells were identified and marked on the plate. Plates were returned to the incubator and allowed to proliferate until 80-90 % confluency was achieved. Cells were then passaged into a 6 well plate and returned to the incubator. Cells were expanded until adequate cell numbers had been reached to freeze cells down, plating into a luciferase assay, DNA extraction for copy number analysis and further expansion.

3.2.4.2 Storage/freezing down cells

Cells were washed with PBS, detached using trypsin and counted. Cells were pelleted by centrifugation and gently resuspended to 1×10^6 cells/mL in freezing media (90 % FBS, 10 % DMSO). 1 mL cell suspension was then added to labelled cryotubes and placed in a freezing container in the -80 °C freezer overnight to allow a controlled rate of freezing (1 °C per min). Cryotubes were then moved to the liquid nitrogen storage within 24 h.

3.2.4.3 Copy number analysis

Cells were harvested (1×10^6 cells/mL) and washed twice with PBS. Cells were then resuspended in 1 mL DNA buffer (1 M Tris-HCL, pH 8.0, 0.5 M EDTA in dH₂O) and

transferred to 1.5 mL sterile Eppendorfs. Cells were centrifuged for 10 min at 10 °C (225 rcf), supernatant removed and the cell pellets resuspended in 300 µL DNA buffer. Proteinase K (2.5 µL: 20 mg/mL) and 20 % SDS (20 µL) was added to the Eppendorfs and were shaken vigorously. Eppendorfs were then incubated overnight at 45 °C. The next morning 350 µL of phenol was added to the Eppendorf's and shaken vigorously for 10 min at room temperature. Eppendorfs were then centrifuged for 10 min at 10 °C (956 rcf). The supernatants were transferred to a new sterile Eppendorf and the volume measured. One part phenol and one part chloroform/isoamyl alcohol (24:1) were added to equal the volume of the supernatants. Eppendorfs were shaken vigorously for 10 min at room temperature then centrifuged for 10 min at 10 °C (956 rcf). The supernatants were transferred to a new sterile Eppendorf and the volume measured. Phenol and chloroform/isoamyl alcohol (24:1) were added to equal the volume of the supernatants. Eppendorfs were shaken vigorously for 10 min at room temperature then centrifuged for 10 min at 10 °C (956 rcf). The supernatants were transferred to a new sterile Eppendorf and the volume measured. 3 M sodium acetate (pH 5.2) was added to equal 1/10th of the volume of the supernatants. 1 mL of 100 % isopropanol was added and the Eppendorfs were rotated end to end for 30 min at 4 °C until the DNA precipitated. The DNA was pelleted by centrifugation (10 min at 10 °C, 956 rcf) and resuspended in 1.5 mL 70 % ETOH. This was repeated twice to wash the pellet, then centrifuged for 20 min at 10 °C, 20817 rcf). The supernatant was removed and the pellet left to air dry for >20 min. The dried DNA pellet was then resuspended in 20 µL of NFW and placed in a thermomixer overnight at 37 °C. DNA was quantified using the Tecan Spark 10M using NanoQuant plate™ with 1 µL DNA. Blanking was completed before

and between sample reads. Quantification was performed by assessing absorbance at A260 nm and quality assessed with A260/280 and A260/A230. Remaining DNA was stored at 4 °C.

DNA was then used to assess copy number by qPCR using primers targeted to an endogenous gene with known copy number and targeted to the luciferase ORF (unknown copy number). GoTaq qPCR Master Mix kit was used for qPCR (Promega, UK, Cat: A6002) and product guidelines were followed (TM318). CXR (reference dye) was added 1 in 100 as required by the QuantStudio Flex 7 (Applied Biosystems Life Tech, Thermo Scientific, UK). Primer stocks were stored at -20 °C in NFW at 100 µM. For DNA copy number analysis, the sequences used are shown in the table below. All primers were designed to span exon boundaries, have GC Clamp, and melting temperature 58-62 °C. Primers were validated before use and all amplified with efficiencies of between 96 % and 100 %.

Table 4 Gene sequences.

The gene name for each primer are shown in the first column, with the direction of prime in the second column. The third column shows the primer sequences in the 5'-3' direction. Primers were purchased from Sigma Aldrich, UK.

Gene	Forward or reverse prime	Sequence
β-actin	Forward	5' CAACTCCATCATGAAGTGTGAC 3'
	Reverse	5' CCACACGGAGTACTTGCGCTC 3'
LXRE-2	Forward	5' GAAGGCGGAGGAGGAAAGC 3'
	Reverse	5' TCTTGAAACCTGAGCTGGGG 3'
Luciferase ORF	Forward	5' GAGATACGCCCTGGTTCCTG 3'
	Reverse	5' GCATACGACGATTCTGTGATTTG 3'

3.3 Time course assays

Cells were maintained as described above (see section 2.1) then 250,000 cells/well plated in 6 well plates. Cells were incubated overnight before treatments of VC

(ETOH), GW3965 (1 μ M), GSK2033 (1 μ M) and epirubicin (25 nM) were treated at various time points (0 h, 0.5 h, 1 h, 2 h, 4 h, 8 h, 16 h and 24 h).

3.4 RNA extraction and quantification

Promega Reliaprep RNA Cell Miniprep System was used for the RNA extraction (Promega, UK, Cat: #Z6012), and product guidelines were followed (TM370). Approximately 5×10^5 cells were harvested and cell pellets re-suspended in 250 μ L BL+TG buffer (Guanidine Thiocyanate + 1-Thioglycerol) and 85 μ L 100 % isopropanol to lyse cells. On column DNA digestion was performed with DNase 1 in Yellow Core Buffer, 0.09 M $MnCl_2$ at room temperature for 15 minutes. 30 μ L NFW was used to elute the RNA and was stored at -80 $^{\circ}C$.

RNA quantification was measured using the Tecan Spark 10M using NanoQuant plateTM with 1 μ L RNA. Blanking was completed before and between sample reads. Quantification was performed by assessing absorbance at A260 nm and quality assessed with A260/280 and A260/A230.

3.5 Reverse transcription

GoScriptTM Reverse Transcription kit (Promega, UK, Cat: A5003) was used for the cDNA synthesis, and product guidelines followed (TM316). 500 ng/reaction of RNA was used as template with 1 μ L random primers. Primers were annealed in a pre-heated block for 5 min at 70 $^{\circ}C$, then immediately placed on ice for 5 min. Mastermix was prepared (NFW, GoScriptTM 5X reaction buffer, $MgCl_2$ (5 mM), PCR Nucleotide mix (0.5 mM), and GoScriptTM Reverse Transcriptase (160u/ μ L) and 15 μ L was added to each sample tube. RT cycle followed in line with product manual. cDNA produced was then diluted 1 in 5 in NFW and stored at -20 $^{\circ}C$.

3.6 Gene expression analysis

3.6.1 Taqman

Taqman Fast Advanced Mastermix (Thermo Fisher, Paisley, UK, Cat: 4444557) was used with Taqman assays (Thermo Fisher, Paisley, UK, Cat: 4331182) on a QuantStudio Flex 7 (Applied Biosystems Life Tech, Thermo Scientific, UK) for gene expression experiments. Taqman assays and Mastermix were stored at -20 °C. Gene expression was analysed using the $\Delta\Delta\text{CT}$ method and normalised the housekeeping gene HPRT1.

Table 5 Taqman Assays.

The gene name for each primer are shown in the first and fourth column, with the company identification number in the second and fifth column. The third column is left blank for separation purposes.

Gene Name	Taqman ID		Gene Name	Taqman ID
HPRT1	Hs02800695_m1		LCP2	Hs01092638_m1
LXRα	Hs00172885_m1		TNFRSF1B	Hs00961750_m1
LXRβ	Hs01027215_g1		ABCB1	Hs00184500_m1
LCAT	Hs01068069_m1		ABCC1	Hs01561483_m1
NCOR1	Hs01094540_m1		ABCG2	Hs01053790_m1
NCOR2	Hs00196955_m1		SLC31A2	Hs00156984_m1
LCOR	Hs00287120_m1		CXCL5	Hs00171085_m1
ABCA1	Hs01059137_m1		BIRC3	Hs00985031_g1
APOE	Hs00171168_m1		GPSM3	HS00254433_m1
DOK2	Hs00929587_m1		SCD1	Hs01682761_m1

3.7 Colony forming assay

The method for cell culture was followed as described above (see section 2.1), and once cells were suspended to 1×10^6 cells/mL, 250 μL /well of cell suspension was

plated into a wells of a 6-well plate and topped up to 2 mL with DMEM-10 %. Cells were incubated overnight and then treated with T0901317 (2.5 μ M), GW3965 (1 μ M), GSK2033 (1 μ M), oxysterols (10 μ M) or vehicle control (VC) (ETOH/DMSO/NFE) and incubated for 24 h. Then epirubicin (25 nM) or VC (nuclease free water) was added for a further 24 h. Cells were then counted and 500 cells per treatment were plated in triplicate in 6 well plates (Nunc, Thermo Fisher, UK, Cat: 10119831). These were incubated for 12 days, until colonies were around 50 cells per colony. Colonies were washed with PBS and stained with a 0.1 % crystal violet staining solution was this in 50 % methanol, 30 % ethanol and 20 % ddH₂O (Sigma, UK, Cat: V5265-250 ML). Colonies were left to air dry overnight then manually counted. The raw data were normalised to the vehicle control samples and presented as mean \pm SD.

3.8 Chemotherapy efflux assay

This assay was designed to utilise the natural fluorescence of the chemotherapy drug epirubicin to measure the effect of LXR ligands on the chemotherapy drug export. Cells were plated (50,000 cells/well) in clear bottom black walled tissue culture 96 well plates (Greiner Bio-One, UK, Cat: 655986) using a p200 multichannel pipette and incubated for 8 h. Cells were pre-treated with either VC (ETOH) or LXR ligands (GSK2033, GW3965 at 1 μ M, 24OHC, 26OHC, SITO, STAN at 10 μ M) for 16 h before a high dose of chemotherapy agent (50 μ M epirubicin) for 1 h. Cells were gently washed with PBS taking care not to disrupt/detach cells and fresh PBS (100 μ L) was placed in the wells and fluorescence was measured using a basic plate reader at 485 nm excitation and 590 nm emissions. Cells were then placed in the incubator with fresh growth media in the wells and wash steps and fluorescence reads routinely measured over the course of 1.5-2 h. Fluorescence reads for treated cells were

normalised to VC cells. For pump inhibitor treatment, drugs were administered to the cells 30 min before epirubicin loading (verapamil - 20 μ M, MK571 – 50 μ M, and KO143 – 15 μ M).

3.9 siRNA knockdowns

Cells were plated in 6 well plates (250,000 cells/well) and incubated overnight. Lipofectamine RNAiMAX (Thermo Fisher, Cat: 13778030), siRNA (origene; catalogue numbers in Table 6) and the universal negative control siRNA (origene; Cat: SR30004) were diluted in OptiMeM (Thermo Fisher, Cat: 31985062) and added to the cells at the final concentration of 30 nM. The cells were incubated for 22 h and the media was changed for fresh DMEM. After 36 h of exposure to the siRNAs, RNA was extracted in BL+TG buffer as described above. RNA was quantified by assessing absorbance at A260 nm and quality assessed with A260/280 and A260/A230, followed by reverse transcription and qPCR analysis.

Table 6 siRNA catalogue numbers.

The gene name for the targeting siRNAs are shown in the first column, with the company identification number in the second column. Each siRNA is provided as three 3 unique siRNA duplexes. Each duplex is individually and collectively validated for silencing efficiency in each cell line.

Gene Name	siRNA ID
LCOR	SR313532
NCOR1	SR306392
NCOR2	SR306393
LXR α	SR322981
LCAT	SR320828

3.10 TCGA Dataset analysis

Genes of interest were analysed in the cBioportal database [229]. The TCGA Nature 2012 study [230] was selected from the section labelled breast, under the

subcategory Invasive Breast Carcinoma. Once selected, mRNA expression z-scores was highlighted and mutations and copy number deselected. Breast cancer subtype was chosen using the PAM50 classification (Basal, Claudin Low, Luminal A, Luminal B, Her2 enriched or Luminal A/B). Finally, the genes of interest were entered into the query box and submitted. Gene expression in the selected patient dataset was then downloaded in a tab delimited format and collected in excel. Data was then imported into graphpad prism and gene expression analysed between BCa subtypes. Statistical analysis was assessed using 2-tailed unpaired t-tests where significance is shown to be * $p < 0.05$, ** $p < 0.01$, *** $p < 0.001$, **** $p < 0.0001$.

3.11 Volcano plots

3.11.1 LXR α target gene plot

Top 100 scoring genes in LXR α -ChIP-Seq datasets sourced from Cistrome.org [231] were downloaded from 7 available datasets in various cell types (macrophages, adipocytes and colorectal cancer cells). Genes that were common in two or more datasets were selected for further analysis (148 genes). The selected genes were then assessed for expression in cBioportal [229] as described in the TGCA method. Not all genes were expressed in the patient dataset (26 genes) and 11 genes were species specific genes with no human equivalent available. An additional 24 genes that are established LXR targets that did not necessarily reach the cut-off scores were added. The final list of 135 genes (**Appendix 1 – A.1**) were assessed for expression in the TGCA dataset [230] of human breast cancers in the PAM50 subtypes. Gene RNA-Seq mRNA expression (log transformed relative to array median) was then correlated with NR1H3/LXR α and NR1H2/LXR β expression. R values (X axis) and P values were plotted in an XY scatter graph to generate the volcano plots. A False Discovery Rate

(FDR) of 1 % was applied followed by a Fisher's exact test used to establish if the number of genes correlating with NR1H3 was significantly different between the two subtypes. Summary of the target gene selection process is shown in **Figure 3.2**.

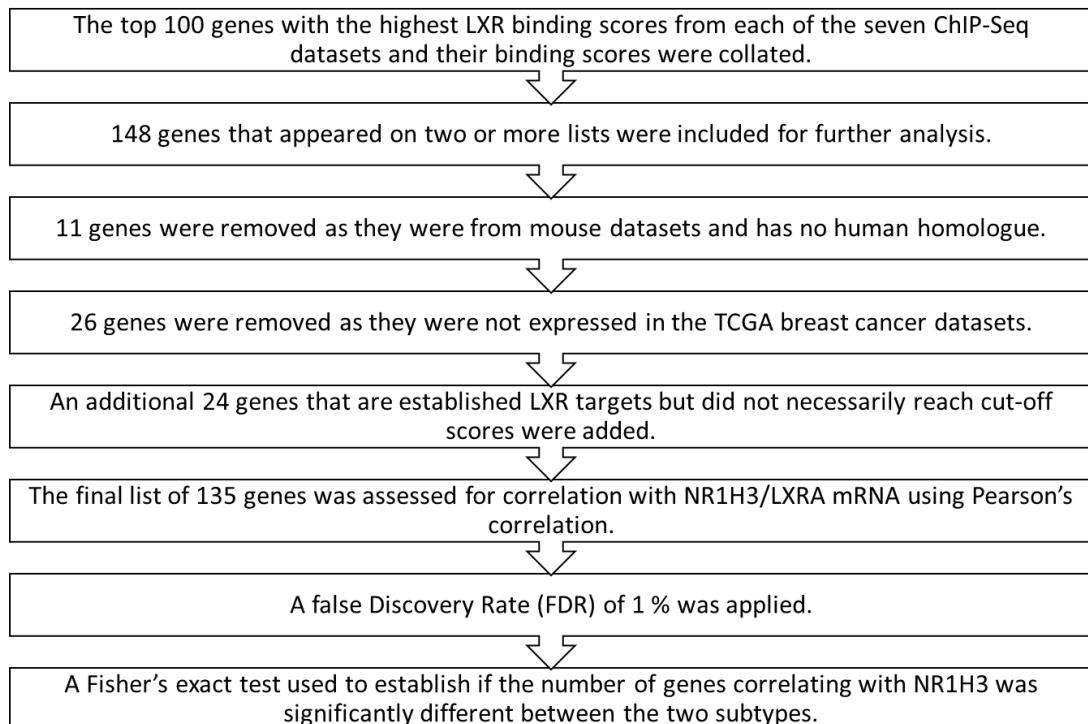


Figure 3. 2 LXR α target gene selection.

Flow diagram describing the gene selection process for the LXR α target gene plot. Exclusion criteria are included and statistical analysis outline.

3.11.2 Systematic literature search for chemotherapy resistance genes

Chemoresistance gene plot

A list of genes implicated in chemotherapy resistance was generated using a literature search. Terms searched were “chemotherapy” and “resistance” and combined into one table of associated chemotherapy genes (see **Appendix A - A.2**). If gene duplicates occurred from different sources multiple references were included in the table, likewise if multiple types of resistance were identified these were incorporated into the table. The literature search was completed in March 2019, the selection process is summarised in **Figure 3.3**.

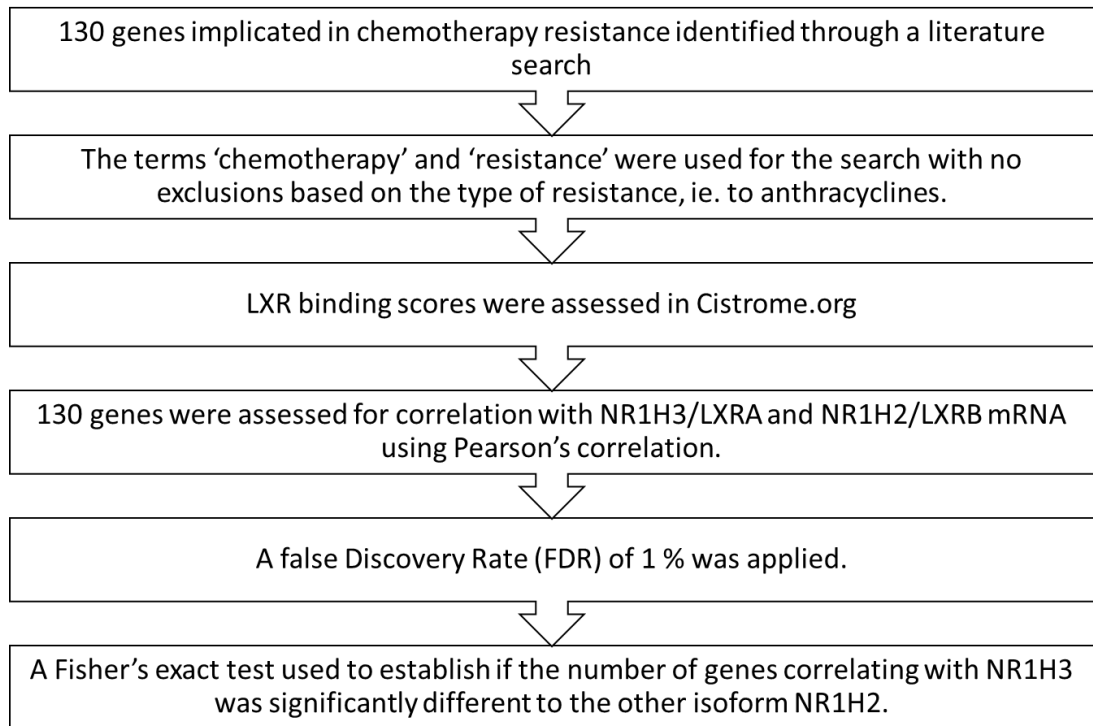


Figure 3. 3 Chemotherapy resistance gene selection.

Flow diagram describing the gene selection process for the chemotherapy resistance gene plot. Exclusion criteria are included and statistical analysis outline.

3.11.3 Evaluation of LXR α binding

Genes identified for the literature search were then assessed in Cistrome.org [231] for LXR α occupancy in their promoter regions, and genes associated with a binding score were assessed for expression in patient tumours in the TGCA dataset [230], however, not all genes were expressed in the patient dataset. The remaining genes were assessed for expression in human breast cancers of the PAM50 subtypes.

Gene expression was then tested for correlation (Pearson's correlation) against NR1H3/LXR α and NR1H2/ LXR β expression. R values (X axis) and P values were plotted in an XY scatter graph to generate the volcano plots. A False Discovery Rate (FDR) of 1 % was applied followed by a Fisher's exact test used to establish if the

number of genes correlating with LXR α was significantly different to the other isoform LXR β .

3.12 Primary breast tumour analysis

69 BCa tumours (41 TNBC, 11 Luminal A, 1 Luminal B, 16 HER2 enriched) were obtained from the Leeds Breast Tissue Bank (LBTB) through two separate ethics applications 09H1326/108 (pilot study with 11 Luminal A and 11 TNBC tumours) and 15/HY/0025 (validation study with 30 TNBC, 16 HER2-positive 1 Luminal B tumours). The total, esterified and free oxysterol concentrations were measured by Dr Hanne Roberg-Larsen (Oslo, Department of Chemistry) using LCMS/MS. Patient tumour characteristics are shown in **Table 7 (09H1326/108) and 8 (15/HY/0025)**.

3.12.1 Tumour characteristics

Table 7 Patient tumour characteristics.

Tumour tissue was obtained from the Leeds Breast Research Tissue Bank at Leeds Teaching Hospital Trust. *denotes tumour size not available for one patient. 22 tumours.

Characteristic	Categories	No. of patients (%) n=22
Subtype Classification	TNBC	9 (40.9)
	Luminal A	11 (50)
	Luminal B	1 (4.55)
	HER2 enriched	1 (4.55)
ER Status	Negative	11 (50)
	Positive	11 (50)
PR Status	Negative	13 (59.1)
	Positive	9 (40.9)
HER2 Status	Negative	20 (90.9)
	Positive	2 (9.1)
Invasive Tumour Grade	1	2 (9.1)
	2	8 (36.4)
	3	12 (54.5)
Invasive Tumour Size*	</= 35mm	14 (63.6)
	>35mm	7 (31.8)
Survival Status	Alive	19 (86.4)
	Deceased	3 (13.6)
Recurrence/Metastasis	None	13 (59.1)
	Local and/or Distal	9 (40.9)

Table 8 Patient tumour characteristics.

Tumour tissue was obtained from the Leeds Breast Research Tissue Bank at Leeds Teaching Hospital Trust. *denotes tumour size not available for one patient. 69 tumours in total.

Characteristic	Categories	No. of patient (%) n= 69
Subtype Classification	TNBC	41 (59.45)
	Luminal A	11 (15.9)
	Luminal B	1 (1.45)
	HER2 enriched	16 (23.2)
ER Status	Negative	58 (84.1)
	Positive	11 (15.9)
PR Status	Negative	60 (86.96)
	Positive	9 (13)
HER2 Status	Negative	52 (75.4)
	Positive	17 (24.6)
Invasive Tumour Grade	1	3 (4.3)
	2	17 (24.6)
	3	49 (71)
Invasive Tumour Size*	</= 35 mm	46 (66.7)
	>35 mm	22 (31.9)
Survival Status	Alive	45 (65.2)
	Deceased	24 (34.8)
Recurrence/Metastasis	None	37 (53.6)
	Local and/or Distal	32 (46.4)

3.12.2 LCMS

The method for LCMS has been previously published [130].

3.12.2.1 Derivatisation with Girard T reagent

Methods for derivatisation with Girard T reagent has previously been described [232] with alterations as described [233]. Analytes were charge tagged following the process outlined and cholesterol oxidase (0.03 mg/mL) from *Streptomyces* sp. (Sigma-Aldrich) was aliquoted in 200 μ L volumes in 50 mM PBS (pH 7.0) and added. The solutions were heated at 37 $^{\circ}$ C for 1 h. Girard T reagent (15 mg – Sigma Aldrich), 15 μ L glacial acetic acid (VWR) and 500 μ L MeOH were added to each sample/standard solution. Samples were kept at room temperature in a dark room overnight. All solutions were kept at 4 $^{\circ}$ C after derivatisation.

3.12.2.2 Breast cancer tumour samples

Breast cancer samples were obtained as mentioned in section 3.12. Each tumour had three consecutive 5 mg slices taken, homogenised in 500 μ L 1.5 nM internal standard mixture solution and 30 μ L autoxidation monitoring solution (6 μ L cholesterol-25,26,27- 13 C, Sigma Aldrich) using an IKA T10 Ultra-Turrax homogeniser. To analyse the free oxysterols within tumour samples, 100 μ L of the sample solution was mixed with 100 μ L isopropanol and placed in an Oasis PRiME HLB 1 cc (30 mg) SPE cartridge (Waters), and the oxysterols were eluted with 200 μ L MeOH. Using an Eppendorf concentrator plus (Hamburg, Germany), solvents were evaporated and the residues reconstituted in 20 μ L of isopropanol. This was followed by derivatisation as detailed above. To measure the total (free and esterified) oxysterol content in tumour samples, alkaline hydrolysis was performed by adding 100 μ L sample solution to 35 μ L 2M KOH (Sigma Aldrich) in MeOH. The sample solution was then heated for 120 min at 60 $^{\circ}$ C then followed by liquid-liquid extraction with n-hexane. 150 μ L of type 1 water was added to the sample followed by n-hexane (150 μ L - VWR) to achieve phase separation. Tumour samples were mixed by vortex for 1 min before centrifugation for 2.5 min at 3000 rpm. The hexane layer was removed and the liquid-liquid extraction repeated twice with 150 μ L n-hexane (combining all the hexane phases at the end). Using an Eppendorf concentrator plus solvents were evaporated and the residues reconstituted in 200 μ L of isopropanol. Sample solution was placed in an Oasis PRiME HLB 1 cc (30 mg) SPE cartridge (Waters), and eluted with 200 μ L MeOH. Using an Eppendorf concentrator plus solvents were evaporated and the residues reconstituted in 20 μ L of isopropanol and followed by derivatisation as detailed above.

3.12.2.3 Chromatographic system

A Dionex UltiMate 3000 UHPLC system was connected to a TSQ Vantage triple quadrupole mass spectrometer (Thermo Fisher Scientific, Waltman, MS, USA) operated in selected reaction mode (SRM). Injection volume was 0.7 μL for column evaluation which was increased to 60 μL when the AFFLSPE-LC system was used. All connections were Thermo Scientific Vipers™ stainless steel fingertight fittings with 180 μm inner diameter (ID). Columns investigated were; ACE SuperC18 core-shell (2.1 mm ID \times 150mm d_p 2.5 μm , core-shell), ACE SuperPhenyl Hexyl (2.1 mm ID \times 150 mm, d_p 2.5 μm , core-shell) (both from Advanced chromatography technologies LTD, Aberdeen, UK), Thermo Scientific HyperSil GOLD C18 (1mm ID \times 50mm, d_p 1.9 μm), Waters Torus 2-PIC (2-picolylamine, 2.1 mm ID \times 100mm, d_p 1.7 μm) and Waters Torus 1-AA (1-aminoanthracene, 2.1 mm ID \times 100mm, d_p 1.7 μm). Also investigated were the in-house packed 0.1 mm ID \times 100 mm columns, using the ACE SuperPhenyl Hexyl particles.

3.12.2.4 Automatic filtration and filter back flush solid phase extraction

A 10 port valve (Waters CapLC selector valve) with a 1 μm in-line filter and a non-line HotSEP C18 SPE column (Teknolab, Ski, Norway) was linked up. Loading mobile phase was 0.1% FA in type 1 water which was delivered by a HitachiL-7110 pump (Merck) with a standard flow rate of 500 $\mu\text{L}/\text{min}$. In position 1, solutions and samples were injected and filtered. Derivatized oxysterols were retained on the SPE column, while surplus derivatization reagent was washed to waste. In position 2, the derivatized analytes were eluted off the SPE column and subsequently separated on an ACE SuperPhenyl Hexyl column (2.1 mm ID \times 100 mm, core-shell) by a Dionex Ultimate 3000 UHPLC pump with a standard flow rate of 650 $\mu\text{L}/\text{min}$. Mobile phase A was

0.1% FA in type 1 water, B was 0.1 % FA in MeOH and C was 0.1 % FA in ACN. Isocratic elution conditions were 57/ 10/33 (v/v/v,A/B/C) for 4.3 min, followed by a 2 min washing step (50/50, v/v, B/C).Including on-line sample clean-up and conditioning of the column, total method run time was 8 min.

3.12.3 Tissue RNA extraction

Three 5 mg slices per tumour were taken from different areas of the breast tissue added to sterile Eppendorf tubes. RNA was extracted following the guidelines issued with the Promega ReliaPrep RNA Tissue Miniprep System. In short, tumour tissue was homogenised in LBA + TG buffer (1-Thioglycerol) to inactivate the ribonucleases present in tissue and pipetted up and down 10 times to shear the DNA. Isopropanol was added and the sample vortexed before transfer to labelled minicolumns. RNA was then bound to the minicolumns by centrifugation at 12,000 x g for 1 min at 21 °C. RNA was washed with RNA wash solution and centrifuged again at 12,000 x g for 30 seconds at 21 °C. RNase-free DNase I enzyme was applied directly to the membrane in a mastermix containing 0.9 M MnCl₂ and yellow core buffer for 15 min at room temperature to digest contaminating genomic DNA. Post-incubation the minicolumns is washed with column wash solution and centrifuged at 12,000 x g for 15 seconds at 21 °C. The bound total RNA is further purified from contaminating salts, cellular components and proteins by washing with RNA wash solution and centrifuged at 12,000 x g for 30 seconds at 21 °C, then again at 12,000 x g for 2 min at 21 °C. To finish, the total RNA is eluted from the membrane by adding nuclease-free water (NFW) and centrifuging one last time at 7000 x g for 1 min at 21 °C. RNA was then stored at 80 °C.

3.12.4 Reverse transcription and qPCR

Tumour cDNA libraries (250 ng each) were generated using the same reagents and procedure used in section 3.5. Gene expression of HPRT1, LXR α , LXR β , ABCA1, ABCB1, LCAT, NCOR1, NCOR2 and LCOR was assessed using Taqman assays as described in section 3.6, in a 384 well plate. Mastermix volume (2.5 μ L) and cDNA volume (2.5 μ L) per reaction totalled 5 μ L per well.

3.12.5 Correlations with LXR expression

The average $\Delta\Delta$ Ct value for the triplicate sections of each tumour were generated for each gene analysed. The average Ct score for ABCA1, ABCB1 and LCAT for each tumour were then correlated with the average Ct score for LXR α and LXR β for each tumour.

3.13 *in vivo* Mouse study

The *in vivo* mouse study was designed to support the colony forming assay data. Dr Erik Nelson (Illinois, Chicago) agreed to collaborate on the work. Treatment plans were designed by the author with guidance from Dr Nelson. All experimental work was completed in Chicago by Dr Nelson's group. All procedures involving animals were approved by the University of Illinois IACUC. Mice were housed in standard IVC cages at up to 5/cage, with standard enrichment. They were provided acidified water and irradiated chow, ad libitum. Mice were 11 weeks old at the start of the study with 10 mice per treatment group. Mice were humanely euthanized by CO₂ followed by a secondary method of either bilateral thoracotomy or decapitation. These methods are consistent with the Panel on Euthanasia of the American Veterinary Medical Association.

3.13.1 Treatment Plan

4T1 cells (ER-negative) were grafted orthotopically into the axial mammary fat pad of BALB/C mice. Mice were treated with either placebo or the LXR ligand GW3965 (daily, 30 mg/kg) 24 h post-graft. Treatments with placebo or epirubicin (every other day, 2.5 mg/kg) commenced 48 h post-graft. Tumour volumes were measured by direct calliper, and plasma, liver and tumour were harvested after 12 days.

3.13.4 Tumour analysis

Mouse tumours were manually homogenised and lysed in TRIzol (Thermo Fisher Scientific) to extract RNA. Once RNA was isolated from tumour tissue cDNA libraries were generated from equal total RNA mass with iScript reverse transcriptase supermix (Bio-Rad). cDNA libraries were then analysed by qPCR with iTaq universal SYBR Green supermix (Bio-Rad) on a CFX384 touch real-time PCR detection system (Bio-Rad). Relative expression of ABCA1, ABCB1, ABCG2, and CXCL5 was determined using the $\Delta\Delta C_t$ method and normalised to the housekeeping gene TBP. Statistical analysis was assessed using 1 Way ANOVA with SNK test.

3.14 MTT assay

TNBC cells (MDA-MB-468 and MDA-MB-231) and Luminal A cells (MCF-7) were seeded in 96 well plates at 2.5×10^4 cells/well. Cells were incubated for 16 h before vehicle (ethanol) or a panel of PSSs were added for 48 h. PSS treatments were in the range of 1 pM to 100 μ M. After 48 h of exposure, media was removed and cells were washed with PBS. Phenol red free DMEM with 10 % FCS was added to each well with MTT reagent at the final concentration of 0.5 mg/mL. Cell were incubated for 4 h at 37 °C before media was removed and replaced with 100 μ L of DMSO/well. Absorbance was read at 540 nm using a CLARIOstar.

Chapter 4

LXR α activity and function is enhanced in triple negative breast cancer relative to Luminal A BCa

4.1 Introduction

Data presented in this chapter have in part been published in a peer-reviewed article [234]. Journal article included in **Appendix B - 1.1**.

Cholesterol is mostly synthesized de novo in the liver, with lesser contributions from diet combining to ensure circulating cholesterol levels are constant. Balanced cholesterol levels are important to ensure extra-hepatic tissues have enough cholesterol to produce a range of metabolites such as bile acids, seco-steroids and steroid hormones [235]. Cholesterol is hydroxylated by members of the cytochrome P450 family (CYPs) producing cholesterol metabolites known as oxysterols [236]. LXR α and LXR β are NRs that bind and respond to oxysterols regulating the expression of genes involved in cholesterol storage, efflux and metabolism. Type 1 NRs such as the ER, AR or the glucocorticoid receptor (GR) bind to ligand in the cytosol, form heterodimers or homodimers and translocate from the cytoplasm into the nucleus to bind to DNA HREs [237-239]. Type 2 NRs such as LXR and RXR remain in the nucleus even in the absence of ligand, binding as heterodimers to DNA [240]. LXR α expression is inducible in the liver, intestine, adipocytes and macrophages, whereas LXR β is expressed ubiquitously. As well as differences in the expression of LXRs, oxysterol concentrations are also diverse between tissues, and relative to each other, with some as high as 1000-fold difference between two oxysterols [204]. Variations in receptor expression and oxysterol concentrations within tissue can also depend on disease status [110]. Oxysterols also have different capabilities in LXR

activation and driving LXR-mediated transcription of target genes, suggesting an element of selective modulation in oxysterol-LXR signaling. An example of this is the oxysterol 26OHC which is the most abundant oxysterol in human tissue but appears to be a fairly weak LXR agonist [69, 241].

The capacity for type 2 nuclear receptors to regulate their target genes is dependent on nuclear localization and genome binding, co-activator and co-repressor expression, ligand bioavailability and expression levels of the receptors themselves. For instance, the expression of co-repressors such as NCOR1 and NCOR2/SMRT dictate how multiple cancers respond to nutritive ligands [94, 95, 242] as discussed in section 1.2.2. LXR β binding affinity for the corepressors NCOR1 and NCOR2 is 100-fold less than LXR α [243]. Furthermore, deregulation of the corepressors NCOR1 and NCOR2/SMRT has been shown to impair sensitivity to ligand in bladder [242] and prostate cancer cells [68, 94] and enhanced coactivator expression has been shown to facilitate growth of malignancies in the breast [244], prostate [245, 246] and pancreas [247]. Assessing the activation potential of oxysterols at different concentrations is required as simply measuring the oxysterol concentrations cannot determine their level of involvement in LXR signaling.

Ligand bioavailability is important for nuclear receptor target gene regulation as type 2 NRs like LXR α and RXR β are poor activators of transcription in the absence of ligand. LXR ligands are typically formed through hydroxylation of cholesterol by cytochrome P450 family members. However, Cytochrome P450 family members are not uniformly expressed in all tissues and may be expressed in specific organs/tissues. CYP46A1, CH25H and CYP27A1 are the enzymes responsible for the conversion of cholesterol to 24OHC, 25OHC and 26OHC respectively and although

they have been detected in many tissues, they are highly expressed in the brain and liver [101]. Interestingly, CYP27A1 was found to be expressed in advanced breast tumour cells and tumour-associated macrophages [105], suggesting support cells in the TME may be enhancing ligand bioavailability in cancer.

Even in the presence of ligands, receptors may not be able to regulate transcription. Other factors such as ligand esterification [101] are involved in nuclear receptor interactions. The expression of enzymes that result in ligand sulfation (SULT2B1) [248] and further modification (CYP7B1) [105] inhibit ligand activation of nuclear receptors and reduce the expression of canonical target genes of LXR. In cancer biology the expression of these enzymes can be altered or skewed to have selective advantages for cancer progression. Identifying altered expression of enzymes involved in oxysterol conversion, esterification and further modification in different subtypes of BCa may help with the understanding of why two alike cancers can have two different responses to treatment.

The function of the oxysterol-LXR axis in cancer seems to be tissue specific as both tumour promoting and tumour suppressive roles have been identified. Oxysterol-LXR signalling is anti-proliferative in lung cancer [249] as it is in almost every cancer cell line studied [68], and impairs angiogenesis and invasion in melanoma [250]. In breast cancer however, 26OHC promotes the growth of ER-positive BCa *in vivo* via the ER [105, 110] and drives the EMT in ER-negative BCa [105]. Furthermore, 26OHC mobilises $\gamma\delta$ -T cells to promote colonisation of ER-negative metastatic tumours [21]. In addition, circulating levels of 25OHC was found to be elevated in patients who had relapsed relative to those with the primary disease [136], and the concentrations of multiple oxysterols are altered in breast cancer tissue relative to healthy tissue [110].

Systematic assessment of oxysterol bioavailability and activation potential when coupled with NR cofactor expression analysis in BCa subtypes is a novel concept that has not been published to date. Given the therapeutic and prognostic value of stratifying breast cancers by hormone receptor status, further definition of the pathways that are altered between subtypes, such as oxysterol-LXR signalling, may provide insight into the evolving roles of cholesterol metabolism in cancer and have the potential to improve patient outcomes.

4.2 Hypothesis and Aims

Dietary and pharmacological interventions that lower cholesterol in humans show the prognosis and incidence of ER-negative breast tumours is improved preferentially in ER-negative tumour subtypes rather than ER-positive ones. Given that cholesterol metabolism into oxysterols produces ligands for LXR in both ER-positive and ER-negative tumours, it is possible that the anti-tumour effect of these cholesterol lowering interventions may be due to differential activation of LXR α between the subtypes.

The hypothesis that is tested in this chapter is that the oxysterol-LXR α signalling pathway is differentially activated between subtypes at the level of ligand synthesis, or receptor and/or co-factor expression.

The aims of this chapter were to:

- Test whether the concentration of side-chain hydroxycholesterols, expression of LXR α , and/or that of its regulatory co-factors, is different between ER-negative and ER-positive breast tumours
- Determine whether LXR α dependent transcription is different between ER-negative and ER-positive breast cancer.
- Establish if LXR α transcriptional activity within breast tumours is associated with patient relapse.

4.3 Results

4.3.1 Expression of LXR α and its regulatory factors, but not ligand concentration, is different between breast cancer subtypes

To determine if there was potential for LXR α activity to be altered between ER dependent breast cancer subtypes distinct approaches were taken. First, publicly available breast cancer RNA-Seq datasets were mined for gene expression data related to differential expression of cholesterol biosynthesis enzymes, cofactor expression and receptor expression. These data were then assessed for patterns consistent with LXR pathway activation or repression. Secondly, primary BCa tumours were acquired from the Leeds Breast Research Tissue Bank and assessed for expression of the same gene expression panel using qPCR. Thirdly, the tissue bank tumours were assessed for oxysterol concentration using LCMS-MS. Fourthly, the LXR α expression and corepressor expression was assessed in ER-negative and ER-positive BCa cell lines to identify representative cell lines for further analysis.

4.3.1.1 LXR α expression is enhanced in triple negative breast cancer relative to Luminal A breast cancer

First, to assess the expression of LXR α in TNBC disease compared to the Luminal A subtype, public data were downloaded from CBioportal [229], TCGA dataset [230] (see methods section 3.10). The RNA-Seq mRNA relative expression of the estrogen receptor (ESR1), progesterone receptor (PGR), LXR α , LXR β and their binding partners the RXRs (RXR α , RXR β and RXR γ) were assessed. The RXRs were included in the analysis as both LXR α and LXR β regulate target genes by forming permissive heterodimers with RXRs [69]. As a control, the median expression of the ESR1 and the PGR were analysed and found to be significantly lower in the TNBC tumours relative to the Luminal A tumour (two-tailed Mann-Whitney U test: ESR1 $p < 0.001$; PGR $p < 0.001$ [Figure 4.1A]) as was expected. Median expression of LXR α ($p < 0.01$) and its binding partner RXR β ($p < 0.05$) were found to be significantly higher in the TNBC tumours relative to the Luminal A tumours (**Figure 4.1A**). LXR β was found to be uniformly expressed across the TNBC and Luminal A subtypes (ns) as was RXR γ (ns). And finally, RXR α was found to be expressed at significantly lower levels in the TNBCs tumours relative to the Luminal A tumours (ns).

To assess if the BCa cell lines (MCF-7, MDA-MB-468 and MDA-MB-231) recapitulated primary TNBC and Luminal A BCa features observed in Figure 4.1A, LXR α and LXR β expression was measured in the BCa cell lines (**Figure 4.1B**). In the TNBC cell line MDA-MB-468, LXR α was expressed at significantly higher levels relative to the Luminal A cell line MCF-7 (1-tailed unpaired t tests; $p < 0.001$) and LXR β was uniformly expressed across all three BCa cell lines (ns). In summary these data show, TNBCs display enhanced LXR α expression and similar LXR β expression levels in primary breast tumours and cells.

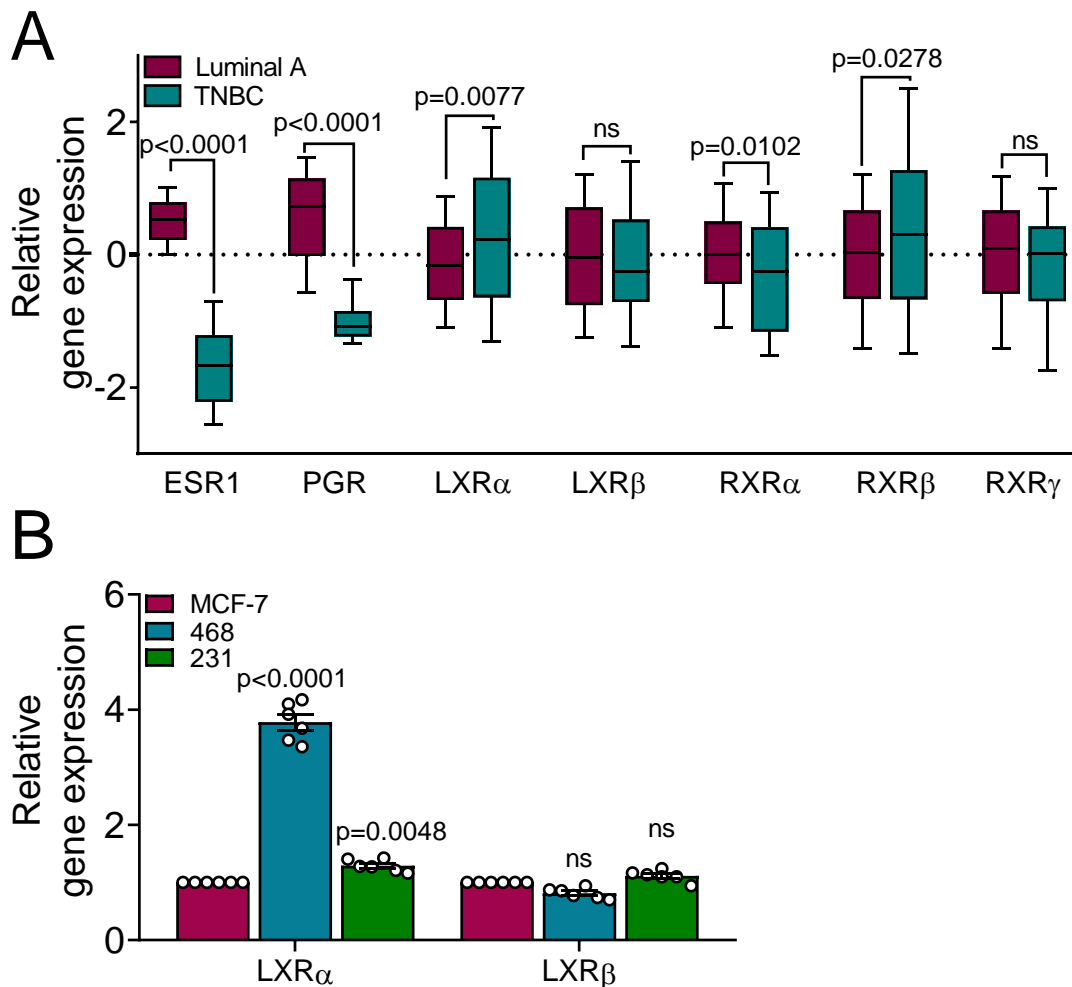


Figure 4.1 Expression of the nuclear receptor LXR α is higher in TNBC compared to Luminal A BCa.

mRNA-Seq data (log transformed relative to array median with 10-90th centiles) for 89 TNBC and 235 Luminal A tumours were obtained [230] for receptor expression analysis from CBioportal (TCGA) [229] (A). Receptor expression is presented as box and whisker plots with median, inter-quartile and 10-90 percentiles shown. Statistical analysis was established using Mann-Whitney U tests. RNA was harvested from TNBC (MDA-MB-468 and MDA-MB-231) and Luminal A/ER-positive (MCF-7) cells and expression of the nuclear receptors LXR α and LXR β was assessed by qPCR (TNBC Δ Ct normalised to MCF-7) (B). Data shown are mean of six independent replicates with SD, statistical analysis was established using two-tailed student t-tests (B).

4.3.1.2 The expression of cholesterol biosynthesis enzymes and genes that metabolise and catabolise LXR ligands are altered in triple negative breast cancers and Luminal A breast cancers.

Next, the expression of genes involved in; the conversion of cholesterol into oxysterols, the esterification of oxysterols and the further modification of oxysterols were assessed in the same dataset used in **Figure 4.1** [230] from cBioportal [229].

First, the expression of genes involved in the conversion of cholesterol to oxysterols

were assessed in the primary tumour datasets (**Figure 4.2A**). CYP27A1, CH25H, CYP46A1 and CYP11A1 are the enzymes responsible for the conversion of cholesterol to 26OHC, 25OHC, 24OHC and 22OHC respectively and in the TNBC and Luminal A tumours, similar expression levels of CYP46A1 (two-tailed Mann-Whitney U test, ns) and CYP11A1 (ns) was observed. CH25H expression however, was lower in the TNBC relative to the Luminal A BCa ($p=0.0002$), and expression of CYP27A1 was enhanced in the TNBC relative to the Luminal A BCa ($p<0.0001$).

LCAT and SOAT1 are enzymes involved in the esterification of oxysterols and their expression in primary tumours were assessed (**Figure 4.2B and Figure 4.2C**). In TNBC primary tumours, expression of LCAT and SOAT1 were found to be elevated compared to Luminal A expression ($p<0.0001$, both genes), whilst expression of the sulphonation enzyme SULT2B1 which modifies the head of the oxysterol structure rendering the ligand incompetent as an LXR ligand, was significantly lower in the TNBC tumours relative to the Luminal A tumours ($p<0.0001$). Additionally, the expression of CYP7B1 was enhanced in the TNBC tumours relative to the Luminal A tumours ($p<0.0001$). These data suggest Luminal A tumours preferentially further modify ligands by sulphonation which could result in fewer ligand-LXR interactions and therefore lower LXR activity.

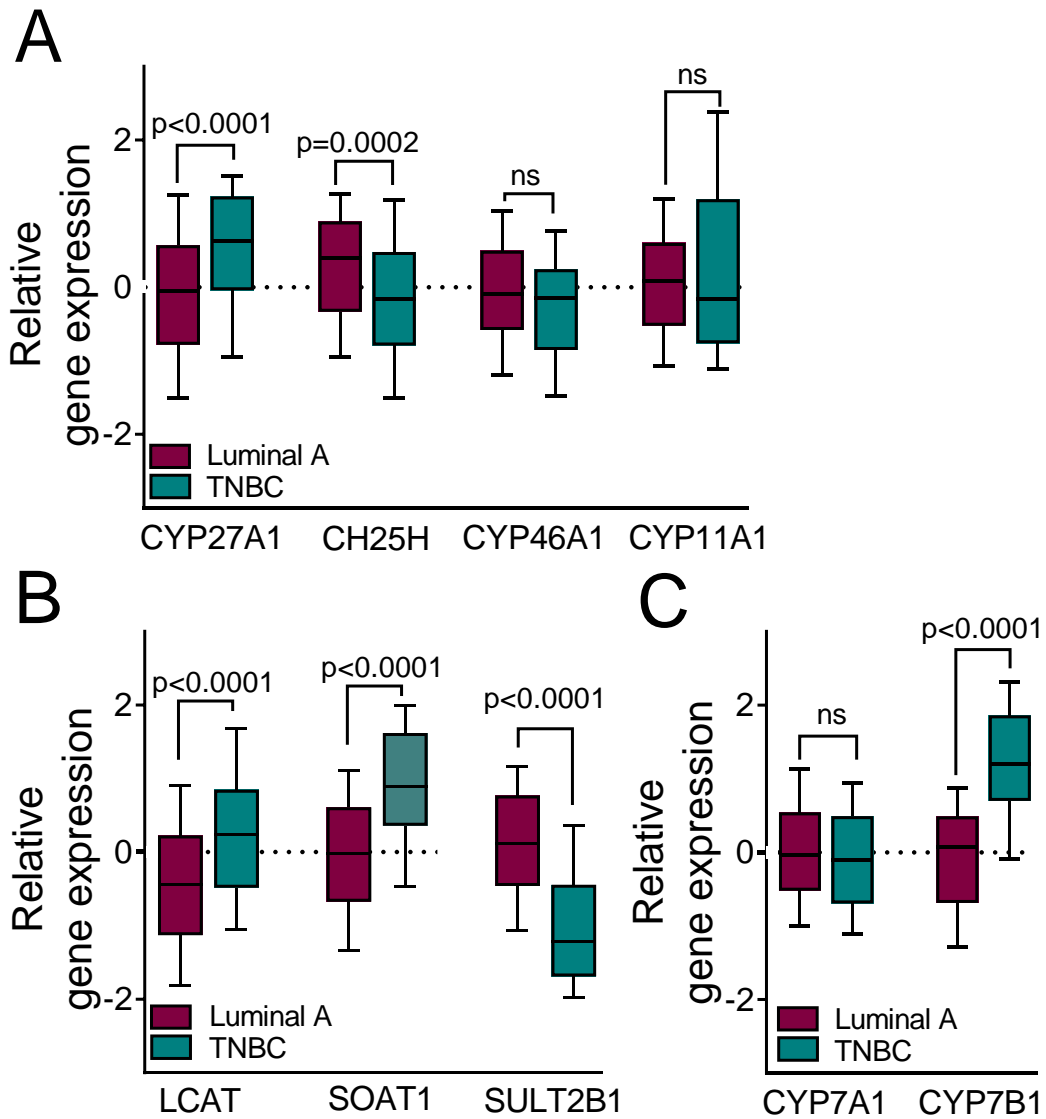


Figure 4.2 The enzymes involved in cholesterol conversion to oxysterols, oxysterol esterification and oxysterol further modification are differentially expressed in TNBC and Luminal A BCa.

mRNA-Seq data (log transformed relative to array median with 10-90th centiles) for 89 TNBC and 235 Luminal A tumours were obtained [14] from CBioportal (TCGA) [13] for expression analysis of the enzymes responsible for cholesterol synthesis, esterification and further modification. Expression is presented as box and whisker plots with median, inter-quartile and 10-90 percentiles shown. Statistical analysis was established using Mann-Whitney U tests.

4.3.1.3 Oxysterol concentration is similar in triple negative breast cancers and Luminal A tumours.

To assess if ligand abundance was different between BCa subtypes we obtained 69 BCa tumours (41 TNBC, 11 Luminal A, 1 Luminal B, 16 HER2 enriched) from the Leeds

Breast Tissue Bank (LBTB) through two separate ethics applications 09H1326/108 (pilot study with 11 Luminal A and 11 TNBC tumours) and 15/HY/0025 (validation study with 30 TNBC, 16 HER2-positive and 1 Luminal B tumours). The total, esterified and free oxysterol concentrations were measured by Dr Hanne Roberg-Larsen (Oslo, Department of Chemistry) using LCMS/MS. Patient tumour characteristics are shown in **Table 7** (09H1326/108) and **8** (15/HY/0025). Total, esterified and free concentrations of 22OHC, 24OHC, 25OHC and 26OHC were measured by LCMS/MS in 22 BCa tumour samples (in triplicate sections) (**Figure 4.3**).

First, 22OHC was undetected in all 3 sections of the 22 BCa tumour samples. Out of the remaining 3 oxysterols measured, 26OHC was the most abundant oxysterol in the TNBC breast tumours (range: 74-3732 ng/mg, mean 908.5 ng/mg) and Luminal A breast tumours (range: 57-2696 ng/mg, mean 438.9 ng/mg). 25OHC was found to be the lowest abundant oxysterol measurable above the Limit of Detection (LOD) and Quantification (LOQ) in both the TNBC tumours (range: 18-262 ng/mg, mean 76.9 ng/mg) and Luminal A tumours (range: 10-780 ng/mg, mean 88.9 ng/mg). 24OHC was found at slightly higher concentrations in the TNBC tumours (range: 34-709 ng/mg, mean 229.7 ng/mg) and Luminal A tumours (range: 26-845 ng/mg, mean 165.1 ng/mg). Analysis of three sections (5 mg each) per tumour showed large intra-tumour variability in oxysterol concentrations (RSD >20). No significant differences were observed in the total, esterified or free oxysterol concentrations between the TNBC and Luminal A tumours (Mann-Whitney U test; ns) (**Figure 4.3**).

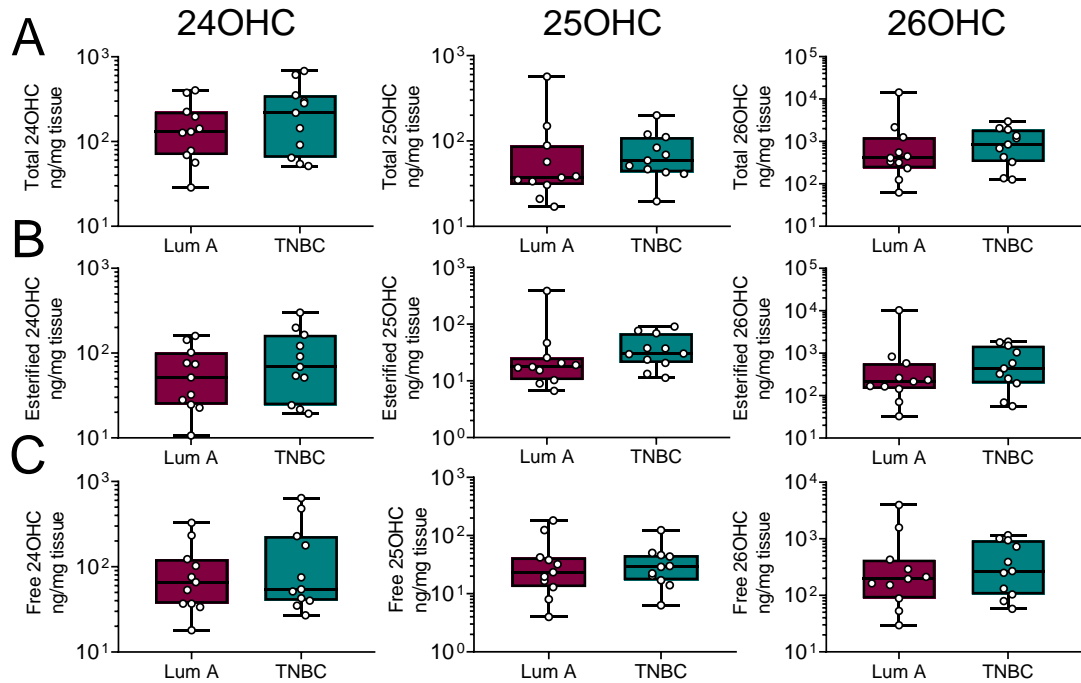


Figure 4.3 Total, esterified and free oxysterol concentrations in TNBC and Luminal A BCa.

The concentrations of total (A), esterified (B) and free (C) oxysterols were measured in Luminal A (purple boxes; n=11) and TNBC (green boxes; n=11) tumours. No statistically significant differences in mean concentrations between ER-subtypes was found (Mann-Whitney U Test). Patient characteristics shown in Table 7 – see methods section 3.12.1.

4.3.1.4 The ratio of esterified to free/total oxysterol concentrations appears to have a relationship in triple negative breast cancers and Luminal A tumours.

To assess if there is a relationship between the amount of esterified to free oxysterols or total to esterified oxysterols in patient breast tumours, correlation analyses were performed. The concentrations of esterified and free 24OHC did not significantly correlate in TNBC or the Non-TNBC tumours (Pearson correlation; ns) (**Figure 4.4A**). Next the correlation of esterified and free 25OHC correlated in the Non-TNBC tumours ($p < 0.01$; $R^2 = 0.82$) but not in the TNBC (ns) (**Figure 4.4A**). And finally, the concentration of esterified and free 26OHC correlated in the Non-TNBC tumours ($p < 0.0001$; $R^2 = 0.89$) and in the TNBC tumours ($p < 0.05$; $R^2 = 0.61$) (**Figure 4.4A**). The concentrations of total to esterified 24OHC however, significantly

correlated in TNBC and the Non-TNBC tumours (TNBC $p=0.0289$; $R^2=0.34$, Non-TNBC $p=0.0086$; $R^2=0.49$) (**Figure 4.4B**). The correlation of total and esterified 25OHC correlated in the Non-TNBC tumours ($p<0.0001$; $R^2=0.96$) but not in the TNBC (ns) (**Figure 4.4B**). And finally, the concentration of total and esterified 26OHC correlated in the Non-TNBC tumours ($p<0.0001$; $R^2=0.89$) and in the TNBC tumours ($p=0.0051$; $R^2=0.54$) (**Figure 4.4B**). Data from the correlation analyses suggested that the ratio of esterified oxysterols (either to free or total) appeared to be important in defining differences between the two subtypes, however large inter-tumour variations were observed and as such further analysis in a larger cohort was required to determine the relationship between esterified oxysterol ratios within tumours.

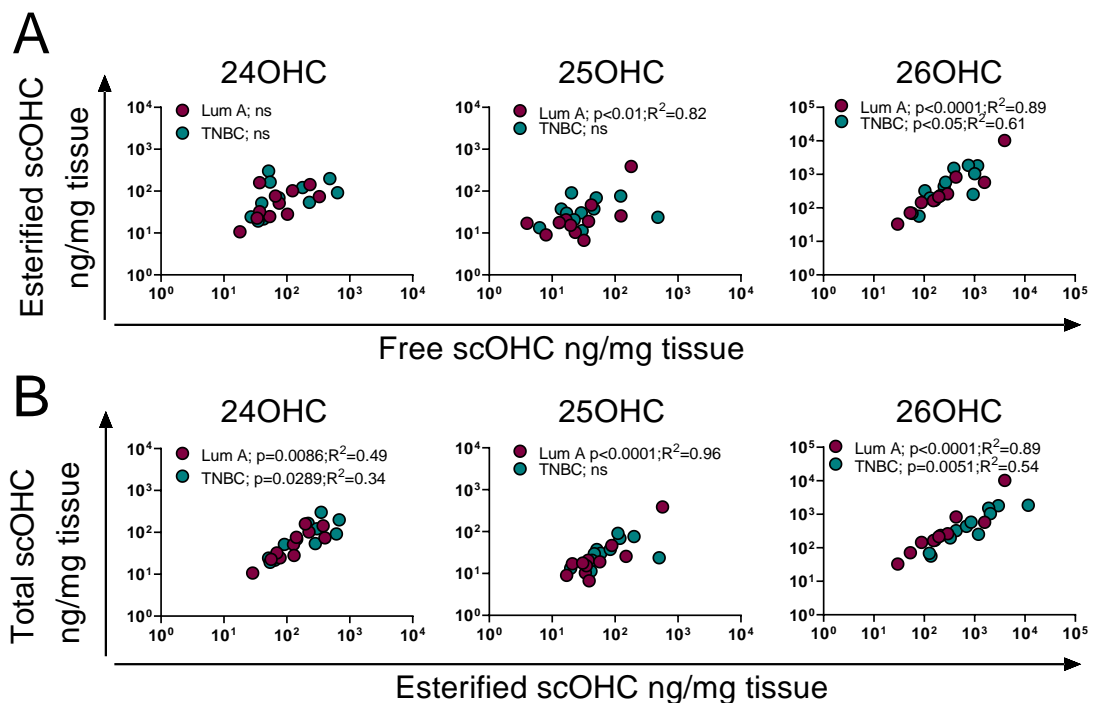


Figure 4. 4 The ratio of 24OHC, 25OHC and 26OHC total to esterified oxysterol concentrations significantly correlate in the Luminal A breast tumours, but only 24OHC and 26OHC correlate in TNBC tumours.

The oxysterol concentrations (total, esterified and free) in 22 patient tumours of two BCa subtypes [TNBC $n=11$, ER-positive $n=11$] were measured by LCMS/MS and compared across subtypes. Free and esterified oxysterol concentrations, and total and esterified oxysterol concentrations were analysed by Pearson correlation and assessed for statistical significance.

4.3.2 LXR cofactor expression is skewed towards transcriptional activation in TNBC and towards repression in ER-positive disease.

To explore the potential for LXR α to be activated and therefore control transcription, publicly available datasets were assessed for the expression of regulatory co-factors which have previously been implicated in the deregulation of nuclear receptor activity [68, 79, 94, 95].

Using the TCGA dataset [230] accessed from cBioportal [229], essential regulators of LXR α activity were assessed in the TNBC and Luminal A subtypes. The cofactors selected for this analysis were chosen if they had been shown previously to physically interact with LXR in a published nuclear receptor/cofactor scan [251], and if they were also reported to interact with LXR in at least one other study. This resulted in 6 co-activators (SRC, NCOA3, EP300, NCOA6, TRRAP and GPS2) and 3 co-repressors (NCOR1, NCOR2 and LCOR) to be selected for assessment. RNA-Seq mRNA expression were downloaded for TNBC and Luminal A primary tumour samples and assessed for differences in median mRNA expression across the two subtypes. Higher median expression of the co-activators SRC (two-tailed Mann-Whitney U test, $p < 0.001$) and TRRAP ($p < 0.001$) was observed in the TNBC relative to the Luminal A BCa subtype, but uniform expression of the remaining co-activators NCOA3, EP300, NCOA6 and GPS2 was observed (ns). (**Figure 4.5A**). Interestingly, decreased expression of all of LXR's co-repressors (NCOR1: $p < 0.001$; NCOR2: $p < 0.001$; LCOR: $p < 0.001$) were observed in the TNBC primary tumour samples (**Figure 4.5B**). The same patterns were observed when the expression of NCOR1, NCOR2 and LCOR was assessed in the breast cancer cell lines (2-tailed unpaired t-tests, $p < 0.001$ for each gene) (**Figure 4.5C**).

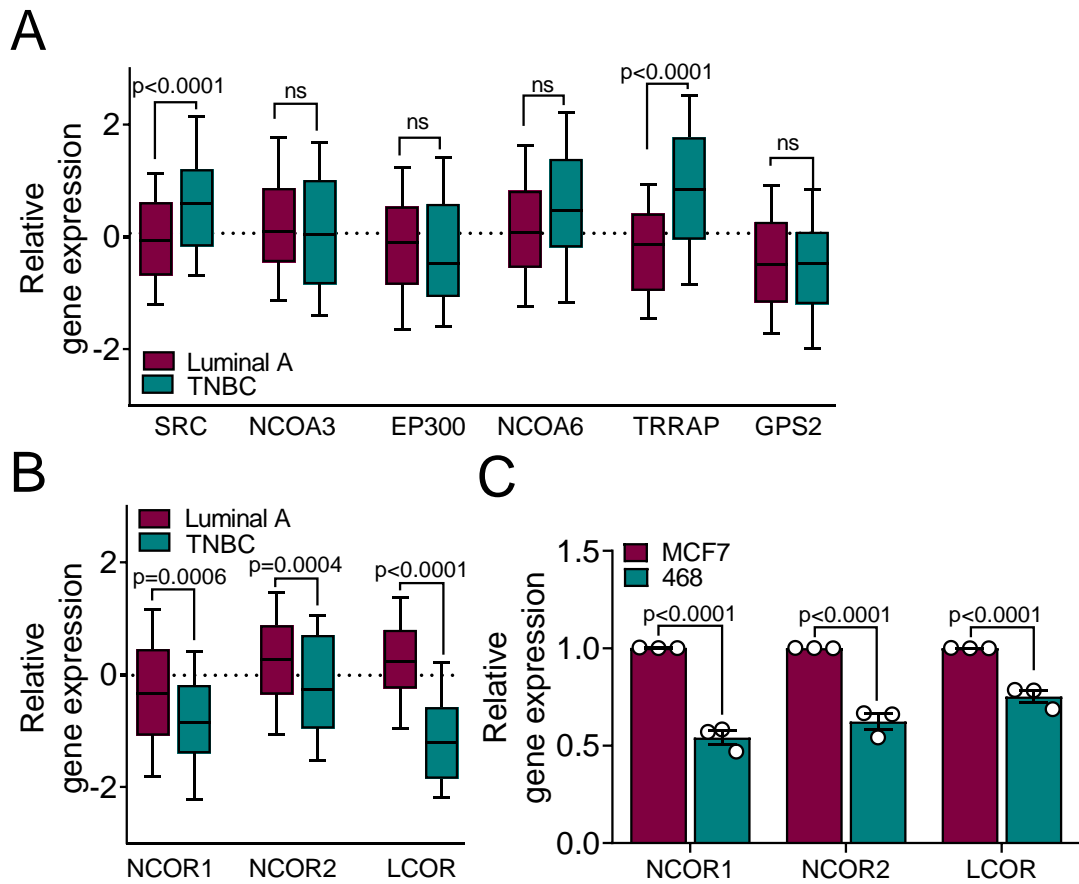


Figure 4.5 Co-activators and co-repressors are differentially expressed in TNBC and Luminal A BCa.

mRNA-Seq data (log transformed relative to array median with 10-90th centiles) for 89 TNBC and 235 Luminal A tumours were obtained [230] for receptor expression analysis from CBioportal (TCGA) [229] and the subtype specific expression of co-activators (A) and co-repressors (B) were assessed. Expression is presented as box and whisker plots with median, inter-quartile and 10-90 percentiles shown. Statistical analysis was established using two-tailed Mann-Whitney U test. RNA was harvested from TNBC (MDA-MB-468) and Luminal A (MCF-7) cells and expression of NCOR1, NCOR2 and LCOR (C) were assessed by TaqMan assays ($\Delta\Delta Ct$ and normalised to MCF-7). Data shown are mean of three independent replicates with SD, statistical analysis was established using 1-tailed unpaired t tests.

4.3.3 Triple negative breast cancer is transcriptionally responsive to LXR ligands and Luminal A BCa is resistant.

In section 4.3.1 the concentrations of all known and measurable endogenous LXR α ligands were found not to be significantly different between tumour subtypes. In 4.3.2 however, expression of LXR α itself, and its regulatory factors such as the co-repressors were found altered in a manner consistent with enhanced responsiveness to ligand. I next hypothesised that such altered expression of LXR α and its cofactors in ER-negative/TNBC disease relative to Luminal A, would be associated with

increased sensitivity to ligand in ER-negative disease relative to ER-positive. This hypothesis was tested through several routes. First, a panel of luciferase reporter cell lines under the control of a multi-LXRE promoter (see methods section 3.2) were generated and luciferase activity measured after exposure to a panel of synthetic and endogenous LXR ligands. As LXR activation has been reported to be anti-proliferative in a wide array of cancer cell lines, MTT assay was used to assess differences in cell number/viability after exposure to ligand. Finally, expression of LXR target genes was assessed by testing for correlation with LXR α (and co-repressors) in ER-negative and ER-positive patient tumour samples, and after treatment with LXR ligands in cell lines representative of both ER- and ER+ disease.

4.3.3.1 Triple negative breast cancer reporters are more responsive to LXR ligands than the Luminal A breast cancer reporter.

In order to assess LXR α responsiveness to ligand in BCa, a panel of BCa and a control cell lines (HepG2 [control], MCF-7, MDA-MB-468 and MDA-MB-231) were stably transfected with a luciferase reporter construct driven by an LXR α responsive promoter. The stable luciferase reporter cell lines: HepG2 [control] (**Figure 4.6A**) and BCa MCF-7, MDA-MB-468 and MDA-MB-231 were treated with a panel of LXR endogenous ligands (**Figure 4.6B**) or synthetic ligands (**Figure 4.6C**) and LXR α activity was determined by luciferase assay. The synthetic controls (agonists: T0901317, GW3965, and antagonist GSK2033) regulated the expression of LXR α in all cell lines from as low as 100 nM to as high as 50 μ M, although signal at this higher concentration was attenuated presumably through a cytotoxic effect. The panel of endogenous LXR ligands were also able to regulate LXR α expression however, a

range in ligand effectiveness to activate LXR α was observed. In the liver HepG2 cells, which were used as a control for LXR α activity (**Figure 4.6A**), endogenous ligands were able to successfully activate LXR α (24OHC, 10-35 fold activation; 25OHC, 5-10 fold activation; 26OHC, 2-10 fold activation; 24,25-EC, 20-50 fold activation). The synthetic ligands T0901317 and GW39965, were able to successfully activate LXR α in all three of the breast cancer reporters, and the synthetic antagonist GSK2033 was able to suppress LXR α (**Figure 4.6A**). The endogenous ligands were able to activate LXR α in the two TNBC reporters, MDA-MB-468 (24OHC, 10-35 fold activation; 25OHC, 5-10 fold activation; 26OHC, 5 fold activation; 24,25-EC, 15-40 fold activation) and MDA-MB-231 (24OHC, 10-35 fold activation; 25OHC, 5-10 fold activation; 26OHC, 2-5 fold activation; 24,25-EC, 15-40 fold activation) in a manner comparable to the HepG2 control reporter. In the MCF-7 reporter however, endogenous ligands were only able to minimally activate LXR α (24OHC, 3 fold activation; 25OHC, 2 fold activation; 26OHC, 2 fold activation; 24,25-EC, 3-5 fold activation) with a clear difference in the response to ligand observed between the two breast cancer subtypes. The endogenous ligand 7KETO was the weakest ligand in the three breast cancer reporters (2-fold activation MCF-7 and MDA-MB-231, 5-fold activation MDA-MB-468) and therefore not included in further analyses. These data indicate that oxysterols robustly activate LXR α in TNBC but the LXR α response is dampened in the Luminal A/ER-positive disease. This is consistent with the observations that co-repressor activity is lower in TNBC tumours and cells relative to Luminal A BCa.

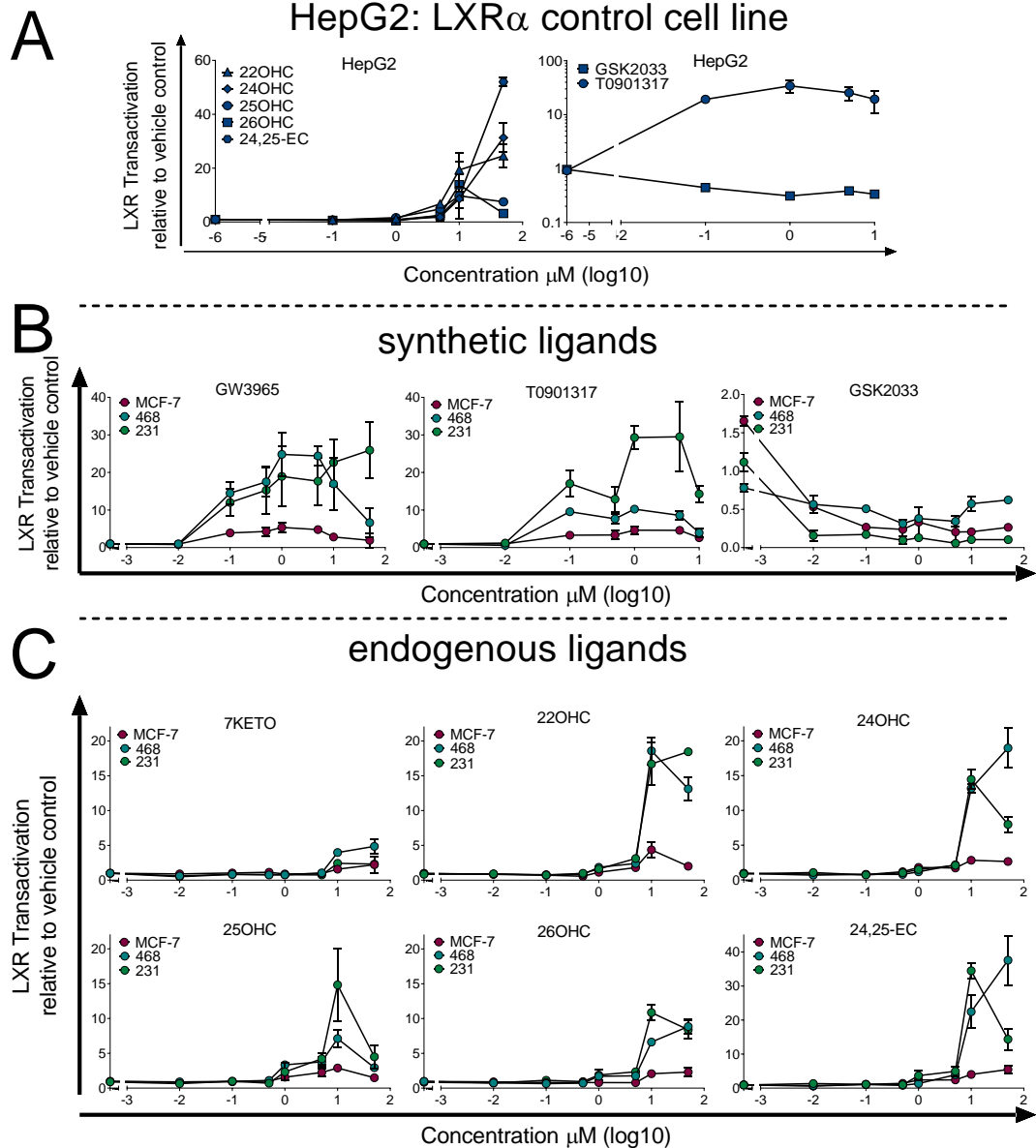


Figure 4. 6 LXR α is transcriptionally responsive to agonists in TNBC but not ER-positive MCF-7 cells.

Liver HepG2 cells, TNBC cells (MDA-MB-468 and MDA-MB-231) and a Luminal A cell line (MCF-7) were stably transfected with an LXR α luciferase positive reporter. HepG2 reporter cells [used as a control] (A) and BCa cells were treated with a panel of LXR ligands: (B) synthetic ([GW3965, GSK2033 – 1 μ M, T0901317 – 2.5 μ M]) and (C) endogenous [7-KETO, 22OHC, 24OHC, 25OHC, 24,25-EC and 26OHC – 10 μ M]) for 16 h. LXR α transactivation was normalised to VC. Data shown are mean of 2-3 independent replicates with SD.

The effects of oxysterols on viability of TNBC and Luminal A/ER-positive cells were next examined – data generated and analysed by Priscilia Lianto (**Figure 4.7**). Luminal A cells (MCF-7) and TNBC cells (MDA-MB-468 and MDA-MB-231) were exposed to oxysterols for 48 h and cell viability assessed by MTT. The Luminal A MCF-7 cells,

were more resistant than the TNBC cells to the treatment with 24OHC (non-linear regression comparison of fits: non-converged for MCF-7), 25OHC (MDA-MB-468; $p < 0.0001$, MDA-MB-231; $p = 0.03$) and 26OHC (MDA-MB-468; $p < 0.0001$) in the micromolar range. The exception to this was treatment with 26OHC in MCF-7 cells compared to TNBC MDA-MB-231 cells (ns). The MDA-MB-231 cells appeared to be more resistant to oxysterol treatment than MDA-MB-468 with 24OHC ($p < 0.0001$), 25OHC ($p < 0.0001$) and 26OHC ($p < 0.0001$) but not as resistant as MCF-7 cells.

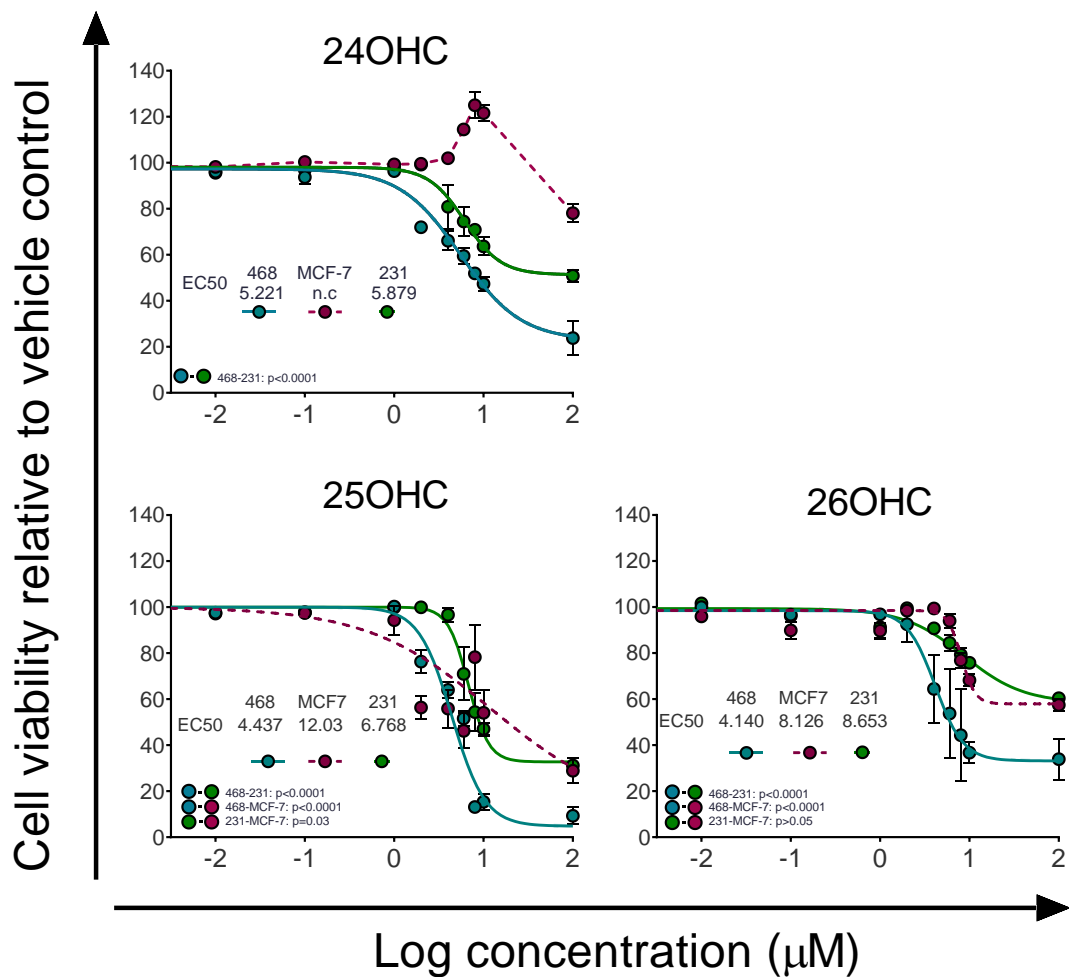


Figure 4. 7 Luminal A BCa cells are insensitive to oxysterol treatment.

The anti-proliferative effects of the oxysterols 24OHC, 25OHC and 26OHC were assessed by MTT in MDA-MB-468, MDA-MB-231 and MCF-7 cells over 48 h with EC50 given in μM. Data are presented as means of 3-4 independent replicates with SEM – data generated by Priscilia Lianto, Thorne laboratory member. Significance was assessed using non-linear fit, significance between MCF-7 and TNBC cells was unable to be assessed as non-linear regression was non-converged for the MCF-7 cells.

4.3.3.2 LXR dependent transcription from endogenous loci is significantly higher in triple negative breast cancer than in Luminal A breast cancer.

A limitation of the luciferase reporter experiment was that the stable construct may not have been embedded in a comparable chromatin environments in the different cell lines. To confirm the results from 4.3.2.1 in a normal, or endogenous, chromatin context, LXR target genes were assessed. To assess this aim, transcriptional output of the LXR target genes ABCA1 and APOE were assessed after treatment with LXR ligands in cell culture, and their expression was tested for correlation with LXR α in the Luminal A and TNBC datasets reported in section 4.3.1.1 [229, 230].

TNBC cells (MDA-MB-468 and MDA-MB-231) and Luminal A BCa cells (MCF-7) were exposed to LXR the synthetic ligand GW3965 and LXR endogenous ligands (24OHC, 26OHC and 24,25-EC) for 4 h and 16 h before RNA was extracted and expression of the canonical LXR target genes ABCA1 and APOE were measured (normalised to HPRT). Enhanced expression of ABCA1 was observed in the MDA-MB-468 and MDA-MB-231 TNBC cell lines relative to the Luminal A cell line MCF-7 (**Figure 4.8**) at both 4 h (**Figure 4.8A**) and 16 h (**Figure 4.8B**). In both TNBC cell lines all agonists increased ABCA1 expression by between 8 and 110 fold (1-tailed unpaired t test; $p < 0.01$ for all). In the Luminal A/ER+ cell line the induction was less and between 3 and 12-fold ($p < 0.05$ for all except 25OHC, ns). Enhanced expression of APOE was also observed in the MDA-MB-468 and MDA-MB-231 TNBC cell lines relative to the Luminal A cell line MCF-7 (**Figure 4.8**) at both 4 h (**Figure 4.8C**) and 16 h (**Figure 4.8D**). In both TNBC cell lines all agonists increased APOE expression by between 1.5 and 5 fold at 16 h ($p < 0.01$ for all). In the Luminal A/ER-positive cell line the LXR response to ligand resulted in down-regulation of APOE ($p < 0.05$ for all).

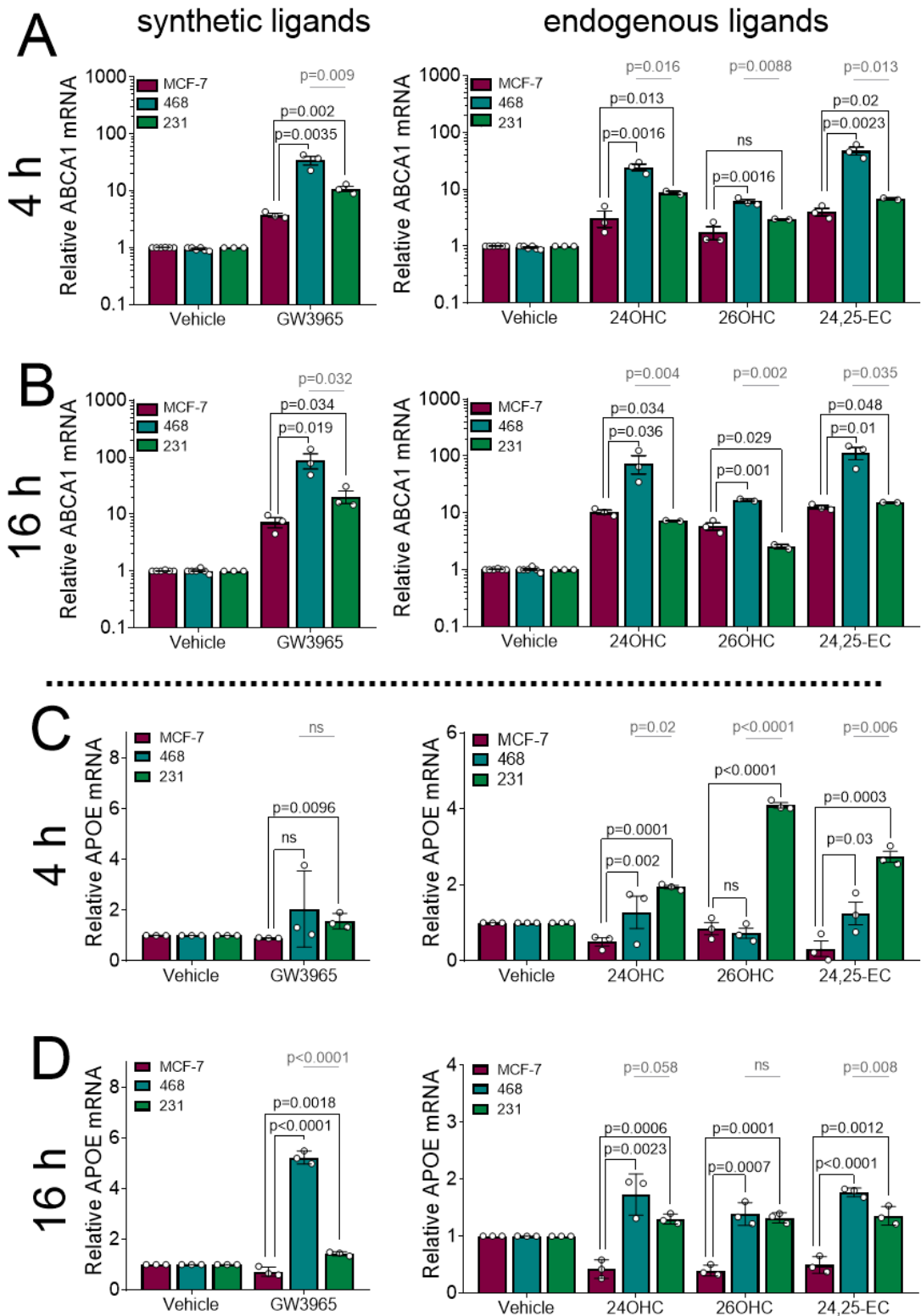


Figure 4. 8 LXR response to ligand is enhanced in TNBC cell cultures relative to Luminal A.

TNBC (MDA-MB-468 and MDA-MB-231) and Luminal A (MCF-7) cells were treated with LXR ligands (synthetic 1 μ M, endogenous 10 μ M) for 4 h and 16 h and expression of ABCA1 (A+B) and APOE (C+D) was assessed by qPCR ($\Delta\Delta$ Ct using HPRT and normalised to vehicle). Data shown are mean of three independent replicates with SD, statistical analysis was established using 1-tailed unpaired t tests. P values in grey represent comparison between MDA-MB-468 and MDA-MB-231 cells.

4.3.3.3 LXR α correlates with ABCA1 and APOE in triple negative breast cancer primary tumours.

To assess whether expression of LXR α and/or LXR β correlates with their target genes, ABCA1 and APOE were assessed for correlation as they are widely accepted as LXR target genes [252-254]. The RNA-Seq mRNA data was downloaded and shown as log transformed relative to array median, with 10-90th centiles was for ABCA1, APOE, LXR α and LXR β in 89 TNBC and 234 Luminal A/ER-positive breast tumours [230] accessed from cBioportal [229]. We then assessed if LXR α or LXR β expression correlates with ABCA1 and/or APOE expression in the two tumour subtypes (**Figure 4.9**). In the TNBC tumours, ABCA1 expression significantly correlated with LXR α expression (Pearson's correlation with linear regression, $p < 0.0001$, $r = 0.502$) but not with LXR β expression (ns). APOE expression also correlated with LXR α in the TNBC tumours ($p < 0.0001$) but did not with LXR β (ns). In the Luminal A/ER-positive tumours, ABCA1 expression failed to correlate with LXR α or LXR β expression, however APOE expression correlated with both LXR α and LXR β expression ($p < 0.0001$).

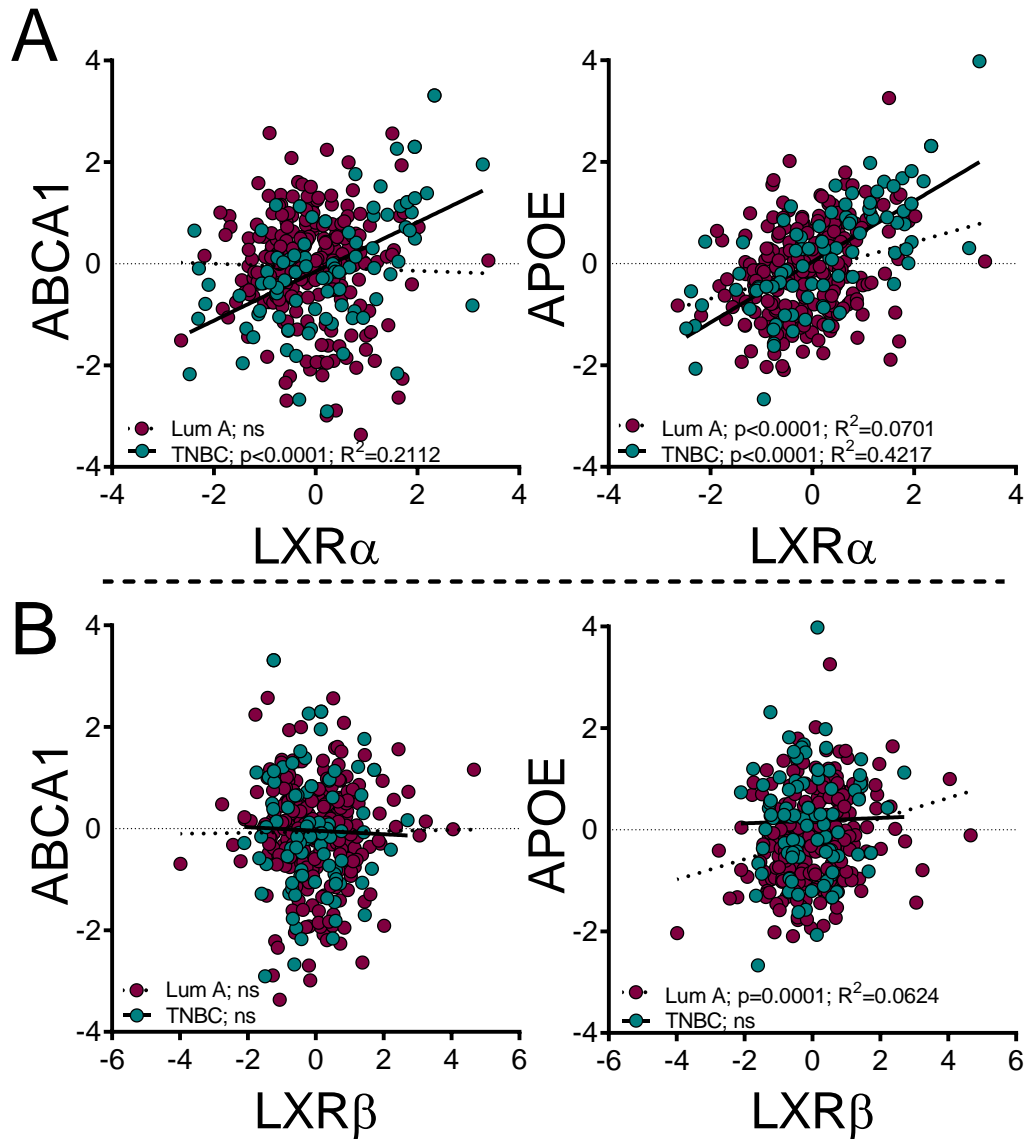


Figure 4. 9 The LXR target genes ABCA1 and APOE significantly correlate with LXR α in TNBC patient tumours but not LXR β .

Expression of the LXR target genes ABCA1 and APOE were correlated with LXR α (A) and LXR β (B) in 81 ER-negative and 234 ER-positive breast tumours [230] accessed from the patient database CBioportal [229]. Statistical significance was assessed using Pearson's correlation test with linear regression.

4.3.3.4 LXR α is more likely to correlate with expression of its target genes in triple negative breast cancer tumours than Luminal A tumours

The next aim was to establish if enhanced LXR activity in the TNBC relative to the Luminal A BCa subtype results in enhanced transcriptional output of most, if not all LXR target genes to remove any selection bias from ABCA1 being a highly researched and robust LXR target. To assess this aim, CHIP-Seq data was mined from the

Cistrome database [231] and genes assessed for LXR α binding in their promoters (method section 3.11.1). Target genes identified in this manner were then assessed for correlation with LXR α in the ER-negative and ER-positive primary BCa tumours datasets from sections 4.3.1.1) [229, 230]. The top most likely LXR target genes in breast tumour tissue identified from these steps were validated in cell cultures.

First, ChIP-Seq data were mined from the Cistrome database [231]. The top 100 genes (defined as having the highest LXR α binding scores) and appearing in at least two from 7 distinct datasets found across three publications [255-257] were selected for further analysis (see **Appendix 1 – A.1** for list of genes and see materials and **methods section 3.11.1** for flow diagram explaining gene selection). Binding scores were assessed in the vehicle control group (VC) compared with the GW3965 treatment group - (shown in **Appendix 1 – A.1**). 135 genes were identified in this manner and their expression data in 81 TNBC and 234 Luminal A BCa were obtained from CBioportal [229, 230]. The expression of these genes was then tested for correlation with LXR α and LXR β in both tumour subtypes. A False Discovery Rate (FDR) of 1 % was used to correct for multiple testing. The data are presented showing correlation coefficient against FDR for TNBC and Luminal A/ER-positive BCa tumours (**Figure 4.11**). In this analysis, LXR α significantly correlated with 48/135 LXR target genes in the TNBC tumours which was significantly more than the 8/135 genes in the Luminal A tumours (Fisher's exact test: $p < 0.0001$). Three genes, which were not previously validated in the literature as *bona fide* LXR target genes (LCP2, DOK2 and TNFRSF1B) were selected from the top 10 strongest correlations to test further *in vitro* and *in vivo*. First, we assessed recruitment of LXR α to target gene promoters are shown in **Figure 4.10A and 4.10B**. Second, we assessed the gene correlations

individually (as previously shown for the canonical LXR target gene ABCA1), to establish if LXR α or LXR β correlate weakly with genes in the Luminal A BCa samples (**Figure 4.10C**). We also included the gene APOE, which is another well-known LXR target gene to the analysis as it significantly correlated with LXR α in the TNBC tumours. As a control, LXR β was tested for correlation with genes identified as having LXR α bound in their promoters LCP2, TNFRSF1B, DOK2 and APOE in the TNBC or Luminal A tumours (with the exception of APOE; Pearson's correlation test: $p < 0.0001$; $R = 0.2499$). Interestingly, the selected target genes (LCP2; $p < 0.0001$, $R = 0.6832$, TNFRSF1B; $p < 0.0001$, $R = 0.6601$, DOK2; $p < 0.0001$, $R = 0.6677$, APOE; $p < 0.0001$, $R = 0.6494$) had much stronger correlations in the ER-negative tumours compared to the ER-positive tumours genes (LCP2; $p = 0.021$, $R = 0.1518$, TNFRSF1B; $p = 0.0048$, $R = 0.1846$, DOK2; $p = 0.0003$, $R = 0.2368$) with the exception of APOE which was equally as strong ($p < 0.0001$; $R = 0.2649$).

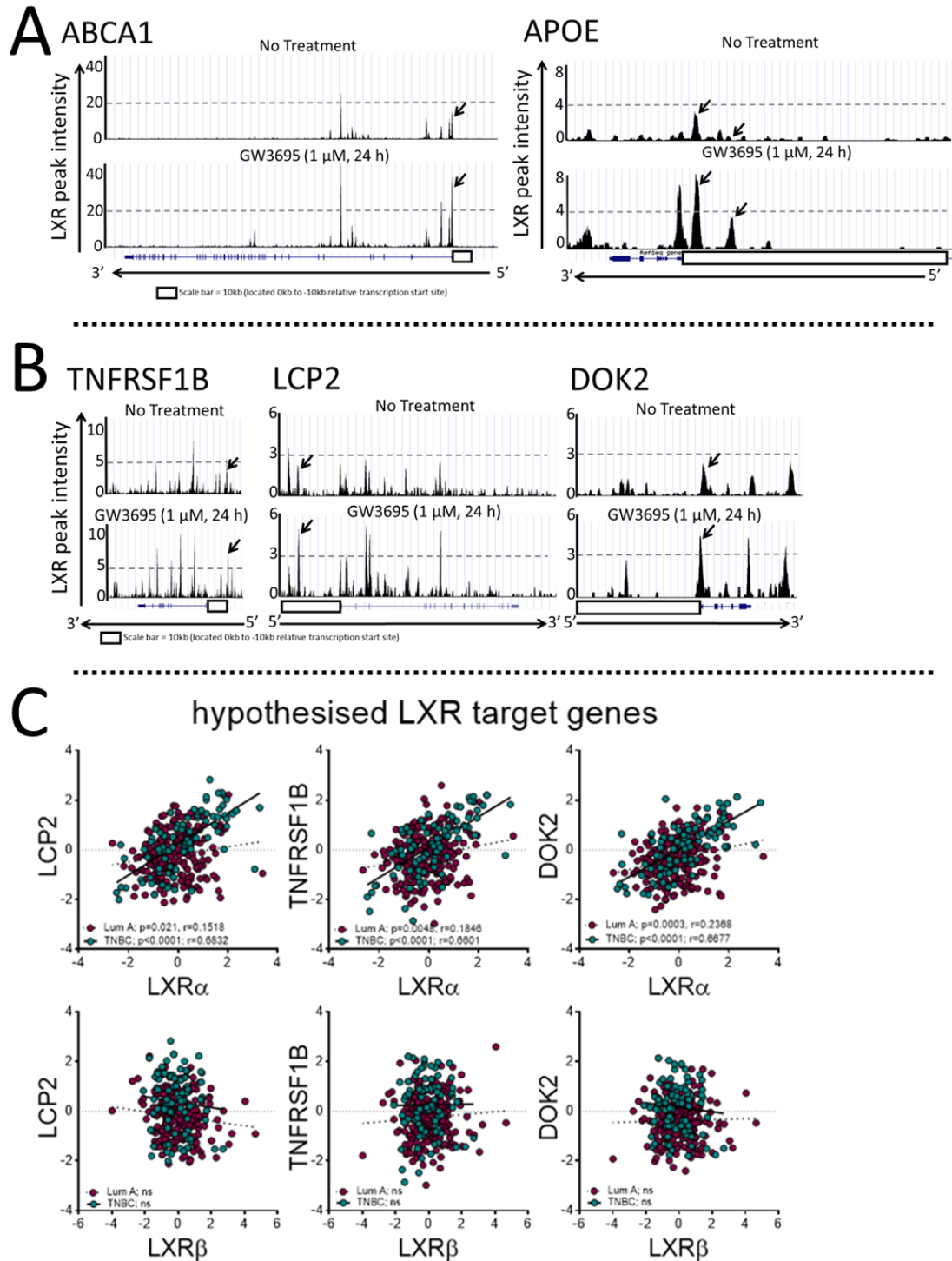


Figure 4. 10 LXR α is recruited to canonical (A) and novel (B) target gene promoters after GW3965 treatment and correlates with the expression of novel target genes in breast tumours.

The promoter regions of the LXR canonical target genes ABCA1 and APOE (A) and the novel target genes TNFRSF1B, LCP2 and DOK2 (B) were assessed for LXR α recruitment in macrophages 24 h post exposure to vehicle control and the LXR ligand GW3965. Peak intensity between treatments are displayed highlighting the increased peak intensity within the 10 kb promoter region after LXR ligand stimulation. Expression of LXR α was correlated with three otherwise novel candidate target genes (C) in 89 TNBC and 234 Luminal A/ER-positive breast tumours accessed from the patient database cBioportal [229], dataset [230]. Statistical significance was assessed using Pearson's correlation test with linear regression.

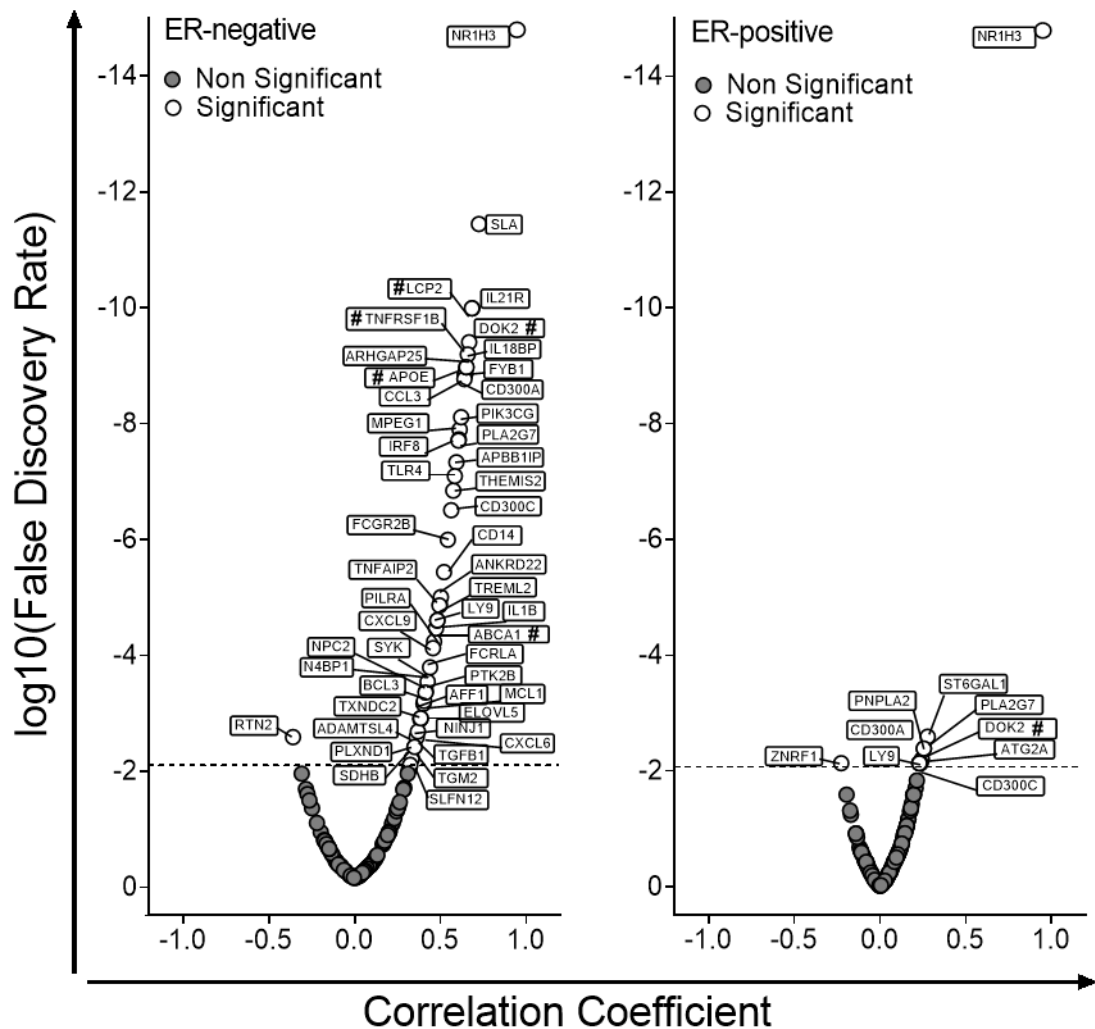


Figure 4. 11 LXR α expression correlates with target genes in ER-negative tumours but not ER-positive.

Genes with top LXR α occupancy scores from the seven LXR α ChIP-Seq datasets [255-257] available at Cistrome [231] were identified. with a further 24 canonical LXR targets identified from literature were added (see methods section 3.11.1). Genes were then correlated with LXR α in 81 ER-negative and 234 ER-positive Luminal A tumours from cBioportal [229], datasets [230]. Data shown are correlation coefficient (R) against correlation significance (on a log₁₀ scale). Fishers' exact test was used to assess significance between LXR α and LXR β correlations with genes implicated in chemoresistance (p<0.0001). Genes marked with a # were later validated by qPCR analysis.

Next, we tested if transcription of the three candidate (LCP2, DOK2 and TNFRSF1B) genes was increased more in TNBC cell lines than Luminal A by treatment with LXR ligands. The LXR synthetic ligand GW3965 (**Figure 4.12A**) and the LXR endogenous ligands 24OHC, 26OHC and 24,25-EC (**Figure 4.12B**) were able to regulate expression

of the novel target genes. In the BCa cells MDA-MB-468, MDA-MB-231 and MCF-7 treatment with GW3965 significantly increased expression of the three candidate genes. Increases in gene expression were generally significantly lower in the Luminal A cells than in the TNBC cell line MDA-MB-468 (1-tailed unpaired t tests: LCP2, $p=0.0059$., DOK2, $p=0.0146$., TNFRSF1B, $p=0.0295$) and MDA-MB-231 (LCP2, $p=0.0131$). However, GW3965 treatment increased the expression of DOK2 and TNFRSF1B to similar levels in the MCF-7 and MDA-MB-231 cells (ns). The LXR endogenous ligands (**Figure 4.12B**) were also able to enhance expression of the novel target genes in TNBC cells relative to the vehicle control. In the MDA-MB-468 cells, expression of LCP2 and DOK2 were not enhanced relative to the MCF-7 cells after treatment with oxysterols (ns). Expression of TNFRSF1B however, was enhanced after treatment with 26OHC ($p=0.002$) in MDA-MB-468 cells compared to the MCF-7 cells. In the MDA-MB-231 cells, expression of LCP2 was not enhanced relative to the MCF-7 cells after treatment with oxysterols (ns). Expression of DOK2 and TNFRSF1B however, were enhanced after treatment with 24OHC (LCP2: $p=0.028$., TNFRSF1B: $p=0.0006$), 26OHC (LCP2: $p=0.003$., TNFRSF1B: $p=0.0005$) and 24,25-EC (LCP2: $p=0.0029$., TNFRSF1B: $p<0.0001$) in MDA-MB-231 cells compared to the MCF-7 cells.

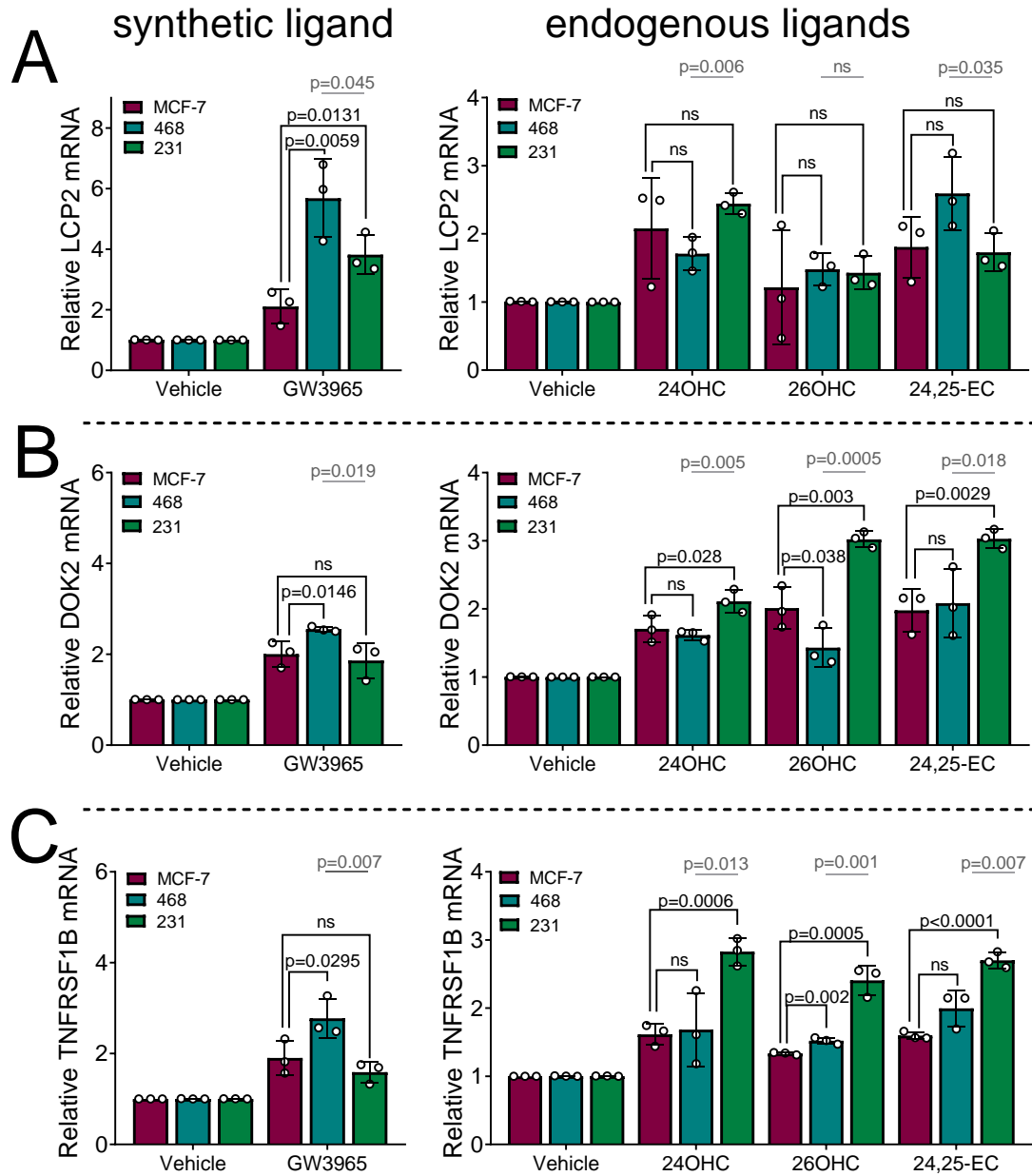


Figure 4. 12 LXR ligands drive expression of hypothesised LXR target genes in TNBC cell cultures relative to Luminal A cells.

TNBC (MDA-MB-468 and MDA-MB-231) and ER-positive (MCF-7) cells were treated with the synthetic LXR ligand GW3965 (1 μ M) or endogenous oxysterols (10 μ M) for 16 h and gene expression of the three novel LXR target genes LCP2 (A), DOK2 (B) and TNFRSF1B (C) was assessed by qPCR ($\Delta\Delta$ cT using HPRT and normalised to vehicle). Data shown are mean of three independent replicates with SD, statistical analysis was established using 1-tailed unpaired t tests. Statistics were used to assess if TNBC cells displayed enhanced transcriptional output of target genes relative to the Luminal A cells. Grey p values and lines represent statistical differences between MDA-MB-468 cells and MDA-MB-231 cells.

In summary, we have established that expressions of LXR target genes are more likely to correlate with expression of LXR α in TNBC than Luminal A BCa and have used false discovery rates to hypothesis and validate novel LXR target genes. LXR ligands

were shown to induce expression of hypothesised LXR target genes in both TNBC and Luminal A cell lines. Furthermore, expression of the target genes were typically enhanced in the TNBC cells relative to the MCF-7 cells. Finally, APOE expression appeared to be down-regulated by LXR ligands in the Luminal A cell line MCF-7, which may be due to enhanced expression of the ligand recruited co-repressor LCOR (as observed in **Figure 4.5**).

4.3.4 Corepressors control LXR α transcriptional responsiveness in breast cancer.

The next aim was to establish if enhanced LXR α luciferase activity and transcriptional output in the TNBC relative to the Luminal A BCa subtype was influenced by the decreased co-repressor expression observed in **Figure 4.5**. To assess this aim NCOR1, NCOR2 and LCOR were knocked down in TNBC and Luminal A BCa cell lines and LXR α luciferase activity and transcriptional output measured by luciferase assay and qPCR respectively.

First, NCOR1, NCOR2 (alone or in combination) or LCOR were knocked down in the cell lines using three targeted siRNAs. RNA was harvested 36 h post transfection and knockdown efficacy validated by Taqman (**Figure 4.13**). NCOR1 expression in MDA-MB-468 and MCF-7 siNCOR1 cells was significantly knocked down to 25 % of the levels in cells transfected with non-targeting control (2-way ANOVA; mean 0.25, $p < 0.001$ for both cell lines) without altering the expression of NCOR2 (mean 1.1, ns for both cell lines) (**Figure 4.13A**). NCOR1 expression in MDA-MB-468 and MCF-7 siNCOR1+2 cells was also significantly knocked down ($p < 0.001$ for both cell lines; MCF7: mean 0.25, MDA-MB-468: mean 0.2). NCOR2 knockdown (**Figure 4.13B**) was similar in the double knockdown (MCF-7: mean 0.25., 468: mean 0.3., $p < 0.001$ for

both cell lines) and in single knockdown (MCF-7: mean 0.2., 468: mean 0.25., $p < 0.001$ for both cell lines) without altering NCOR1 expression (mean 1.0, ns for both cell lines), therefore demonstrating knockdown specificity of different NCOR genes. Additionally, LCOR expression in MDA-MB-468 and MCF-7 siLCOR cells (**Figure 4.13C**) was also significantly knocked down (MCF-7: mean 0.5., 468: mean 0.4., $p < 0.001$ for both cell lines).

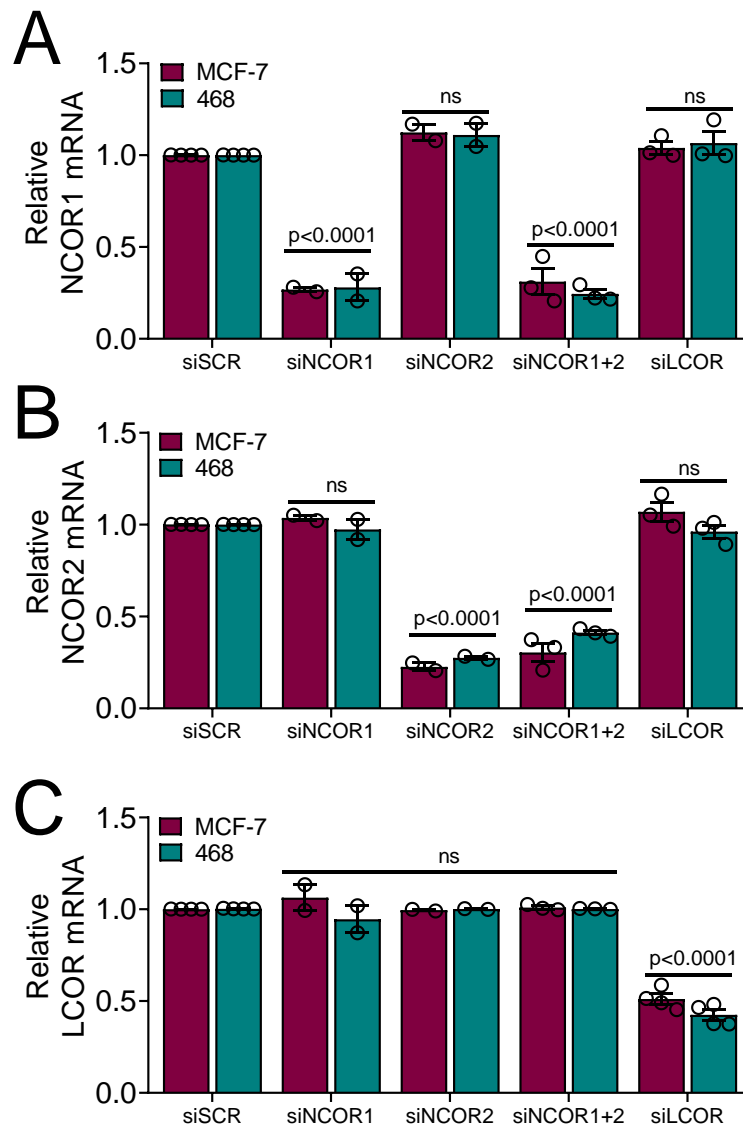


Figure 4. 13 NCOR1, NCOR2 and LCOR were successfully knocked down in MDA-MB-468 and MCF-7 cells.

LCOR, NCOR1 (siNCOR1) and NCOR2 (siNCOR2) either alone or in combination (siNCOR1+2) were knocked-down in the LXR α luciferase reporter MCF-7 and MDA-MB-468 cells. Gene expression of the corepressors NCOR1 (A), NCOR2 (B) and LCOR (C) were assessed by qPCR 36 h post silencing. Statistical significance was established using 2-way ANOVA and mean of 2-3 independent replicates with SEM are presented.

Since LXR transcriptional response to ligand and corepressor expression appear to be associated we assessed if knockdown of corepressors NCOR1, NCOR2 and LCOR equalized the response to ligand between the two BCa subtypes. So after validating the knockdowns, LCOR, NCOR1, NCOR2 and NCOR1+2 together were knocked down in MDA-MB-468 and MCF-7 luciferase reporters and treated with VC or 26OHC for a further 16 h. LXR α transactivation was measured by luciferase assay and mRNA assessed using qPCR. MDA-MB-468 cells transfected with universal negative control siRNA (siSCR) and treated with 26OHC showed significant increase in luciferase signal similar to **Figure 4.7** (2-way ANOVA; MCF-7: mean 2-fold., 468: mean 3-fold., $p < 0.01$) which again, was significantly more than the MCF-7 cells (**Figure 4.14A**). Interestingly, knockdown of NCOR1 enhanced response to 26OHC (mean 2.5-fold, $p < 0.001$ both cell lines), NCOR2 (mean 2.5-fold, $p < 0.001$ both cell lines) and NCOR1+2 (MCF-7: mean 4-fold., 468: mean 4.4-fold., $p < 0.001$ both cell lines) and restored sensitivity of LXR α to ligand in the MCF-7 cell line, equalizing the expression of NCOR1, NCOR2 and NCOR1+2 to match that of the MDA-MB-468 cells (ns). Knockdown of LCOR also enhanced response to 26OHC in both cell lines (MCF-7: mean 5-fold., 468: 5.5-fold., $p < 0.0001$ both cell lines), and equalised the sensitivity of LXR α to ligand in MCF-7 to match that of the MDA-MB-468 cells (ns), **Figure 4.14B**.

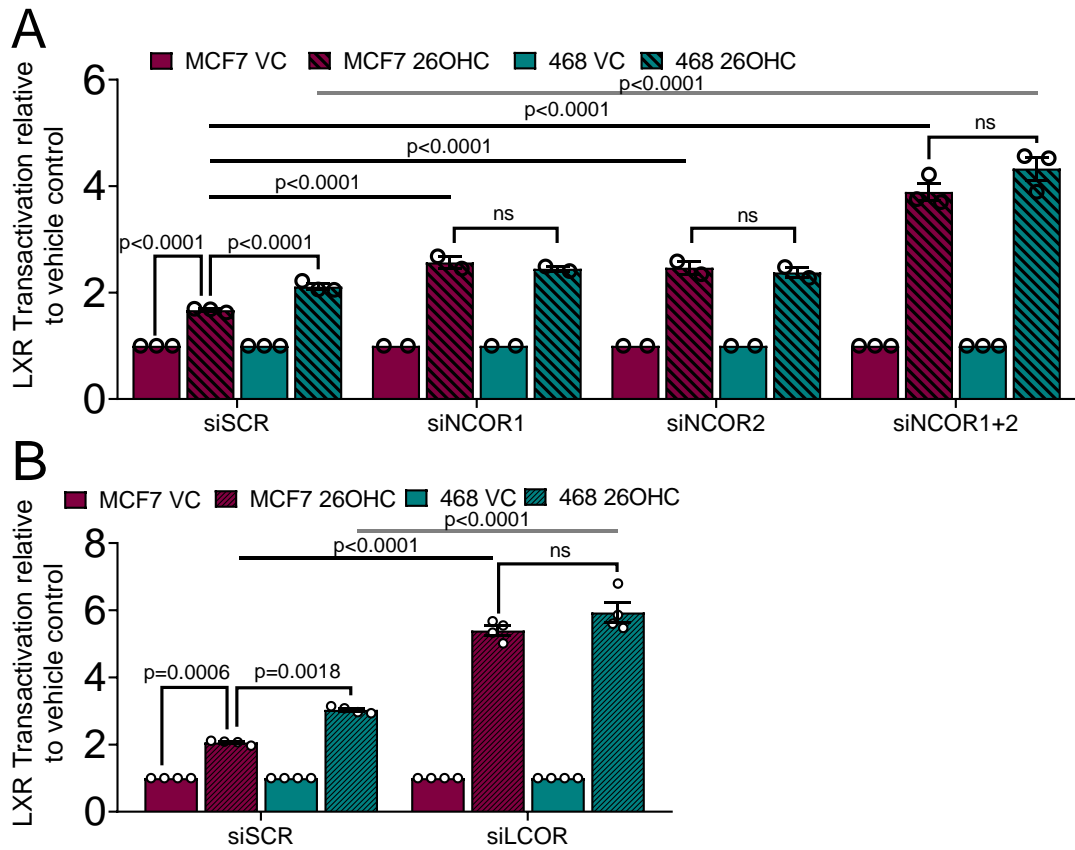


Figure 4. 14 NCOR and LCOR knockdown restores sensitivity to ligand..

LCOR, NCOR1 (siNCOR1) and NCOR2 (siNCOR2) either alone or in combination (siNCOR1+2) were knocked-down in the LXR α luciferase reporter MCF-7 and MDA-MB-468 cells and treated with vehicle control (VC) or 26OHC (10 μ M) for 16 h. LXR α transactivation was assessed 36 h post silencing in luciferase assays (A+B). Statistical significance was established using 2-way ANOVA (* p <0.05, ** p <0.01, *** p <0.001) and mean of 2-3 independent replicates with SEM are presented.

Furthermore, expression of ABCA1 and APOE was assessed after knockdown of LCOR, NCOR1, NCOR2 and NCOR1+2 (**Figure 4.15**). Expression of the LXR target genes ABCA1 and APOE were enhanced in the MCF-7 cells post knockdown of NCOR1 (1-way ANOVA: ABCA1 and APOE p <0.001) and NCOR1+2 (ABCA1 and APOE p <0.001). NCOR2 knockdown enhanced the expression of ABCA1 however not significantly, but was able to significantly enhance the expression of APOE (p <0.05). Enhanced transcriptional output of LXR target genes was also observed in the MDA-MB-468 cells post knockdown of NCOR1 (ABCA1; p <0.001., APOE; p <0.001), NCOR2 (ABCA1; p <0.05., APOE; p <0.05) and NCOR1+2 (ABCA1; p <0.001., APOE; p <0.001).

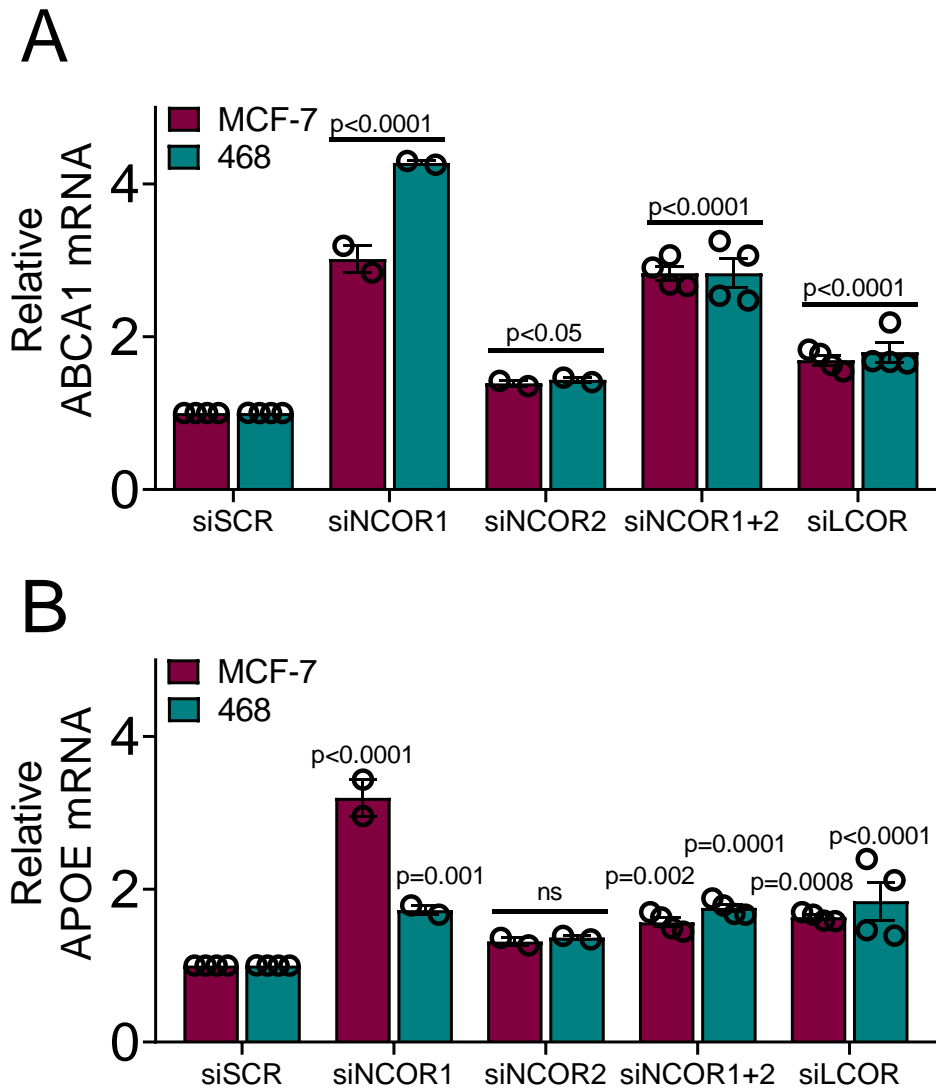


Figure 4. 15 NCOR1, NCOR2 and LCOR knockdown enhances expression of LXR target genes ABCA1 and APOE in TNBC and Lumina A reporter cells.

LCOR, NCOR1 (siNCOR1) and NCOR2 (siNCOR2) either alone or in combination (siNCOR1+2) were knocked-down in the LXR α luciferase reporter MCF-7 and MDA-MB-468 cells. Gene expression of the canonical LXR target genes ABCA1 (A) and APOE (B) were assessed by qPCR 36 h post silencing. Statistical significance of gene expression analyses was established using 1-way ANOVA comparing knockdown cells to cell line specific siSCR (using $\Delta\Delta C_t$ and normalised to HPRT1). Mean of 2-4 independent replicates with SEM are presented.

Since LXR transcriptional response to ligand was equalized by knockdown of corepressors NCOR1, NCOR2 and LCOR between the two BCa subtypes we wanted to assess whether corepressor knockdown also made the MCF-7 cells more sensitive to ligand in MTT assays (**Figure 4.16A**). In MCF-7 cells, knockdown of NCOR1 (non-linear regression comparison of fits: $p<0.001$), NCOR2 ($p,0.001$) and LCOR (no p

value: ambiguous) made the Luminal A cells more sensitive to treatment with 26OHC. In MDA-MB-468 cells, knockdown of NCOR1 ($p < 0.001$), NCOR2 ($p < 0.001$) and LCOR ($p < 0.001$) also made the TNBC cells more sensitive to treatment with 26OHC. In summary, corepressors have been shown to be important factors dictating the differential transcriptional activity of LXR between BCa subtypes.

Next, we measured LXR transcriptional output of its target genes after LXR α silencing to assess for LXR α control. First, we transfected MDA-MB-468 and MCF-7 LXR α luciferase reporter cells with LXR α siRNA complexes and measured LXR α transactivation after stimulation with ligands (**Figure 4.16B**). 26OHC was able to induce LXR α transactivation in the MDA-MB-468 and MCF-7 siSCR transfected cells but in the MDA-MB-468 and MCF-7 siLXR α cells; ligand driven LXR α activity was significantly attenuated (2-way ANOVA, 26OHC; $p < 0.0001$, for both cell lines). After validation of successful knockdown, RNA was harvested from MDA-MB-468 and MCF-7 cells transfected with siLXR α complexes and expression of ABCA1 and APOE was assessed by TaqMan assays (normalized to HPRT1) (**Figure 4.16C**). In cells transfected with siLXR α complexes gene expression of ABCA1 was reduced ($p < 0.0001$ for both cell lines), as was APOE expression ($p < 0.0001$ for both cell lines) validating these targets as LXR α regulated genes.

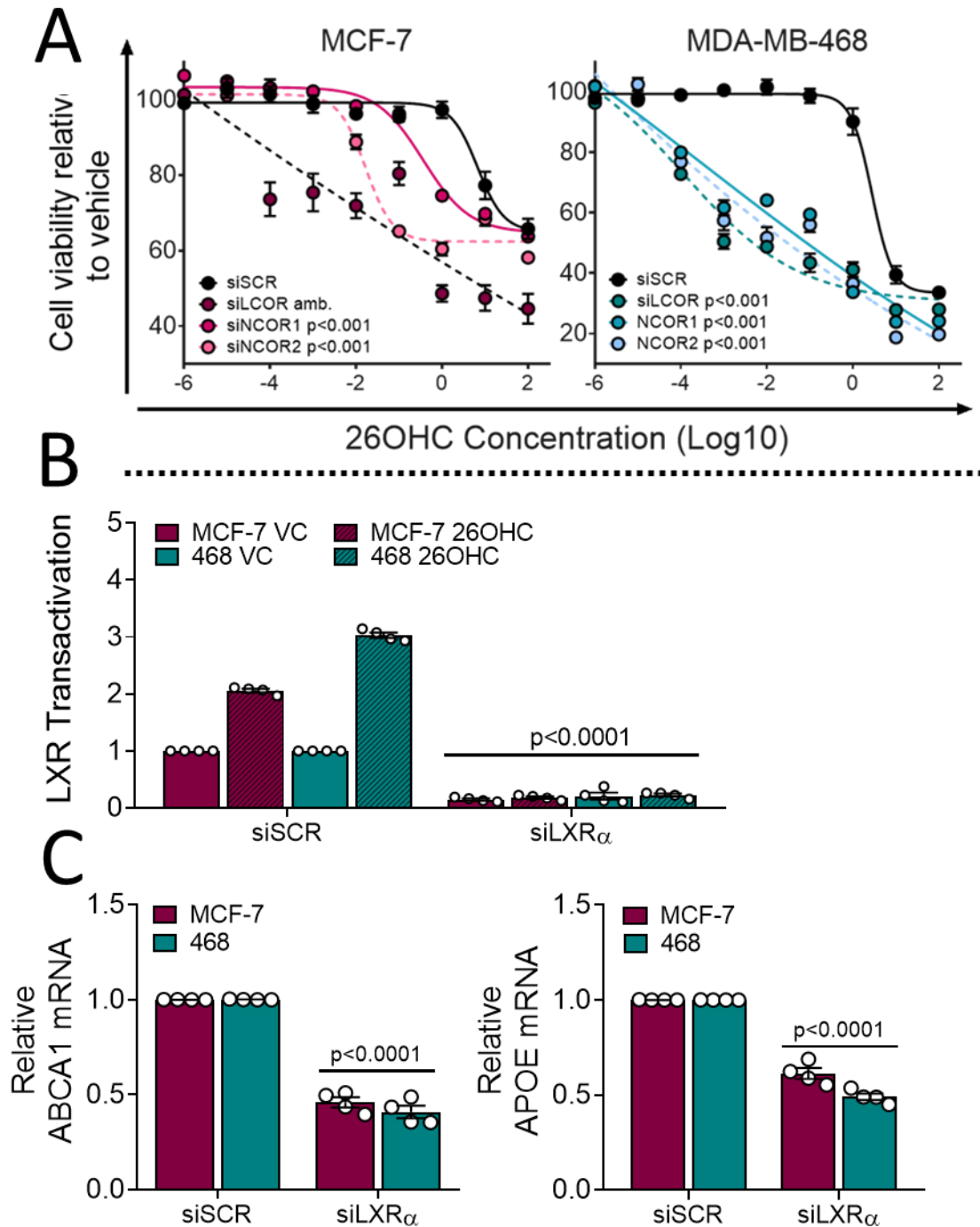


Figure 4. 16 Knockdown of corepressors increases sensitivity to ligand, and knockdown of LXR α in attenuates the expression of LXR target genes ABCA1 and APOE.

The corepressors LCOR, NCOR1 and NCOR2 were knocked down in MCF-7 and MDA-MB-468 cells and their response to ligand assessed relative to the universal negative control. LXR α was knocked-down in MCF-7 and MDA-MB-468 LXR α -luciferase reporter cells and were treated with vehicle control (VC) or 26OHC (10 μ M) for 16 h to validate LXR α specificity (A). After knockdown of LXR α the expression of the LXR target genes ABCA1 and APOE were analysed by qPCR. Statistical significance was established using 2-way ANOVA (*p<0.05, **p<0.01, ***p<0.001, p<0.0001) and mean of 4 independent replicates with SEM are presented..

4.3.5 Enhanced LXR α activity and function increases the risk of patient relapse.

Enhanced LXR α activity and function has been shown in the TNBC disease relative to the Luminal A disease, but whether this impacts on the patient prognosis, independently of subtype is unclear. To assess whether enhanced LXR α activity is a signature of poor prognosis in TNBC patients, we assessed tumours for oxysterol content, LXR α target gene expression, and gene signatures through correlations between gene expression profiles in tumours in 69 breast tumour samples from the Leeds Breast Tissue Bank (09H1326/108 - 22 tumours, 15/HY/0025 - 47 tumours).

First, we assessed whether markers of LXR α activity are associated with worse prognosis within the TNBC subtype by assessing patient primary tumours for expression of the LXR α target gene ABCA1 in patients who had either suffered an event or not. Events are defined as patients who have suffered a breast cancer relapse but may still be alive or patients who had died from breast cancer. No events are classified as patients who have had no relapse, were disease free and are alive after at least 3 years. To test this aim, RNA was extracted from 69 tumours from a mixture of breast tumour subtypes (**Table 7** – section 3.12.1) and gene expression analysed by qPCR. In TNBC tumours, patients who had suffered an event had significantly higher expression of ABCA1 (Mann-Whitney U Test; $p=0.0036$) relative to patients who had not suffered an event (**Figure 4.17**). In the Non-TNBC tumours, patients who had suffered an event did not have significantly higher expression of ABCA1 (ns) than those who were alive and disease free after at least 3 years (**Figure 4.17**). Tumour expression of ABCA1 was then assessed alongside patient survival to assess whether expression is predictive of survival in Kaplan Meier graphs (**Figure 4.17B**). ROC curves were used to establish the expression cut offs for high and low

expression levels. TNBC tumours with higher expression of ABCA1 (>1) were found to have worse survival than those with lower ABCA1 expression (<1; Logrank test, $p=0.031$). In non-TNBC tumours however, ABCA1 expression was found to have no effect on patient survival (ns).

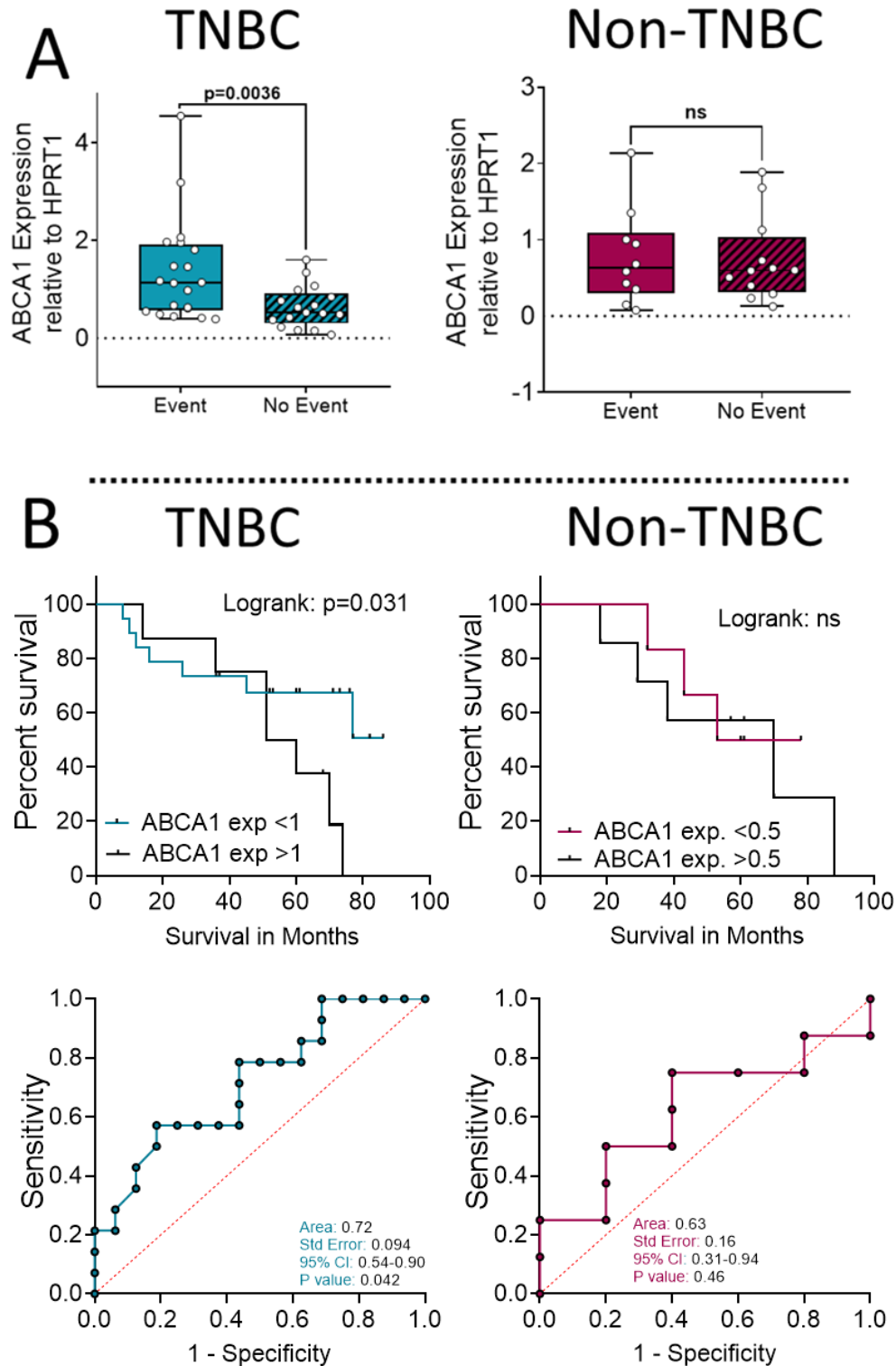


Figure 4. 17 Enhanced expression of ABCA1 was observed in patient tumours who relapsed compared to those with primary disease.

RNA was isolated from 69 breast cancer patient tumours (41 TNBC, 28 HER2 enriched or hormone receptor positive [HR+]) and the expression the canonical LXR target gene ABCA1 was analysed by qPCR. Expression of the target genes were assessed in patients who had suffered a recurrence or BCa related death (Event) and those that had not had (No Event) with at least 3 years follow up from diagnosis. Statistical differences were established using Mann-Whitney U Tests. Patient survival is shown in a Kaplan Meier graph for the TNBC (28) and Non-TNBC (13) subtypes due to significant differences in ABCA1 expression between event and no event groups. Statistical differences were established using a Logrank test, expression cut offs established using ROC curves.

4.4 Discussion

The purpose of this study was to establish if a difference in LXR α activity between ER-negative and ER-positive subtypes of breast cancer could explain why clinical interventions that impact on cholesterol have greater impacts on TNBC than ER-positive disease [5, 46-48, 122, 220, 221, 258]. In this chapter, it was established that although ligand synthesis and concentration were indistinguishable between subtypes, the expression of LXR α and its regulatory factors is skewed towards insensitivity to ligand in ER-positive breast cancers and a more responsive and transcriptionally poised state in the ER-negative breast cancers. As a transcription factor, it would be expected that on balance, and in the absence of other variables, LXR target genes should be more highly expressed in the presence of high levels of LXR. This was found to be the case in ER-negative, but not ER-positive disease. This difference in LXR target gene expression was explained by significantly higher expression of the corepressors NCOR1, NCOR2 and LCOR in the ER-positive disease and was reversible by genetic knockdown of these factors. These data indicate that ER-negative tumours are more sensitive to the increased oxysterols levels that are produced by in high cholesterol environments than ER-positive tumours. Given the role of LXR-oxysterol signaling in BCa, the observations presented here may explain why ER-negative disease is more likely to be ameliorated by cholesterol lowering interventions such as statins and nutrition such as plant-based diets and diets low in saturated fat [46, 47, 220].

Nuclear receptor repression through elevated corepressor expression has been observed in other cancers including bladder [242] and prostate [94, 95], as a mechanism to reduce antiproliferative effects, but this is the first report of reduced

CoR expression that facilitate a NR's activity and associates with worse prognosis. Here, the antiproliferative effects of oxysterol-LXR signaling were assessed through MTT assays and surprisingly found a more sensitive environment in the antiproliferative response to oxysterols in the aggressive ER-negative disease. The ER-positive breast cancer cells MCF-7 have previously been shown to be more sensitive to LXR induced cell cycle arrest than the ER-negative MDA-MB-231 breast cancer cells after exposure to synthetic LXR ligands [134]. Interestingly, LXR stimulation was shown to induce expression of the LXR target gene ABCA1 in the BCa cells with a more enhanced transcriptional output observed in the ER-negative cells compared to the ER-positive cells, which matches our observations in this study. The differences in antiproliferative effects observed in the study by Vedin *et al* [134], compared to our study may be due to the nature of LXR specific synthetic agonists. The LXR ligands used in our study were oxysterols, which are estrogenic and show the antiproliferative actions of oxysterols on ER and LXR in ER-positive cells. As demonstrated in this chapter, there are notable differences in nuclear receptor biology between BCa subtypes beyond those of ER and PR expression. Furthermore, responsiveness to ligands in the subtypes is controlled by corepressor expression and indicates differential cholesterol metabolism between subtypes.

In some tumour types it appears there may be selective advantages associated with the retention of LXR signaling which compensates for the antiproliferative actions of the oxysterol-LXR axis. The oxysterol signaling pathway has been associated with the metastasis of breast cancer cells in ER-negative disease [21]. It would be interesting to determine if repressed LXR activity is required for the initial primary tumour development to impair its antiproliferative actions, and in later stage disease returns

to support migration. Consistent with this is the observation that 25OHC is elevated in serum of breast cancer patients at relapse compared to those with primary disease [136].

Gene expression patterns and responsiveness to ligand appear to be altered in cancer biology. With the use of nuclear receptor cofactor expression as therapeutic biomarkers, it may be possible to reinstate pre-cancer gene expression responsiveness through targeting of corepressors such as NCOR. NCOR1 for example, was identified as an independent prognostic marker in a cohort of mixed breast cancer subtypes [259]. Interestingly for the treatment of ER-positive breast cancers, tamoxifen depends on NCOR1 recruitment to the ER to repress the activity of the receptor and therefore its target genes [260]. Additionally, our data suggest corepressor expression levels are high in pre-treatment ER-positive tumours, which may be to prevent LXR and other nuclear receptors driving anti-proliferative effects. This may cause impacts on oxysterol dependent ER activity, which as several oxysterols are estrogenic and pro-proliferative when liganded with the ER, high corepressor activity may impede oxysterol-ER dependent proliferation.

LCOR is another corepressor of great interest in this chapter. LCOR recruitment is somewhat different to that of NCOR. LCOR is a ligand recruited corepressor and its recruitment to promoters by agonists, and can repress gene expression rather than enhance or activate gene transcription [261]. In this study, LCOR expression was found to be higher in the ER-positive primary breast tumours as well as the ER-positive breast cancer cells (MCF-7), which has previously been associated with improved survival in BCa patients [262]. In support of the observations where ER-positive BCa displayed enhanced LCOR expression, LXR ligands also down-regulated

the expression of APOE but only in the ER-positive breast cancer cells, implicating LCOR as the corepressor recruited in the MCF-7 cells to impair activation of the LXR target gene APOE. This was further supported by increased expression of APOE in MCF-7 cells that had LCOR silenced/knocked down (**Figure 4.15B**).

4.5 Summary

In this chapter LXR α activity and function has been established as subtype specific. Oxysterols have been confirmed as natural LXR agonists in TNBC and Luminal A BCa cell lines. Enhanced LXR α activity has been identified in the TNBC tumours and cell lines and are poised for response to ligand relative to the Luminal A subtype. These findings were established through mining publicly available datasets, qPCR analyses, western blot protein analysis, MTT assays and the generation of LXR α -luciferase reporter cell lines. We also assessed publicly available datasets to assess correlations of potential LXR target genes to validate highly correlated genes by qPCR. Furthermore, we performed knockdowns to assess subtype response to ligand after co-repressor gene silencing and established NCOR1, NCOR2 and LCOR knockdown restored sensitivity to the Luminal A cell line comparable to the TNBC response to ligand. And finally, we showed enhanced LXR α activity in patients who had relapsed compared to those that had not through methods of LCMS/MS and genes expression analyses in patient primary tumours.

Chapter 5

LXR links cholesterol hydroxylation to chemotherapy resistance in breast cancer.

5.1 Introduction

LXR and oxysterol signalling have been linked to the progression of BCa in multiple studies [21, 105, 110]. In the previous chapter, the differential expression of cofactors and ligand concentration were explored as mechanistic reasons for why TNBC and Luminal A BCa subtypes process and respond to cholesterol differently. In TNBC subtype, lower expression of corepressors was identified as a likely reason for enhanced LXR α activity relative to the Luminal A BCas. Knockdown of the corepressors NCOR1, NCOR2 and LCOR enhanced LXR response to ligand in both Luminal A and TNBC cell lines and the response to some ligands was equalised. LXR ligands are known to be anti-proliferative in a wide variety of cancer cell lines [68, 249], so it remains unclear why TNBC, the more aggressive form of BCa, would deregulate expression of its co-factors to have enhanced oxysterol signalling.

In addition to their anti-proliferative actions, oxysterols are also known to have proapoptotic and cytotoxic effects on tumour cells. Oxysterols are consequential of the enzymatic or non-enzymatic oxidation of cholesterol. The enzymatic conversion of cholesterol to oxysterols involves the enzymes belonging to the cytochrome P450 family (CYPs) and are responsible for the synthesis of 24OHC and 26OHC. The synthesis of 25OHC occurs when cholesterol is hydroxylated by CH25H, an enzyme that utilises diiron cofactors to catalyse hydroxylation (**Figure 5.1**). The non-enzymatic conversion or auto-oxidation involves reactive oxygen and nitrogen species (ROS) such as hydroxyl radical or hydrogen peroxide, and an example of this includes the synthesis of 7-ketocholesterol. The overproduction of ROS as a

bipproduct of cholesterol auto-oxidation is linked to the proapoptotic effects of oxysterols as shown in 7-ketocholesterol treated RPE cells, which have been shown to significantly enhance mitochondrial DNA damage [263]. Furthermore, oxysterol induced apoptosis is facilitated by internal mitochondrial pathways [264, 265] and an external Fas/Fas death receptor-dependent pathway [266] of which highlight an exploitable mechanism through targeting of the LXRs.

Total cholesterol, LDL-C and oxysterol levels have been shown to be elevated in tumours relative to healthy tissue [110, 176-178], yet low total serum cholesterol and LDL-C levels have been observed in patients with cancer [179, 180] suggesting cholesterol may accumulate within tumours or be synthesised by tumour microenvironment support cells. Oxysterols have been shown to promote BCa tumour growth [105, 110], metastasis [21], and to induce LXR-dependent EMT in ER-negative tumours [105]. Furthermore, elevated oxysterol levels have been found in patient serum at relapse [136] and knockdown of CYP27A1, the rate-limiting enzyme in the synthesis of 26OHC, resulted in the reduction of hypercholesterolemia-promoted tumour growth in mice [105]. Wu *et al*, supported these studies by the Nelson group [21, 105], demonstrating 26OHC promotes ER-positive BCa growth via diminished CYP7B1 expression [110]. Moreover, larger tumours derived from TNBC BCa cells were observed in mice with high circulating LDL-C compared to mice with low LDL-C [51]. Research so far has shown oxysterols have links to BCa progression and the enhanced LXR activity in TNBC may be contributing to the higher risk of relapse associated with this subtype.

Recurrence of cancer is common in the TNBC subtype and relapse often occurs due to the failure or lack of response to anticancer therapies resulting in the

development of chemotherapy resistance [56]. The active efflux of chemotherapy agents from within a cell is a key mechanism of chemoresistance [61]. Several members of the ATP-binding cassette transporters (ABC-transporters), including BCRP [226, 267], p-gp/ABCB1 [224, 268] and MDRP [225, 269] are linked with unsuccessful drug effect and cancer cell survival. Importantly, 24OHC has been shown, via LXR α , to regulate expression of the p-gp/ABCB1 in the BBB [228]. Additionally, as oxysterols are known to have cytotoxic and proapoptotic effects it may provide insight into oxysterol induced expression of the p-glycoprotein/ABCB1. Given the enhanced LXR α activity and function in TNBCs, and that p-glycoprotein is an important clinical factor associated with chemotherapy resistance, if p-gp/ABCB1 is regulated by LXR α in BCa it may be a previously unidentified route of chemotherapy resistance in TNBC.

5.2 Hypothesis and Aims

Oxysterols are moderately reactive with DNA, proteins, and lipids, and if further metabolised form bile acids that have increased propensity to react with cellular components. A tumour that has developed in a cholesterol rich environment is pre-equipped (*de novo*) with detoxification mechanisms that not only allow removal of potentially cytotoxic metabolite metabolites but xenobiotics such as chemotherapy agents as well. Enhanced LXR activity in TNBC promotes chemoresistance by direct activation of drug efflux proteins.

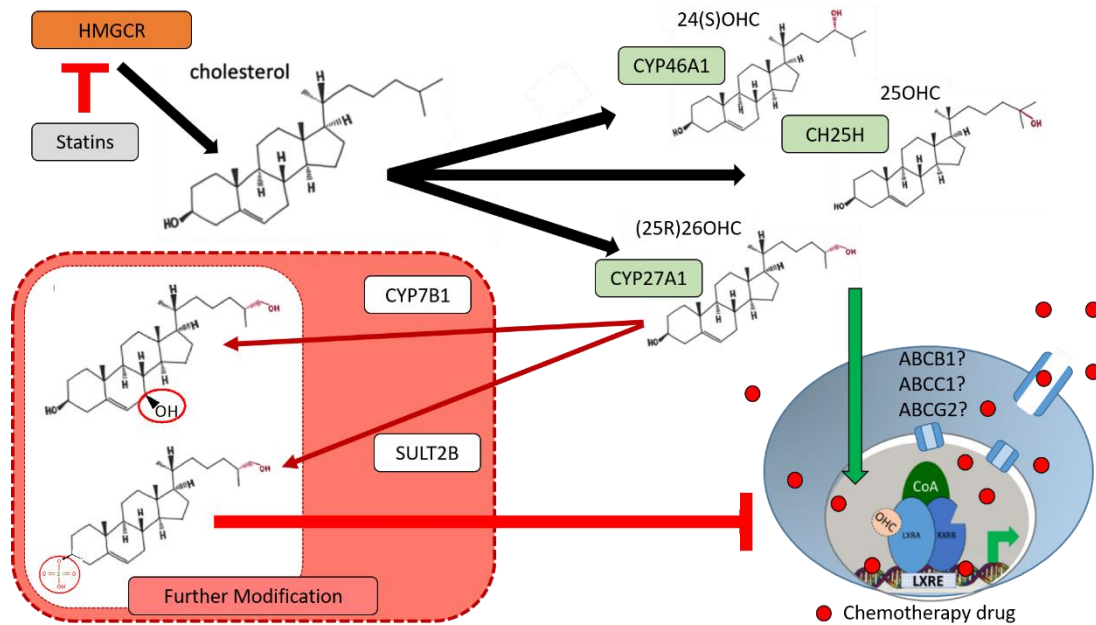


Figure 5. 1 Do LXR ligands alter the efficacy of chemotherapy drugs?

HMGCR is the enzyme responsible for the synthesis of cholesterol. Cholesterol can be modified by enzymes such as CYPs (shown are CYP46A1 and CYP27A1) to convert cholesterol to their hydroxylated state as oxysterols (24OHC and 26OHC). Other enzymes such as CH25H utilise diiron cofactors to catalyse hydroxylation for the conversion of cholesterol to oxysterols (25OHC), or conversion can occur through auto-oxidation or non-enzymatic means. Oxysterols can then bind to and activate LXR α in breast cancer cells. Further modifications such as sulphonation (SULT2B1) or hydroxylation of the B ring (CYP7B1) however, inactivate the oxysterols impairing their ability to interact with LXR. Here we hypothesise that oxysterols can reduce chemotherapy efficacy through up-regulation of genes involved in chemotherapy drug export.

The aims of this chapter were to:

- Establish if LXR α regulation alters cancer cell line responses to chemotherapy.
- Determine whether LXR regulates expression of genes implicated in chemoresistance.
- Establish if LXR α activity is associated with worse chemotherapy efficacy in breast cancer patients.

5.3 Results

5.3.1 LXR activation protects breast cancer cells from chemotherapy assault.

To establish if LXR ligands alter chemotherapy response in breast cancer cell lines colony forming assay, MTT assay, and mouse xenografts were performed. First, we performed colony forming assays to assess the effects of LXR α regulation during chemotherapy treatments. Luminal A BCa cell cultures (MCF-7) and TNBC cell cultures (MDA-MB-468 and MDA-MB-231) were pre-treated with LXR synthetic ligands (T0901317, GW3965 and GSK2033) for 24 h before the chemotherapy agent epirubicin for a further 24 h. Cells were then counted and 500 live cells/well were plated per treatment group and left to recover and form colonies for 12 days. After the recovery period colonies were stained with crystal violet and colonies counted (**Figure 5.2**).

The LXR agonist T0901317 enhanced colony formation and cell survival when given as a pre-treatment before epirubicin in all BCa cells (paired t-tests; $p < 0.01$) as did the LXR agonist GW3965 ($p < 0.01$). Furthermore, the LXR antagonist GSK2033 decreased colony formation and cell survival when given as a pre-treatment before epirubicin in TNBC cells ($p < 0.05$), but not in MCF-7 cells (ns). No effects on colony forming efficiency were observed in the LXR ligand treatment groups in the absence of epirubicin (ns), indicating the increased colony formation is likely due to rescue from epirubicin rather than enhanced inherent colony forming capacity.

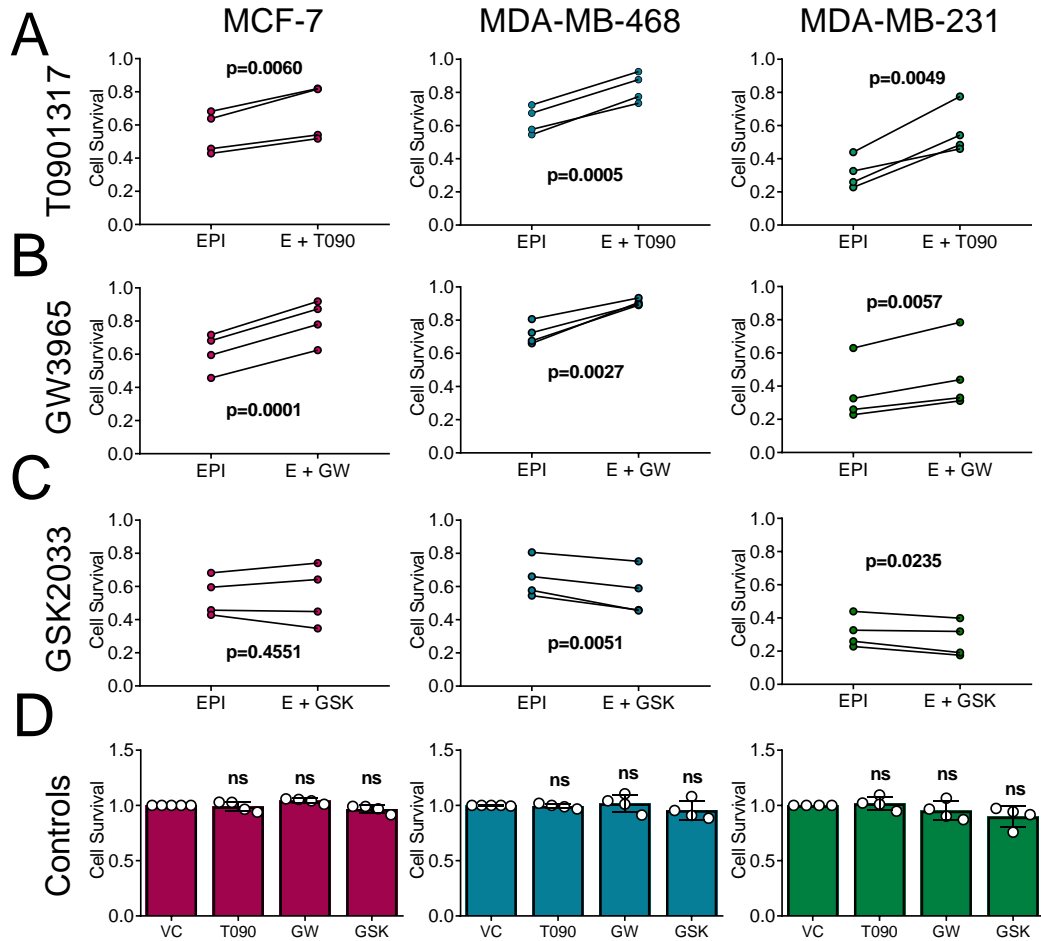


Figure 5. 2 Treatment of breast cancer cell cultures with synthetic LXR ligands protects against subsequent exposure to the chemotherapy agent epirubicin.

ER-positive (MCF-7) and triple negative (MDA-MB-468 and MDA-MB-231) breast cancer cell cultures were treated with the synthetic LXR ligands (a) T0901317 (T090), (b) GW3965 (GW), (c) GSK2033 (GSK) at 1 μ M, or vehicle control, for 24 h before exposure to epirubicin (25 nM) for a further 24 h. Each line shows an independently replicated experiment (generated from the mean of 3 technical repeats) comparing the effect on colony formation of epirubicin alone (EPI) or first pre-treating cells with ligand (EPI + T090/GW/GSK). In (d) cells were treated with LXR ligands but not exposed to epirubicin. p-values show results from paired t-tests (a, b and c) or one-way ANOVA (d) after correction for multiple testing. Data shown are mean of 4 independent replicates with SEM.

Next, the colony forming assays were repeated to determine if endogenous LXR ligands (oxysterols) recapitulated the chemoresistance inducing effects of synthetic LXR agonists. Luminal A breast cancer cell cultures (MCF-7) and TNBC cell cultures (MDA-MB-468 and MDA-MB-231) were pre-treated with LXR endogenous ligands (24OHC, 24,25-EC and 26OHC) for 24 h before the chemotherapy agent epirubicin for a further 24 h (**Figure 5.3**). 24OHC enhanced the number of cells able to establish

a colony when given as a pre-treatment before epirubicin in TNBC cells (paired t-tests; $p < 0.01$), but not in MCF-7 cells (ns). 24,25-EC enhanced colony formation when given as a pre-treatment before epirubicin in all BCa cells (paired t-tests; $p < 0.05$), as did 26OHC (paired t-tests; $p < 0.01$). These data (**Figure 5.2 and 5.3**) demonstrate that activation of the LXR pathway with synthetic agonists or endogenous ligands, increases the ability of several breast cancer cell types to resist chemotherapy and form colonies.

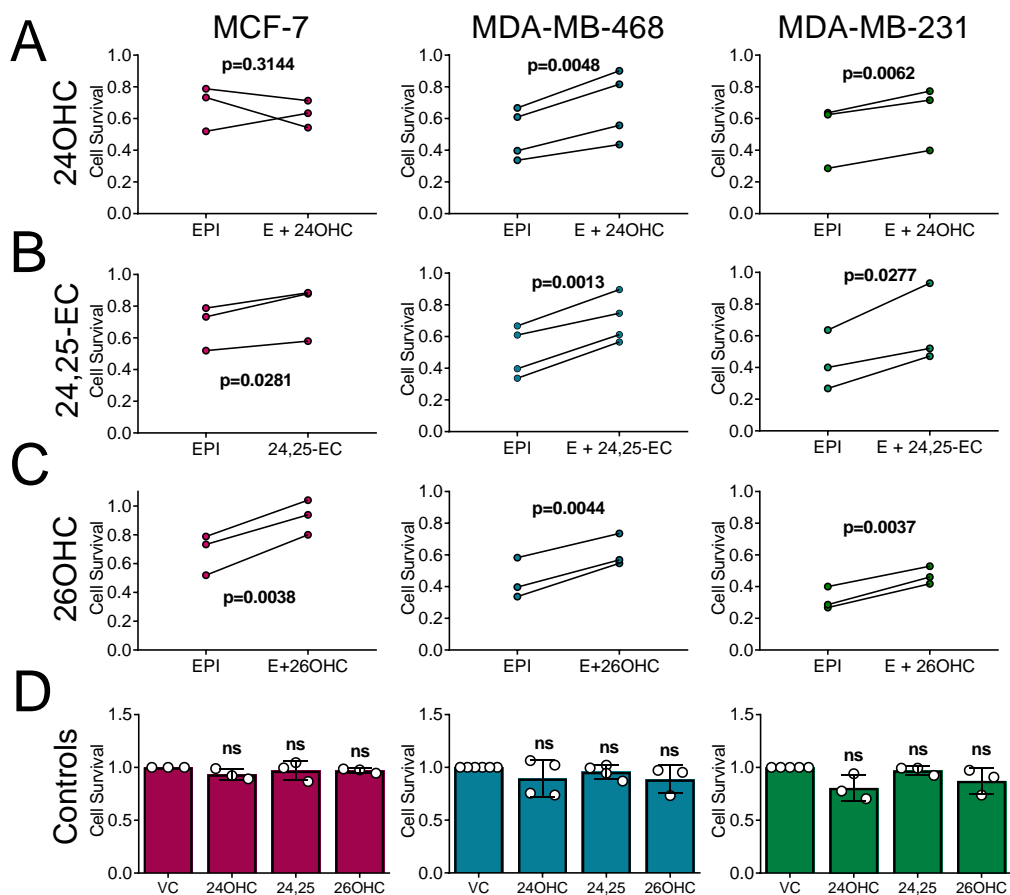


Figure 5. 3 Treatment of breast cancer cell cultures with endogenous LXR ligands protects against subsequent exposure to the chemotherapy agent epirubicin.

ER-positive (MCF-7) and triple negative (MDA-MB-468 and MDA-MB-231) breast cancer cell cultures were treated with the endogenous LXR ligands (a) 24-hydroxycholesterol (24OHC), (b) 24,25-epoxycholesterol (24,25-EC), (c) 25,26-hydroxycholesterol (26OHC) at 10 μ M, or vehicle control, for 24 h before exposure to epirubicin (25 nM) for a further 24 h. Each line shows an independently replicated experiment (generated from the mean of 3 technical repeats) comparing the effect on colony formation of epirubicin alone (EPI) or first pre-treating cells with ligand (EPI + 24OHC/24,25-EC/26OHC). In (d) cells were treated with LXR ligands but not exposed to epirubicin. p-values show results from paired t-tests (a, b and c) or one-way ANOVA (d) after correction for multiple testing. Data shown are mean of 3-4 independent replicates with SEM.

The next aim was to determine if oxysterols impair the ability of epirubicin to induce cell death, by using mitochondrial function as a surrogate marker of cell viability/cell number in MTT assays (NB: these experiments were performed and analysed by Priscilia Lianto).

The MTT assays (**Figure 5.4**) showed significant reductions in epirubicin efficacy after exposure to 24OHC in the MCF-7 cells at 1 μ M (2-tailed unpaired t-tests; $p=0.004$) and 10 μ M ($p=0.025$), MDA-MB-231 cells at 1 μ M ($p=0.0026$) and 2.5 μ M ($p=0.0013$) and MDA-MB-468 cells at 1 μ M ($p=0.0452$) and 2.5 μ M ($p=0.0198$) and 10 μ M ($p<0.0001$). Significant reductions in epirubicin efficacy were observed after exposure to 25OHC in the MCF-7 cells at 2.5 μ M ($p<0.0001$) only, MDA-MB-231 cells at 2.5 μ M ($p=0.0074$) and 10 μ M ($p=0.0136$) and MDA-MB-468 cells at 2.5 μ M ($p=0.002$) only. Furthermore, significant reductions in epirubicin efficacy were observed after exposure to 26OHC in the MCF-7 cells at 1 μ M ($p=0.0048$) and 2.5 μ M ($p=0.0056$), MDA-MB-231 cells at 10 μ M ($p=0.0167$), and in MDA-MB-468 cells at 10 μ M ($p<0.0001$). In summary these data show oxysterols reduce the efficacy of the chemotherapy drug epirubicin.

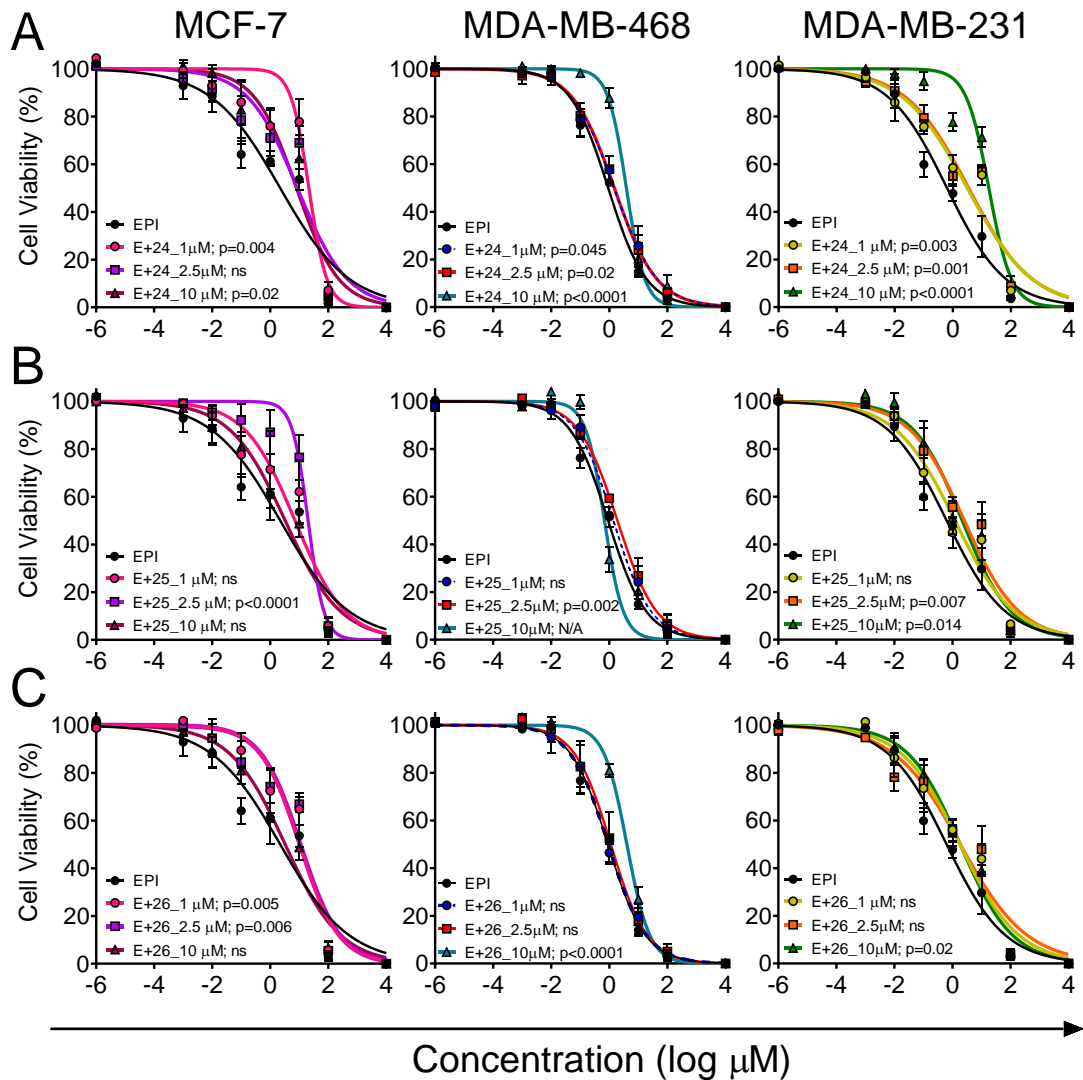


Figure 5. 4 Oxysterols alter the efficacy of the chemotherapy agent epirubicin.

The anti-proliferative effects of epirubicin alone and in the presence of oxysterols were assessed by MTT in MDA-MB-468, MDA-MB-231 and MCF-7 cells over 72 h. Cells were treated with ligand treatment for 24 h alone (A: 24OHC, B: 25OHC and C: 26OHC), then with epirubicin for a further 48 h. Data are presented as means of 3 independent replicates with SEM and non-linear regression. Experiments performed and data analysed by Priscilia Lianto.

5.3.2 The oxysterol-LXR axis regulates genes which promote chemotherapy resistance in triple negative breast cancer.

To establish the molecular mechanisms through which LXR appeared to be exerting chemotherapy resistance, hypothesis driven and hypothesis generating approaches were taken. The initial candidate for LXR-mediated chemoresistance was p-gp/ABCB1; previous reports had identified p-gp/ABCB1 was regulatable by the LXR ligand 24OHC albeit in the BBB [228]. To identify other molecular effectors of LXR-

mediated chemotherapy resistance, the following steps were performed: i) a systematic review to identify all genes previously implicated in breast cancer chemoresistance (**Appendix A – A.2**); ii) evidence for LXR α binding to the promoters of these genes was then sought by mining CHIP-Seq data public databases [231]; iii) assessment of correlations between mRNA expression of LXR α and chemotherapy resistance target genes; iv) validation of top targets in BCa cell lines.

5.3.2.1 Systematic Literature Review.

Pubmed was searched (**for search criteria and flow diagram see methods section 3.11.2**) and 130 genes identified as potential candidates (**Appendix A - A.2**) containing a range of chemotherapy mechanisms including DNA repair (BRCA1, BRCA2, XRCC1), detoxification (ABCC1, ABCG2, CBR1) and evasion of apoptosis (BIRC3, BCL2, TP53)..

5.3.2.2 LXR α binding.

CHIP-Seq data was mined from the Cistrome database [231] to check for LXR α binding (see **Appendix A – A.3** for list of genes and binding scores).

5.3.2.3 Assessment of chemotherapy resistance gene expression in breast cancer patient tumours.

Genes were then assessed for mRNA expression levels [230] in the CBioportal database [229]. The expression of genes implicated in chemoresistance was then assessed for any correlations with LXR α and LXR β . A False Discovery Rate (FDR) of what 1 % was used to correct for multiple testing (denoted with a dotted line). The analysis is shown as a volcano plot showing correlation coefficient against FDR in ER-negative BCa tumours (**Figure 5.5**). We observed that LXR α significantly correlated with 11/130 chemoresistance genes in the TNBC tumours which was significantly more than 0/130 genes for LXR β (Fisher's exact test: $p < 0.0001$). A mixture of

previously identified LXR targets (p-gp/ABCB1 and MMP9) and apparently novel, aside from their listing in Cistrome ChIP-Seq analyses (SLC31A2, BIRC3, NFKB1, TFPI2, TRIM2, ERBB3, GPSM3, FPGS, and CXCL5) were found. Of these, five genes (SLC31A2, BIRC3, p-gp/ABCB1, GPSM3 and CXCL5) with the strongest positive correlations were followed further to test the *in-silico* predictions that these genes should be inducible in the TNBC cells. Recruitment of LXR α to target gene promoters are shown in

Appendix 2 – A.2.

Next, gene correlations were performed individually to show how LXR α and LXR β correlate with genes in the TNBC and Luminal A BCa samples (**Figure 5.6**). LXR β failed to significantly correlate with the selected chemotherapy resistant genes SLC31A2, BIRC3, and CXCL5 in the TNBC and Luminal A patient tumours (Pearson's correlation test: ns), but GPSM3 significantly correlated with LXR β in the Luminal A patient tumours ($p < 0.0001$; $R = 0.4688$) as well as in the TNBC tumours ($p = 0.0016$; $R = 0.3455$). Expression of p-gp/ABCB1 only weakly correlated with LXR β expression in the TNBC tumours ($p = 0.05$; $R = 0.2146$) but not with the Luminal A BCas. Interestingly, the selected chemoresistance genes (SLC31A2; $p < 0.0001$, p-gp/ABCB1; $p < 0.0001$, GPSM3; $p < 0.0001$, and CXCL5; $p < 0.0001$) had much stronger correlations in the TNBC tumours except BIRC3 which was equally as strong ($p < 0.0001$) compared to the Luminal A tumours genes (SLC31A2; $p = 0.0085$, p-gp/ABCB1; ns, GPSM3; $p = 0.0002$, CXCL5; ns).

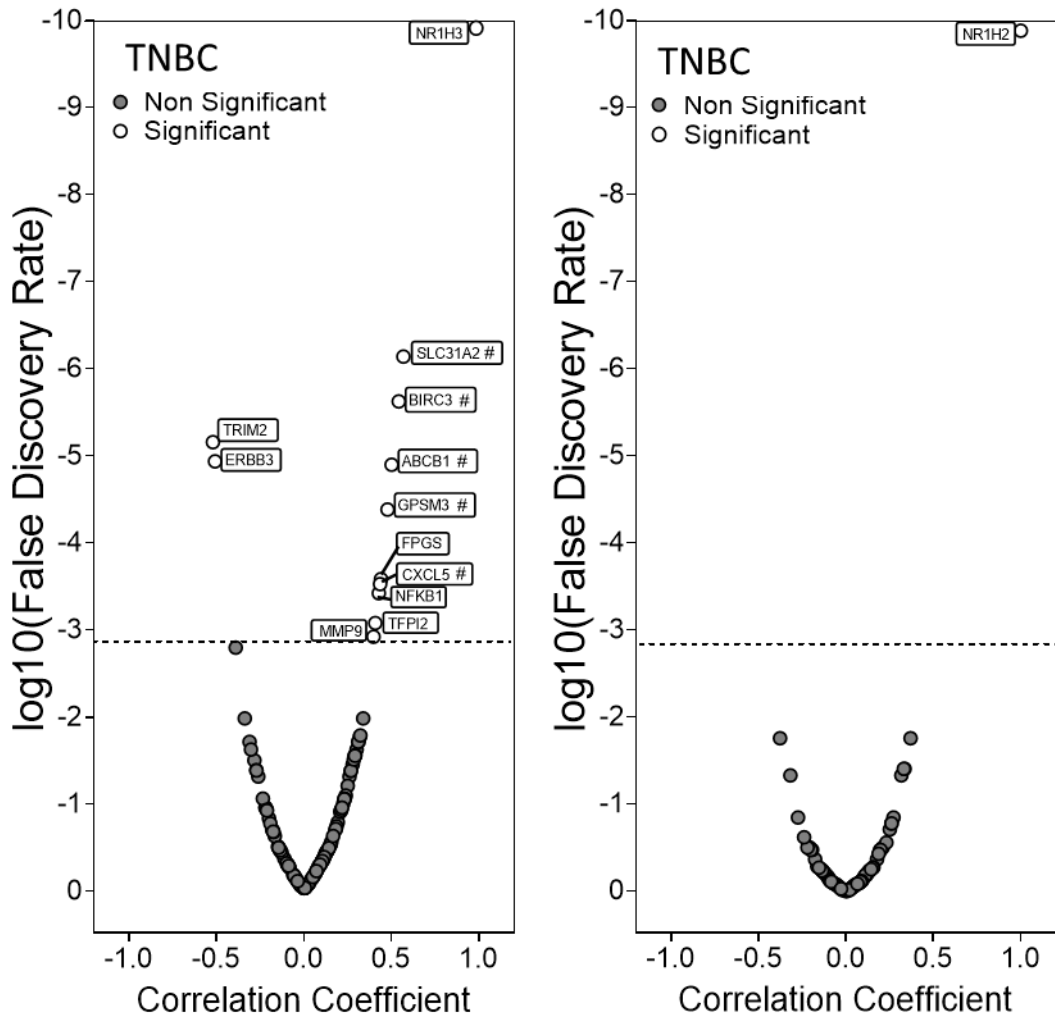


Figure 5. 5 LXR α is significantly more likely to correlate with chemoresistance genes in TNBC..

130 genes implicated in chemotherapy resistance in cancer were identified from literature and included for analysis if they appeared in the top 50 % of LXR α bound scores and the genes were found bound to their promoters in a mouse macrophage ChIP-Seq dataset [256] accessed from Cistrome [231]. These genes were then assessed for correlation with LXR α and LXR β expression in 89 TNBC primary breast tumours [229, 230]. Data display the correlation coefficient (R) against correlation significance (on a log₁₀ scale). Fishers' exact test was used to assess significance between LXR α and LXR β correlations with genes implicated in chemoresistance ($p < 0.0001$). Genes marked with a # were later validated by qPCR analysis.

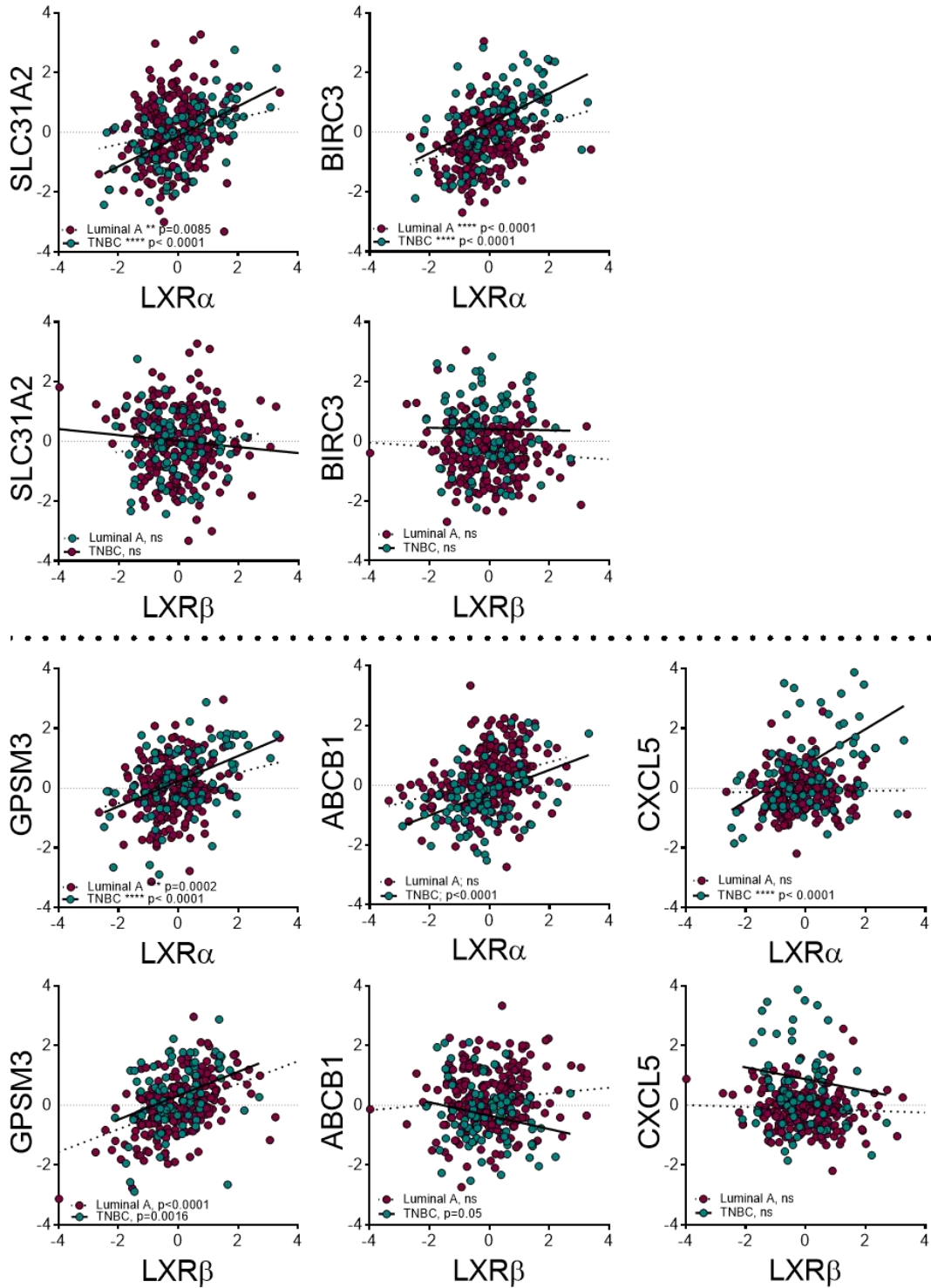


Figure 5. 6 Examples of the some of the strongest correlating genes with LXR α in TNBC and Luminal A BCa patient tumours.

Expression of genes implicated in chemoresistance were correlated with LXR α and LXR β in 89 TNBC and 234 Luminal A/ER-positive breast tumours [230] accessed from the patient database CBioportal [229]. Statistical significance was assessed using Pearson's correlation test with linear regression.

5.3.2.4 *In vitro* validation of chemotherapy resistance genes as LXR α targets.

To clarify if the chemotherapy resistance genes identified as correlated with LXR α expression and had LXR α binding in their promoters, were targets, their transcriptional output was assessed after treatment with LXR ligands. Expression of the chemotherapy efflux pump p-gp/ABCB1 was significantly increased in MDA-MB-468 by all agonists ($p < 0.05$) and by all endogenous agonists in MDA-MB-231 cells ($p < 0.01$) (**Figure 5.7**). In MCF-7 cells, agonists either had no effect or decreased expression ($p < 0.05$), which was reminiscent of how APOE responded previously (**Figure 4.8**). GSK2033 prevented 26OHC mediated induction in both TNBC cell lines (468 $p = 0.0038$, 231 $p = 0.0008$).

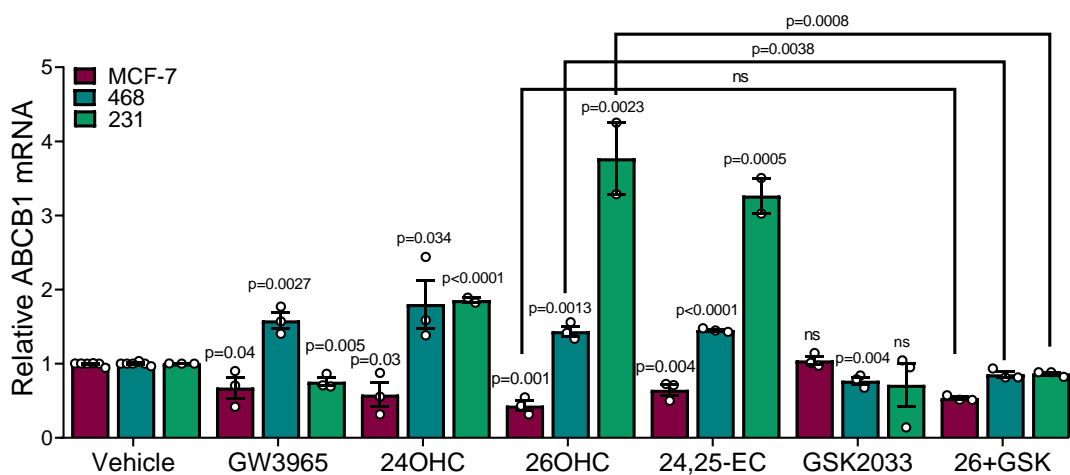


Figure 5. 7 LXR ligands induce expression of the p-glycoprotein/ABCB1 in TNBC cells but downregulates its expression in Luminal A cells in an LXR dependent manner.

TNBC (MDA-MB-468 and MDA-MB-231) and ER-positive (MCF-7) cells were treated with LXR ligands (synthetic 1 μ M, endogenous 10 μ M) for 16 h and expression of p-gp/ABCB1 was assessed by qPCR ($\Delta\Delta$ ct using HPRT and normalised to vehicle). Data shown are mean of 2-3 independent replicates with SD, statistical analysis was established using 1-tailed unpaired t tests.

LXR ligands also regulated three of the remaining four chemoresistance genes selected for further analysis (**Figure 5.8**). In both TNBC lines, GSPM3 and CXCL5 were significantly altered ($p < 0.05$) whilst BIRC3 induced in MDA-MB-468 only. In MCF-7 cells, BIRC3 and CXCL5 expression was altered by LXR ligand (**Figure 5.8**). In no cell

line was SLC31A2 regulated (ns). Taken with the data presented above, p-gp/ABCB1 was the strongest candidate for LXRs chemotherapy resistance effects. P-gp/ABCB1 responded to all ligands in both TNBC cell lines, was correlated with LXR α , and had demonstrable recruitment of LXR to its promoter. P-gp/ABCB1 was selected for more detailed evaluation as the link between LXR and chemotherapy resistance.

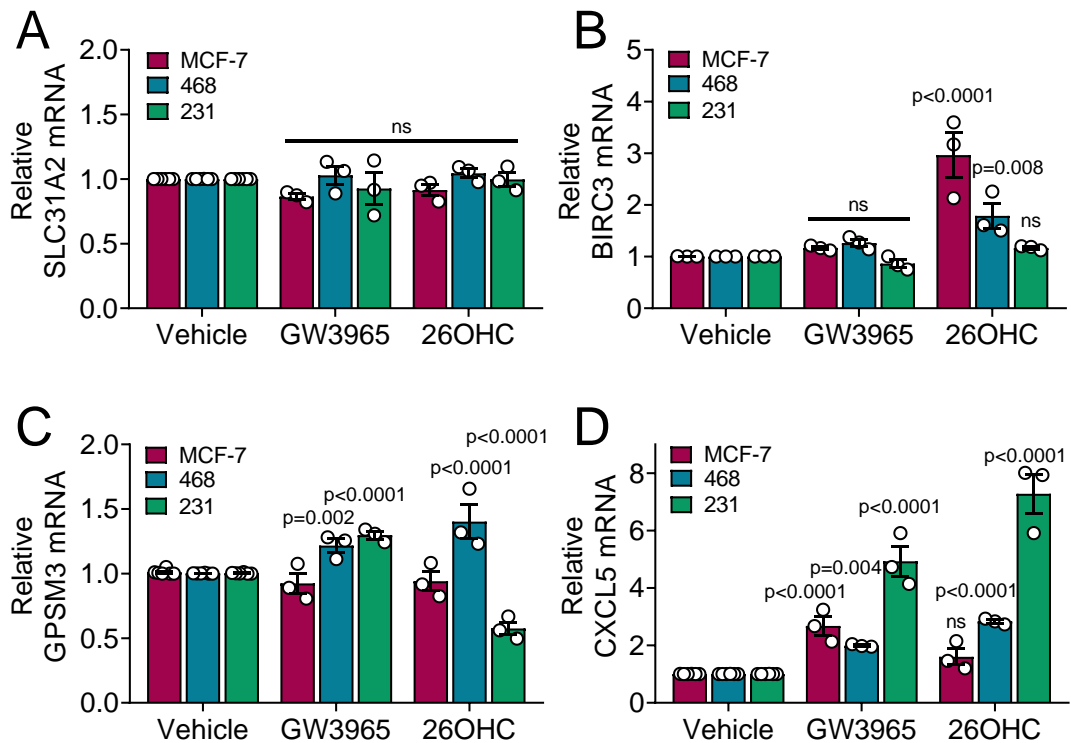


Figure 5. 8 LXRs ligands also drive transcription of predicted genes involved in chemoresistance in TNBC.

TNBC (MDA-MB-468 and MDA-MB-231) and Luminal A/ER-positive (MCF-7) cells were treated with LXR ligands (synthetic 1 μ M, endogenous 10 μ M) for 16 h and expression of SLC31A2 (A), BIRC3 (B), GPM3 (C), CXCL5 (D) was assessed by qPCR ($\Delta\Delta$ Ct using HPRT and normalised to vehicle). Data shown are mean of three independent replicates with SD, statistical analysis was established using 1-tailed unpaired t tests.

5.3.3 LXR regulates chemotherapy drug efflux from breast cancer cells.

As p-gp/ABCB1 expression was shown to be induced by 24OHC in literature (albeit in the BBB) [228], and later in TNBC cells (Figure 5.6), our aim was to establish a functional role for enhanced p-gp/ABCB1 expression in TNBC. To explore this role, a new assay was developed to exploit the natural fluorescence of epirubicin in a high throughput (96-well plate) and time resolved system; epirubicin efflux was measurable in time-matched using signal decay rates under different experimental conditions. In the TNBC cell lines, pre-treatment with the LXR ligand GW3965 (**Figure 5.9**) and endogenous ligands (**Figure 5.10**) significantly enhanced the export of epirubicin relative to control. Verapamil (a p-gp/ABCB1 inhibitor), but not MK571 or KO131 (BCRP and MRP1 inhibitors) enhanced epirubicin loading (**Figure 5.11**) and reversed LXR dependent efflux in TNBC cell lines but not MCF-7 and reversed LXR dependent efflux (**Figure 5.9-11**). In summary, these data suggest that LXR can increase epirubicin efflux, this was only observed in TNBC cell lines, and it is dependent on p-gp/ABCB1.

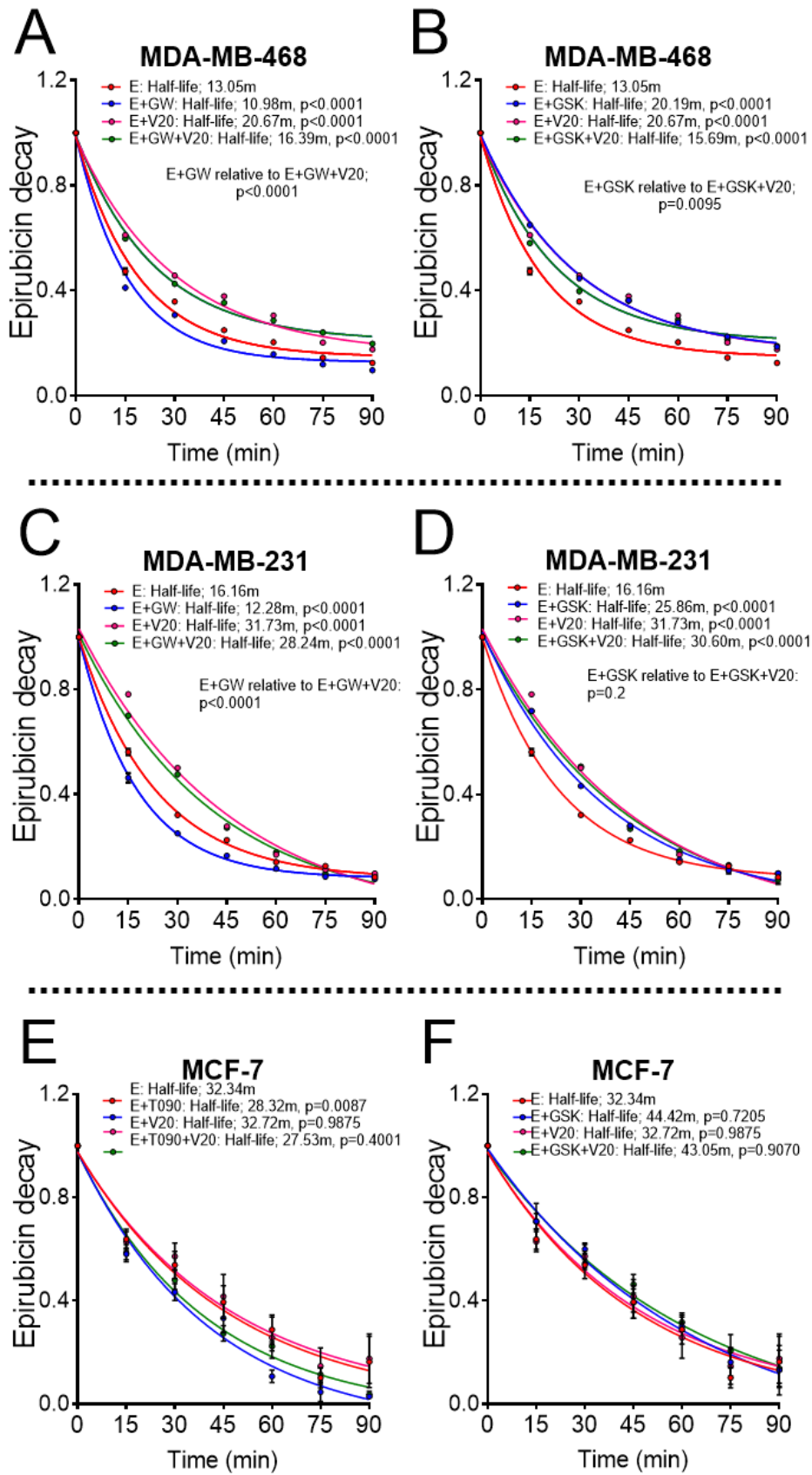


Figure 5. 9 The synthetic LXR ligand GW3965 enhances epirubicin export via p-gp/ABCB1 in TNBC cells.

MDA MDA-MB-468 (A+B), MDA-MB-231 (C+D) and MCF-7 (E+F) cells were pre-treated with LXR ligands GW3965 (A+C) or T0901317 (E), GSK20333 (B, D, F) or vehicle for 16 h. Cells were then treated with the p-gp/ABCB1 specific inhibitor verapamil 20 μ M (V20) or vehicle for 30 min, before cells were loaded with epirubicin (50 μ M) for 1h. Fluorescence of epirubicin was measured at 15 min intervals for 90 min. Mean and standard error of the mean of 3 independent replicates (performed with 6 technical replicates) with SEM is shown. The half-life of the intra-cellular epirubicin signal was determined using dissociation one phase exponential decay, (n=3).

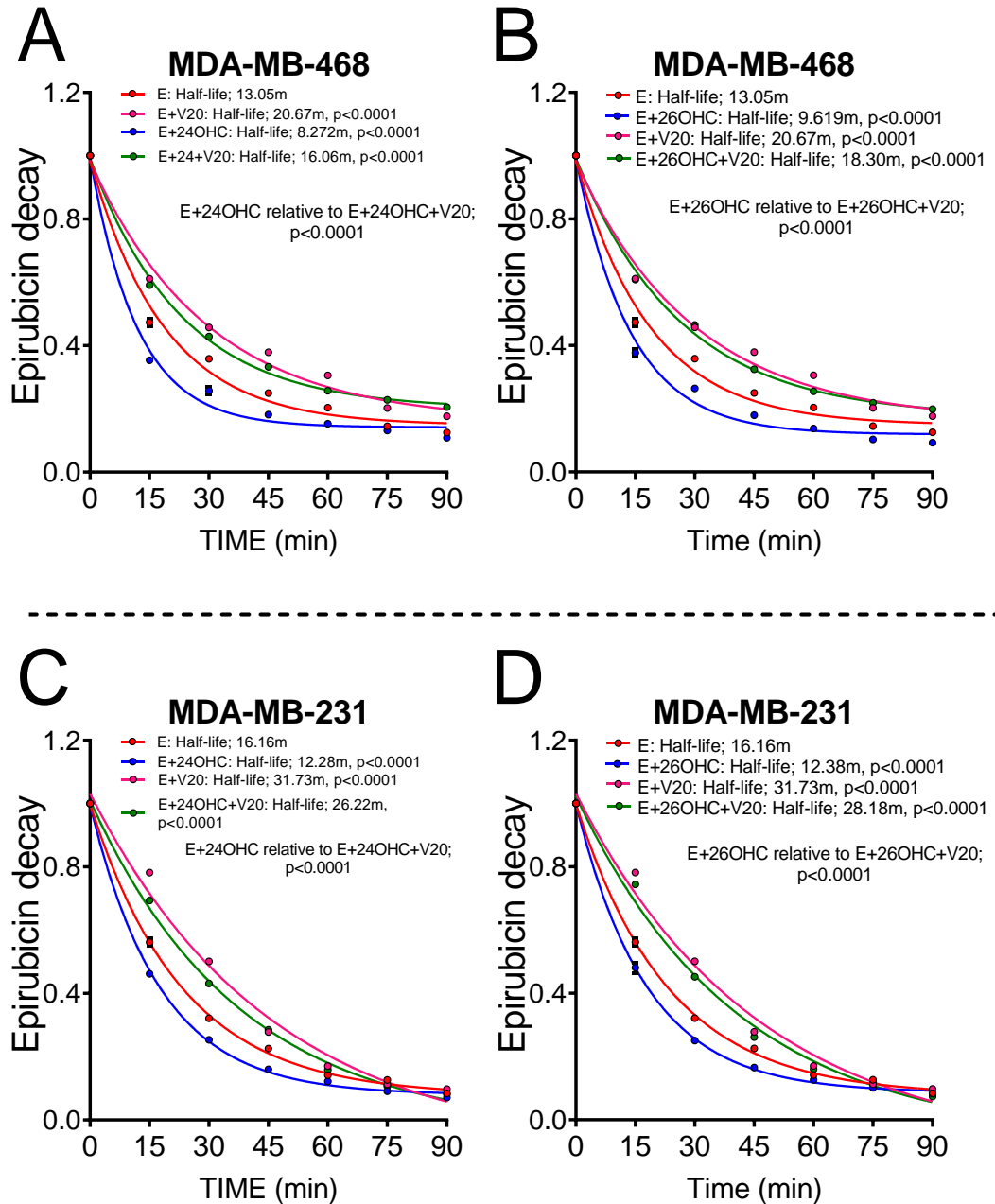


Figure 5. 10 Oxysterols enhance epirubicin export and is reversed by verapamil in TNBC cells.

MDA-MB-468 (A+B) and MDA-MB-231 (C+D) cells were pre-treated with the LXR ligands 24OHC (A+C) and 26OHC (B+D) or vehicle for 16h. Cells were then treated with the p-gp/ABCB1 specific inhibitor verapamil 20 μ M (V20) or vehicle for 30 min, before cells were loaded with epirubicin (50 μ M) for 1h. Fluorescence of epirubicin was measured at 15 min intervals for 90 min. Mean and standard error of the mean of 3 independent replicates (performed with 6 technical replicates) with SEM is shown. The half-life of the intra-cellular epirubicin signal was determined using dissociation one phase exponential decay, (n=3).

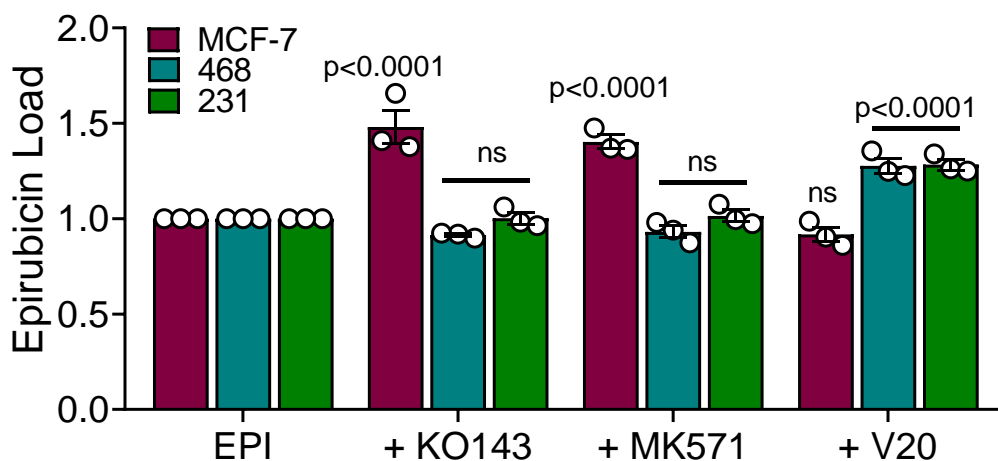


Figure 5. 11 The p-gp/ABCB1 inhibitor verapamil increases intra-cellular retention of epirubicin in TNBC cells but not MK571 and KO143 inhibitors.

TNBC (MDA-MB-468 and MDA-MB-231) and Luminal A/ER-positive (MCF-7) cells were seeded into black 96-well plates and after 24 h they were pre-treated with KO143 (BCRP/ABCG2 inhibitor), MK571 (MRP1/ABCC1 inhibitor) or verapamil [V20] (p-gp/ABCB1 inhibitor) for 30 minutes before a treatment of epirubicin (50 μ M) for 1 h. Cells were washed with PBS and epirubicin within the cells was measured fluorescently. Data shown are mean of three independent replicates with SEM, statistical analysis was established using 2-way ANOVA and corrected for multiple tested.

5.3.4 P-gp/ABCB1 dependent chemoresistance is partially dependant on LXR α in breast cancer.

To prove LXR α was responsible for mediating the chemotherapy resistance effects of the ligands tested knockdown of LXR α expression was performed (and validated), and qPCR and colony forming assays repeated. To further investigate if p-gp/ABCB1 was an LXR α target gene, co-factors that were previously shown to regulate LXR α 's ability to control its target genes (Chapter 4) were also inhibited.

First, LXR α knockdowns were validated by measuring LXR α and LXR β mRNA expression post gene silencing relative to universal negative control (siSCR) (**Figure 5.12**). 48 h after transfection, LXR α expression was reduced by 70 % in MCF-7 cells (2-way ANOVA; p<0.0001) and 60 % in MDA-MB-468 cells (**Figure 5.12A**, p<0.0001). LXR β expression was unaffected (**Figure 5.12B**, ns).

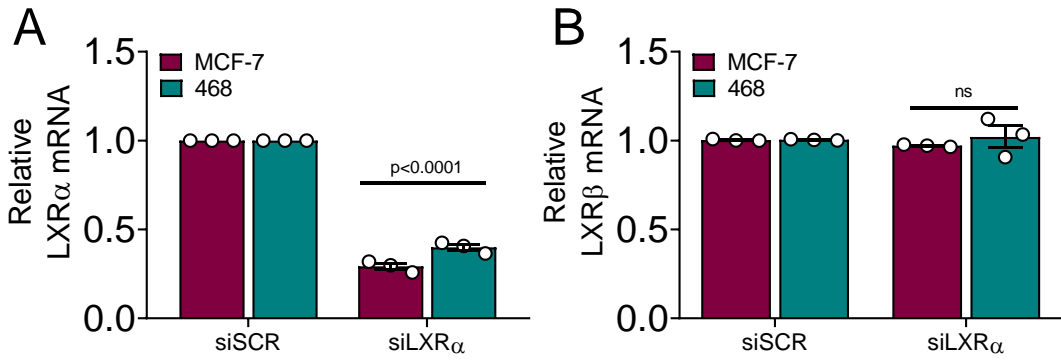


Figure 5.12 Knockdown of LXRα in BCa cells.

LXRα was knocked-down in TNBC (MDA-MB-468) and Luminal A (MCF-7) parental cells. Gene expression of LXRα (A) and LXRβ (B) were assessed by qPCR 36 h post silencing using $\Delta\Delta Ct$ (normalised to HPRT1). Statistical analysis was performed using 2-way ANOVA and is representative of 3 independent replicates with SEM.

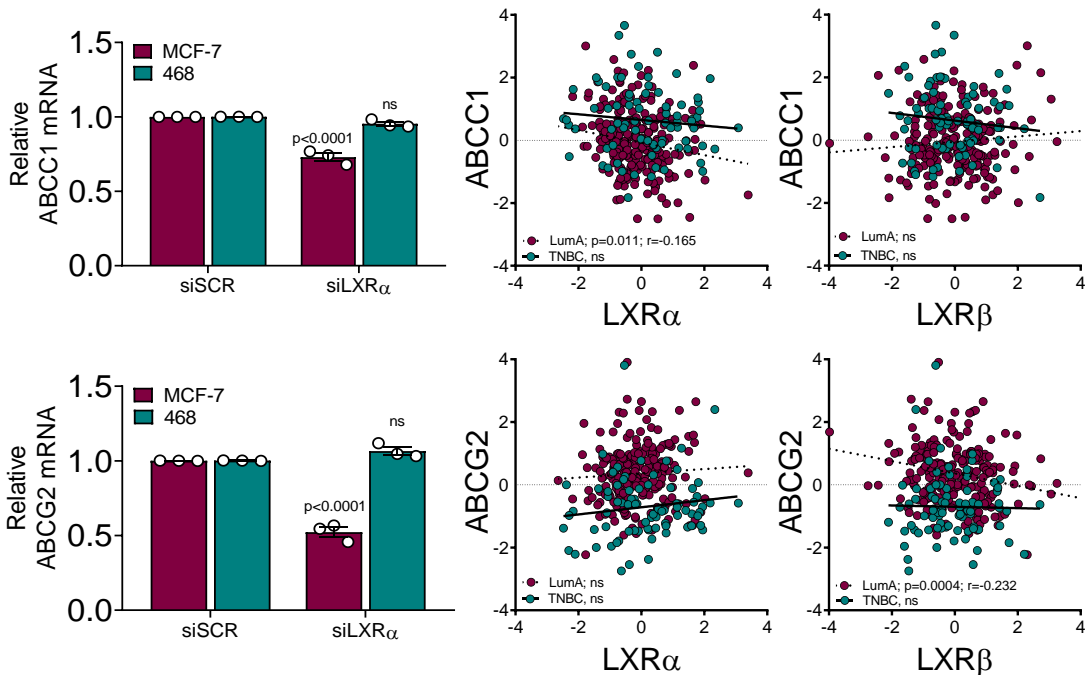


Figure 5.13 Knockdown of LXRα attenuates ABCG2 and ABCC1 expression in ER-positive cells.

LXRα was knocked-down in TNBC (MDA-MB-468) and Luminal A (MCF-7) parental cells. Gene expression of ABCG2 and ABCC1 were assessed by qPCR 36 h post silencing using $\Delta\Delta Ct$ (normalised to HPRT1). Statistical analysis was established using 2-way ANOVA and is representative of 3 independent replicates with SEM.

Next, we show a series of knockdowns in MCF-7 and MDA-MB-468 cells and the expression of the chemoresistance genes p-gp/ABCB1 and BIRC3 post gene silencing (relative to the universal negative control) using Taqman assays (**Figure 5.14**). In

LXR α silenced cells, p-gp/ABCB1 and BIRC3 expression was significantly reduced relative to the universal negative control in MDA-MB-468 cells (2-way ANOVA: p-gp/ABCB1 $p < 0.0001$, BIRC3 $p = 0.0024$) as was BIRC3 expression in the MCF-7 cells ($p = 0.0004$). p-gp/ABCB1 expression however, was significantly enhanced in the LXR α silenced MCF-7 cells ($p < 0.0001$). In LCOR silenced cells, p-gp/ABCB1 and BIRC3 expression was significantly enhanced in the MDA-MB-468 cells (p-gp/ABCB1 $p < 0.0001$, BIRC3 $p = 0.0002$) and in the MCF-7 cells (p-gp/ABCB1 $p = 0.0252$, BIRC3 $p = 0.0001$). In NCOR1+2 silenced cells, p-gp/ABCB1 expression was also significantly enhanced relative to the universal negative control in the MDA-MB-468 cells (p-gp/ABCB1 $p < 0.0001$, BIRC3 $p = 0.0002$) but only BIRC3 expression was enhanced in the MCF-7 cells (p-gp/ABCB1 ns, BIRC3 $p < 0.0001$).

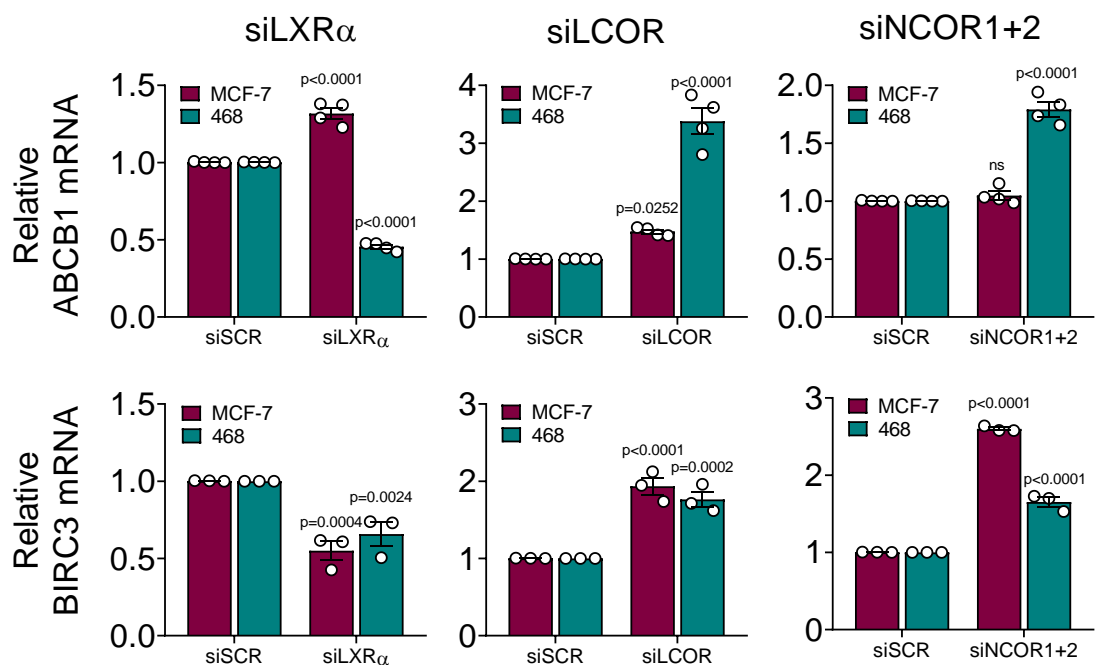


Figure 5.14 Knockdown of LXR α , LCOR and NCOR alters p-gp/ABCB1 and BIRC3 expression.

LXR α , LCOR, NCOR1+2 was knocked-down in TNBC (MDA-MB-468) and Luminal A/ER-positive (MCF-7) parental cells. Gene expression of p-gp/ABCB1 and BIRC3 were assessed by qPCR 36 h post silencing using $\Delta\Delta C_t$ (normalised to HPRT1). Statistical analysis was established using 2-way ANOVA and is representative of 3 independent replicates with SEM.

Finally, we assessed LXR α dependent chemoresistance by silencing LXR α in MDA-MB-468 and MCF-7 cells followed by colony forming assays (**Figure 5.15**). In universal negative control MDA-MB-468 cells, pre-treatment with GW3965 significantly improved cancer cell survival and colony formation during chemotherapy treatment (paired t-tests; $p=0.0022$). In LXR α silenced MDA-MB-468 cells, pre-treatment of GW3965 before epirubicin treatment restored TNBC cell sensitivity to chemotherapy treatment (ns). In universal negative MCF-7 cells, pre-treatment with GW3965 also significantly improved cancer cell survival and colony formation during chemotherapy treatment ($p=0.0034$). However, in LXR α silenced MCF-7 cells, pre-treatment of GW3965 before epirubicin treatment not only restored TNBC cell sensitivity but was able to enhance cell sensitivity to chemotherapy treatment ($p=0.0171$).

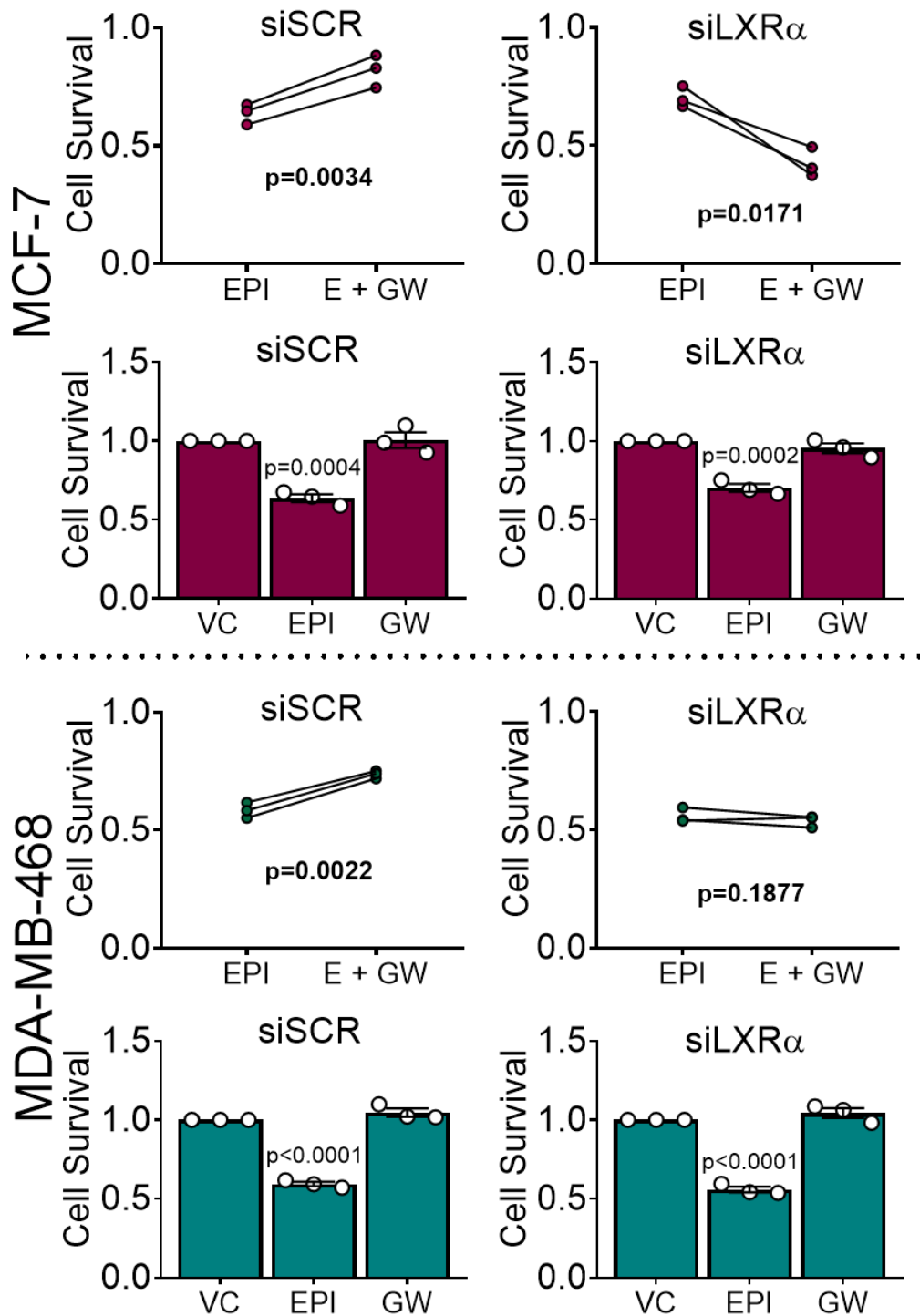


Figure 5. 15 Knockdown of LXR α increases chemotherapy efficacy demonstrating chemoresistance is LXR dependent.

LXR α was knocked-down in TNBC (MDA-MB-468) and Luminal A (MCF-7) parental cells. Post gene silencing cells were plated into colony forming assays and pre-treated with either VC or GW3965 (1 μ M) for 24 h. Cells were then treated with either VC or a dose of the chemotherapy agent epirubicin (25 nM) for a further 24 h, before 500 cells/treatment were plated in triplicate wells and incubated for 12 days. Colonies were then stained with crystal violet and counted. Statistical analysis was established using paired t-tests. Data shown are of 3 independent replicates with SEM.

5.3.5 Enhanced p-gp/ABCB1 expression correlates with LXR α expression in breast cancer patient tumours.

To establish if enhanced LXR α activation is a marker of worse prognosis, BCa tumours were assessed for increased expression of p-gp/ABCB1 in patients who had suffered an event (relapse) and those who had not (no event). The expression of p-gp/ABCB1 was also correlated with LXR α expression to assess the relationship between expression of the genes.

First, we established whether patient tumours displayed enhanced p-gp/ABCB1 expression, and if this is altered in patients who had relapsed compared to those who had not. RNA was extracted from the 69 patient primary tumours and gene expression analysed by Taqman assays (normalised to HPRT1). In Non-TNBC tumours, patients who has suffered an event did not have significantly altered expression of p-gp/ABCB1 (Mann-Whitney U Test; ns) when compared to patients who had not suffered an event (**Figure 5.16**). Interestingly, in the TNBC tumours, patients who has suffered an event had significantly higher expression of p-gp/ABCB1 ($p=0.003$) relative to patients who had not suffered an event (**Figure 5.16A**). Tumour expression of ABCB1 was then assessed alongside patient survival to assess whether expression is predictive of survival in Kaplan Meier graphs (**Figure 5.16B**). ROC curves were used to establish the expression cut offs for high and low expression levels. TNBC tumours with higher expression of p-gp/ABCB1 (>0.175) were found to have worse survival than those with lower p-gp/ABCB1 expression (<0.175 ; Logrank test, $p=0.018$). In non-TNBC tumours however, p-gp/ABCB1 expression was found to have no effect on patient survival (ns).

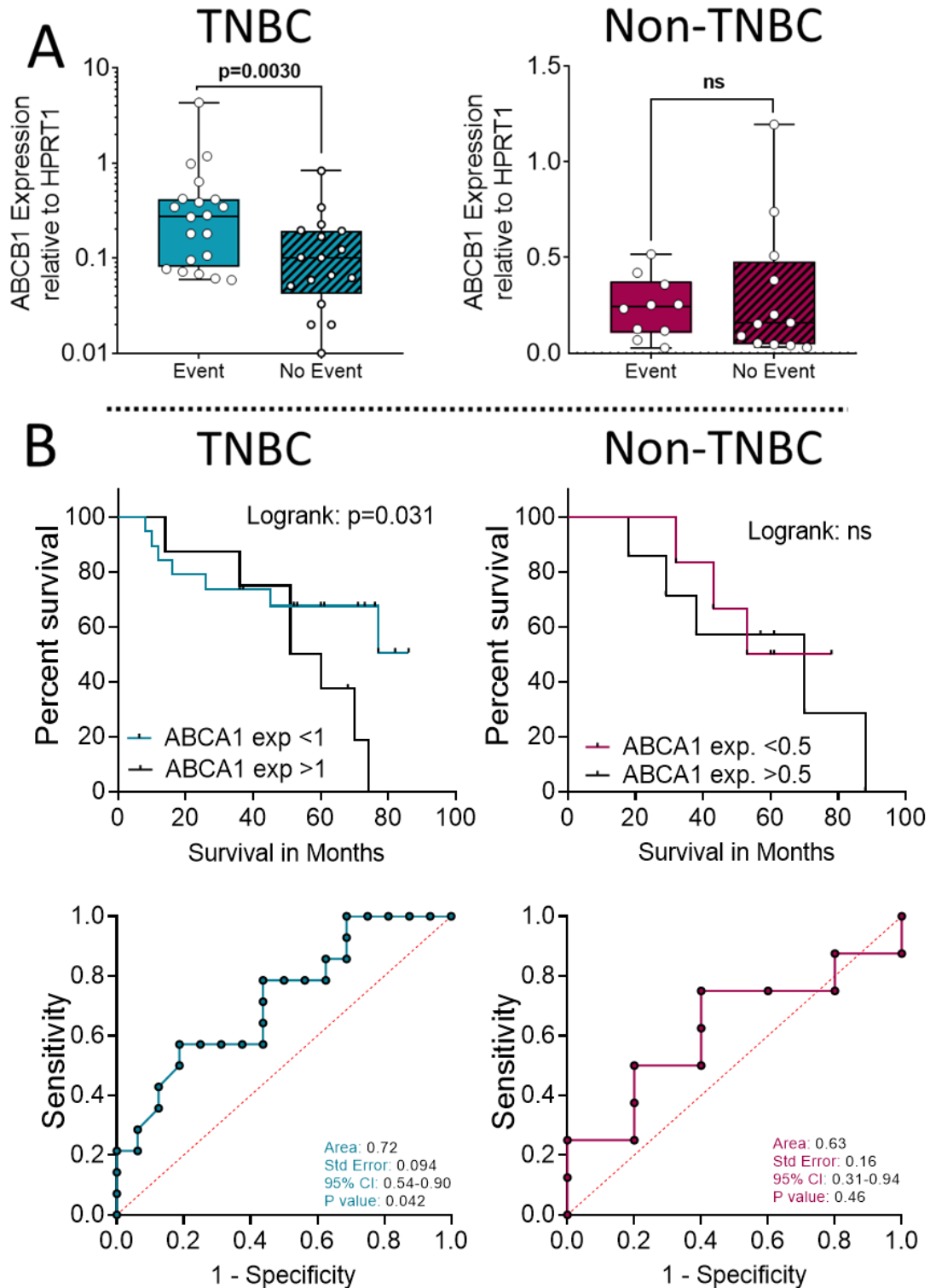


Figure 5. 16 Increased expression of p-gp/ABCB1 was observed in TNBC breast tumours.

RNA was isolated from 69 breast cancer patient tumours (41 TNBC, 28 HER2 enriched or hormone receptor positive [non-TNBC]). mRNA expression p-gp/ABCB1 was analysed by qPCR. Expression of p-gp/ABCB1 was assessed between patients who had suffered a recurrence or death (Event) and those that had not had (No Event). Statistical differences were established using Mann-Whitney U Tests. Patient survival is shown in a Kaplan Meier graph for the TNBC (28) and Non-TNBC (13) subtypes due to significant differences in p-gp/ABCB1 expression between event and no event groups. Statistical differences were established using a Logrank test, cut offs established using ROC curves.

After measuring p-gp/ABCB1 expression in the patient primary tumours, LXR α and LXR β expression were tested for correlation with the expression of p-gp/ABCB1 (**Figure 5.17A and Figure 5.17B**) to establish if patient tumours with higher LXR α expression are likely to have higher expression of p-gp/ABCB1. First, LXR α expression was correlated with p-gp/ABCB1 expression (**Figure 5.17A**). In the TNBC patients who had suffered an event LXR α was found to have a particularly strong correlation with p-gp/ABCB1 expression (Pearson correlation; $p < 0.0001$). In the TNBC tumours which did not have an event, LXR α did not significantly correlate with the expression of p-gp/ABCB1 (ns). LXR α also correlated with p-gp/ABCB1 expression in the Non-TNBC patients who had suffered an event ($p = 0.0235$) but did not correlate with those who had not had an event (ns).

Next, LXR β expression was tested for correlation with p-gp/ABCB1 expression (**Figure 4.17B**). In the TNBC patients who had suffered an event, LXR β expression strongly correlated with p-gp/ABCB1 expression ($p < 0.0001$). In the TNBC patient tumours who had not had an event, LXR β failed to significantly correlate with the expression of p-gp/ABCB1 (ns). In the Non-TNBC patients who had relapsed, LXR β expression also correlated with p-gp/ABCB1 expression ($p = 0.017$) however the correlation was not as strong as in the TNBC tumours. In the Non-TNBC patients who had not had an event, LXR β expression also weakly correlated with p-gp/ABCB1 expression ($p = 0.0321$).

In summary, patient tumours from those who had suffered an event (BCa death or relapse) had strong LXR α and correlations with p-gp/ABCB1 expression in the TNBC group, and a weak but significant correlation in the non-TNBC group. Furthermore,

patient tumours from those who had not suffered any event (healthy and alive) had no LXR α correlations with p-gp/ABCB1 expression in the TNBC or Non-TNBC group.

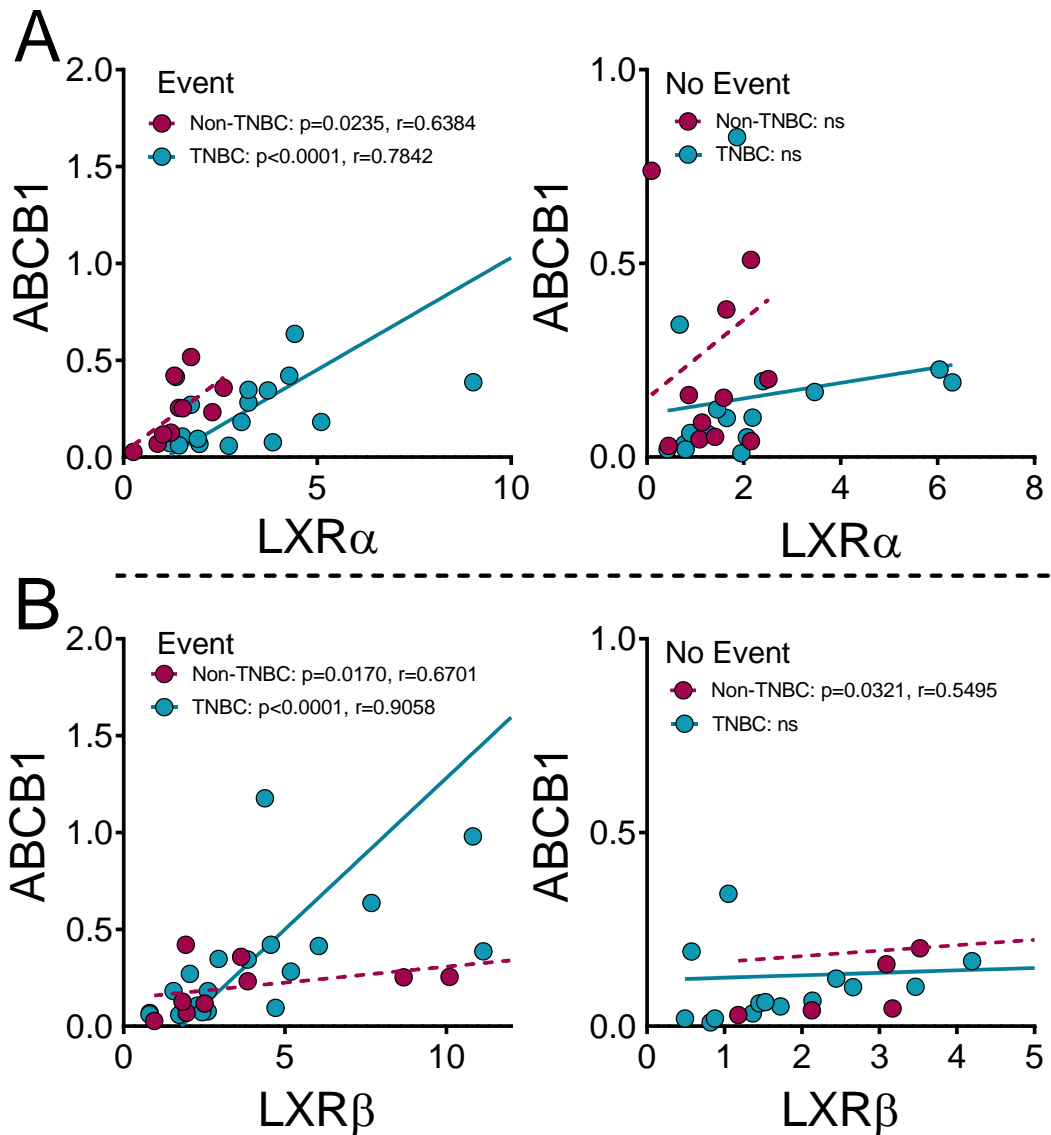


Figure 5.17 LXR α and LXR β expression strongly correlates with ABCB1 in TNBC patient tumours who have relapsed. .

RNA was isolated from 69 breast cancer patient tumours (41 TNBC, 16 HER2 enriched and 12 hormone receptor positive [non-TNBC]) and the expression of p-gp/ABCB1 was analysed by qPCR. Statistical differences were established using Mann-Whitney U Tests. Expression of LXR α and LXR β were then correlated with p-gp/ABCB1. Statistical significance was established using Pearson correlation with linear regression.

5.3.6 LXR ligands reduce the efficacy of the chemotherapy agent epirubicin *in vivo*.

To validate the hypothesis proposed above that LXR activation confers chemotherapy resistance, an animal model was developed.

The 4T1 TNBC cells were orthotopically grafted into the axial mammary fat pad of BALB/C mice and split into four treatment groups: placebo, GW3965 (daily, 30mg/kg), epirubicin (every other day, 2.5mg/kg) and GW3965+epirubicin (Full details in M+M). Tumour size was measured daily, and after 12 days tumours harvested, weighed and markers of LXR activation and chemotherapy resistance measured. The tumours in mice treated with GW3965+epirubicin were larger than the tumours in mice treated with epirubicin ($p=0.03$) (**Figure 5.18**) and had significantly higher expression of chemotherapy resistance gene ABCB1 and canonical LXR target gene ABCA1 (**Figure 5.19**). As expected GW396, which is antiproliferative, slowed tumour growth compared to placebo. In summary, treatment with LXR agonist concurrently with chemotherapy reduces epirubicin efficacy in mice.

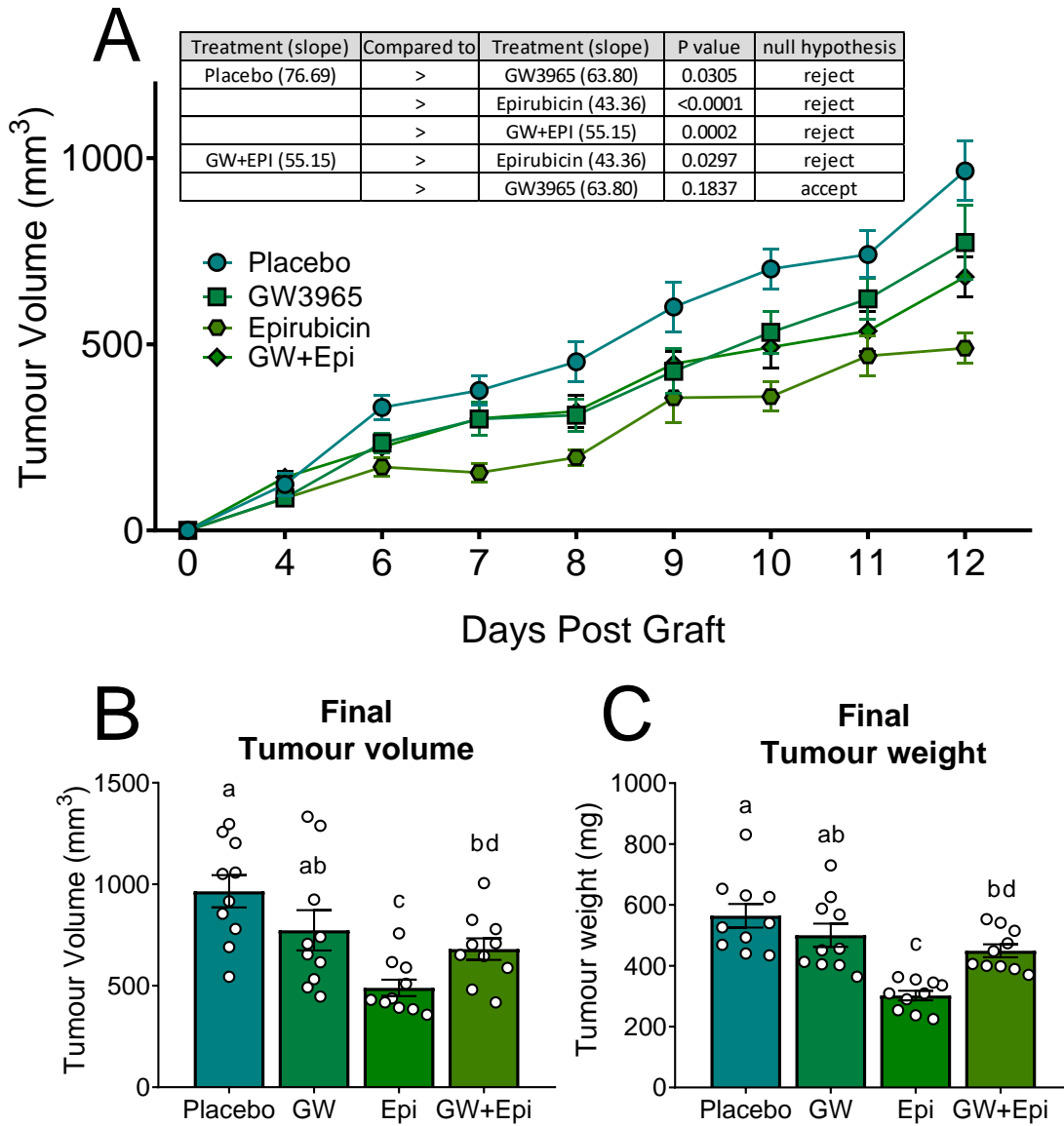


Figure 5. 18 LXR agonists reduce anti-tumoural efficacy of epirubicin in TNBC cells grafted into mice.

4T1 cells (TNBC) were grafted orthotopically into the axial mammary fat pad of BALB/C mice. Mice were treated with either placebo or the LXR ligand GW3965 (daily, 30 mg/kg) 24 h post-graft. Treatments with placebo or epirubicin (every other day, 2.5 mg/kg) commenced 48 h post-graft. Tumour volumes measured by direct calliper (A), plasma, liver and tumour were harvested after 12 days. Statistical analysis was assessed using non-linear regression. Tumours were dissected out and weighed (B). Statistical analysis was assessed using 1 Way ANOVA with SNK test, with 10 mice per group and shown with SD. Different letters denote statistical differences. Mouse study completed in Chicago in the lab group of Erik Nelson.

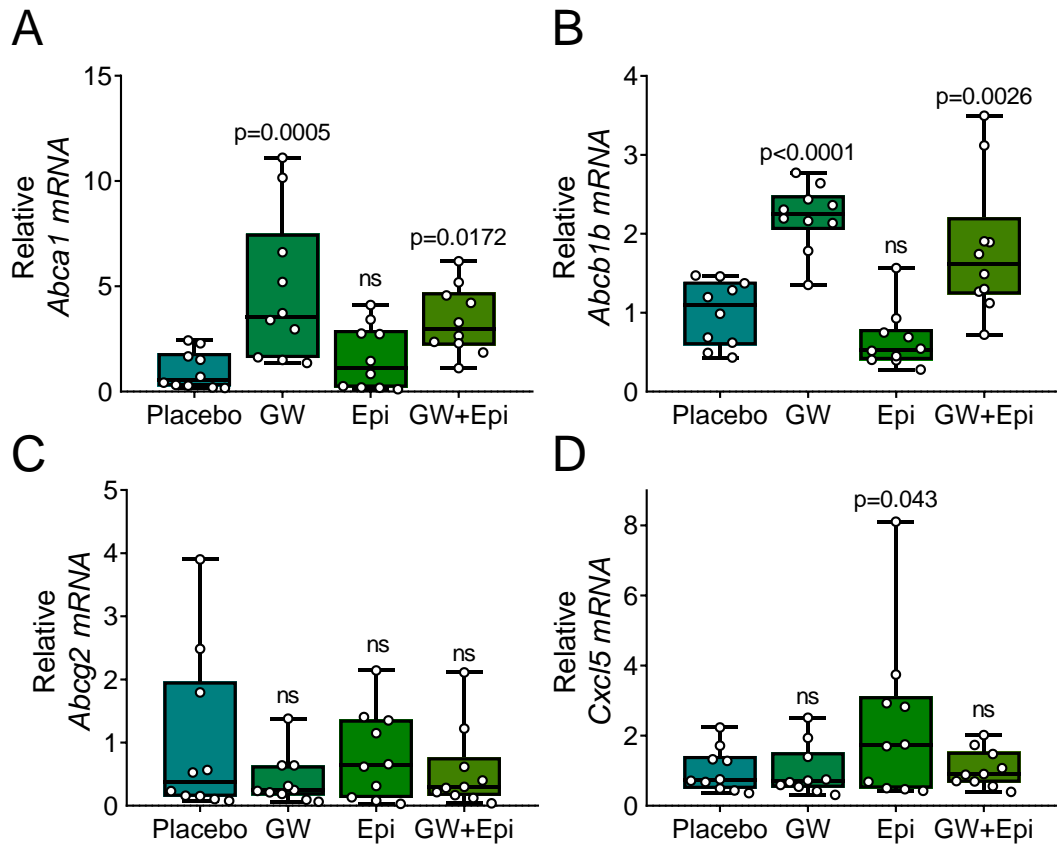


Figure 5. 19 Mice treated with LXR agonists have enhanced expression of *Abca1* and *Abcb1b*.

4T1 cells (TNBC) were grafted orthotopically into the axial mammary fat pad of BALB/C mice. Mice were treated with either placebo or the LXR ligand GW3965 (daily, 30 mg/kg) 24 h post-graft. Treatments with placebo or epirubicin (every other day, 2.5 mg/kg) commenced 48 h post-graft. Tumours were dissected out and weighed after 12 days. Total RNA was isolated from tumour tissue and expression of *Abca1* (A), *Abcb1b* (B), *Abcg2* (C), and *Cxcl5* (D) was assessed by qPCR analysis. Statistical analysis was assessed using 1 Way ANOVA with SNK test, with 10 mice per group and shown with SD. Different letters denote statistical differences. Mouse study completed in Chicago in the laboratory group of Erik Nelson.

5.4 Discussion

New roles for oxysterol-induced LXR targets in the progression of breast cancer are emerging. The purpose of this study was to establish if LXR α activity was linked to chemotherapy resistance in TNBC. In this chapter oxysterol activation of LXR was found to reduce the efficacy of epirubicin, a common anthracycline given to TNBC patients, via activation of the membrane bound drug efflux pump p-gp/ABCB1. Regulation by LXR α of p-gp/ABCB1 and several other genes implicated in chemotherapy resistance (BIRC3, GPSM3 and CXCL5) was identified by combining

data mined from public databases, with cell biology and mouse xenograft experiments and analysis of primary tumours from TNBC patients. BCa subtype specific differences were observed, with p-gp/ABCB1 appearing the dominant efflux pump in TNBC, whereas BCRP and MRP1 were dominant in Luminal A BCa. LXR α control of p-gp/ABCB1 expression was confirmed by siRNA knockdown of LXR α , as expression of p-gp/ABCB1 was attenuated in the TNBC cells but not in the MCF-7 cells, and knockdown of LXR α in colony forming assays restored epirubicin efficacy in both TNBC and Luminal A cells.

In the present study, LXR agonists reduced the efficacy of epirubicin, a common chemotherapy agent given to TNBC patients to either down-stage tumours before breast conserving surgery, or after surgery to eliminate residual tumour. The data presented are consistent with the hypothesis that activation of LXR α by excessive oxysterol production that results from high LDL-cholesterol levels may therefore promote a *de novo* chemotherapy resistance during tumour growth. The analysis of gene expression in primary tumours, mouse xenograft models and in cell lines suggested this chemotherapy resistance could be due to upregulation of the xenobiotic transporter p-gp/ABCB1. The fluorescence-based efflux assay developed during this chapter demonstrated that LXR dependent epirubicin efflux was entirely driven by p-gp/ABCB1. P-gp/ABCB1 expression was higher in TNBC when patients went on to relapse or die from their disease, but interestingly, p-gp/ABCB1 and LXR α expression only correlated (suggesting functional regulation of p-gp/ABCB1 by LXR α) in patients who relapsed or died.

5.4.1 Enhanced p-gp/ABCB1 expression predicts reduced survival in triple negative breast cancer patients

A key finding of this chapter showed enhanced expression of p-gp/ABCB1 in BCa tumours from patients who had relapsed relative to those that had not. Reassuringly, Kim *et al*, made similar observations of enhanced p-gp/ABCB1 expression in breast tissues post neoadjuvant chemotherapy which was associated with reduced survival by 20 % [270]. Kim *et al*, also showed a significant 40 % reduction in survival in patients who had high BCRP expression post neoadjuvant chemotherapy relative to those with low expression [270]. In another study, the expression of p-gp/ABCB1 was assessed in two MDA-MB-231 cell lines, one which was doxorubicin resistant and the other doxorubicin sensitive. Immunocytochemical staining of the doxorubicin sensitive MDA-MB-231 cells for p-gp/ABCB1 was undetected, however the doxorubicin resistant MDA-MB-231 cells showed strong cytoplasmic and nuclear staining of p-gp/ABCB1 expression [271]. These data support our findings of a p-gp/ABCB1 enhanced chemotherapy resistance mechanism in ER-negative breast cancers which could provide useful as a prognostic marker for poor response to treatment and increased risk of relapse.

So far attempts at targeting p-gp/ABCB1 in clinic have failed due to side effects such as, cardiotoxicity [272], unwanted interactions with drug metabolizing enzymes [273] and altered pharmacokinetics of anti-cancer drugs [274]. Failures in targeting p-gp/ABCB1 suggest cancer specific mechanisms of regulation are required to successfully reverse the reduced chemotherapy efficacy caused by up-regulation of p-gp/ABCB1.

5.4.2 Oxysterols regulate the p-glycoprotein via LXR α in the blood brain barrier

LXR ligand upregulation of p-gp/ABCB1 in TNBC is a novel finding of this study. So far, LXR α regulation of p-gp/ABCB1 has only been identified in the BBB in a study by Saint-Pol *et al* [228]. Saint-Pol *et al*, showed treatments of 24OHC and 26OHC enhanced expression of the LXR target gene ABCA1 in BCECs and the apical-to-basolateral transport (influx) of A β peptides across BCECs. Furthermore, the ABCA1 inhibitor probucol failed to significantly alter the apical-to-basolateral transport (influx) of A β peptides across BCECs suggesting ABCA1 was not directly involved in the influx. The expression of p-gp/ABCB1 was assessed and found to be significantly induced by the treatment with both oxysterols. Although no other studies have shown LXR α regulation of p-gp/ABCB1 there are other studies that have found enhanced p-gp/ABCB1 expression in breast cancers [270, 271]. As my finding is unique, confirmatory reports will be required to allow subsequent follow up, although the work by Saint-Pol [228], and the support of enhanced p-gp/ABCB1 in breast tumours [270, 271] supply circumstantial evidence for oxysterol:LXR α regulation of p-gp/ABCB1. For follow up experiments, validation of LXR α regulation of p-gp/ABCB1 by means of CHIP-Seq is required – see future work in **Section 8.6**.

5.4.3 P-gp/ABCB1 is regulated in triple negative breast cancer and BCRP in ER-positive breast cancer cells

Through the development of a chemotherapy efflux assay, p-gp/ABCB1 was shown to be upregulated by LXR agonists which was attenuated by treatment with verapamil in the TNBC cells. In ER-positive cells, verapamil had no effect on chemotherapy efflux but the BCRP and MDRP inhibitors MK571 and K0143 respectfully enhanced the chemotherapy loading. Encouragingly, Kim *et al*, observed similar results when they investigated the effects of MK571 on the loading of another

chemotherapy drug doxorubicin, which is also often used for the treatment of breast cancer [269]. Intracellular doxorubicin was significantly enhanced by treatment with MK571 in the ER-positive T47D cells when measured by flow cytometry [269]. These findings support those observed in the current study but in the ER-positive MCF-7 cells. This suggests BCRP inhibitors may increase the chemotherapy drug load of other similar chemotherapy drugs and in other ER-positive BCa cells. This suggestion warrants further cell line comparisons and clinical testing.

5.4.4 Oxysterols promote *in vivo* tumour growth and LXR-dependent metastasis

Other novel findings in this chapter include the *in vitro* and *in vivo* experiments showing LXR agonists reduce the efficacy of the chemotherapy drug epirubicin and enhance expression of p-gp/*Abcb1b* in BCa cells and mice treated with the LXR agonist GW3965. A similar study by Nelson *et al*, demonstrated GW3965 treatments retarded the growth of primary tumours in MMTV-PyMT mice (which is in line with our observations), but was able to promote the formation of metastatic cancers in the mice lungs [105]. LXR-dependent metastatic tumour growth was established through pre-treatment with 26OHC prior intravenous injection readily metastasized in ER-negative Met1 cells to the mice lungs [105]. LXR agonists have not been shown to reduce the efficacy of epirubicin, however reduced efficacy of other BCa therapies have been identified. Bougaret *et al*, showed co-cultures of mature adipocytes with breast cancer cells in overweight and obese patients reduced the efficacy of Tamoxifen therapy in the ER-positive MCF-7 cells [275]. The observations in this chapter showing LXR agonists reduce the efficacy of epirubicin in both BCa cells and a mouse study are strongly supported by the findings in mice grafted with the same ER-negative 4T1 cells by Nelson *et al* [105], and the reduced efficacy of Tamoxifen in

adipocytes [275]. Furthermore, the observations of the enhanced p-gp/ABCB1 expression from this chapter further develop the research implicating p-gp/ABCB1 and LXR α activity in chemotherapy failure and the development of chemotherapy resistance.

5.5 Summary

In this chapter we have shown LXR α activation leads to chemoresistance in BCa through a series of colony forming assays, MTT assays and gene expression analysis. We have also identified subtype specific LXR α -regulation of p-gp/ABCB1 in TNBC cells and ABCG2 and ABCC1 in Luminal A cells through the development of a chemotherapy efflux assay, gene silencing and data mining. Furthermore, LXR α -dependent chemoresistance has been demonstrated through knockdown of LXR α followed by colony forming assays and gene expression analyses. Finally, we showed enhanced p-gp/ABCB1 expression leads to poorer prognosis through the means of gene expression analyses and correlations in RNA from patient tumours who had relapsed and those who had not. And this was further supported through the design and execution of a mouse study which demonstrated LXR agonists reduce the anti-tumoural efficacy of epirubicin in TNBC cells grafted into mice also through enhanced p-gp/ABCB1 expression.

Chapter 6

Fibroblasts activate LXR α in adjacent triple negative breast cancer epithelial cells.

6.1 Introduction

The tumour microenvironment can be diverse with large variations between host cell (macrophages, fibroblasts and adipocytes) presence at the site of breast cancers. *In vitro* cell studies suggest that tumour growth is influenced by the tumour stroma [276], which includes the extracellular matrix (ECM). The deposition of the ECM is one of the key functions of fibroblasts along with regulation of inflammation, epithelial differentiation, and wound healing [277, 278]. Many of the constituents of the ECM, such as collagen and fibronectin, are synthesised by fibroblasts [278, 279]. Fibroblasts are also known to regulate expression of CYP enzymes responsible for the synthesis of oxysterols [142], but whether these support cells are generating oxysterols for epithelial cells is unknown. Fibroblasts have been linked to the progression of cancer [280, 281], and CAF-promoted tumour growth [282]. Furthermore, patients who have tumours with enhanced support cell microenvironments often have a poor prognosis, allowing the cancer cells to employ TME-driven metastatic and proliferative behaviours via paracrine signalling [143-145].

Given that tumours supported by cancer-associated fibroblasts tend to have poorer prognosis and fibroblasts have been shown to regulate the expression of CYP enzymes and produce 24OHC, 26OHC, 25OHC and 24,25-EC it may be plausible to suggest cancer-associated fibroblasts may be able to regulate LXR α through the synthesis and secretion of oxysterols.

6.2 Hypothesis and Aims

Cancer-associated fibroblasts not only have migratory capacities but they have been shown to promote tumour growth and progression. In this chapter, the hypothesis that cancer-associated fibroblasts activate LXR α in BCa cells was tested.

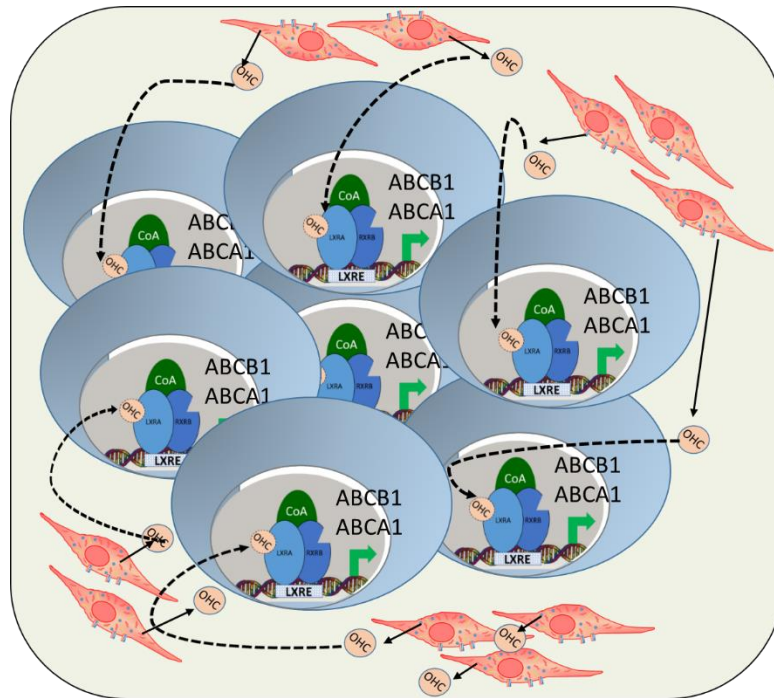


Figure 6. 1 Fibroblasts may secrete oxysterols into the tumour microenvironment.

Cancer associated fibroblasts (CAFs) have the ability to synthesise and secrete oxysterols into to the tumour microenvironment (TME). Oxysterols may be sequestered into the BCa cells activating LXR α and driving LXR target genes.

The aims of this chapter were to:

- Measure oxysterol concentrations in cell lines to relative contributions to the tumour microenvironment.
- Determine if fibroblasts can drive LXR α dependent transcription in adjacent cancer cells in co-culture.
- Differentiate between juxtacrine and paracrine activation of LXR α investigate origins.

6.3 Results

6.3.1 Cancer-associated fibroblasts have high concentrations of oxysterols.

Epithelial cancer cells create a tumour microenvironment around the site of cancer made up of all different kinds of support cells [140]. To establish whether fibroblasts can activate LXR α in epithelial breast cancer cells, oxysterol content in epithelial cells and fibroblasts was measured and a series of co-cultures of fibroblasts and epithelial breast cancer cells were performed.

First, to identify if fibroblasts (cancer-associated and non-cancer associated) have high levels of oxysterols relative to epithelial cancer cells oxysterol concentrations were measured in breast cancer cells lines (MCF-7, MDA-MB-468 and MDA-MB-231) a healthy breast cell line (HB2) and two fibroblast cell lines (LaCAF; cancer-associated fibroblast, NF2; non-cancer associated fibroblast) by methods of fast liquid chromatography LCMS/MS (completed by Dr Hanne Roberg-Larsen, Oslo) (**Figure 6.2**). In general, results showed LaCAFs had significantly higher concentrations of oxysterols (24OHC, 26OHC and 24,25-EC) than epithelial breast cells (1 way ANOVA, at least $p < 0.05$). NF2 cells did not have higher concentrations of oxysterols compared to epithelial (ns), with the exception of 25OHC (at least $p < 0.01$ for all epithelial cells). Finally, LaCAFs had significantly higher oxysterol concentrations than the NF2 cells (at least $p < 0.05$ for 24OHC, 26OHC and 24,25-EC) with the exception of 25OHC (ns).

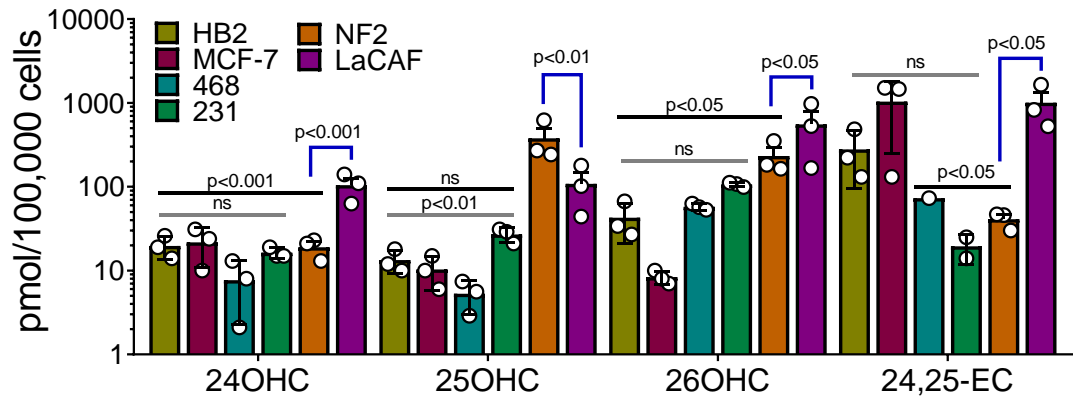


Figure 6. 2 Cancer-associated fibroblasts have high concentrations of oxysterols relative to epithelial cells.

Epithelial cells (HB2, MCF-7, MDA-MB-468 and MDA-MB-231) and fibroblasts (non-cancer associated NF2 and cancer-associated LaCAF) were individually cultured. 500,000 cells of each cell line (in triplicate from different passages) were pelleted and sent to Oslo to be measured by LCMS/MS (LCMS/MS completed by HRL). Statistical analysis was assessed by 1-way ANOVA, grey lines represent comparisons between NF2 cells and epithelial cells, black lines for comparisons between LaCAFs and epithelial cells and blue lines between NF2 and LaCAFs. Data shown are of 2-3 independent replicates with SD.

6.3.2 Fibroblasts activate adjacent LXR α epithelial triple negative breast cancer cells

To establish if cancer-associated fibroblasts can activate LXR α in breast cancer epithelial cells co-culture experiments were performed with epithelial breast cancer luciferase reporter cell lines. Conditioned media from CAFs and non-cancer associated fibroblasts was collected and epithelial breast cancer luciferase reporter cell lines exposed to increasing percentages to assess if LXR α is possible without cell to cell contact.

To identify if cancer-associated fibroblasts can regulate LXR α in breast cancer epithelial cells we co-cultured cancer-associated fibroblasts with epithelial breast cancer luciferase reporter cell lines and measured the LXR α transactivation after 16 h by luciferase assay (**Figure 6.3**). MDA-MB-468 and CAF co-cultures showed as the fibroblast percentage relative to the epithelial breast cell reporters increased so did

the LXR α activation plateauing around 80 % then a reduction in LXR α activation was observed (1-way ANOVA: 20-120 %; 1.5-2 fold increase, at least $p < 0.05$). MDA-MB-231 and CAF co-cultures also showed as the fibroblast percentage relative to the epithelial breast cell reporters increased so did the LXR α activation (20-120 %; 1.4-2 fold increase, at least $p < 0.001$). Surprisingly, MCF-7 and CAF co-cultures showed no matter what the fibroblast percentage relative to the epithelial breast cell reporters, fibroblasts failed to regulate LXR α activity (ns for all percentages).

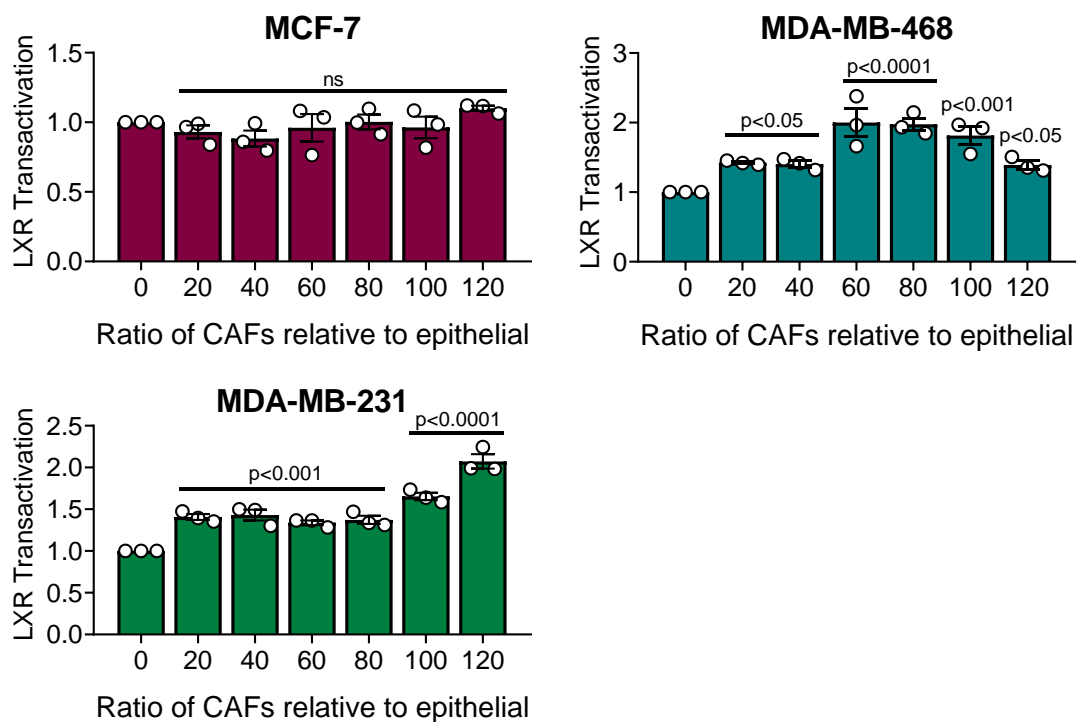


Figure 6. 3 Fibroblast co-cultures with epithelial cells activate LXR α in TNBC luciferase reporters but not ER+ luciferase reporters.

Cancer associated fibroblasts (LaCAFs) were seeded into 96 white walled clear bottomed plates 48 hours before epithelial cells were added. Epithelial cells were incubated for the 8 h cells are usually given to attach and regain usual morphology plus a further 16 h to represent treatment/stimulation time. LXR α transactivation was measured by luciferase assay and normalised to total epithelial cells (0). Statistical analysis was assessed by 1-way ANOVA with the Holm-Sidak multiple correction test. Data shown are of 3 independent replicates with SEM.

To establish if CAF conditioned media could regulate LXR α in breast cancer epithelial cells, LXR α breast cancer reporter cells and the liver cell line HepG2 [control] were exposed to CAF conditioned media for 16 h and LXR α transactivation measured by luciferase assay. (**Figure 6.4**). MDA-MB-468 cultures showed as the fibroblast conditioned media percentage increased so did the LXR α activation plateauing around 20-30 % then a reduction in LXR α activation was observed (1-way ANOVA: 10-40 %; 1.3-1.5 fold increase, at least $p < 0.05$, 50 %, 75 % and 100 %; no increase, ns). MDA-MB-231 cultures also showed as the fibroblast conditioned media percentage increased so did the LXR α activation plateauing around 20-30 % then a reduction in LXR α activation was observed (10-30 %; 1.3-1.4 fold increase, at least $p < 0.01$, 40 %; no increase ns, 50-100 %; decrease, at least $p < 0.001$). Again, MCF-7 cultures showed no matter what the fibroblast conditioned media percentage, fibroblasts failed to regulate LXR α activity (ns for all percentages). HepG2 cultures however, showed as the fibroblast conditioned media percentage increased so did the LXR α activation plateauing around 75-100 % with response significantly more robust (10-100 %; 3-6 fold increase, at least $p < 0.01$).

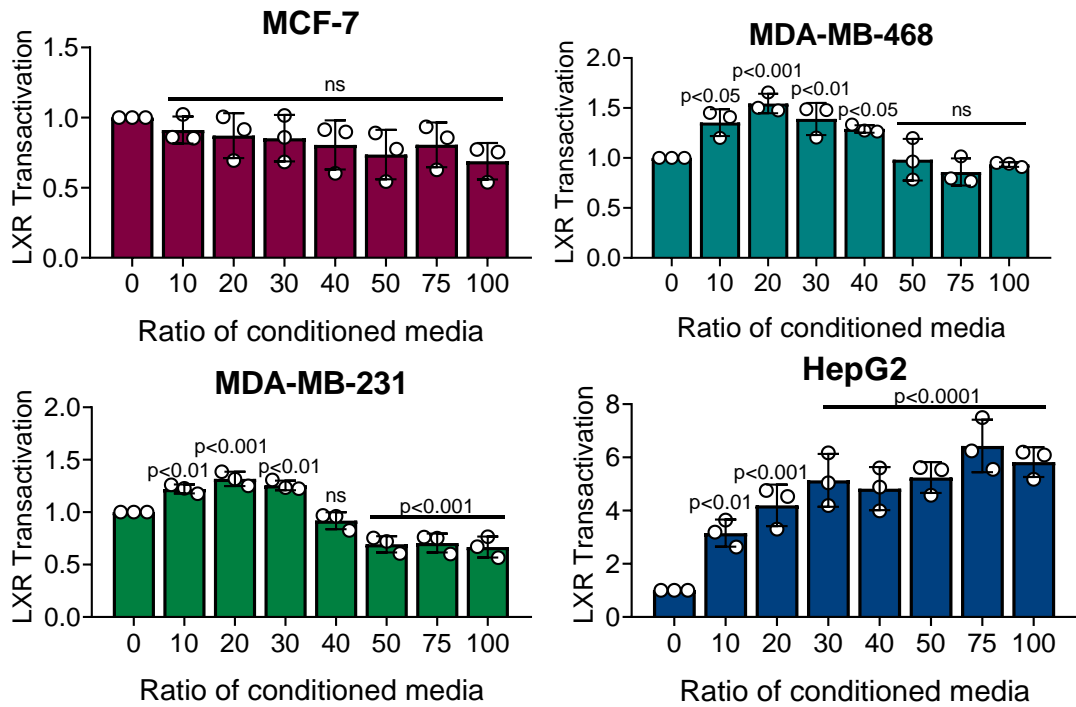


Figure 6. 4 LaCAF conditioned media activates LXR α in TNBC and liver HepG2 cell reporters.

Cancer associated fibroblasts (LaCAFs) and parental epithelial cells were seeded into T75 flasks 24 h before conditioned media was collected. Epithelial reporter cells were seeded into 96 white walled clear bottomed plates incubated for 8 h. Fresh conditioned media was added for 16 h before LXR α transactivation was measured by luciferase assay and normalised to complete epithelial conditioned media (0). Statistical analysis was assessed by 1-way ANOVA with the Holm-Sidak multiple correction test. Data shown are of 3 independent replicates with SEM.

Next, NF2 conditioned media was assessed to see if it could also regulate LXR α in breast cancer epithelial cells, so LXR α breast cancer reporter cells and the liver cell line HepG2 [control] cells were exposed to NF2 conditioned media for 16 h and measured LXR α transactivation by luciferase assay. (Figure 6.5). MDA-MB-468 cultures showed as the NF2 conditioned media percentage increased so did the LXR α activation plateauing around 50-75 % then a reduction in LXR α activation was observed (1-way ANOVA: 10-100 %; 1.4-1.8 fold increase, at least p<0.01). MDA-MB-231 cultures also showed as the NF2 conditioned media percentage increased so did the LXR α activation plateauing around 50-75 % then a reduction in LXR α activation was observed (20-100 %; 1.4-1.5-fold increase, p<0.01). Interestingly, MCF-7

cultures also showed as the NF2 conditioned media percentage increased so did the LXR α activation plateauing around 50-75 % then a reduction in LXR α activation was observed (30-75 %; 1.2-1.3 fold increase, at least $p < 0.01$., and 100 %; no increase ns). HepG2 cultures also showed as the NF2 conditioned media percentage increased so did the LXR α activation plateauing around 50-75 % with response more moderate compared to the CAF conditioned media (10-100 %; 1.5-2.2 fold increase, at least $p < 0.05$).

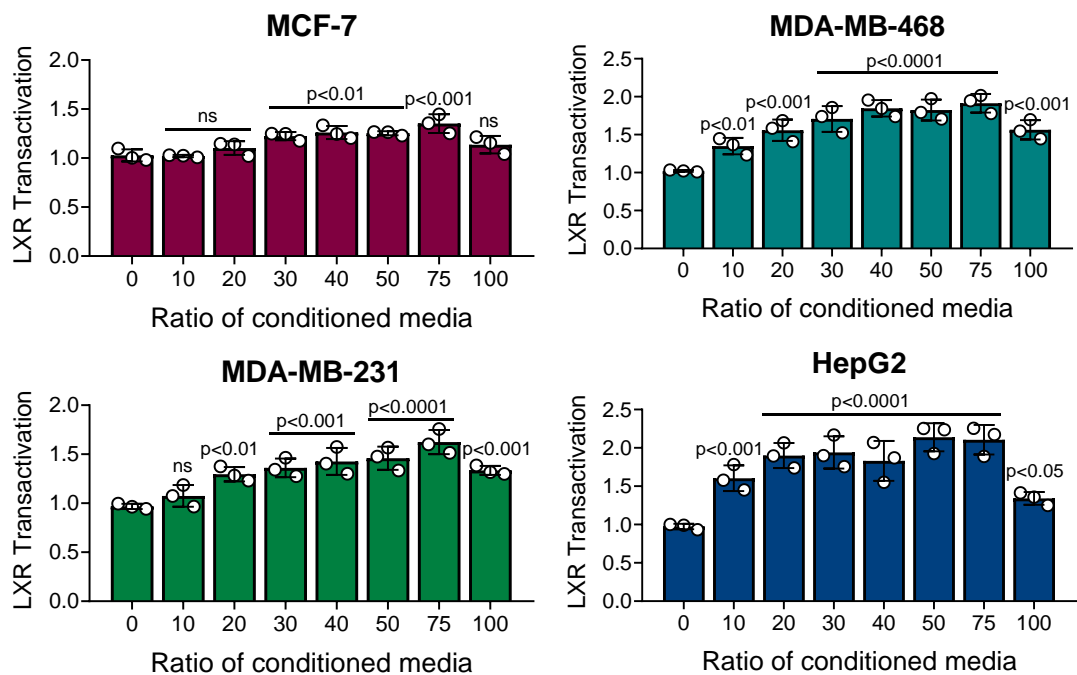


Figure 6. 5 NF2 conditioned media activates LXR α in Luminal A, TNBC and liver HepG2 cell reporters.

Non-cancer associated fibroblasts (NF2s) and parental epithelial cells were seeded into T75 flasks 24 h before conditioned media was collected. Epithelial reporter cells were seeded into 96 white walled clear bottomed plates incubated for 8 h. Fresh conditioned media was added for 16 h before LXR α transactivation was measured by luciferase assay and normalised to complete epithelial conditioned media (0). Statistical analysis was assessed by 1-way ANOVA with the Holm-Sidak multiple correction test. Data shown are of 3 independent replicates with SEM.

6.4 Discussion

The purpose of this study was to establish if cancer associated fibroblasts could activate LXR α in BCa cells. LXR α activation was assessed after co-culture with the fibroblasts or after exposure to conditioned media taken from the cultured fibroblasts.

In this chapter fibroblasts were found to have higher levels of oxysterols than breast cancer epithelial cells and non-cancer associated fibroblasts when measured by LCMS/MS. Strangely there have been no reports published showing the comparison of oxysterol concentrations between epithelial BCa cells and fibroblasts. There have been a few reports where fibroblast production of oxysterols has been validated [283, 284] and concentrations reported for 24,25-EC (56 ng/mg/h), 25OHC (11ng/mg/h) and 26OHC (14 pmol/mg/h) in fibroblast conditioned media and/or fibroblast cells [146-148]. Interestingly, a recent study by Shi *et al*, measured protein expression of CYP27A1 in the breast cancer cell lines MCF-7 and MDA-MB-231, showing enhanced expression in the MDA-MB-231 cells relative to the MCF-7 cells [285]. Furthermore, the same study also measured the oxysterol concentrations in THP-1 monocytes/macrophages and found expression of CYP27A1 to be at least x10 higher in the support cells than the epithelial cells [285]. This study supports the hypothesis that TNBC cells require/benefit from oxysterols relative to Luminal A, but also the hypothesis that support cells in the TME have higher concentrations of oxysterols than epithelial cells.

Oxysterol concentrations have not been previously measured in the breast cancer cell lines before, as such no direct comparison to published data can be made. However, comparison to oxysterols in other epithelial cells can be made. A recent

study by Hong *et al*, measured the oxysterol concentrations in GES-1 and GES-1^{SULT2B1-/-} cells. After conversion to match the units of this study, oxysterol concentrations were found to be within the range of concentrations identified in the breast epithelial cells measured in this chapter [in bold]. 24OHC was found to average at 2 pmol/100,000 cells in GES-1 cells and 20 pmol/100,000 cells in GES-1^{SULT2B1-/-} cells [**this study BCa cells average: 10 pmol/100,000 cells**], 24,25-EC at 35 pmol/100,000 cells in GES-1 cells and 200 pmol/100,000 cells in GES-1^{SULT2B1-/-} cells [**BCa cells range: 100-1000 pmol/100,000 cells**], 25OHC at 2 pmol/100,000 cells in GES-1 cells and 5 pmol/100,000 cells in GES-1^{SULT2B1-/-} cells [**BCa cells average: 20 pmol/100,000 cells**], and 26OHC at 2 pmol/100,000 cells in GES-1 cells and 10 pmol/100,000 cells in GES-1^{SULT2B1-/-} cells [**BCa cells average: 10-100 pmol/100,000 cells**] [286]. Interestingly, the GES-1^{SULT2B1-/-} cells have comparable oxysterol concentrations to those measured in the BCa cell lines, but the GES-1 cells appear to have lower amounts. To date, there has been no direct comparison between oxysterol concentrations in non-cancer associated fibroblasts and cancer-associated fibroblasts, may be because the hypothesis has not been considered. As the higher concentrations of oxysterols in fibroblasts relative to epithelial cells is a unique finding, confirmatory studies in isolated primary fibroblasts (non-cancer associated and CAFs) and primary breast cancer cells including LCMS/MS with matched tumour section immunohistochemistry analysis of the oxysterol synthesis enzymes will be required to allow subsequent follow up. Additionally, the oxysterol concentrations in epithelial and fibroblasts co-cultures should be assessed as cross-talk between cells may increase the demand for oxysterol production. Finally, knockout of the

oxysterol synthesis enzymes in fibroblasts would be interesting to assess whether production of oxysterols is compensated for in epithelial cells.

Another key finding in this chapter was that CAFs drive LXR α signalling in MDA-MB-468 and MDA-MB-231 cells by CAFs. Camp *et al* showed similar findings where TNBC co-cultures with fibroblasts enhanced the expression of ABCA1 but did not in the Luminal BCa co-cultures [287]. The similar findings in the study by Camp *et al* and this one gives great confidence in the results, particularly as the data presented by Camp *et al*, included the same MCF-7 cell used in this chapter. Camp *et al* also used alternative cell lines to the ones used in this study (SUM102, SUM149, HCC1937, ZR-75-1, T47D), and found that TNBC co-cultures with fibroblasts enhanced the expression of ABCA1 but failed to do so in the Luminal BCa co-cultures. This means we can suppose epithelial cell co-cultures with fibroblasts activate LXR α in multiple TNBC and therefore further testing would be warranted. However, this chapter has expanded the findings of Camp and colleagues as the data from conditioned media experiments show paracrine rather than juxtacrine signalling is the most likely form of communication and a secreted factor, most likely oxysterol(s), is responsible.

There is increasing recognition that the tumour microenvironment support cells can influence the behaviour of tumour epithelial cells contributing to and defining patient outcomes [281, 288]. In response to tumourigenesis, breast stromal arrangement changes increasing the numbers of cancer-associated fibroblasts within the tumour site [289, 290], which has been shown to increase tumour cell proliferation and angiogenesis [291]. Although there is limited research that has been published showing LXR α modulation in BCa epithelial cells by fibroblasts there is evidence showing fibroblasts have the capacity to produce oxysterols [146-148]

which are known LXR ligands. In this chapter we have presented data supporting the hypothesis that fibroblasts activate LXR α in epithelial BCa cells when cultured with fibroblasts and when exposed to fibroblast conditioned media suggesting cell-to-cell contact is not required or is dispensable. The study by Camp *et al*, performed two methods of epithelial BCa cell co-cultures with fibroblasts, through direct contact co-culture and through the use of transwell to impair cell-to-cell contact. As discussed above, direct contact co-culture of TNBC cells with fibroblasts enhanced the expression of ABCA1 but failed to do so in the Luminal BCa co-cultures. Co-cultures of TNBC cells with fibroblasts using the transwell method enhanced the expression of ABCA1 in both the fibroblast and the epithelial cells. Co-cultures of Luminal A BCa cells with fibroblasts using the transwell method enhanced the expression of ABCA1 in the epithelial cells but failed to do so in the fibroblasts. This study by Camp and colleagues strengthens the hypothesis that fibroblasts activate LXR α in epithelial BCa cells and supports the observations in this chapter of LXR α induced paracrine signalling.

6.5 Summary

In this chapter we have established that fibroblasts support LXR α enhanced TNBC cancer cells through the secretion of oxysterols. We have also identified that fibroblasts produce almost x10 higher amounts of oxysterols than breast epithelial cells. Through co-culture assays we discovered cancer-associated fibroblasts were not able to activate MCF-7 LXR α -driven reporters but significantly increased LXR α activity in the TNBC reporters. Furthermore, CAF and NF2 conditioned media were also able to increase LXR α activity in the TNBC and HepG2 liver luciferase reporters showing cell-to-cell contact is not essential and oxysterol activation of the reporters is secretion dependent. Finally, MCF-7 co-cultures with CAFs and CAF conditioned media were not able to alter Luminal A LXR α activity, however the NF2 conditioned media was able to increase LXR α activation suggesting cross-talk between CAFs and Luminal A BCa cells is reduced.

Chapter 7

Phytosterols antagonise oxysterol-mediated LXR α activation and chemosensitize triple negative breast cancer cells.

Data presented in this chapter have in part been published in a peer-reviewed article [131]. Journal article included in **Appendix B - 1.2**.

7.1 Introduction

Plant based diets that are rich in phytosterols are known to lower LDL-C and are associated with reduced risk of primary and recurrent breast cancer [48]. In normal biology however, phytosterols are essential components of plant cell membranes and have equivalent cellular functions in plants to those of cholesterol in mammals. At the molecular level, relatively little is known about the biological functions of phytosterols (outside of their role as cholesterol lowering sterols) in normal or diseased tissues. In animal models and *in vitro* studies, anti-cancer properties for phytosterols have been suggested including the inhibition of BCa growth and metastasis [292-294]. Furthermore, plant rich diets [220] and healthy dietary patterns associated with PSS intake have lower cancer incidence and improved survival [219].

7.1.1 Phytosterol intake is associated with a reduction in cancer risk

Recently Jiang *et al*, published a systematic evaluation of the existing research focusing on dietary total phytosterols [295]. The meta-analysis consisted of 11 case-control and case-cohort studies assessing the relative risk associated with phytosterol intake and cancer risk. The relative risk (RR) for the highest intake compared to the lowest intake for total phytosterol intake RR=0.63 (95 % CI = 0.49-0.81) [295]. Individual phytosterol intake was also assessed, with β -sitosterol

RR=0.74 (95 % CI = 0.54-1.02), campesterol RR=0.72 (95 % CI = 0.51-1.00) stigmasterol RR=0.83 (95 % CI = 0.60-1.16), β -sitostanol RR=1.12 (95 % CI = 0.96-1.32) and campestanol RR=0.77 (95 % CI = 0.65-0.90 [295]) but due to large heterogeneity no individual associations could be made. Data shown suggest that high total phytosterol intake is inversely associated with cancer risk.

Other studies have also looked at cancer risk and dietary patterns. Results from the Women's intervention nutrition study (WINS) showed dietary patterns that lower fat intake were associated with reduced risk of BCa relapse [48]. The WINS design included two groups, one was a control group and the other a low-fat (15 % energy from fat) group which were asked to lower their consumption of oils, high fat dressings and spreads, opt for low fat dairy products, fish, poultry, meat and egg whites, consume smaller portions and substitute low fat beverages, desserts and snacks with high fat items. The intervention group were also asked to increase their fruit, vegetables, grain products and legume intake. Results from the intervention showed a significant ($p < 0.001$) decrease in dietary fat (33.3 fat grams/per day) at 12 months [95 % CI = 32.2-34.5] in the intervention group relative to the control group (51.3 fat grams/per day) at 12 months [95 % CI = 50.0-52.7] which was maintained through the 5 years of observations. In line with reduced dietary fat intake the intervention group had a mean body weight which was 6 pound lighter than the control group after the 5 years of observations ($p < 0.005$). Dietary patterns were designed to reduce dietary fat intake and increase consumption of fruit and vegetables. Furthermore, implemented dietary patterns were associated with a reduction in the hazard ratio (HR) for BCa relapse events when compared to the control group, HR=0.76 (95 % CI, 0.60-0.98, adjusted Cox model analysis $p = 0.034$).

When groups were further classified by ER status, HR for relapse events was further reduced in the intervention group with ER-negative BCas, HR=0.58 (95 % CI, 0.37-0.91, adjusted Cox model analysis p=0.018) compared to the control group however, significance was lost in ER-positive BCas relative to the control group, HR=0.85 (95 % CI, 0.63-1.14, adjusted Cox model analysis p=0.277).

7.1.2 Phytosterol effects on cells

PSS intake has been associated with reduced BCa risk, but the exact mechanism behind the reduced relapse rates is not clear. Other researchers have performed *in vitro* experiments to assess the response to phytosterol treatments in various cell line models. For example, the tumour growth of multiple human cancer cell lines has been shown to be inhibited by treatments of β -sitosterol, such as; colon [296], liver [297], lung [298], prostate [292, 299] and breast [300]. Additionally, rats treated with β -sitosterol 20 mg/kg three times per week for 24 weeks had induced apoptosis in renal cancer cells [301]. Furthermore, treatments of β -sitosterol also inhibited proliferation and metastasis in renal cancer cells in the rats [301], which is in support of other similar observations where high intakes of phytosterols has anticancer effects [302-305]. The anti-cancer properties of phytosterols are thought to be acting through induced apoptosis [306], inhibition of cholesterol synthesis [307], promotion of cell cycle arrest [308, 309] and through inhibition of cell invasion and migration [308, 309].

7.1.3 Phytosterols alter oxysterol signalling

Phytosterols alter oxysterol signalling in several ways as summarised in **Figure 7.1**. First, phytosterols have been shown to alter oxysterol signalling through inhibition of cholesterol uptake. Lutjohann *et al*, showed patients given 0.5 g sitostanol (three times a day) had an average reduction in cholesterol absorption by 34 % and increased cholesterol content in faecal matter [210]. Furthermore, there was no significant rise in cholesterol synthesis following sitostanol mediated reductions in cholesterol absorption [210]. Second, phytosterols alter oxysterol signalling through inhibition of HMGCR, the rate limiting enzyme in cholesterol synthesis. Yang *et al*, showed significant reductions in HMGCR at the protein level after treatment with campesterol and stigmasterol in cultured Y1-BS1 adrenal cells [172]. Furthermore, no significant changes were observed in cells after treatment with phytosterols showing changes in HMGCR levels were not due to changes in cholesterol levels [172]. And finally, phytosterols can also alter oxysterol signalling through inhibition of CYP family members, which are required for the conversion of cholesterol to oxysterols. Brauner *et al*, showed co-incubation of cholesterol with either campesterol (77 ± 9 pmol x mg protein/min) or sitosterol (106 ± 16 pmol x mg protein/min) significantly inhibited the generation of 26OHC when compared to treatment of cholesterol alone (285 ± 23 pmol x mg protein/min) [211].

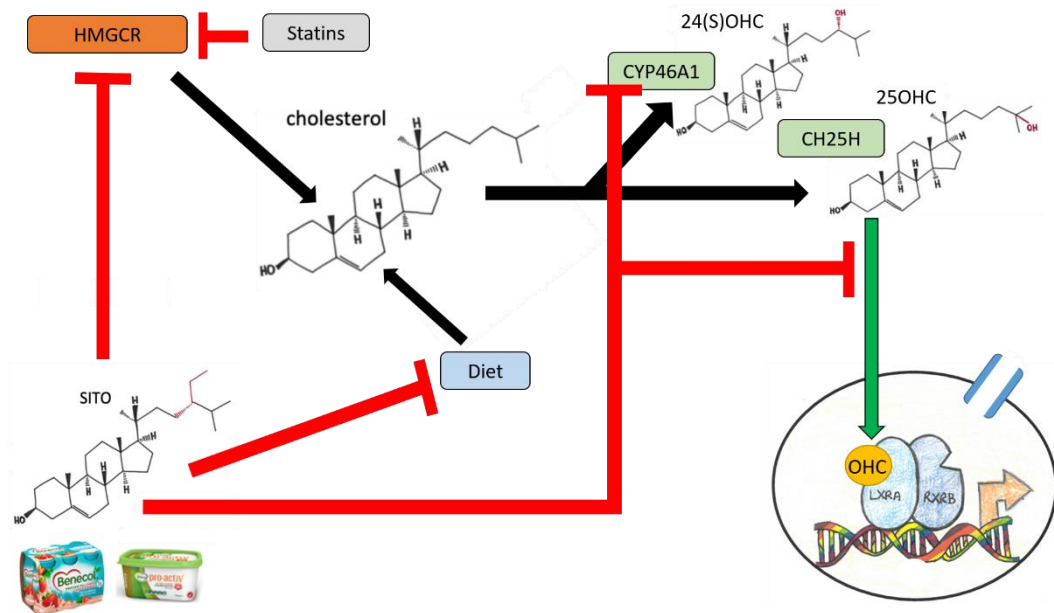


Figure 7. 1 Phytosterols alter oxysterol signalling in several ways.

Phytosterol intake can alter oxysterol signalling in three ways: 1) inhibition of HMGCR the enzyme required to synthesise cholesterol, 2) Inhibition of cholesterol uptake from the diet and 3) inhibition of CYP family members required to convert cholesterol to oxysterols and therefore reduce LXR α activity.

7.1.4 Phytosterols have tissue specific effects.

Phytosterols have been shown to behave as selective LXR modulators (SLiM) which is defined as LXR ligands that have diverse effects in different tissues. Phytosterols are very similar in structure to oxysterols and cholesterol and it appears they can alter mammalian physiology if accumulated at sufficient concentrations. Interestingly, phytosterol treatments have been shown to induce [66] and repress LXR target gene expression [109, 211, 213, 214]. For example, Kaneko *et al* showed SITO, CAMP, BRASS and STIG were able to activate LXR α driven luciferase HEK293 cells at 10 μ M [66] however in CHO-7 cells, SITO was unable to effectively activate LXR [172]. Plat, Nichols and Mensink, showed the expression of canonical LXR target gene ABCA1 is enhanced by treatment of phytosterols (SITO, STAN and CAMP) in Caco-2 cells [212] but Brauner *et al*, found that co-treatment of cholesterol with

either CAMP or SITO attenuated cholesterol mediated ABCA1 expression, suggesting phytosterols may be able to moderate LXR's response to ligand [211] but in a tissue/cell specific manner.

7.2 Hypothesis and Aims

PSS are able to impact on the oxysterol:LXR α axis at multiple points, including direct binding to LXR α as selective LXR modulators (SLiM) leading to changes in transcription targets. In this chapter the hypothesis that PSS could inhibit LXR α signalling in breast cancer was tested, and if through this altered transcriptional activity PSS are able to counteract the chemotherapy resistance mechanisms observed in chapter 5.

The aims of this chapter were to:

- Identify whether phytosterols act as selective modulators of LXR α in BCa cell lines.
- Determine whether phytosterols can alter LXR target gene transcription.
- Establish if phytosterols can reduce LXR-driven chemoresistance in TNBC.

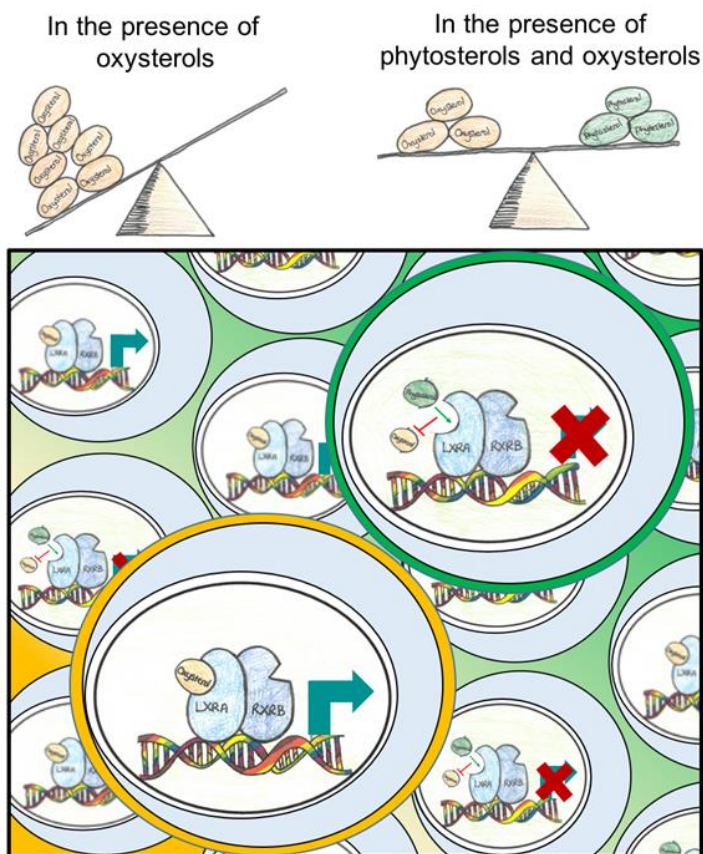


Figure 7. 2 Graphical abstract.

In the presence of oxysterols, oxysterols can bind to LXR and are able to regulate LXR target genes in breast cancer cells. In the presence of oxysterols and phytosterols however, phytosterols will compete with oxysterols for LXR α binding in breast cancer cells suppressing the LXR activity. Image previously published by Hutchinson *et al* [131].

7.3 Results

7.3.1 Phytosterols weakly modulate LXR.

In the literature, phytosterol interactions with LXR have shown a variety of results. For example, in HEK293 cells phytosterols (SITO, CAMP, BRAS and STIG at 10 μ M) were shown to behave as LXR agonists [66] but in other cell types such as CHO-7 cells failed to activate LXR α reporters [172]. MTT assays (see methods section 3.14) were performed to assess the anti-proliferative effects of phytosterol treatments and luciferase reporter systems (see methods section 3.2) were used to assess LXR α response after phytosterol treatments alone and in combination with oxysterols in BCa cell lines.

First, MTT assays were performed to assess the anti-proliferative effects in BCa cell lines after treatment with a range of phytosterol concentrations (**Figure 7.3**). All cell lines were unaffected by phytosterol treatments below 100nM (NB: MTT assays performed by Priscilia Lianto).

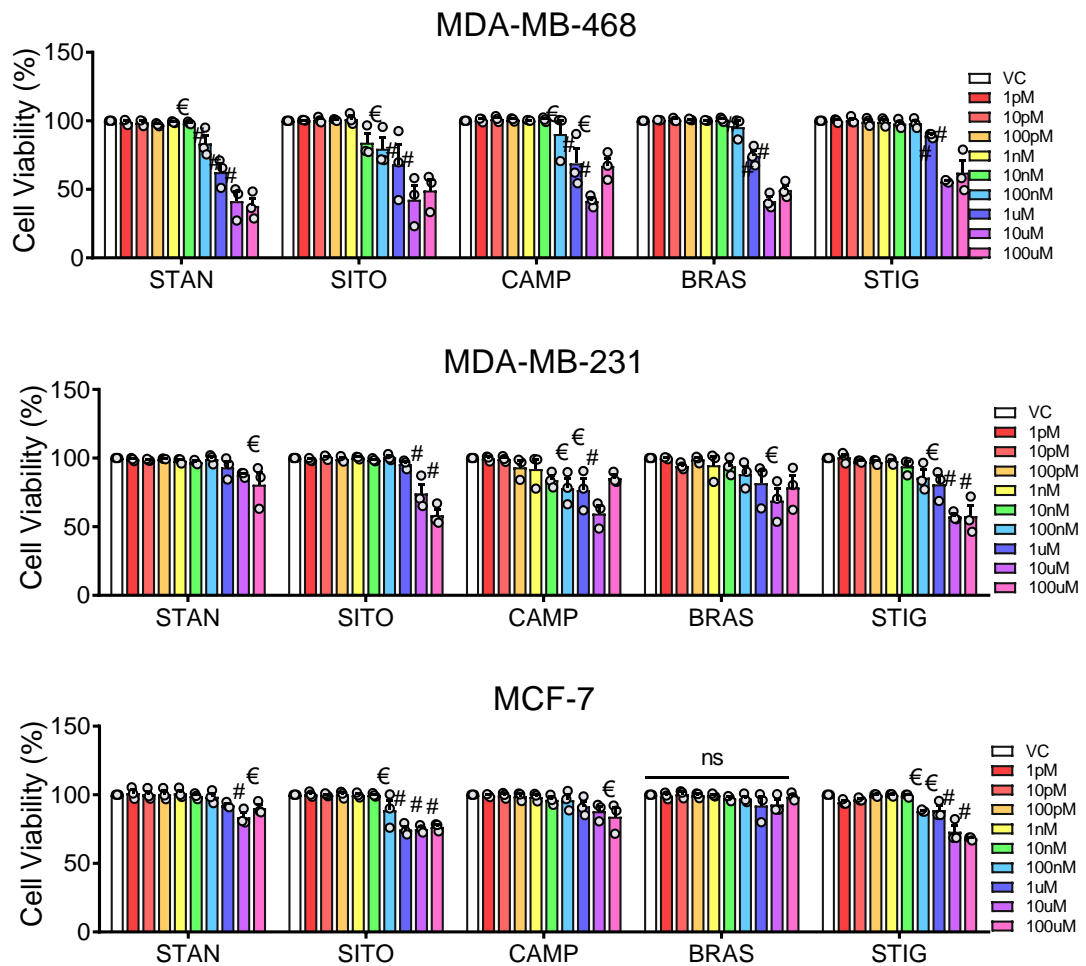


Figure 7. 3 Phytosterols are anti-proliferative in breast cancer cell cultures.

The anti-proliferative effects of STIG, SITO, CAMP, BRASS and STIG over 48 h was assessed by MTT in MDA-MB-468, MDA-MB-231, and MCF-7 cells. Cell viability relative to vehicle control was measured after treatment with plant sterols and stanols (PSSs) at indicated concentrations. Data are presented as mean of three independent replicates (open circles) with SEM. For assessing changes between individual concentrations and vehicle, one-way ANOVA with Holm-Sidak correction for multiple testing and post-test for linear trend was performed. Significance levels are indicated by € = $p < 0.05$ and # = $p < 0.0001$. Linear trend was significant for all PSS in all cell lines except for BRAS in MCF-7 (ns). Data generated and analysed by Priscilia Lianto.

At 100nM and above there were differences between the cell lines in their response to the phytosterols. MDA-MB-468 cells were the most sensitive to phytosterol

treatment with significant reductions in cell viability after treatment with STAN, SITO, CAMP and BRAS at 100 μ M (1 way-ANOVA: $p < 0.0001$), 10 μ M (at least $p < 0.05$) and 1 μ M (at least $p < 0.05$). MCF-7 cells were the most resistant to phytosterol treatment with complete resistance to BRAS at all concentrations tested (ns). SITO most effective phytosterol at altering cell viability across all three cell lines ($p < 0.0001$ at 100 μ M and 10 μ M, $p < 0.05$ for 1 μ M in 468 and MCF-7 cells). The MDA-MB-231 cells were more sensitive to phytosterol treatments than the MCF-7 cells, but not as sensitive as the MDA-MB-468 cells.

Next, we assessed phytosterol regulation of LXR α luciferase reporters. MDA-MB-468, MDA-MB-231 and MCF-7 reporter cells were treated with a panel of phytosterols at a range of concentrations for 16 h and LXR α transactivation measured by luciferase assay (**Figure 7.4**). The range of phytosterols failed to significantly alter LXR α activity in the MDA-MB-468 cells at all concentrations except for STAN at 100 nM (1 way-ANOVA; $p < 0.05$). The range of phytosterols failed to significantly alter LXR α activity in the MDA-MB-231 cells at all individual concentrations. However, in the MCF-7 cells BRAS (50 μ M, $p < 0.05$) and STIG (1 pM, 100 nM., 5 μ M, 10 μ M and 50 μ M., $p < 0.05$) were able to activate LXR α by a small fraction. Linear trends were assessed for each phytosterol; MDA-MB-468 (SITO; slope=0.017, $R^2=0.09$, $p=0.038$), MDA-MB-231 (STAN; slope=-0.03, $R^2=0.025$, $p=0.002$., SITO; slope=-0.015, $R^2=0.063$, $p=0.03$., and BRAS; slope=0.018, $R^2=0.061$, $p=0.033$) and MCF-7 (BRAS; slope=0.049, $R^2=0.25$, $p=0.0002$., STIG; slope=0.023, $R^2=0.15$, $p=0.0049$). Overall, the range of phytosterols were not able to sufficiently alter LXR α activation.

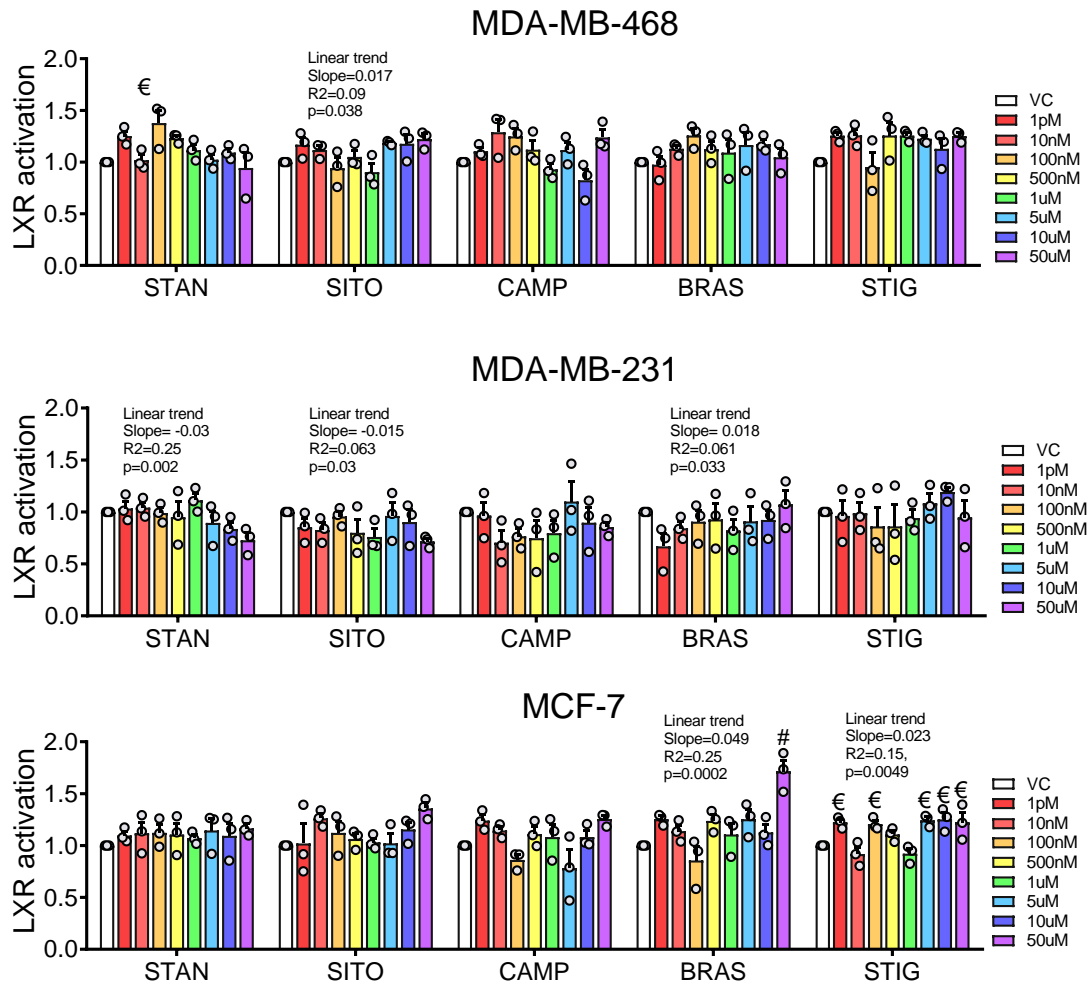


Figure 7. 4 LXR α is only weakly modulated by PSSs treatment in breast cancer cell lines.

A luciferase reporter driven by an LXR alpha (LXR α) responsive promoter was stably transfected into MDA-MB-468, MDA-MB-231, and MCF-7. Relative luciferase activity was measured after treating with PSSs at indicated concentrations for 16 h and is shown normalised to vehicle control (VC). Data are presented as mean of three independent replicates (open circles) with SEM. For assessing changes between individual concentrations and vehicle, one-way ANOVA with Holm-Sidak correction for multiple testing and post-test for linear trend was performed. Significance levels are indicated by € = $p < 0.05$ and # = $p < 0.0001$, or for linear trend Slope, R² and p value are indicated.

7.3.2 Phytosterols antagonise oxysterol-LXR α activation.

The phytosterol treatments were not able to strongly alter LXR α activity in the breast cancer reporters. Phytosterols when taken to reduce LDL-C, have an effect when cholesterol and oxysterol levels are high. So, to test their ability to alter LXR α activity when stimulated by the cholesterol derivatives oxysterols, we used luciferase reporter systems and gene expression analyses to assess cell LXR α response after co-treatment with oxysterols and phytosterol in BCa cell lines.

First, we assessed LXR α response after co-treatment with oxysterols and phytosterols in BCa reporter cell lines. MDA-MB-468, MDA-MB-231 and MCF-7 LXR α reporter cell lines were treated with oxysterols and phytosterols alone and in combination for 16 h and LXR α transactivation measured by luciferase assay. In the MDA-MB-468 reporters (**Figure 7.5**) treatment with oxysterols at 1 μ M (2-way ANOVA: $p < 0.05$) and 10 μ M ($p < 0.0001$) increased LXR α activity. When oxysterols were given as co-treatments with phytosterols, the phytosterols antagonised the oxysterol activation of LXR α at 1 μ M (24OHC; all PSS, $p < 0.0001$., 25OHC; all PSS, $p < 0.0001$., 24,25-EC; all PSS, $p < 0.0001$., 26OHC; all PSS, $p < 0.05$) and 10 μ M (24OHC; all PSS, $p < 0.0001$., 25OHC; all PSS at least, $p < 0.05$., 24,25-EC; all PSS except CAMP (ns), $p < 0.0001$., 26OHC; all PSS except STIG (ns) at least, $p < 0.05$).

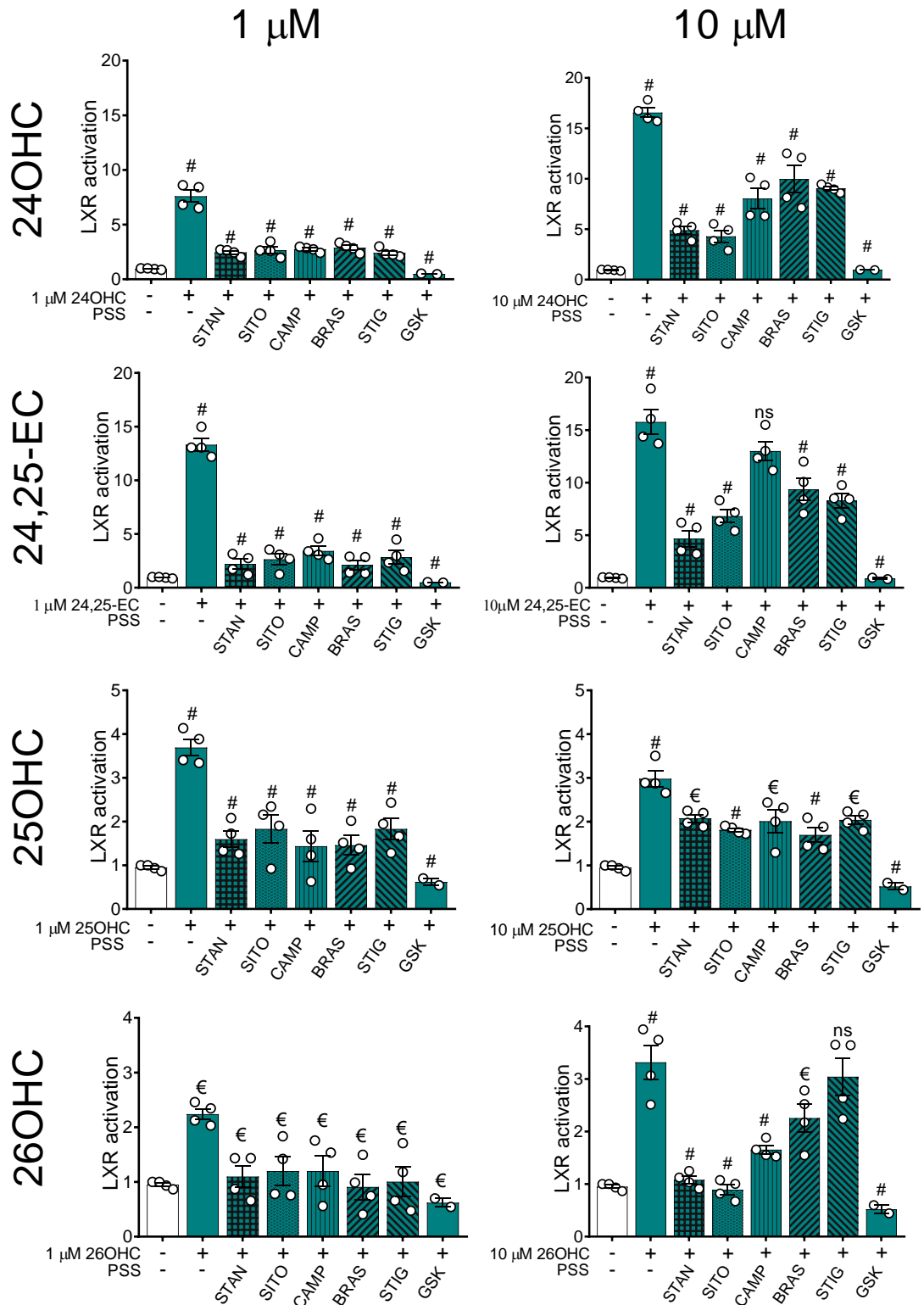


Figure 7. 5 Phytosterols antagonise oxysterol-LXR α activation in TNBC MDA-MB-468 cell cultures.

Oxysterol-mediated LXR α activity was measured in the presence of oxysterols alone (24OHC, 25OHC, 26OHC, 24,25-EC) or in combination with PSS (STAN, SITO, CAMP, BRAS, STIG) or the synthetic LXR antagonist GSK2033. PSS were applied to TNBC cells in doses of 10 μ M, and oxysterols in 1 μ M and 10 μ M as indicated. Error bars show SEM of four biological replicates. Two-way ANOVA used for statistical analysis were € = $p < 0.05$, and # = $p < 0.0001$.

In the MDA-MB-231 reporters (**Figure 7.6**) treatment with oxysterols at 1 μM ($p < 0.05$) and 10 μM ($p < 0.0001$) increased LXR α activity. When oxysterols were given as co-treatments with phytosterols, the phytosterols antagonised the oxysterol activation of LXR α at 1 μM (24OHC; all PSS except STAN (ns) at least, $p < 0.05$., 25OHC; all PSS, $p < 0.05$., 24,25-EC; all PSS, $p < 0.05$, 26OHC; only STAN, $p < 0.05$) and 10 μM (24OHC; all PSS, $p < 0.0001$, 25OHC; all PSS except BRAS (ns), $p < 0.0001$, 24,25-EC; all PSS except BRAS (ns), $p < 0.0001$, 26OHC; all PSS, $p < 0.0001$).

In the MCF-7 reporters (**Figure 7.7**) treatment with oxysterols at 1 μM (all OHC except 26OHC $p < 0.05$) and 10 μM ($p < 0.0001$) increased LXR α activity. When oxysterols were given as co-treatments with phytosterols in the MCF-7 cell line, the phytosterols were also able to antagonise the oxysterol activation of LXR α at 1 μM (24OHC; all PSS except SITO (ns) at least, $p < 0.05$, 25OHC; all PSS at least, $p < 0.05$., 24,25-EC; all PSS except STAN (ns), $p < 0.05$, 26OHC; all PSS except SITO (ns), $p < 0.05$) and 10 μM (24OHC; all PSS, $p < 0.0001$, 25OHC; all PSS except BRAS and STIG (ns), $p < 0.0001$, 24,25-EC; all PSS at least, $p < 0.05$, 26OHC; all PSS except BRAS and STIG (ns), $p < 0.0001$).

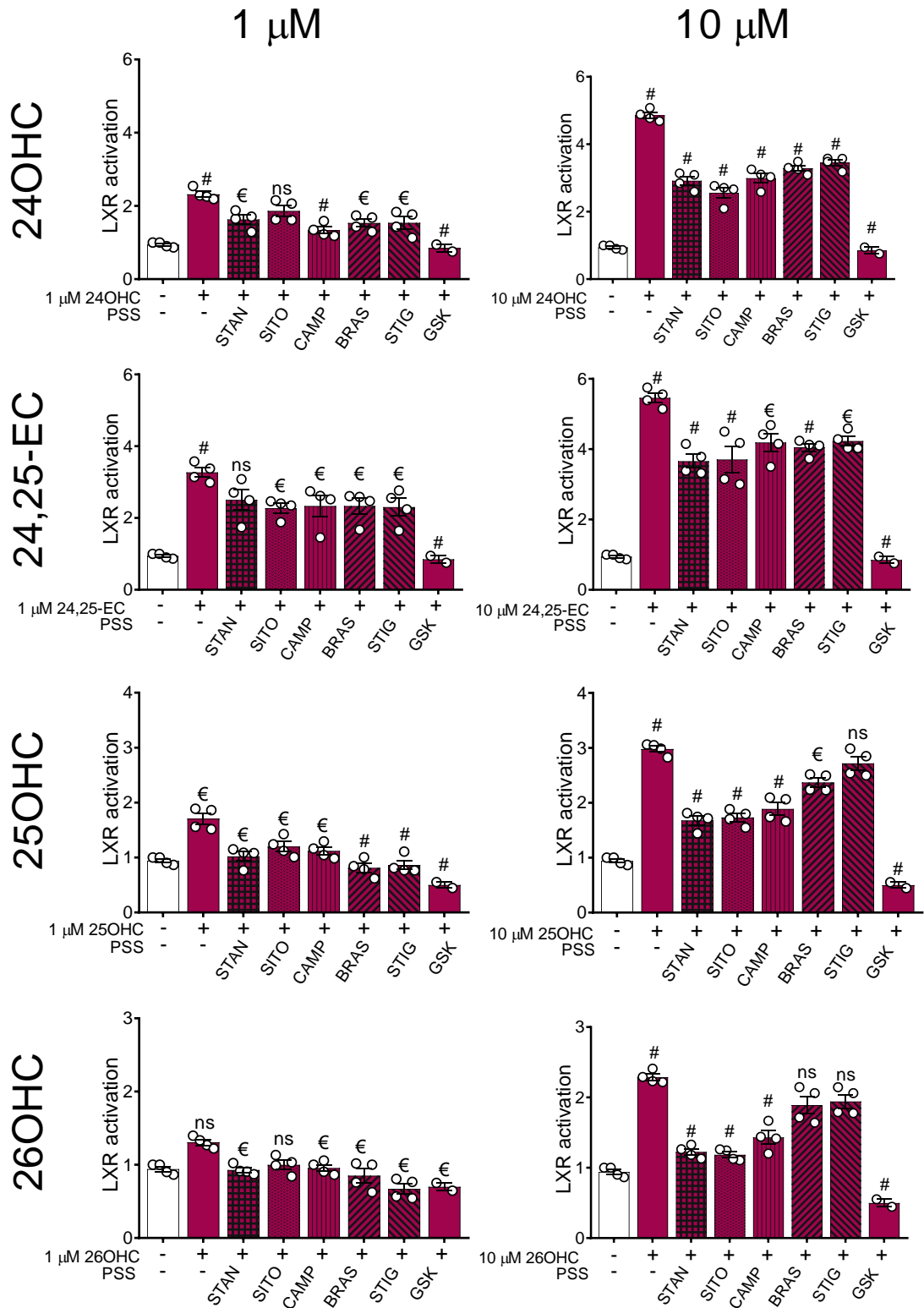


Figure 7.7 Phytosterols antagonise oxysterol-LXR α activation in ER-positive MCF-7 cell cultures.

Oxysterol-mediated LXR α activity was measured in the presence of oxysterols alone (24OHC, 25OHC, 26OHC, 24,25-EC) or in combination with PSS (STAN, SITO, CAMP, BRAS, STIG) or the synthetic LXR antagonist GSK2033. PSS were applied to ER-positive cells in doses of 10 μ M, and oxysterols in 1 μ M and 10 μ M as indicated. Error bars show SEM of four biological replicates. Two-way ANOVA used for statistical analysis were € = $p < 0.05$, and # = $p < 0.0001$.

Additional to the luciferase oxysterol and phytosterol co-treatments, phytosterols were also included as single treatments as controls (**Figure 7.8**). Treatments of phytosterols (STAN, SITO, CAMP, BRAS and STIG) in MDA-MB-468, MDA-MB-231 and MCF-7 luciferase reporters were unable to regulate LXR α activity at 10 μ M as single treatments (Two-way ANOVA; ns). The LXR antagonist GSK2033 was included as a control to compare reduced LXR α activity in the three BCa cell lines ($p < 0.0001$).

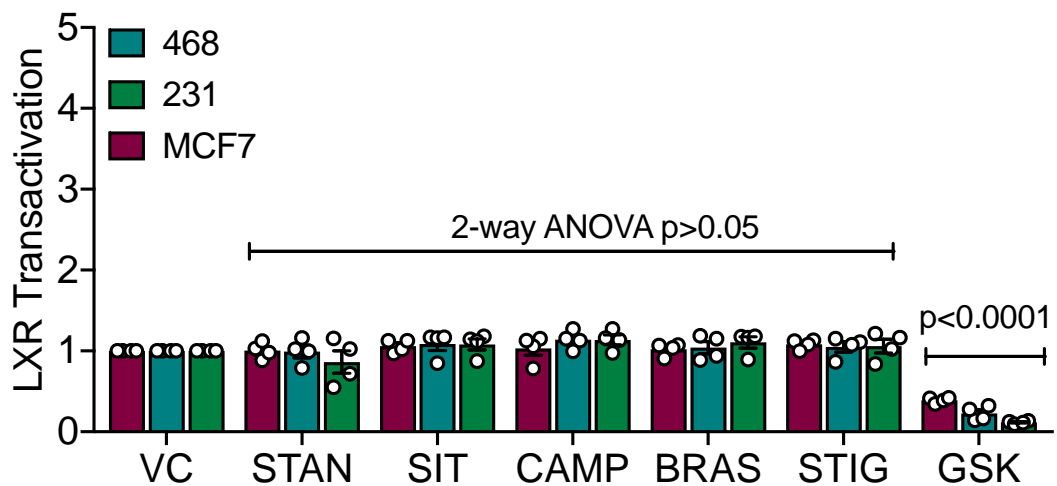


Figure 7. 8 LXR α activity when treated with phytosterols at 10 μ M.

Hormone receptor negative (a) MDA-MB-468 and (b) MDA-MB-231 luciferase reporter cells, and hormone receptor positive (c) MCF-7 luciferase reporter cells were treated with PSS (10 μ M) for 16 h and LXR α activity was assessed by luciferase assay and normalised to VC. Data shown are mean of four independent replicates with SEM. Two-way ANOVA with Holm-Sidak correction for multiple testing was used to determine statistical significance.

Next, the data were analysed to establish efficiency of inhibition. (**Figure 7.9**). First the percentage efficiency that each phytosterol impairs the activation of LXR α by each oxysterol in each cell line at 1 μ M and 10 μ M were calculated and presented as boxplots. Results showed that in the co-treatments treated with 1 μ M oxysterol and 10 μ M phytosterol there was no significant difference (Two-way ANOVA, ns) between phytosterols for the breast cancer cell lines (**Figure 7.9A**). In the co-treatments treated with 10 μ M oxysterol and 10 μ M phytosterol (**Figure 7.9B**)

however, STAN and SITO were significantly more efficient at antagonising oxysterol activation of LXR α in the three BCa cell lines (Two-way ANOVA).

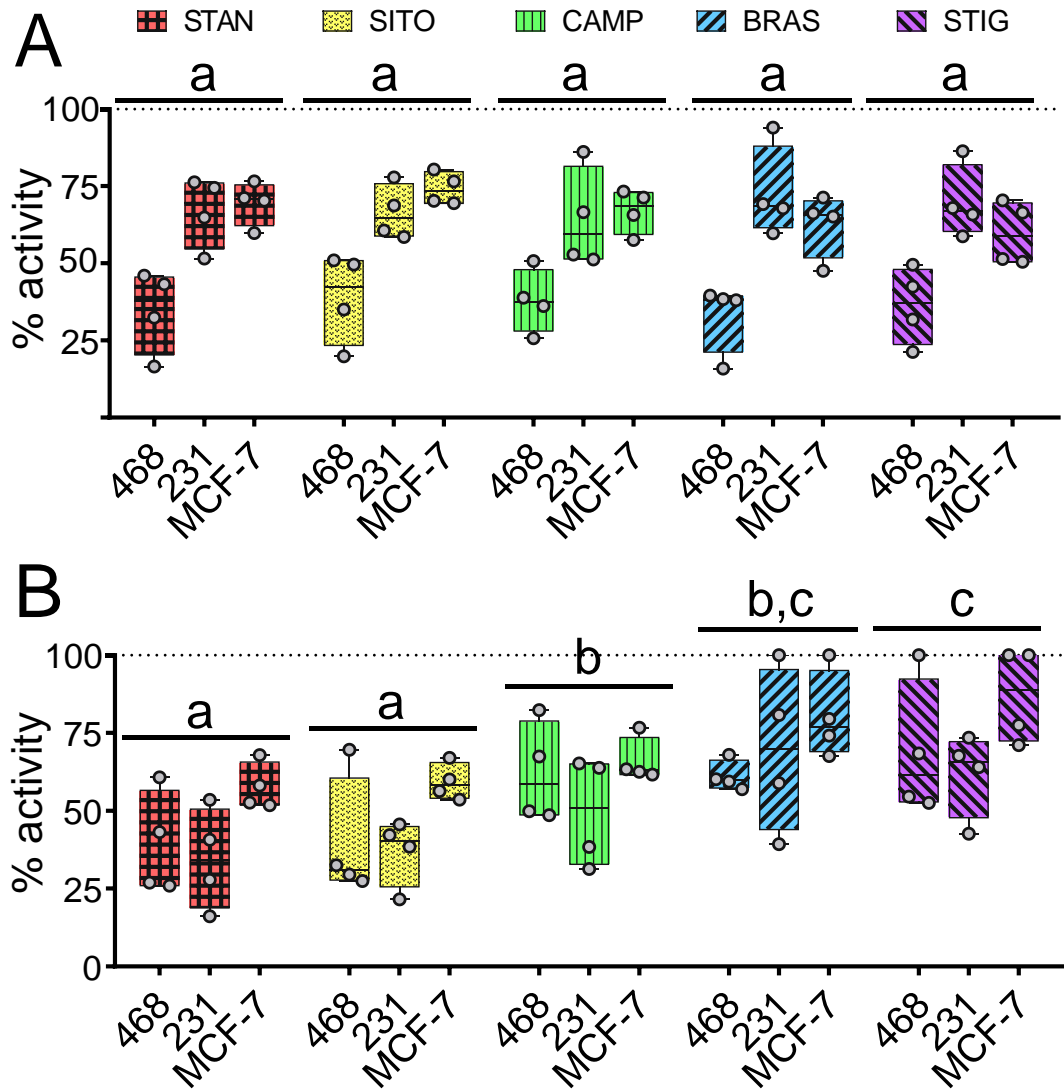


Figure 7.9 Inhibition of oxysterol induced LXR α activity by PSS and cell lines.

The percentage efficiency with which each PSS impairs activation of LXR α by each oxysterol was calculated in each cell line for both low (1 μ M (a)) and high (10 μ M (b)) dose PSS treatment. Individual oxysterols are represented by circles with range and mean shown in box plots. Statistical differences in the abilities of different PSS to impair oxysterol mediated LXR α activation are denoted by different letters (shared letters indicate no significant difference between PSS). Statistical significance was determined using two-way ANOVA. Data shown are of 4 independent replicates with SEM.

After phytosterols were found to inhibit oxysterol mediated activation of LXR α , oxysterol and phytosterol co-treatments were repeated in the parental cell lines to determine whether co-treatment altered LXR transcriptional output of its target genes ABCA1 (**Figure 7.10**) and APOE (**Figure 7.11**).

MDA-MB-468, MDA-MB-231 and MCF-7 parental cell lines were exposed to co-treatments of 24OHC, 26OHC and GW3965 alone and in combination with SITO and STAN for 16 h. RNA was harvested, and gene expression analysed with Taqman assays. In MDA-MB-468 cells, treatment with LXR agonists enhanced expression of ABCA1 (1-way ANOVA, $p < 0.0001$) which was attenuated by co-treatment of 24OHC, 26OHC and GW3965 with phytosterols (SITO and STAN, $p < 0.0001$, all co-treatments). In MDA-MB-231 cells, treatment with LXR agonists enhanced expression of ABCA1 ($p < 0.0001$) which was also attenuated by co-treatment of 24OHC, 26OHC and GW3965 with phytosterols (SITO and STAN, $p < 0.0001$, all co-treatments). And finally in MCF-7 cells, treatment with LXR agonists enhanced expression of ABCA1 ($p < 0.0001$) which was also attenuated by co-treatment of 24OHC, 26OHC and GW3965 with phytosterols (SITO and STAN, $p < 0.0001$, all co-treatments).

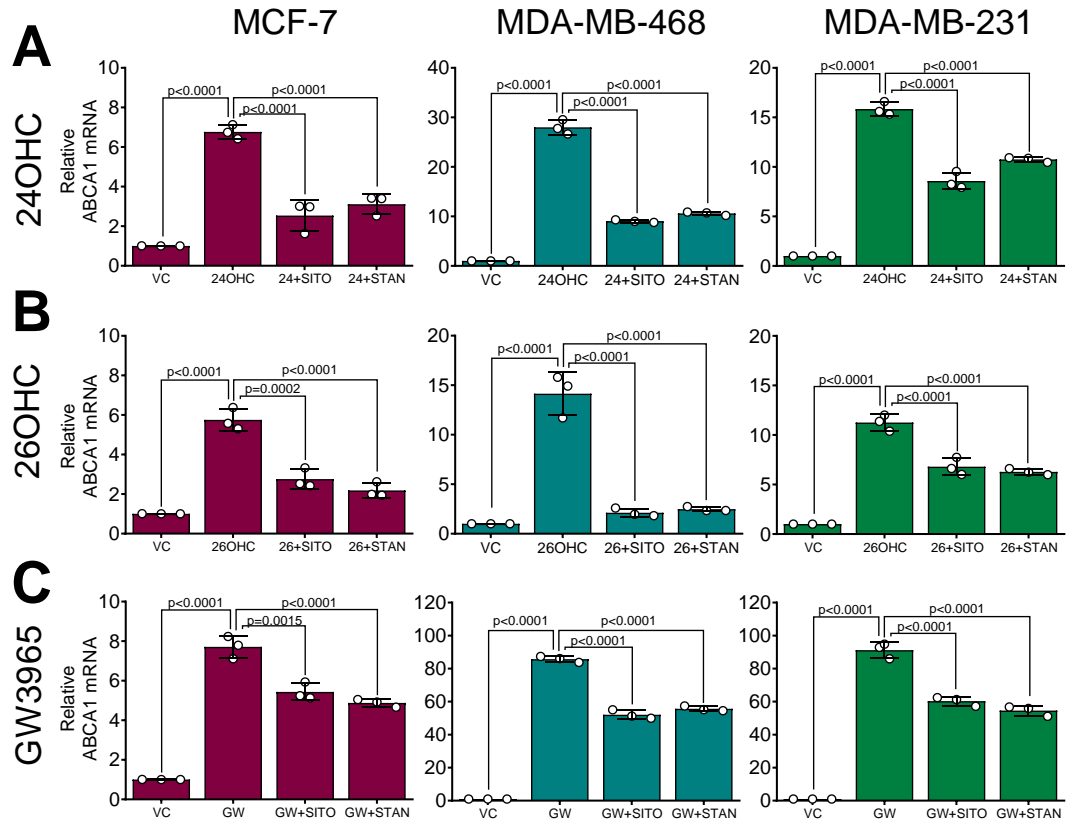


Figure 7. 10 Phytosterols antagonise oxysterol-LXR activation of the canonical target genes ABCA1.

TNBC MDA-MB-468 and MDA-MB-231 cells, and Luminal A MCF-7 cells were treated with LXR ligands 24OHC (A), 26OHC (B) and GW3965 (C) (synthetic 1 μ M, oxysterol 10 μ M) for 16 h alone or in combination with SITO or STAN and expression of ABCA1 was assessed by qPCR ($\Delta\Delta$ Ct using HPRT and normalised to vehicle). Data shown are mean of three independent replicates (circles) with SEM. One-way ANOVA with Holm-Sidak correction for multiple testing was performed.

In MDA-MB-468 cells, treatment with LXR agonists enhanced expression of APOE ($p < 0.0001$) which was attenuated by co-treatment of 24OHC, 26OHC and GW3965 with phytosterols (SITO and STAN, $p < 0.0001$, all co-treatments). In MDA-MB-231 cells, treatment with LXR agonists enhanced expression of APOE ($p < 0.0001$) which was attenuated by co-treatment of 24OHC with phytosterols (SITO, $p < 0.05$., STAN, $p < 0.0001$), 26OHC with phytosterols (SITO and STAN, $p < 0.0001$) and GW3965 with phytosterols (SITO and STAN, $p < 0.0001$). In MCF-7 cells, treatment with LXR agonists drastically decreased expression of APOE ($p < 0.0001$) which was not able to be

further attenuated by co-treatment of 24OHC, 26OHC and GW3965 with phytosterols (SITO and STAN, ns, all co-treatments).

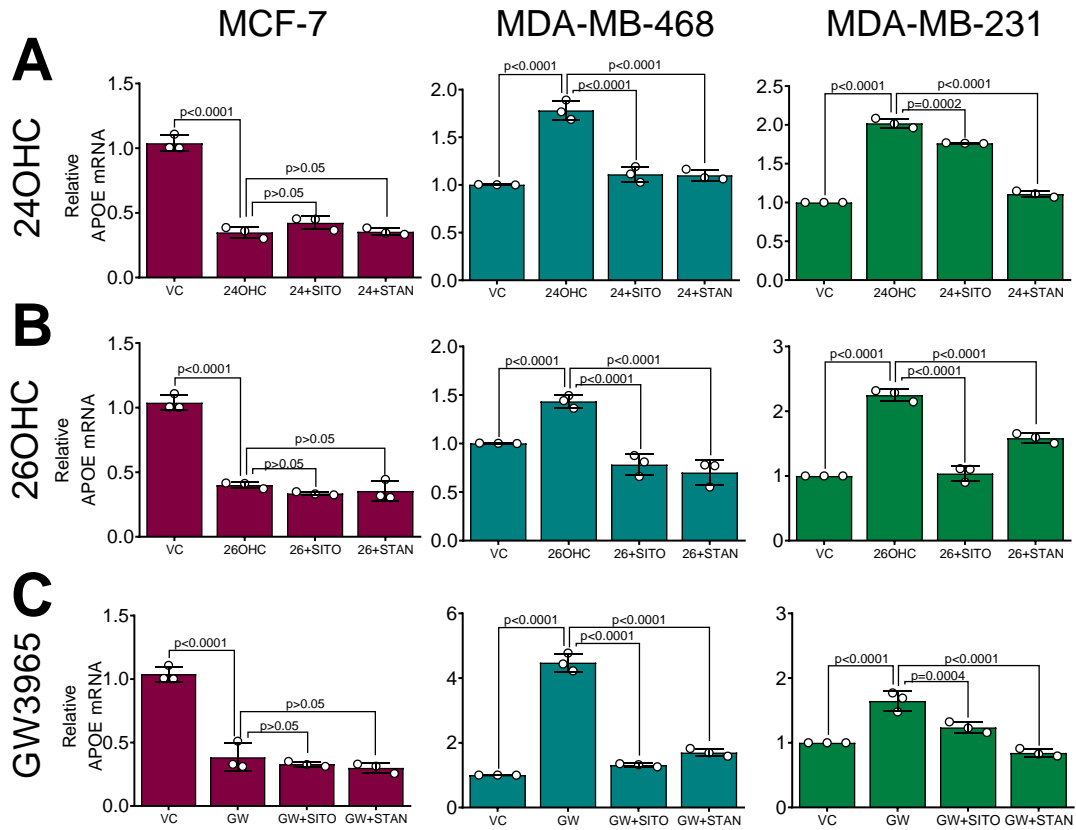


Figure 7. 11 Phytosterols antagonise oxysterol-LXR activation of the canonical target genes APOE.

TNBC MDA-MB-468 and MDA-MB-231 cells, and Luminal A MCF-7 cells were treated with LXR ligands 24OHC (A), 26OHC (B) and GW3965 (C) (synthetic 1 μ M, oxysterol 10 μ M) for 16 h alone or in combination with SITO or STAN and expression of APOE was assessed by qPCR ($\Delta\Delta$ Ct using HPRT and normalised to vehicle). Data shown are mean of three independent replicates (circles) with SEM. One-way ANOVA with Holm-Sidak correction for multiple testing was performed.

Furthermore, expression of ABCA1 and APOE was measured after single treatment of phytosterols SITO and STAN (Figure 7.12). In MDA-MB-468 cells individual treatments of SITO and STAN were unable to alter the expression of ABCA1 or APOE (1-way ANOVA; SITO and STAN, ns). In MDA-MB-231 cells individual treatments of SITO and STAN increased the expression of ABCA1 (SITO, p=0.016., STAN, p=0.03) and APOE (SITO and STAN, p<0.0001). And finally, in MCF-7 cells individual treatments of SITO and STAN were unable to alter the expression of ABCA1 (SITO

and STAN, ns) but significantly reduced the expression of APOE (SITO and STAN, $p < 0.0001$).

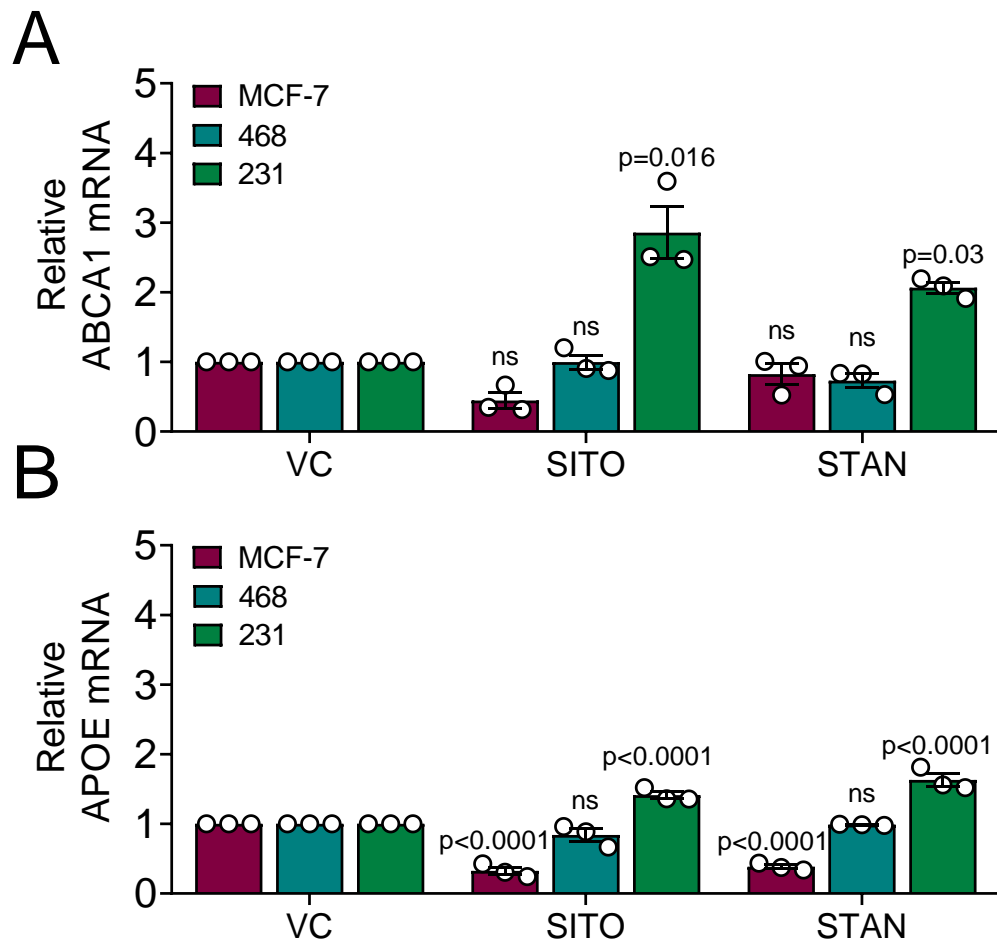


Figure 7.12 Phytosterols weakly regulate of LXR target genes.

TNBC MDA-MB-468 and MDA-MB-231 cells, and Luminal A MCF-7 cells were treated with PSS (10 μ M) for 16 h and expression of ABCA1 (A) and APOE (B) was assessed by TaqMan assays ($\Delta\Delta$ Ct using HPRT and normalised to vehicle). Data shown are mean of three independent replicates with SEM. One-way ANOVA with Holm-Sidak correction for multiple testing was used to determine statistical significance.

7.3.3 Phytosterols attenuate the oxysterol-LXR driven expression of the p-glycoprotein/ABCB1.

Phytosterols have been shown to antagonise LXR α activity and the transcriptional output target genes involved in cholesterol efflux in the TNBC cells. As shown in chapter 5, LXR α controls the regulation of genes involved in the development of

chemoresistance such as p-gp/ABCB1 in TNBC cells, which when knocked down or silenced was able to reverse the chemoprotective effects. To establish if phytosterols can impair oxysterol-mediated expression of LXR α driven expression of p-gp/ABCB1 and therefore reduce the chemoprotective effects previously demonstrated, we treated cells with co-treatments of phytosterols and oxysterols and assessed the regulation of p-gp/ABCB1 through gene expression analyses and chemotherapy efflux assays.

To assess if phytosterols can inhibit oxysterol-LXR expression of the chemotherapy efflux pump p-gp/ABCB1, co-treatments of the phytosterols SITO and STAN were administered to MDA-MB-468, MDA-MB-231 and MCF-7 cells with either 24OHC, 26OHC or GW3965 and expression of p-gp/ABCB1 measured using qPCR (**Figure 7.13**). In MDA-MB-468 cells, treatment with LXR agonists enhanced expression of p-gp/ABCB1 (1-way ANOVA, $p < 0.0001$) which was attenuated by co-treatment of 24OHC, 26OHC and GW3965 with phytosterols (SITO and STAN, at least $p < 0.001$ for all co-treatments). In MDA-MB-231 cells, treatment with LXR agonists enhanced expression of p-gp/ABCB1 ($p < 0.0001$) which was attenuated by co-treatment of 24OHC with phytosterols ($p < 0.0001$), 26OHC with phytosterols ($p < 0.0001$) and GW3965 with phytosterols ($p < 0.0001$). In MCF-7 cells however, treatment with LXR agonists decreased expression of p-gp/ABCB1 ($p < 0.0001$) which was not able to be further attenuated by co-treatment of 24OHC, 26OHC or GW3965 with phytosterols (ns).

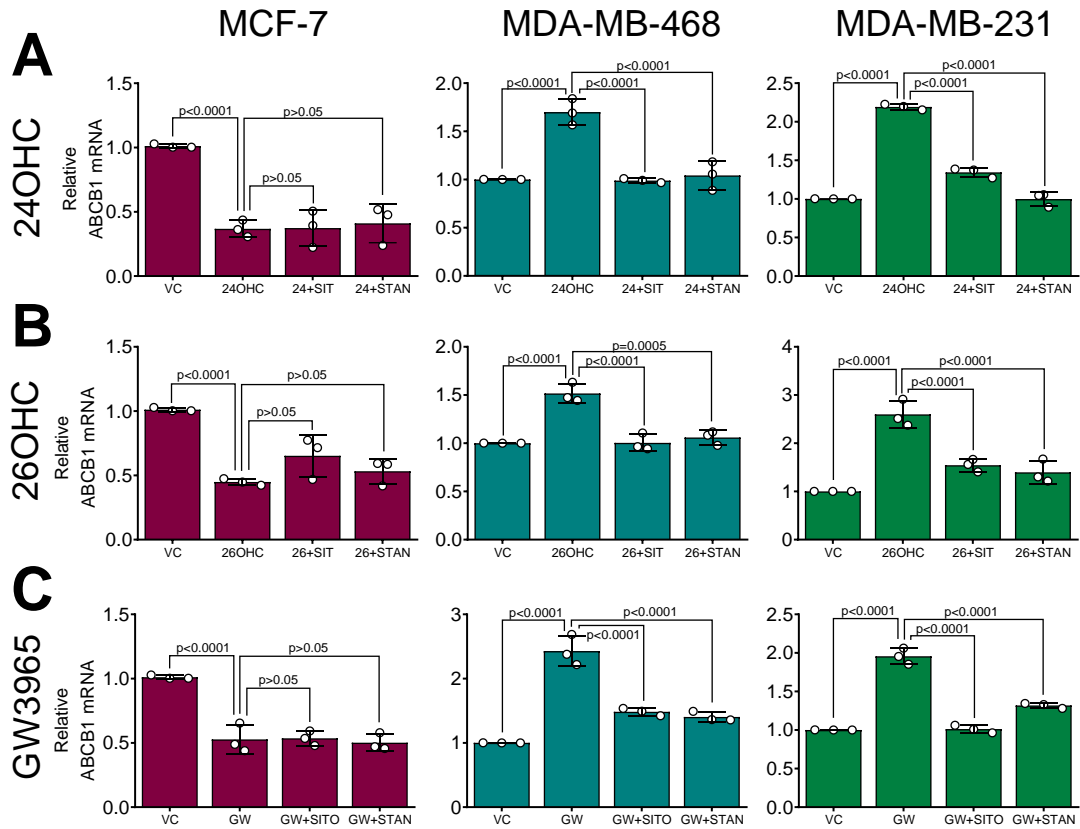


Figure 7.13 Phytosterols antagonise oxysterol-LXR activation of p-gp/ABCB1.

TNBC (a) MDA-MB-468 and (b) MDA-MB-231 cells, and Luminal A (c) MCF-7 cells were treated with LXR ligands (synthetic 1 μ M, oxysterol 10 μ M) for 16 h alone or in combination with SITO or STAN and expression of p-gp/ABCB1 was assessed by qPCR ($\Delta\Delta$ Ct using HPRT and normalised to vehicle). Data shown are mean of three independent replicates (circles) with SEM. One-way ANOVA with Holm-Sidak correction for multiple testing was performed.

Furthermore, we measured expression of p-gp/ABCB1 after single treatment of phytosterols SITO and STAN (**Figure 7.14**). In MDA-MB-468 cells individual treatments of SITO and STAN were unable to alter the expression of p-gp/ABCB1 (1-way ANOVA, ns) or in MDA-MB-231 cells (ns). In MCF-7 cells however, individual treatments of SITO and STAN significantly reduced the expression of p-gp/ABCB1 ($p < 0.0001$).

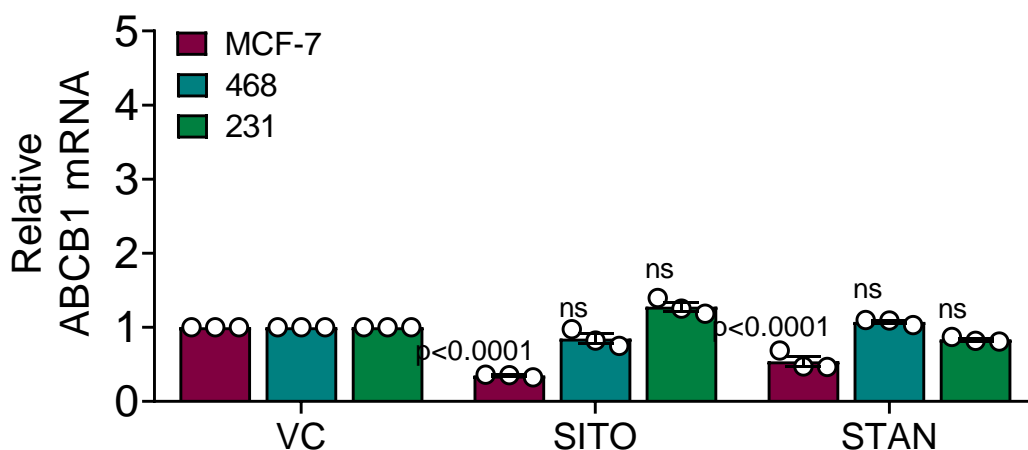


Figure 7. 14 Phytosterols downregulate the expression of p-gp/ABCB1 in Luminal A cells.

TNBC MDA-MB-468 and MDA-MB-231 cells, and Luminal A MCF-7 cells were treated with PSS (10 μ M) for 16 h and expression of p-gp/ABCB1 was assessed by qPCR ($\Delta\Delta$ Ct using HPRT and normalised to vehicle). Data shown are mean of three independent replicates with SEM. One-way ANOVA with Holm-Sidak correction for multiple testing was used to determine statistical significance.

As gene expression of p-gp/ABCB1 was significantly reduced by co-treatment of phytosterols with oxysterols in the TNBC cells, chemotherapy efflux assays were performed to identify if the reduction in p-gp/ABCB1 expression by the co-treatments also reduced the export of epirubicin (**Figure 7.15**). MDA-MB-468 and MDA-MB-231 cells were pre-treated with phytosterols and oxysterols in combination and alone for 16 h before epirubicin for 1 h. **Figure 7.15** shows oxysterols in co-treatment with sitosterol (SITO) and (**Figure 7.16**) shows oxysterols in co-treatment with sitostanol (STAN).

In TNBC cells (MDA-MB-468 **Figure 7.15A**, MDA-MB-231 **Figure 7.15B**), oxysterol treatment with 24OHC and 26OHC before chemotherapy treatment enhanced the export of epirubicin (dissociation one phase exponential decay; $p < 0.0001$) relative to the epirubicin only treated cells. Treatment with SITO before chemotherapy treatment slowed down the export of epirubicin ($p < 0.001$). Interestingly, co-treatment of oxysterols with SITO reversed the enhanced expression of epirubicin slowing down the rate of exportation ($p < 0.0001$). Additionally, the co-treatment of

oxysterols with SITO further slowed down the export of epirubicin in the MDA-MB-468 cells ($p < 0.0001$) but was only able to in MDA-MB-231 cells with co-treatment of 26OHC+SITO ($p < 0.0001$).

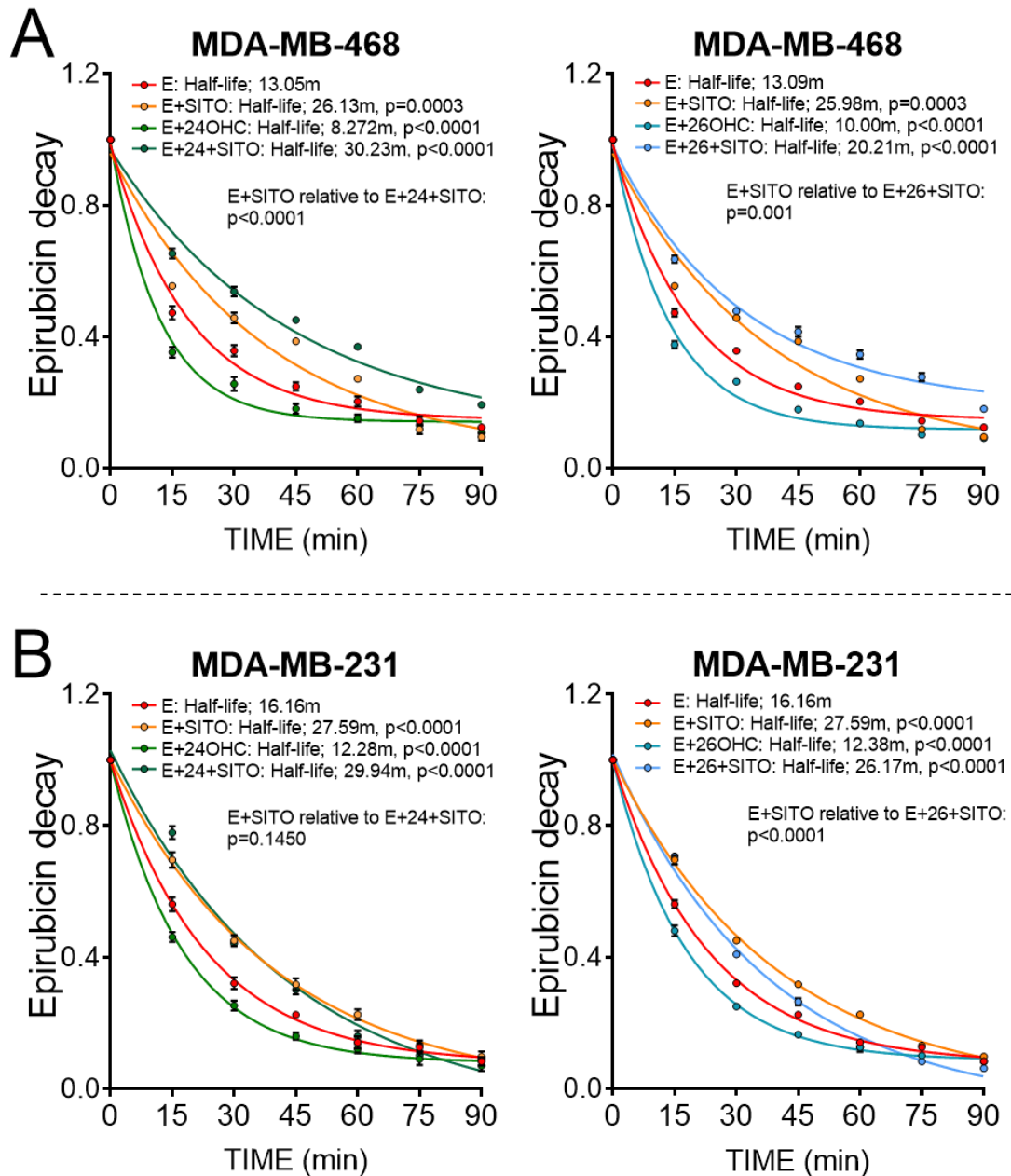


Figure 7.15 Sitosterol reverses the OHC-LXR effects of enhanced epirubicin exportation.

MDA-MB-468 (A) and MDA-MB-231 (B) cells were pre-treated with LXR ligands (24OHC, 26OHC) alone or combination with a phytosterol (β -sitosterol) or vehicle for 16 h. Cells were then exposed to epirubicin (50 μ M) for 1 h. Fluorescence of epirubicin was measured at 15 min intervals for 90 min. Statistical analysis of half-life was assessed using dissociation one phase exponential decay. **Data shown are of 3 independent replicates with SEM.**

In TNBC cells (MDA-MB-468 **Figure 7.16A**, MDA-MB-231 **Figure 7.16B**), oxysterol treatment with 24OHC or 26OHC before chemotherapy treatment enhanced the export of epirubicin (dissociation one phase exponential decay; $p < 0.0001$) relative to the epirubicin only treated cells. Treatment with STAN in both TNBC cell lines before chemotherapy treatment slowed down the export of epirubicin (at least $p = 0.001$). In MDA-MB-468 and MDA-MB-231 cells co-treatment of 24OHC with STAN reversed the enhanced expression of epirubicin slowing down the rate of exportation ($p < 0.0001$) as did the co-treatment of 26OHC with STAN ($p < 0.0001$). Additionally, the co-treatment of 24OHC with STAN further slowed down the export of epirubicin (at least $p < 0.01$) relative to the treatment of E+STAN, as did the co-treatment of 26OHC with STAN ($p < 0.0001$).

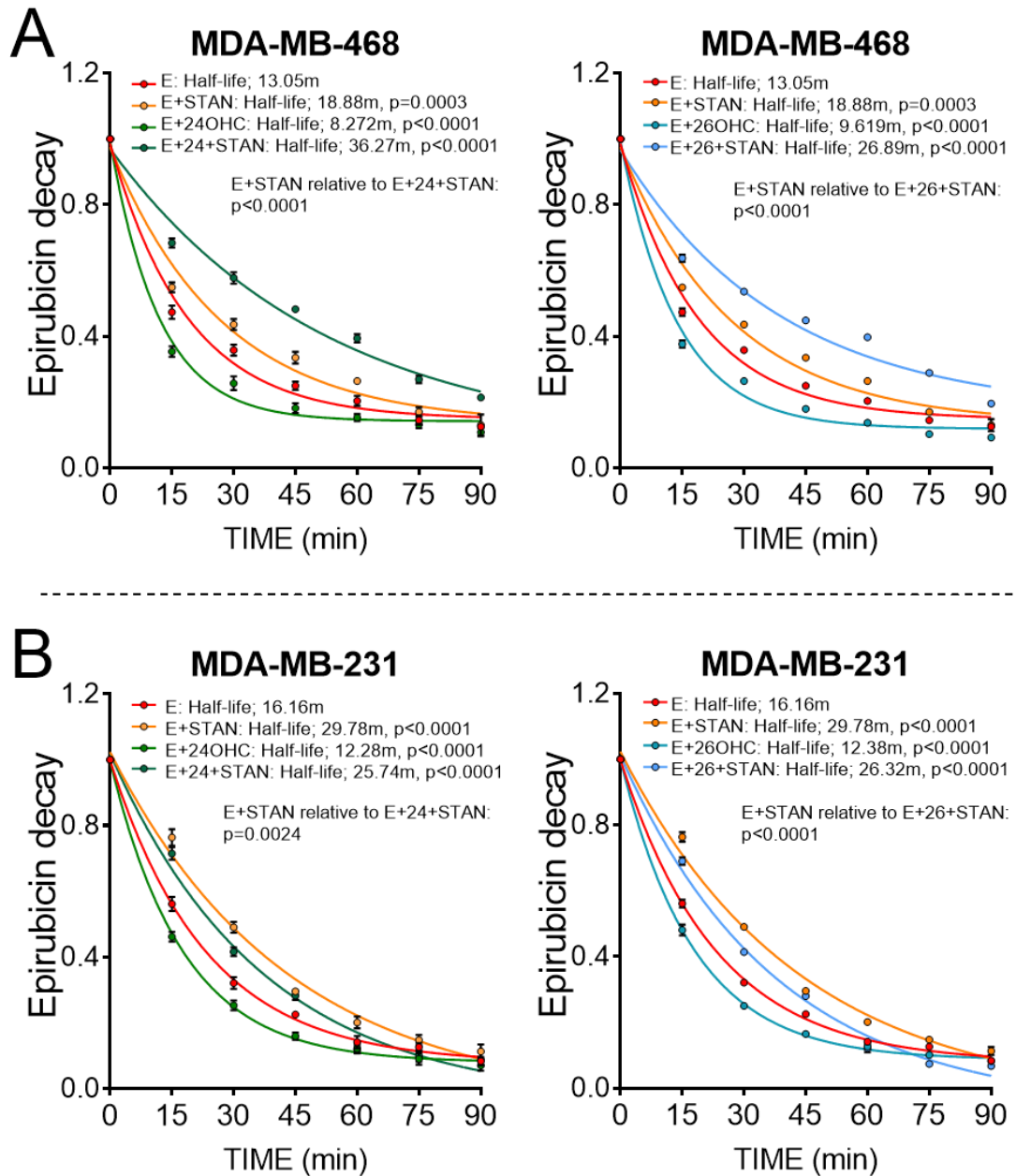


Figure 7. 16 Sitostanol reverses the OHC-LXR effects of enhanced epirubicin exportation.

MDA-MB-468 (A) and MDA-MB-231 (B) cells were pre-treated with LXR ligands (24OHC, 26OHC) alone or combination with a phytosterol (β -sitostanol) or vehicle for 16 h. Cells were then exposed to epirubicin (50 μ M) for 1 h. Fluorescence of epirubicin was measured at 15 min intervals for 90 min. Statistical analysis of half-life was assessed using dissociation one phase exponential decay. **Data shown are of 3 independent replicates with SEM.**

In summary, phytosterols antagonise oxysterol-mediated expression of p-gp/ABCB1 in TNBC. Phytosterols have also been shown to reverse the oxysterol-LXR effects of enhanced epirubicin export when given as a co-treatment.

7.4 Discussion

Plant based diets that are rich in phytosterols are known to lower LDL-C and are associated with reduced risk of primary and recurrent breast cancer [48]. Typically, 0.04-5 % of consumed PSSs are absorbed [210, 310-312] but this can vary from person to person based on the individual genetics or pathologies [210, 311], but also on the chemistry of specific PSSs [210, 312]. Absorption of dietary cholesterol is more efficient than the absorption of phytosterols however, phytosterols circulate in much higher concentrations than cholesterol derivatives. In the general population phytosterols circulate at around 20 μM , although in some high PSS intake individuals PSS concentrations have been found to be in excess of 100 μM [204]. Cholesterol circulates at concentrations between 4-5 mM [313] which is around 50-200 times higher than PSS concentrations. Although lower than cholesterol concentrations, PSS circulating concentrations are around 5,000-20,000 times higher than 17β -estradiol (1 nM), 20-100 times higher than Vitamin D (50 nM) and up to 1000 times higher than most oxysterols [314].

In this chapter, cells have been treated with phytosterols in the concentrations of 1 μM and 10 μM which is below the mean physiological serum concentration of 20 μM from serum [204]. Within this range PSSs have been shown to have modest effects on LXR α activity and cell proliferation in TNBC and Luminal BCa cell cultures and were unable to repress or induce LXR α when not in competition for binding. However, phytosterols when given as a co-treatment were able to significantly attenuate the oxysterol-LXR α activation as measured by luciferase and analysis of LXR target genes ABCA1 and APOE by qPCR. These changes were further influenced by cell line. Furthermore, phytosterols when given as a co-treatment were able to significantly

attenuate the oxysterol-LXR activation of p-gp/ABCB1. And finally, phytosterols were able to antagonise oxysterol:LXR enhanced export of epirubicin in TNBC cells in a manner similar to the p-gp/ABCB1 inhibitor verapamil suggesting an alternative route for reducing p-gp/ABCB1 mediated chemotherapy resistance.

From these data, we have shown that categorising phytosterols as LXR agonists or antagonists is too simplistic when key factors such as the presence of other ligands and cell type can alter how the ligand interacts with LXR α . In these BCa cell lines, phytosterols have been found to behave as competitive inhibitors of LXR α . Furthermore, these data may have implications for the development of novel therapeutic drugs targeting LXR α as PSS rich diets may alter the efficacy of LXR α targeting.

In the three breast cancer cell lines MDA-MB-468, MDA-MB-231 and MCF-7, the extent to which phytosterols attenuated the oxysterol:LXR α pathway depended on which oxysterol they were competing with. The most efficient inhibitors of oxysterol-driven LXR activation were SITO and STAN. The most effective drivers of LXR α activations were 24,25-EC and 24OHC (which is in agreement with previous reports [241]). Interestingly Ras *et al*, previously reported no differences in the ability of phytosterols and phytostanols at lowering LDL-cholesterol [315]. SITO and STAN are almost identical in structure except for a single double bond in the B-ring structure. Given that no significant differences were observed between SITO and STANs percentage efficiency with which each PSS impaired oxysterol activation of LXR α , suggests the double bond on the B-ring structure does not impact on interactions with LXR. For example, SITO and STIG are almost identical except for the unsaturated bond between the 22nd and 23rd carbon in the side chain (**Figure 1.4**) which appears

to be an adequate change altering the ability of STIG to compete with oxysterols for LXR α binding. Plat, Nichols and Mensink, measured ABCA1 expression after exposure to SITO, STAN and CAMP and found all three PSSs to induce ABCA1 expression in Caco2 cells [212]. Furthermore, they found SITO and STAN significantly increased ABCA1 expression by approximately 3.5 fold and CAMP by 3 fold which is in line with the observations shown in this chapter demonstrating SITO and STAN as the most efficient LXR ligands tested [212]. Hac-Wydro *et al*, specifically compared SITO and STIG and their interactions with 2-oleoyl-1-palmitoyl-3-phosphocholine (POPC) molecules, finding SITO had stronger affinity for the molecules than STIG as a consequence of their structure, namely the double bond in the side chain of STIG [316]. Furthermore, unsaturated bonds in the side chain like the one in STIG, makes the side chain bulkier and less flexible and allows for decreased rotational freedom [316]. Additionally, unsaturated bonds in the side chain makes the ligand more prone to enzymatic attack or oxidation. Supporting this, one study used a series of synthetic STIG derivatives with alterations on either carbon 22 or carbon 23 and found the altered STIG derivatives were able to selectively regulate the LXR target gene ABCA1 [317]. Furthermore, robust activation of ABCA1, SCD1 and FASN was observed by altered stigmastane ligands (addition of a hydroxyl group at C24) [318]. A study by Yang *et al* however, showed STIG was able to regulate ABCA1 in culture mouse adrenal cells but SITO failed to alter ABCA1 levels [319]. Furthermore, they investigated the structural requirements for ligand LXR activation and found unsaturation of the cholesterol side chain was required for LXR activation by sterols [319]. There are clear research gaps in the understanding of phytosterols and their selective modulation of LXR, particularly in understanding why some phytosterols

appear to be more efficient ligands than others and in a tissue dependent manner. This is a critical factor for the successful therapeutic targeting of LXR which has disease promoting and disease prevention capacities through the LXR-oxysterol signalling cascades.

Oxysterols and phytosterols are closely related, both displaying similar structures and functions in their natural host. It is in part the reason we suspected phytosterols to behave in a selective manner combined with other evidence supporting this selective modulator hypothesis include the work completed by Kaneko *et al*, who showed SITO, CAMP, BRASS and STIG were able to activate LXR α driven luciferase HEK293 cells at 10 μ M [66]. In CHO-7 cells however, SITO was unable to successfully activate LXR α [172]. Plat, Nichols and Mensink performed qPCR analysis after treatments with phytosterols and showed SITO, CAMP and STAN were able to enhance ABCA1 expression in Caco2 cells [212], but contrary to this Brauner *et al*, showed co-treatment of cholesterol with CAMP or SITO attenuated cholesterol driven ABCA1 expression in the same cell line [211]. Furthermore, in HepG2 cells phytosterols were found to downregulate the expression of LXR target genes (HMGCR, LDLR, SR-BI and NPC1L1) [109] and downregulate expression of ABCG5 and ABCG8 in Caco2 cells [214]. These findings support the conclusion that understanding the modulation of LXR in conjunction with other factors such as cell type and the presence of other ligands is essential for therapeutic targeting of LXR.

In this study oxysterols have been shown to have the capacity to robustly regulate LXR α . As isolated ligands, phytosterols were unable to significantly alter LXR α activity but as a co-treatment with oxysterols were able to attenuate oxysterol-driven LXR α luciferase BCa reporters. Furthermore, co-treatment of oxysterols with phytosterols

were also able to significantly attenuate transcription of LXR target genes. One gene in particular, p-gp/ABCB1 is a well-known chemotherapy efflux pump which we showed to be under the control of LXR α in chapter 5. In this chapter the expression of p-gp/ABCB1 was assessed after co-treatment of phytosterols with oxysterols and was found to reduce the expression of p-gp/ABCB1. Additionally, co-treatment of phytosterols with oxysterols slowed down the export of epirubicin in chemotherapy efflux assays, reversing the effects of pre-treatment with just the oxysterols. These results suggest a phytosterol rich diet may have beneficial effects for patients undergoing chemotherapy treatment.

7.5 Summary

In this chapter we have demonstrated that phytosterols as single treatments are able to weakly modulate LXR α in luciferase reporters and they are anti-proliferative at micromolar concentrations. Although phytosterols do not appear to do much in the absence of oxysterols, in the presence of oxysterols they impair oxysterol mediation of LXR α and its target genes ABCA1 and APOE. Furthermore, we identified a therapeutic method to silence the chemoprotective effects in TNBC cells caused by LXR α regulation of p-gp/ABCB1 through co-treatment of phytosterols and oxysterols.

Chapter 8

8.0 Discussion

8.1 LXR α activity is enhanced in triple negative breast cancer

The purpose of this research was to explore and identify new therapeutic targets in TNBC. Chapter 4 of this thesis has focused on identifying a therapeutic target that is altered between BCa subtypes. LXR α was found to be expressed at much higher levels in TNBC primary patient tumours along with its alternative binding partner RXR β , suggesting altered cholesterol pathways in BCa subtypes. Presented in chapter 4 are results showing enhanced LXR α activity and response to ligand in the TNBC subtype relative to the Luminal/ER-positive subtype, which appears to be influenced by lower levels of corepressors relative to the Luminal A subtype. Interestingly, LXR stimulation in BCa cells has been shown to induce expression of ABCA1 with enhanced transcriptional output observed in ER-negative cells compared to the ER-positive cells, which matches the observations in this chapter with those of Vedin *et al* [134]. Reassuringly, Vedin and colleagues also observed enhanced transcriptional output of LXR target genes (ABCA1 and SREBP1c) in ER-negative MDA-MB-231 cells relative to ER-positive MCF-7 and T47D cells, which strongly agrees with our findings as two of the cell lines used in the Vedin study were the same cell lines used here. Furthermore, they observed the same findings in the T47D and SK-BR3 cells suggesting the enhanced ER-negative response to ligand may be true for many ER-negative cell lines.

8.2 Fibroblasts can activate LXR α in BCa cells.

Through a series of fibroblast co-cultures and conditioned media experiments, fibroblasts have been shown to activate LXR α BCa reporters successfully. Oxysterol concentrations within CAFs and non-cancer associated fibroblasts were measured by LCMS/MS (completed by Dr. Hanne Roberg-Larsen, Oslo) and were found to have significantly higher concentrations of oxysterols (except 25OHC) than epithelial BCa cells. Conditioned media taken from fibroblast cultures were exposed to LXR α BCa reporters and LXR α transactivation measured by luciferase assay. Results showed that CAF conditioned media successfully activated LXR α TNBC reporters and the control liver HepG2 reporter but failed to activate the Luminal A BCa reporter. Conditioned media from the non-cancer associated fibroblasts successfully activated all LXR α BCa reporters as well as the control liver HepG2 reporter. These data imply fibroblasts do not require direct cell-to-cell contact with BCa epithelial cells to activate LXR α , but in fact secrete factors to interact with LXR α in the BCa reporters. The study by Camp *et al*, performed two methods of epithelial BCa cell co-cultures with fibroblasts, through direct contact co-culture and through the use of transwell insert culture dishes to impair cell-to-cell contact. Both methods of TNBC cells co-culture with fibroblasts enhanced the expression of ABCA1 but contact culture failed to do so in the Luminal BCa co-cultures. Co-cultures of Luminal A BCa cells with fibroblasts using the transwell method enhanced the expression of ABCA1 in the epithelial cells but failed to do so in the fibroblasts. This study by Camp and colleagues strengthens the hypothesis that fibroblasts activate LXR α in epithelial BCa cells and supports the observations in this chapter of LXR α induced paracrine signalling.

Further research is needed to establish whether fibroblasts secrete enhanced levels of oxysterols to cancer epithelial cells in the TME enabling the activation of LXR α . A study by Axelson *et al*, measured the production of oxysterols in normal human fibroblasts after incubation in media containing 10 % FCS for 24 h [146]. Measurements of 24OHC, 25OHC and 26OHC in fibroblast cells and the conditioned media were assessed. After subtracting the oxysterol content observed in the FCS control cell measurements showed no production of 24OHC, 3 pmol of 25OHC and 5 pmol of 26OHC. In fibroblast conditioned media oxysterols concentrations increased to 77 pmol of 26OHC but no secretion of 24OHC and a decrease in 25OHC. The concentrations of oxysterols in the human fibroblasts are much lower than observed in the breast fibroblasts in this chapter, but it does provide evidence that fibroblasts secrete oxysterols. To follow up this study, samples of conditioned media from multiple types of TME cells (fibroblast, macrophages and adipocytes) could be assessed for oxysterol content by LCMS/MS from single cultures and co-cultures (cell-to-cell and using transwell) with epithelial BCa cells.

The role of macrophages in the TME [320] is also an area of interest as they too possess the ability to synthesise and secrete oxysterols [321], and LXR ligands have been shown to induce ABCA1 in macrophages [322]. Shi *et al*, measured protein expression of CYP27A1 in the breast cancer cell lines MCF-7 and MDA-MB-231 and the THP-1 human monocytes/macrophages. Western blot analysis showed epithelial BCa cell expression of CYP27A1 to be relatively low compared to the THP-1 monocytes/macrophages, and enhanced expression of CYP27A1 in the MDA-MB-231 cells relative to the MCF-7 cells [285]. Both the findings in this chapter and the literature that support our LCMS/MS analysis results provide confidence in the data

collected and pave the way for further analysis of other TME support cells and their role in oxysterol synthesis and secretion contributing to the ER-negative/TNBC enhanced LXR α activity.

8.3 Enhanced LXR activity predicts poorer patient outcome and reduced treatment efficacy

In chapter 5, LXR α was shown to have a central role in the development of chemotherapy resistance. LXR ligands, the oxysterols, were identified as mediators of reduced chemotherapy drug efficacy in TNBC and Luminal A BCas. Through a series of knockdowns and chemotherapy efflux assays LXR α was shown to regulate p-gp/ABCB1 in TNBC but not Luminal A BCas. Supporting these findings was a study by Saint-Pol *et al*, who showed oxysterol induction of p-gp/ABCB1 increasing efflux across the BBB [228]. Other than this one study showing regulation by LXR α in the brain no other published records exist. This may not be a complete novel discovery, but it is a novel finding for BCa with clinical implications particularly for those with high LDL-C. The LXR α regulation of p-gp/ABCB1 in BCa is of great importance, and although no other studies can be directly compared due to the novelty of this discovery other studies can support aspects of this research. For example, Kim *et al*, made similar observations of enhanced p-gp/ABCB1 expression in breast tissues post neoadjuvant chemotherapy which was associated with reduced survival by 20 % [270]. Furthermore, Kim and colleagues also showed a significant 40 % reduction in survival in patients who had high BCRP expression post neoadjuvant chemotherapy relative to those with low expression which links in with the LXR α regulation of BCRP in Luminal A BCa [270]. In another study, the expression of p-

gp/ABCB1 was assessed in two MDA-MB-231 cell lines, one which was doxorubicin resistant and the other doxorubicin sensitive. Immunocytochemical staining of the doxorubicin sensitive MDA-MB-231 cells for p-gp/ABCB1 was undetected, however the doxorubicin resistant MDA-MB-231 cells showed strong cytoplasmic and nuclear staining of p-gp/ABCB1 expression [271]. These data support our findings of a p-gp/ABCB1 enhanced chemotherapy resistance mechanism in ER-negative breast cancers which could provide useful as a prognostic marker for poor response to treatment and increased risk of relapse. To follow up on these novel findings, validation studies showing LXR α control of p-gp/ABCB1 are required in these and other cell lines using ChIP-Seq techniques.

8.4 Phytosterols antagonise the oxysterol:LXR axis

Data presented in chapter 7 explore the role of phytosterols as selective LXR α modulators. Phytosterols were shown to have little effect on LXR α in the absence of ligand but when in the presence of ligand, they were able to antagonise oxysterol-mediated LXR α activation and expression of its targets ABCA1, APOE and P-gp/ABCB1. Brauner *et al*, showed the induction of HEK293 LXR α reporters by treatment of 26OHC but not by phytosterols (CAMP and SITO), but co-cultures of 26OHC with either SITO or CAMP increased the LXR α response [211]. In contrast, Brauner *et al*, also found no change in ABCA1 expression by phytosterol treatment in Caco2 cells but co-treatment of cholesterol with either CAMP or SITO in the same cell line attenuated cholesterol mediated ABCA1 expression[211], therefore phytosterols may be able to moderate LXR's response to ligand but in a tissue/cell specific manner. This is further supported by their oxysterol production experiments

where Brauner and colleagues showed co-incubation of cholesterol with either campesterol (77 ± 9 pmol x mg protein/min) or sitosterol (106 ± 16 pmol x mg protein/min) significantly inhibited the generation of 26OHC when compared to treatment of cholesterol alone (285 ± 23 pmol x mg protein/min) in HepG2 cells [211]. Additionally, in Caco2 cells CYP27A1 was shown to be increased by treatment with cholesterol and attenuated by co-treatment with either SITO or CAMP [211].

8.5 Future prospective

The design of this study was split into four key sections; i) to identify a therapeutic target in TNBC, ii) to assess the target's role in chemotherapy resistance, iii) to assess the regulation of the target in the TME, and iv) to identify compounds that can be used to impair and reduce the activity of the target in TNBC. The research presented in this thesis, have highlighted LXR α activity is enhanced in TNBC, LXR α activation reduced the efficacy of chemotherapy treatment through up-regulation of p-gp/ABCB1, fibroblasts activate LXR α through cell-to-cell contact and paracrine signalling and finally that phytosterols antagonise oxysterol-mediated LXR α activation.

LXR α activity and cholesterol status is increasingly recognised as important in pathology, particularly in the field of cancer. Understanding mechanisms that reduce treatment and chemotherapy efficacy is important to be able to predict better patient outcomes. Identifying enhanced LXR α activity in the TNBC subtypes and their readiness to respond to ligand has the potential to assess individual cholesterol status alongside the standard tumour classification to identify individuals who may be at a higher risk. This is supported by the WCRF-CUP report which assessed intake

of non-starchy vegetables (which are high in phytosterols) and the associated risk of BCa. The report found no significant difference between high and low non-starchy vegetable intake and risk of unspecified BCa, RR=0.95 (95 % CI, 0.88-1.33) per 200 g per day [37]. However, when phytosterol intake was assessed in 3950 cases of ER-negative BCas specifically, there was a significant inverse association RR=0.79 (95 % CI, 0.63-0.98) per 200 g per day. Furthermore, when non-starchy vegetable intake was assessed in 1,229 cases of ER-positive BCas there was no significant association [37]. Similar observations from the Women's intervention nutrition study (WINS) support these findings, in which dietary patterns that lower fat intake were associated with reduced risk of BCa relapse [48]. Although phytosterol intake was not directly measured, diets rich in fruit and vegetables and low in fat are more likely to have higher levels of phytosterols than diets which are low in fruit and vegetables. Implemented dietary patterns in the WINS intervention when classified by estrogen receptor status show HR for relapse events was reduced in the intervention group with ER-negative BCas, HR=0.58 (95 % CI, 0.37-0.91, adjusted Cox model analysis $p=0.018$) compared to the control group however, no significance was observed in ER-positive BCas relative to the control group, HR=0.85 (95 % CI, 0.63-1.14, adjusted Cox model analysis $p=0.277$) [48]. Data presented in chapter 4 of this thesis show TN/ER-negative BCas are more susceptible than Luminal A/ER-positive BCas at the molecular level to modulation by LXR α , which explains how these reports by Chlebowski [48] and the WCRF-CUP [37] show reductions in fat intake and increases in non-starchy vegetables are protective against TNBC/ER-negative disease but not ER-positive disease.

Based on these findings, clinical trials with phytosterols in the lead up to and during chemotherapy treatments for BCa patients are warranted. The evidence supplied in this thesis with the supporting evidence already published suggest the inclusion of phytosterols to treatment plans before and during chemotherapy treatment has the potential to improve BCa outcomes, particularly those belonging to the TNBC subtype. The most recent study by Jiang *et al* showed relative risk for the highest phytosterol intake compared to the lowest for total phytosterol intake was associated with a reduction in cancer risk, RR=0.63 (95 % CI = 0.49-0.81) [295]. This study included multiple different cancer types and therefore shows phytosterol intake to reduce cancer risk is applicable to other cancers not just BCa.

Kumar *et al*, conducted one of the largest retrospective ER-negative tumour studies during which they analysed data from 2,141 female participants who had a BCa incident. The study assessed statin use among the women previous to the BCa incidence and identified women taking lipophilic statins for more than a year had proportionally fewer ER/PR-negative tumours OR=0.63 (95% CI 0.43-0.92: p=0.02) relative to women who did not use statins or had been for less than a year [122]. Phytosterols are already given to patients at higher risk of cardiovascular disease and are therefore known to be safe and not have cytotoxic side effects. The daily intake guidelines given to CVD patients is 2-3 g/day which is achievable through a diet rich in fruit, vegetables and nuts. This highlights the simplicity of changing patient diets to include manageable amounts of phytosterols per day to improve their response to chemotherapy treatments and reduce their risk of relapse.

8.6 Future work

To further support the findings of this PhD project a number of experiments remain to validate LXR α control of p-gp/ABCB1. This project has mainly focused on LXR α control of p-gp/ABCB1 at the RNA level and therefore control at the protein level would be the obvious next steps. This includes treatment of cells with LXR ligands (oxysterols and phytosterols alone and in combination), protein extraction and western blot analyses with a p-gp/ABCB1 antibody and a HPRT1 housekeeping antibody. The remaining patient tumour samples obtained from the Leeds Breast Tissue bank should also have protein extracted and western blot analyses performed with a p-gp/ABCB1 antibody and a HPRT1 housekeeping antibody to assess whether p-gp/ABCB1 protein expression is predictive of survival using Kaplan Meier plots. Furthermore, tissue for immunohistochemistry was also acquired from the Leeds Breast Tissue bank to validate the cBioportal datasets.

In this project siRNA knockdowns were used for targeted gene silencing at the RNA level. This could be strengthened using techniques such as CRISPR which knocks out the target gene at the DNA level. The CRISPR method is much more specific and is a guaranteed gene knockout, whereas siRNA knockdown gives only a partial knockdown and has the potential to have non-specific effects.

The final future suggestion to strengthen this project is to perform a ChIP-Seq experiment in TNBC cells after treatment with a VC and LXR ligands for 16 h. After crosslinking and chromatin shearing, the chromatin can be incubated with protein-specific antibodies to immunoprecipitate the DNA-protein complex. The DNA can then be extracted and sequenced, providing sequences of the protein-binding sites with the gene of interest promotor (p-gp/ABCB1). This experiment would provide

the validation necessary to show LXR α binds in the promotor region of p-gp/ABCB1 controlling the expression.

Chapter 9

9.0 Conclusion

TNBCs have been shown to have enhanced LXR α activity and are poised for response to ligand relative to Luminal A breast cancers. TNBC patients who had relapses were shown to have enhanced LXR α activity. LXR α regulates the expression of p-gp/ABCB1 in TNBC but not in Luminal A BCa, and LXR α regulates the expression of ABCG2 and ABCC1 in Luminal A BCa but not TNBC. Oxysterols are endogenous LXR ligands which reduced the efficacy of epirubicin in BCa cell cultures and in ER-negative grafted 4T1 BCa cells in BALB/C mice. Phytosterols were shown to have little effect on LXR α in the absence of ligand, but when in the presence of ligand antagonised oxysterol-mediated LXR expression of ABCA1, APOE and p-gp/ABCB1. Furthermore, phytosterols when given as a co-treatment were able to decrease the export of epirubicin in a similar manner to that of the p-gp/ABCB1 inhibitor verapamil suggesting possible new roles for phytosterols in improving BCa patient response to chemotherapy. A summary of the main findings are shown in **Figure 9.1**.

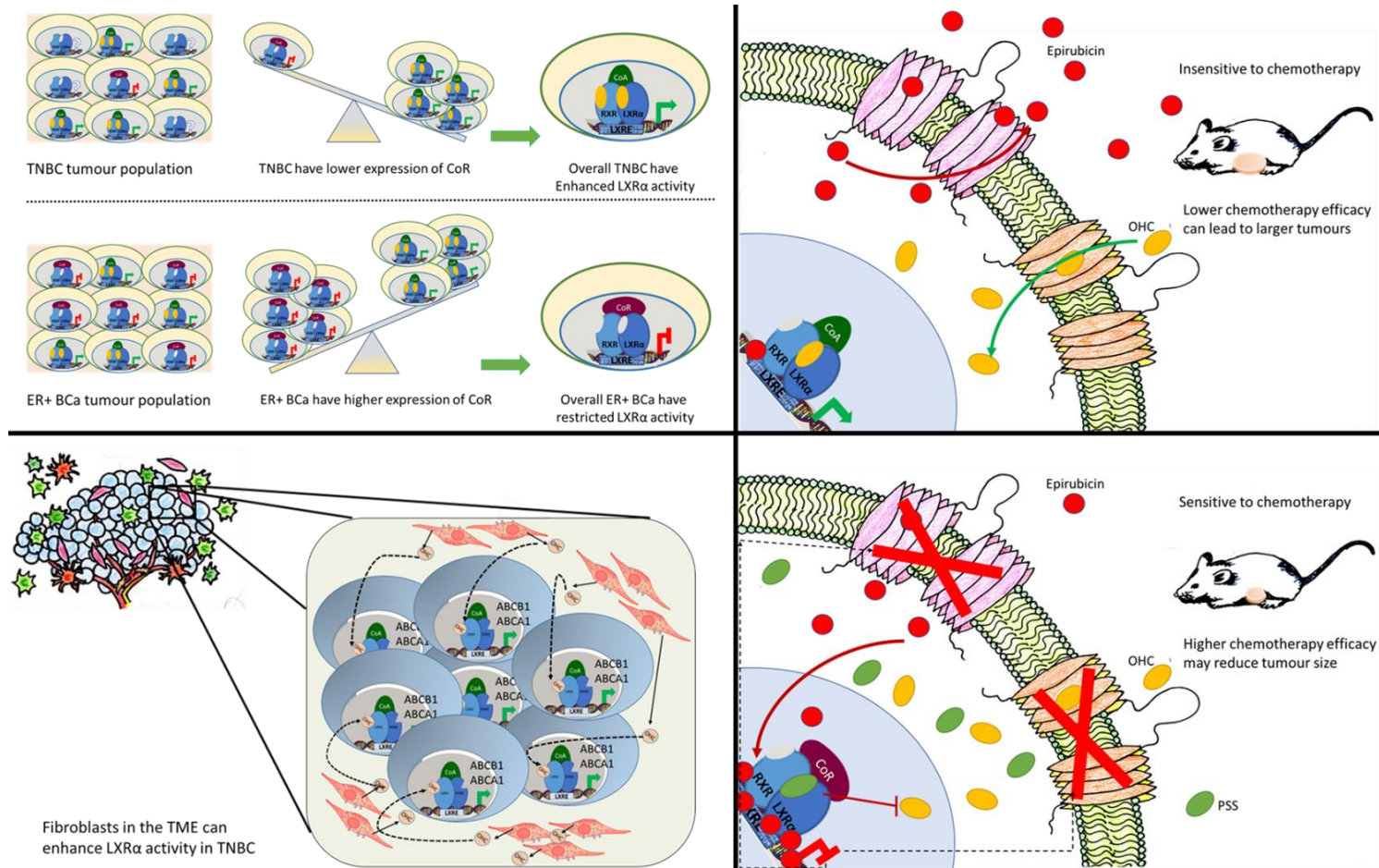


Figure 9. 1 LXRαs role as a therapeutic target – a summary of key findings.

The overall enhanced expression of LXRα in TNBC (shown in the top left box) has protective effects on tumour cells when pre-treated with oxysterols (OHC) during chemotherapy treatment (top right). This protective effect resulted in larger tumours in mice when treated with LXR ligands and was associated with worse survival. In addition to enhanced LXRα expression in TNBC, fibroblasts were also found to activate TNBC LXRα reporters through paracrine signalling. Finally, phytosterols (PSS) inhibit oxysterol-mediated expression of LXRα and reduces the export of epirubicin through attenuation of the p-glycoprotein.

Chapter 10 Additional outcomes of this PhD

10.1 Oral Presentations

1. Hutchinson, S.A., Battaglia, S., Roberg-Larsen, H., Lianto, P., Hughes, T.A., and Thorne, J.L. Oxysterol signalling is retained in ER-negative and suppressed in ER-positive breast cancer. FENS. October 2019.
2. Hutchinson, S.A., Lianto, P., Moore, J.B., Hughes, T.A., and Thorne, J.L. Phytosterols inhibit the oxysterol-LXR axis in breast cancer cells. 1st Annual Nutrition and Cancer Networking Meeting. July 2019.
3. Hutchinson, S.A., Battaglia, S., Roberg-Larsen, H., Vaghela, K., Hughes, T.A., and Thorne, J.L. Innate chemo-resistance in breast cancer driven by LXR signalling. ENOR, September 2018.
4. Hutchinson, S.A., Røberg-Larsen, H., Hughes, T.A., and Thorne, J.L. Could the dietary advice for cardio-vascular disease prevention also reduce breast cancer relapse rates? Fourth international congress of Translational Research in Human Nutrition. Nutrition and Cancer. Clarmont-Ferrand. 2017. Winner of best OC.
5. Hutchinson, S.A., Roberg-Larsen, H., Hughes, T.A., and Thorne, J.L. Could the dietary advice designed for cardio-vascular disease prevention work to prevent tertiary relapse of triple negative breast cancer? 4th Food Science & Nutrition PhD Conference, November 2017. Key note oral communication.
6. Hutchinson, S.A., Battaglia, S., Campbell, M.J., Harrowven, D.C., Hughes, T.A., Wastall, L.M., and Thorne, J.L. European Network for Oxysterol Research.

Oxysterols: Players in Different Metabolic Leagues, Bonn, 2015. Winner of best OC.

10.2 Poster Presentations

1. Hutchinson, S.A., Battaglia, S., Roberg-Larsen, H., Hughes, T.A., and Thorne, J.L. Cholesterol metabolism and chemo-resistance in breast cancer. SfE BES, November 2018.
2. Hutchinson, S.A., Battaglia, S., Roberg-Larsen, H., Hughes, T.A., and Thorne, J.L. Cholesterol metabolism and chemo-resistance in breast cancer., 5th Food Science & Nutrition PhD Conference, November 2018.
3. Hutchinson, S.A., Roberg-Larsen, H., Hughes, T.A., and Thorne, J.L. Could the dietary advice for cardio-vascular disease prevention also reduce breast cancer relapse rates? Yorkshire Breast Cancer Symposium, June 2017.

10.3 First author publications

10.3.1 Methods chapter

1. Hutchinson, S.A., and Thorne, J.L. 2019. A stable luciferase reporter system to characterise LXR regulation by oxysterols and novel ligands. Lipid-Activated Nuclear Receptors, Springer Protocols, London. Editors: Matthew C. Gage, and Ines Pineda-Torra.

10.3.2 Peer-reviewed journal articles

1. Hutchinson, S.A., Lianto, P., Moore, J.B., Hughes, T.A., and Thorne, J.L. Phytosterols antagonise side-chain oxysterol mediated activation of LXR in breast cancer cells. *International Journal of Molecular Science*. **2019**, 20 (13), 3241.

2. Hutchinson, S.A., Battaglia, S., Roberg-Larsen, H., Lianto, P., Hughes, T.A., and Thorne, J.L. ER-negative breast cancer is highly responsive to hydroxycholesterol signalling. *Nutrients*, **2019**, 11, 2618.

10.3.3 Peer-reviewed journal articles in preparation

1. Hutchinson, S.A., Lianto, P., Roberg-Larsen, H., Nelson, E.R., Hughes, T.A., and Thorne, J.L. Oxysterol activation of LXR α during chemotherapy reduces treatment efficacy and leads to chemoresistance in TNBC. **2020**.

10.4 Additional contributions

10.4.1 Peer-reviewed journal articles

1. Solheim, S., Hutchinson, S.A., Lundanes, E., Wilson, S.R., Thorne, J.L., and Roberg-Larsen, H. Fast liquid chromatography-mass spectrometry reveals side chain oxysterol heterogeneity in breast cancer tumour samples. *Journal of Steroid Biochemistry and Molecular Biology*. **2019**, DOI: 10.1016/j.jsbmb.2019.02.004.
2. Thorne, J.L., Battaglia, S., Baxter, D.E., Hayes, J.L., Hutchinson, S.A., Jana, S., Millican-Slater, R.A., Smith, L., Teske, M.C., Wastall, L.M., and Hughes, T.A. Mir-19b non-canonical binding is directed by HuR and confers chemosensitivity through regulation of P-glycoprotein in breast cancer. *Biochimica et Biophysica Acta (BBA) - Gene Regulatory Mechanisms*. **2018**, 1861 (11), 996-1006.

10.4.2 BSc/MSc student projects

1. Kate Sykes – LXR α and chemoresistance in TNBC. 2017. BSc.
2. Kishan Vaghela – LXR α and chemoresistance in TNBC. 2018. MSc.

Appendix A

A.1 Table of LXR α target genes and their genomic binding scores (identified using the Cistrome database).

The top 100 scoring genes for 7 different LXR α ChIP-Seq datasets are shown. Each of the 7 datasets (which include mouse macrophages, human adipocytes and human colorectal cancer cells) are shown in columns with the appropriate reference and the cell line at the top. The genes are listed in the first column on the left in alphabetical order and their corresponding binding scores for each study in the following 7 columns. Scores that are in black text are scores that were within the top 100 scoring genes for that dataset. Scores that are in grey text are scores that were not within the top 100 scoring genes for that dataset. Each gene has at least two binding scores that successfully appeared in the top 100 scoring genes.

	Oishi, Y., et al, 2017.				Galhardo, M., et al., 2013. Savic, D., et al., 2016.		
	Macrophage No Treatment	Macrophage GW3965	Macrophage KLA6H	Macrophage KLA1H	Adipocyte	Colorectal Cancer GW3965 2H	Colorectal Cancer GW3965 48H
A130077B15RIK	1.88	3.512	2.019	3.097	0	0	0
ABCA1	3.58	3.29	3.865	3.332	0.948	1.981	2.382
ABCG1	2.58	2.922	2.266	3.073	1.652	2.21	2.0945
ABLIM3	0	0	0	0	0	3.1305	3.5665
ADAMTSL4	3.818	4.073	3.281	1.974	0	1.3845	1.1115
AFF1	3.423	3.556	1.849	3.958	0	1.761	2.3825
AIM1L	0.396	0.437	0.343	0.343	0	3.023	3.3815
AMZ2	3.215	2.785	3.644	3.95	0	0.4725	0.847
ANKRD22	0.683	1.636	1.24	0.706	0.603	2.754	3.383
AP2S1	0.725	0.728	0.626	0.726	0	3.1435	3.0865
APBB1IP	3.033	3.747	2.462	2.407	0	0.107	0.152
ARHGAP25	3.596	4.148	2.676	3.394	0	0.319	0.643
ARHGAP26-AS1	0	0	0	0	0	2.9995	2.667
ASPH	1.855	4.37	2.822	2.944	0	2.1115	2.15

ATG2A	1.616	2.342	1.572	2.431	0	2.078	3.343
B330016D10RIK	2.336	3.478	3.71	3.18	0	0	0
BCL3	2.421	3.108	3.292	2.807	0	4.512	3.878
BMF	1.58	2.439	2.388	1.242	0	3.408	3.9315
C14ORF182	0	0	0	0	0	2.028	2.119
C1ORF159	0	0	0	0	0	2.795	3.32
C1QTNF1-AS1	0	0	0	0	0	3.3795	3.4415
C6ORF222	0	0	0	0	0	3.5385	3.133
CAPN2	1.459	1.931	1.558	1.661	0	3.889	3.3725
CAPN5	0.508	1.931	1.568	1.091	0	4.036	3.1095
CCDC19	0	0	0	0	0	1.5575	3.647
CCL3	2.979	2.949	3.086	3.237	0	0.2015	0.352
CCL6	3.403	4.196	3.416	3.304	0	0	0
CCL9	3.16	3.875	2.839	3.578	0	1.593	0
CD14	3.055	3.463	2.708	3.845	0.486	2.3265	2.247
CD300A	4.041	4.719	1.777	3.602	0	1.367	1.6455
CD300C	3.206	2.986	1.799	3.069	0	0.074	0.1225
CD300LB	3.664	3.376	1.664	3.325	0	0.169	0.217
CLCF1	1.453	3.264	3.114	2.473	0	3.299	2.672
CLDN7	1.831	1.662	1.505	1.143	0.294	2.075	3.568
CTDNEP1	2.132	2.243	1.959	1.461	0.187	2.0865	3.375
CTDSP1	3.398	2.552	2.789	2.027	0	2.4175	2.346
CYTH4	3.783	3.311	2.335	3.074	0	0.497	0.6645
DDX47	1.023	0.88	0	0	0	3.348	3.582
DNAJC17	0.959	0.19	0.152	0.756	0	2.9305	3.0395
DOK2	1.759	2.843	2.747	3.306	0	0.512	0.512
DUSP1	2.593	2.63	2.496	2.319	0	3.3765	3.9665
E230016K23RIK	3.231	3.942	2.995	3.607	0	0	0
E230025N22RIK	3.103	3.22	2.269	3.469	0	0	0

EHD1	1.794	2.368	1.529	2.866	0	2.802	3.472
EHF	0	0	0	0	0	3.8045	2.903
ELF3	0.744	1.155	0.744	1.314	0	3.42	3.346
ELP5	2.132	2.244	1.959	1.464	0.189	2.094	3.39
FAM83E	1.473	1.743	0.942	1.7	0	3.515	3.3635
FCGR2B	2.136	4.169	3.928	2.687	0	0.409	0.4555
FCRLA	2.328	3.889	2.757	2.435	0	0.899	1.3235
FEM1A	2.693	3.623	3.101	2.425	0.595	1.3795	1.7125
FIZ1	0.256	1.773	0.79	1.105	0	3.169	3.292
FLOT1	1.678	2.642	2.549	2.901	0	3.308	3.189
FYB	3.254	3.948	3.119	3.076	0	0.7515	0.5905
GM13031	2.687	3.679	2.792	1.809	0	0	0
GM14005	1.858	2.989	3.501	4.307	0	0	0
GM19510	3.025	3.425	4.473	3.341	0	0	0
GM2848	1.679	3.618	2.845	2.845	0	0	0
GPRC5C	1.231	2.793	0.428	2.113	0	3.4955	3.229
HCG27	0	0	0	0	0	3.1945	3.5385
IER3	1.699	2.677	2.639	2.976	0	3.343	3.23
IL1B	1.506	2.671	2.748	3.021	0	2.4235	2.1675
IL21R	3.381	4.466	3.09	3.984	0	0.3435	0.4955
ITGB6	0.059	0.029	0.033	0.209	0	3.287	3.1685
JUP	1.07	1.823	0.566	0.498	0	3.3015	2.966
KRT7	0.383	0.667	0.759	0.653	0	3.416	3.4625
LCP2	2.711	3.765	2.77	3.961	0	0.0135	0.5135
LINC00880					0	3.819	3.545
LINC01226					0	2.352	3.4795
LOC100503496	2.582	2.471	2.755	3.229	0	0	0
LOC100506499	0	0	0	0	0	3.8165	1.94
LOC101928093	0	0	0	0	0	3.0705	3.1675

LOC254099	0	0	0	0	0	3.4	1.9805
LOC731656	0	0	0	0	0	3.6505	3.606
LTBR	1.653	2.152	1.422	1.884	0	3.4655	3.2635
LY9	3.46	3.665	1.806	2.926	0	0.756	0.7805
MAPK6	0.812	1.723	1.028	1.419	0.135	3.331	3.7225
MCL1	4.279	4.495	3.655	2.297	0	1.2855	1.5605
MGRN1	3.456	4.423	3.16	3.353	0	1.283	1.448
MIR101C	4.51	2.906	4.317	3.499	0	0	0
MIR192	1.641	2.166	1.541	2.528	0	2.9125	3.733
MIR194-2	1.635	2.16	1.535	2.518	0	2.912	3.7315
MIR26B	3.394	2.451	2.787	1.977	0	2.442	2.354
MIR6076	0	0	0	0	0	3.6895	2.779
MIR6749					0	2.4065	3.397
MIR6750					0	2.5795	3.508
MIR8085	0	0	0	0	0	3.9775	3.497
MPEG1	3.952	5.67	2.183	3.195	0	1.6755	1.7955
MSL1	1.905	3.241	3.265	3.088	0	1.981	2.2855
N4BP1	3.185	3.073	2.214	3.151	0	1.363	1.591
NDST1	4.492	3.72	1.577	2.665	0	1.552	1.9775
NINJ1	2.954	3.484	2.441	2.619	0	1.442	2.606
NR1D1	1.991	3.211	3.659	3.259	0	2.3405	2.442
OMP	0.385	0.898	1.23	0.515	0	3.808	3.276
PDE4B	2.176	2.776	3.329	3.392	0	0.03	0.017
PGC	1.275	1.949	0.416	1.486	0	3.3635	3.287
PIGC	1.298	1.549	0.434	1.62	0	3.6525	3.406
PIK3CG	2.286	3.206	3.416	3.956	0.552	0.519	0.742
PILRA	3.799	2.98	3.319	2.347	0	0.296	0.5855
PILRB1	3.737	2.891	3.06	2.359	0	0.3405	0.4225
PLA2G7	2.649	3.452	2.784	3.047	0	0.3365	0.4055

PLAU	2.942	2.493	2.301	3.535	0	1.938	2.1345
PLXND1	2.017	3.61	2.541	3.5	0	0.9205	0.863
PNPLA2	4.061	3.586	1.942	2.232	0	2.0065	1.9595
PPM1N	1.587	2.016	1.709	3.105	0	2.3235	2.8845
PRKCD	2.956	3.829	3.205	2.869	0	2.154	2.33
PTK2B	3.399	3.037	2.382	3.366	0	1.7165	1.8775
RALB	1.796	1.457	0.185	1.797	0	3.0205	3.4605
RALGDS	2.782	3.06	2.138	3.286	0	2.6305	3.2175
RHOV	1.876	1.752	1.271	1.717	0	3.282	3.259
RPL18	1.654	1.963	1.069	1.79	0	3.362	3.2965
RPLP2	3.605	3.533	1.682	2.159	0	1.846	1.7275
RTN2	1.52	2.081	1.666	3.041	0	2.3765	2.9505
SBSN	1.093	1.463	0.561	0.527	0.039	1.9105	3.483
SCNN1A	1.589	2.267	1.278	1.862	0	3.4695	3.2685
SDHB	2.85	3.865	3.069	1.901	0	0.693	1.379
SLA	3.115	2.811	1.966	3.294	0	0.229	0.6185
SLC2A4	2.275	1.766	1.675	1.278	0.596	1.9825	3.204
SLFN2	2.381	3.811	2.057	3.409	0	0	0
SMAD3	1.235	1.206	1.921	1.875	0	3.695	3.4055
SMIM5	0	0	0	0	0	3.638	3.5235
SMIM6	0	0.027	0.296	0.256	0	3.689	3.5365
SNAR-E	0	0	0	0	0	3.5265	3.46
SNORA52	3.652	3.519	1.711	2.158	0	1.8605	1.761
SNRNP35	2.964	3.157	2.319	3.293	0.014	1.4695	1.2415
SOCS3	1.542	2.541	1.914	3.162	0.662	2.499	2.6945
SPACA4	1.24	1.469	0.784	1.607	0	3.5865	3.3715
SPHK2	1.658	2.131	1.146	1.884	0	3.367	3.3025
ST6GAL1	3.009	3.593	3.023	2.83	0	0.684	0.2845
SULT2B1	0.644	0.603	0.199	1.145	0	3.968	3.8135

SYK	1.535	3.545	2.991	3.575	0	0.945	0.7315
SYNJ2	3.049	3.515	1.844	2.089	0	2.55	1.8535
TAGLN2	2.45	2.304	2.309	2.473	0	3.033	3.542
TANK	1.808	3.528	1.457	1.104	0.594	2.368	1.9025
TEC	3.44	3.953	2.71	3.579	0	1.1565	1.686
TFEB	2.443	2.668	1.567	1.989	0	3.4555	3.4055
TGFB1	3.797	3.099	2.846	2.793	0	1.0155	0.707
TGFBI	2.365	3.847	1.462	1.411	0.543	2.6185	2.4415
TGM2	3.658	3.647	4.156	2.886	0.172	3.179	2.8655
THEMIS2	2.897	3.848	1.854	3.383	0.067	1.092	1.078
TICAM1	2.225	3.758	2.829	2.435	0.12	1.0705	1.599
TMCO6	2.486	3.059	1.999	3.309	0.602	2.3785	2.3185
TMEM154	4.251	3.55	2.661	2.319	0	0.3375	0.461
TMEM185B	1.121	1.471	0.434	1.121	0	2.7235	3.539
TMEM72	1.468	2.243	3.042	4.138	0	1.1515	0.7675
TNFAIP2	2.33	2.221	2.022	1.991	0	3.947	3.645
TREML2	2.112	4.558	1.575	3.257	0	1.078	0.586
TRIM31	0.661	0.79	0.646	0.648	0	4.728	3.652
TRIM40	0.514	0.691	0.503	1.091	0	4.378	3.4775
TRNFRSF1B	3.183	3.911	4.32	3.843	0	0.891	1.416
TRP53COR1	1.885	2.604	2.883	3.262	0	0	0
TSKU	0.947	1.673	0.72	0.166	0.411	2.9435	3.674
TXNDC2	2.661	4.012	2.997	3.222	0	2.0835	2.202
UBALD1	3.179	4.162	3.048	3.167	0	1.3075	1.29
VASP	1.955	2.23	1.97	3.204	0	2.4965	3.0555
ZFYVE19	0.956	0.189	0.152	0.754	0	2.93	3.034
ZNF524	0.261	1.821	0.811	1.132	0	3.1485	3.296
ZNF598	1.289	0.905	1.344	1.662	0	2.867	3.1385
ZNRF1	1.883	1.862	4.023	3.055	0	1.0075	1.01

5031414D18RIK	3.344	4.637	1.512	2.904	0	0	0
---------------	-------	-------	-------	-------	---	---	---

A.2 Table of genes associated with chemotherapy resistance.

A systematic review was completed to identify a list of genes associated with chemotherapy resistance. The first column includes the genes listed in alphabetical order. The second and third column include the type of associated resistance and the reference for each article describing the resistance. For genes with multiple types of resistance are labelled multidrug resistance and those that do not state the exact chemotherapy drug are labelled chemotherapy resistance.

Gene	Type of resistance	Reference
ABCB1	Anthracyclines	[323]
ABCC1	Anthracyclines	[323]
ABCC3	Anthracyclines	[323]
ABCC5	Anthracyclines	[323]
ABCC9	Anthracyclines	[323]
ABCG1	Multidrug Resistance	[324]
ABCG2	Anthracyclines	[323]
ADD3	Multidrug Resistance	[325]
AGER	Chemotherapy Resistance	[326]
AKAP11	Multidrug Resistance	[325]
AKR1A1	Anthracyclines	[323]
AKT1	Cisplatin	[327]
AOX1	Multidrug Resistance	[325]
APAF1	Cisplatin	[328]
APOBEC3	Tamoxifen	[329]
ASK1	Platinum	[330]
ATP7A	Cisplatin	[331]
ATP7B	Platinum	[332]
BCL2	Platinum	[330]
BIRC2	Multidrug Resistance	[325]
BIRC3	Chemotherapy Resistance	[333]
BMI1	Doxorubicin	[334]
	Paclitaxel	[334]
	Cisplatin	[334]
BRCA1	Cisplatin	[335]

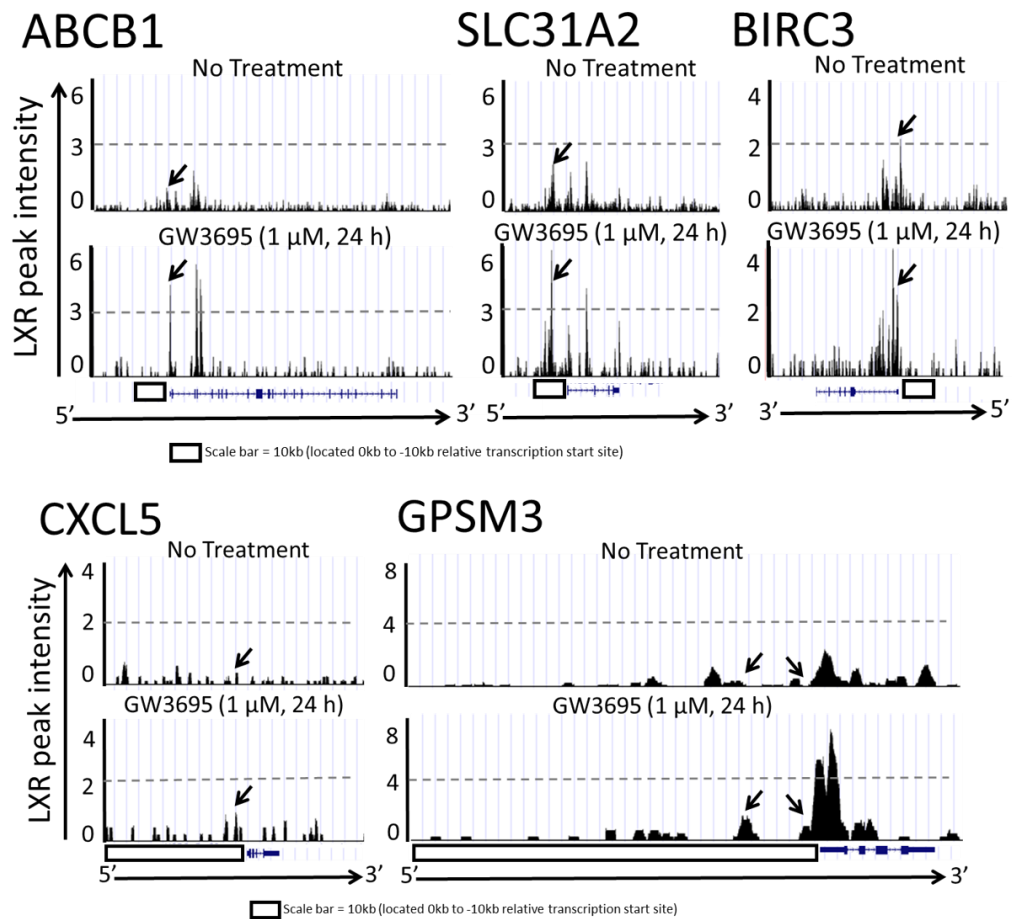
BRCA2	Cisplatin	[335]
CAT	Multidrug Resistance	[325]
CAV1	Doxorubicin	[336]
	Gemcitabine	[336]
CBR1	Anthracyclines	[323]
CCNB2	Multidrug Resistance	[325]
CDK2	Multidrug Resistance	[325]
CDKN1A	Multidrug Resistance	[337]
CDKN2A	Multidrug Resistance	[337]
CHEK1	Gemcitabine	[338]
CHEK2	Gemcitabine	[338]
COL1A1	Sorafenib	[339]
	Cisplatin	[339]
COX17	Platinum	[340]
CTH	Multidrug Resistance	[325]
CXCL12	Gemcitabine	[341]
CXCL5	Chemotherapy Resistance	[342]
DDIT4	5-fluorouracil	[343]
DKK3	Multidrug Resistance	[325]
DRAP1	Multidrug Resistance	[325]
DUSP4	Multidrug Resistance	[325]
EGFR	Multidrug Resistance	[344]
EMP2	Multidrug Resistance	[325]
ERBB2	Cyclophosphamide	[345]
	Methotrexate	[345]
	5-fluorouracil	[345]
ERBB3	Multidrug Resistance	[346]
ERCC1	Cisplatin	[347]
ERCC2	Cisplatin	[348]
ERK1	Platinum	[330]
ERK2	Platinum	[330]
FAM129A	Multidrug Resistance	[349]
FANCL	Cisplatin	[350]

FBLN1	Anthracyclines	[351]
	Taxanes	[351]
FBXO32	Multidrug Resistance	[337]
FDFT1	Multidrug Resistance	[325]
FPGS	Methotrexate	[352]
FYN	Multidrug Resistance	[325]
GPSM3	Multidrug Resistance	[325]
HMCN1	Multidrug Resistance	[353]
HMGA2	Multidrug Resistance	[325]
HMGN3	Multidrug Resistance	[325]
HSP90	Cisplatin	[354]
IGFBP7	Multidrug Resistance	[325]
IL24	Multidrug Resistance	[337]
JNK	Cisplatin	[355]
KRAS	Cisplatin	[356]
LAMC1	Multidrug Resistance	[357]
LTBP2	Multidrug Resistance	[325]
MCAM	Multidrug Resistance	[358]
MEST	Multidrug Resistance	[325]
MLH1	Cisplatin	[338]
	Carboplatin	[338]
MMP13	Chemotherapy Resistance	[359]
MMP9	Multidrug Resistance	[360]
MMRN2	Chemotherapy Resistance	[361]
MTDH	Doxorubicin	[362]
	Paclitaxel	[362]
	Cisplatin	[363]
MXI1	Multidrug Resistance	[325]
NFKB1	Cisplatin	[364]
NFKB2	Anthracyclines	[364]
	Taxanes	[364]
	5-fluorouracil	[365]
NMT2	Multidrug Resistance	[325]

NOS3	Anthracyclines	[323]
NQO1	Anthracyclines	[323]
NUDT4	Multidrug Resistance	[325]
P83/RHOBTB2	Chemotherapy Resistance	[366]
PAR4	Chemotherapy Resistance	[367]
PDCD4	Multidrug Resistance	[337]
PTEN	Cisplatin	[368]
RAB20	Multidrug Resistance	[325]
RAD51	Doxorubicin	[369]
	Cisplatin	[369]
	Etoposide	[369]
RAF1	Doxorubicin	[370]
	Etoposide	[370]
RASSF1	Multidrug Resistance	[337]
RRM1	Gemcitabine	[371]
S100BP	Chemotherapy Resistance	[326]
SCD1	Chemotherapy Resistance	[372]
SERPINB2	Multidrug Resistance	[325]
SERPINE1	Multidrug Resistance	[325]
SKP2	Paclitaxel	[373]
SLC22A1	Cisplatin	[374]
SLC22A12	Anthracyclines	[323]
SLC22A3	Irinotecan	[375]
	Cisplatin	[375]
	Oxaplatin	[375]
SLC28A3	Anthracyclines	[323]
SLC31A2	Chemotherapy Resistance	[376]
SLCO1B3	Docetaxel	[377]
SRC	Anthracyclines	[378]
SRD5A1	Multidrug Resistance	[325]
STAT3	Doxorubicin	[379]
	Carboplatin	[380]
	Chemotherapy Resistance	[381]

SULF1	Multidrug Resistance	[382]
SULT1A1	Tamoxifen	[352]
SULT2B1	Anthracyclines	[323]
TFPI2/RAGE	5-fluorouracil	[383]
TIP60	Doxorubicin	[334]
TMEM97	Multidrug Resistance	[384]
TOP1	Gemcitabine	[385]
	Platinum	[385]
TOP2A	Multidrug Resistance	[386]
TP53	Anthracyclines	[387]
	Etoposide	[387]
	Mitomycin	[387]
TP73	Multidrug Resistance	[337]
TRIM2	Tamoxifen	[388]
TUBB3	Gemcitabine	[385]
	Platinum	[385]
TYMP	5-fluorouracil	[352]
UCLH1	Multidrug Resistance	[325]
WWOX	Multidrug Resistance	[337]
XIAP	Platinum	[330]
	Taxanes	[330]
	Doxorubicin	[330]
XPA	Cisplatin	[348]
XRCC1	Cisplatin	[348]
ZFP36L2	Multidrug Resistance	[325]

A.3 LXR α binding in the promotor of genes associated with chemotherapy resistance.



LXR recruitment to the promoters of genes associated with chemotherapy resistance.

Images of LXR binding in gene promotor regions were generated using the Cistrome database [1]. LXR α binding was assessed in a ChIP-Seq mouse macrophage dataset provided by Oishi, Y., *et al*, 2017 [2] with no treatment (ID: 72545) and after GW3965 treatment for 24 h (ID: 72544). These datasets were selected out of the available 11 datasets as these were the only datasets that had paired datasets comparing no treatment and treatment with an LXR agonist. Genes of interest were then individually assessed for LXR α binding in the gene promotor regions. Each gene was visualised using the UCSC genome browser function in Cistrome, aligned and cropped to only include the gene of interest and 10 kb immediately upstream of the gene sequence representing the promotor region. Datasets were presented showing no treatment sequences placed above the LXR agonist treatment sequences for direct comparison. Arrows are used to suggest/predict areas of LXR binding (the largest peak within the promotor region that shows an increase with the LXR treatment compared to no treatment).

Appendix B Published manuscripts

B.1 ER-Negative Breast Cancer Is Highly Responsive to Cholesterol Metabolite Signalling



ER-Negative Breast Cancer Is Highly Responsive to Cholesterol Metabolite Signalling

Samantha A Hutchinson ¹, Priscilia Lianto ¹, Hanne Roberg-Larsen ²,
Sebastiano Battaglia ³, Thomas A Hughes ⁴ and James L Thorne ^{1,*}

¹ School of Food Science and Nutrition, University of Leeds, Leeds LS2 9JT, UK; fssah@leeds.ac.uk (S.A.H.); fspl@leeds.ac.uk (P.L.)

² Department of Chemistry, University of Oslo, 0315 Oslo, Norway; hanne.roberg-larsen@kjemi.uio.no

³ Center for Immunotherapy, Roswell Park Cancer Institute, Buffalo, 14263 NY, USA; Sebastiano.Battaglia@RoswellPark.org

⁴ School of Medicine, University of Leeds, Leeds LS9 7TF, UK; t.hughes@leeds.ac.uk

* Correspondence: j.l.thorne@leeds.ac.uk; Tel.: +44-113-343-0684

Received: 27 September 2019; Accepted: 25 October 2019; Published: 1 November 2019

Abstract: Interventions that alter cholesterol have differential impacts on hormone receptor positive and negative-breast cancer risk and prognosis. This implies differential regulation or response to cholesterol within different breast cancer subtypes. We evaluated differences in side-chain hydroxycholesterol and liver X nuclear receptor signalling between Oestrogen Receptor (ER)-positive and ER-negative breast cancers and cell lines. Cell line models of ER-positive and ER-negative disease were treated with Liver X Receptor (LXR) ligands and transcriptional activity assessed using luciferase reporters, qPCR and MTT. Publicly available datasets were mined to identify differences between ER-negative and ER-positive tumours and siRNA was used to suppress candidate regulators. Compared to ER-positive breast cancer, ER-negative breast cancer cells were highly responsive to LXR agonists. In primary disease and cell lines LXRA expression was strongly correlated with its target genes in ER-negative but not ER-positive disease.

Expression of LXR's corepressors (NCOR1, NCOR2 and LCOR) was significantly higher in ER-positive disease relative to ER-negative, and their knock-down equalized sensitivity to ligand between subtypes in reporter, gene expression and viability assays. Our data support further evaluation of dietary and pharmacological targeting of cholesterol metabolism as an adjunct to existing therapies for ER-negative and ER-positive breast cancer patients.

Keywords: cholesterol; hydroxycholesterol; breast cancer; LXR; oestrogen receptor status; corepressors

1. Introduction

Cholesterol is predominantly synthesized *de novo* in the liver with lesser amounts obtained from the diet. Dietary intake, *de novo* synthesis, metabolism and excretion, combine to balance circulating cholesterol levels ensuring extra-hepatic tissues are sufficiently equipped to produce a range of metabolites including steroid hormones, bile acids and *seco*-steroids. Side-chain hydroxycholesterols (scOHCs) are typically formed through hydroxylation of cholesterol by specialized members of the

Cytochrome P450 family, which bind and activate the Liver X Receptor-alpha (LXRA; gene name *NR1H3*) and beta (LXRB; gene name *NR1H2*) transcription factors [1,2]. LXR target genes are typically involved in cholesterol and fatty acid metabolism. In normal tissue, expression of LXRA is inducible in the liver, intestine, macrophages and adipocytes, whilst expression of LXRB is more ubiquitous. As well as differences in expression of LXRA and LXRB, local concentrations of the scOHCs differ

Nutrients 2019, 11, 2618; doi:10.3390/nu11112618

www.mdpi.com/journal/nutrients

considerably between tissues, and relative to each other, sometimes by as much as 1000-fold [3] and variance can also depend on disease status [4]. Furthermore, the different scOHCs have varying capacities to activate LXR-mediated transcription, imposing an element of selective modulation onto signalling. 26-OHC (commonly referred to as 27-OHC [5]) for example is the most abundant scOHC, but is a relatively weak LXR agonist [1,6]. Moreover, there is little difference in scOHC concentrations between breast cancer subtypes [7].

Transcriptional activity of the LXRs, like the other members of the Nuclear Receptor (NR) superfamily, is not just regulated by ligand bioavailability; chromatin environment, cross-talk and competition for response element binding [8] with other NRs, as well as cell- and tissue-type dependent expression of cofactors are also key mediators. For example, the expression of corepressors such as NCOR1 and

NCOR2/SMRT determine how several cancers respond to nutritive ligands [9–11]. LXRA has a 100-fold higher binding affinity than LXR_B for the corepressors NCOR1 and NCOR2 [12] and deregulation of these corepressors allows prostate and bladder cancer cells to evade cancer suppressive signals of Vitamin D (through repression of Vitamin D Receptor (VDR)) and omega-3 fatty acids (through repression of peroxisome proliferator-activated receptors (PPARs)) by impairing sensitivity to ligand [10,11,13]. Simply measuring scOHC concentrations does not sufficiently determine their contributions to LXR signalling; concentration and activation potential should be assessed in combination.

In cancer, the function of the scOHC-LXR signalling axis appears site specific as both tumour suppressive and promoting roles have been described. For example, scOHC-LXR signalling impairs invasion and angiogenesis in melanoma [14] and is anti-proliferative in lung cancer in vivo [15], as it is in almost every cancer cell line studied in vitro [13]. In Oestrogen Receptor (ER)-positive Breast Cancer (BCa) however 26-OHC promotes growth in vivo via ER- α [4,16]. In ER-negative BCa 26-OHC drives the epithelial-to-mesenchymal transition [16] and promotes colonization of metastatic sites in through mobilization of $\gamma\delta$ -T cells [17]. Furthermore, concentrations of several scOHCs are altered in BCa relative to normal tissue [4], and 25-OHC is elevated in the circulation of BCa patients who have relapsed compared to those with primary disease [18].

We recently evaluated LXR ligand bio-availability in a small BCa cohort [7] and found large inter tumoural heterogeneity in oxysterol content, but no difference in ligand concentrations between tumour subtypes. Systematic evaluation of scOHC bioavailability and activation potential, coupled

with analysis of NR cofactor expression between BCa subtypes has not been performed previously. Given the prognostic and therapeutic value of stratifying BCa by hormone receptor status, further delineation of the pathways that are altered between these subtypes, such as scOHC-LXR signalling, may help advance understanding about the emerging roles of cholesterol metabolism in cancer and improve outcomes for patients.

2. Materials and Methods

2.1. Cell Culture and Transfections

MCF7, T47D, MDA-MB-468 and MDA-MB-231 cell lines were originally obtained from ATCC. All cells were maintained at 37 °C with 5% CO₂ in a humidified incubator and cultured in Dulbecco's Modified Eagle Medium (DMEM, Thermo Fisher, Altrincham, UK Cat: 31966047) supplemented with 10% fetal calf serum (FCS) (Thermo Fisher, UK, Cat: 11560636). Routine passaging of cells was completed every 3–4 days, and

seeded at 1×10^6 live cells per T75 tissue culture treated flask (Nunc, Thermo Fisher, UK, Cat: 10364131) to maintain confluence between 20% and 80%.

For transfection with siRNA, cells were plated in 6-well plates (MDA-MB-468 cells: 1.5×10^5 cells/well; MCF7 cells: 1×10^5 cells/well) and incubated overnight. Lipofectamine RNAiMAX (Thermo Fisher, Cat: 13778030), siNCOR1 (Cat: SR306392), siNCOR2 (Cat: SR306393) or siLCOR (Cat: SR313532), or the scrambled siRNA (Cat: SR30004) were diluted in OptiMeM (Thermo Fisher, Cat: 31985062), combined according to manufacturer's instructions, and added to the cells at a final concentration of 30 nM. The cells were incubated for 20 h and the media was changed for fresh DMEM. Cells were plated for luciferase or qPCR assays after 36 h, and for MTT at 24 h, knockdown was confirmed at mRNA level at 36 h.

2.2. Drugs and Reagents

Drugs stocks were stored at -20°C as follows: GSK2033 (gift from Dr Carolyn Cummings—University of Toronto, Toronto, ON, Canada) at 20 mM diluted in DMSO. GW3965 (Cayman, Ann Arbor, MI, USA, Cat: 71810) at 100 mM diluted in DMSO. Hydroxycholesterols were sourced from Avanti Polar Lipids (Alabaster, AL, USA): 7-ketocholesterol (7-KETO) (Cat: 700015), 22R-hydroxycholesterol (22-OHC) (Cat: 700058), 24S-hydroxycholesterol (24-OHC) (Cat: 700071), 25-hydroxycholesterol (25-OHC) (Cat: 700019), 26-hydroxycholesterol (26-OHC) (Cat: 700021) and 24(R/S),25-epoxycholesterol (24,25-EC) (Cat: 700037). Stocks of 10 mM were prepared in nitrogen flushed ethanol (NFE) to prevent auto-oxidation. Puromycin Hydrochloride (Santa Cruz, CA, USA; Dallas, TX, USA, Cat: sc-108071) stocks diluted in Nuclease Free Water and stored as 25 mg/mL aliquots.

2.3. Luciferase Reporter Assay

This method has been reported previously [19]. Briefly, 3×10^4 cells were plated in each well of a 24-well plate and incubated overnight. Signal Lentiviral particles (LXRA) were purchased from Qiagen, Manchester, UK (Cat: CLS-7041L) and transduced into the cells using 8 $\mu\text{g}/\text{mL}$ SureEntry transduction reagent at MOI at manufacturer's recommendations. After 18 h the particles were removed and fresh DMEM supplemented with 0.1 mM Non Essential Amino Acids (Thermo Fisher, Cat: 12084947) and 100 U/mL penicillin and 100 $\mu\text{g}/\text{mL}$ streptomycin (Thermo Fisher, Cat: 10378016) were added to the cells. Cells were passaged and puromycin used to select successfully transduced cells. For luciferase quantitation, 30,000 transfected cells/well were seeded into 24-well plates, and allowed to attach under normal culture conditions for 8 h. Cultures were treated with ligands, inhibitors or vehicle control as indicated in figure legends for 16 h. Luciferase assays were carried out by transferring

cell lysates to white-walled 96-well plates and luminescence was assessed using the Tecan Spark 10M.

2.4. qPCR

Cells were plated in 6-well plates (2.5×10^5 cells/well) and incubated overnight before treatment with Vehicle Control (ETOH) or LXRA ligands. mRNA analysis was performed as described previously [20,21]. Briefly, Promega Reliaprep™ RNA Cell Miniprep System was used for the RNA extraction (Promega, Southampton, UK, Cat: #Z6012), and product guidelines were followed using approximately 5×10^5 cells. On column DNase 1 digestion was performed and RNA was eluted in 30 μ L nuclease free water. RNA was stored at -80°C . GoScript™ Reverse Transcription kit (Promega, UK, Cat: A5003) was used for the cDNA synthesis, and product guidelines followed (TM316), using 500 ng total RNA/reaction and 0.5 $\mu\text{g}/\mu\text{L}$ random primers. cDNA produced was then diluted 1 in 5 in nuclease free water and stored at -20°C . For gene expression analysis, Taqman Fast Advanced Mastermix (Thermo Fisher, Paisley, UK, Cat: 4444557) was used with Taqman assays (Thermo Fisher, Paisley, UK, Cat: 4331182) on a QuantStudio Flex 7 (Applied Biosystems Life Tech, Thermo Fisher, Paisley, UK) in 384-well plates. Taqman assays and Mastermix were stored at -20°C .

Taqman ID's used were *HPRT1*: Hs02800695_m1; *ABCA1*: Hs01059137_m1; *APOE*: Hs00171168_m1; *DOK2*: Hs00929587_m1; *LCP2*: Hs01092638_m1; *TNFRSF1B*: Hs00961750_m1; *LCOR*: Hs00287120_m1; *NCOR1*: Hs01094540_m1; *NCOR2*: Hs00196955_m1. Gene expression was analysed using the $\Delta\Delta\text{cT}$ method and normalised to *HPRT1*. *HPRT1* was confirmed as the most suitable housekeeping gene from a panel of 18 housekeeping genes tested in MCF7 and MDA-MB-468 cell lines treated with a panel of sterols at various time points and in various concentrations (Thermo Fisher, Paisley, UK, Cat: 4367563).

2.5. MTT Assays

The human BCa cell lines (MCF7, MDA-MB-468) were cultured in DMEM (glucose 4.5 g/L) supplemented with 10% fetal bovine serum (FBS) at 37°C in a humidified 5% CO_2 incubator. Seeding density was determined empirically for each cell line and for each time point. Then, 2×10^4 cells/well for MDA-MB-468 cell line and 3×10^4 cells/well for MCF7 were seeded in 96-well plates. After overnight incubation, media was removed and replaced with the fresh media (200 μL) with vehicle control (0.1% ethanol flushed with N_2) or 10 μM , or 100 μM 26-OHC (in vehicle) for indicated time points. Cells were washed with PBS and 90 μL phenol-red free DMEM was added with 10 μL of diluted MTT reagent at 37°C for 4 h incubation. Media was removed and 100 μL of DMSO was added, absorbance was read using a CLARIOstar plate reader at 540 nm.

2.6. The Cancer Genome Atlas Gene Expression Analysis

To establish the possible regulators of LXR activity, cofactors were included if they physically interacted with LXR in a previously performed NR/cofactor scan [22], and if the interaction had been reported in at least one other study. Based on these criteria, a total of six coactivators and three corepressors were selected for further analysis. mRNA expression of was assessed using the array-median centered gene expression obtained from <http://cBioportal.org> [23], deposited by The Cancer Genome Atlas (TCGA) BCa dataset [24]. Data collection and analysis was performed as described previously [25,26]. Expression data were obtained for 81 Basal (ER-/PR-/Her2-) and 234 Luminal A (ER+/PR+/Her2-) tumours and were compared using two-tailed Mann–Whitney U tests using Bonferroni correction for multiple testing where indicated [27].

2.7. Transcription Factor-Target Gene Correlation Analysis

NR1H3/LXRA binding to gene promoters was assessed in all available ChIP-Seq datasets deposited into the <http://cistrome.org> portal [28]. LXRA binding scores were obtained from seven ChIP-Seq datasets, from three publications that had deposited LXRA binding information for mouse monocytes either untreated or exposed to LXRA agonist GW3965 [29], human colorectal cancer cells treated with GW3965 at 2 or 48 h [30] (both time points had duplicate ChIP-Seq datasets associated with them, which were averaged to give a 2 h list and a 48 h list), and untreated human adipocytes [31]. Processed ChIP-Seq data were accessed and the 100 genes with the highest LXRA binding scores in each of the seven datasets were included for further analysis. If a gene was present in the top 100 bound genes in only one dataset it was excluded from further analysis (resulting in 148 genes appearing in multiple lists). Eleven genes (from mouse datasets) were excluded as they did not have human orthologs, and a further 26 were excluded as they were not expressed in the TCGA dataset resulting in a 111 gene list. To this list, 24 canonical LXR targets identified from the literature were included in analysis, even if they did not necessarily reach the cut-off criteria outlined above. The entire list of 135 genes was then assessed for Pearson correlation with NR1H3/LXRA in the 81 ER-negative and 234 ER-positive breast tumours from TCGA [24]. The Pearson's correlation coefficient was calculated between each of the 135 genes and LXRA and the resulting *p* values were corrected for False Discovery Rate (FDR). Lastly, Fisher's exact test was used by building a contingency table to test the null hypothesis that the number of genes with FDR of 1% is the same in the two diseases. Flow diagram of gene selection and exclusion methodology can be found in Supplementary Materials (Figure S1).

3. Results

3.1. LXR Activation Potential Is Retained in ER-Negative Disease but Dampened in ER-Positive Disease

Previous studies examining differences in LXR signalling across BCa ER-subtypes have reported strong anti-proliferative actions of synthetic LXR agonists in ER-positive cell lines, but enhanced transcription from canonical gene loci such as ABCA1 and SREBP1c in ER-negative cell lines [32]. To explore differences in how breast cancer cells respond to LXR stimulation by synthetic and endogenous ligands, we generated LXRA-regulated luciferase reporter cell lines representing ER-negative (MDA-MB-468, MDA-MB-231) and ER-positive (MCF7, T47D) BCa, as well as a control liver cell line (HEPG2). Dose-response experiments were performed with synthetic LXR ligands (agonists: T0901317 and GW3965 [33]; inhibitor: GSK2033 [34]). At nanomolar and micromolar concentrations in MDA-MB-468 cell culture, GW3965 treatment resulted in up to a 25-fold induction of LXR driven luciferase activity and T0901317 resulted in up to 10-fold induction (Figure 1a). When attempting to stimulate LXR-mediated transcription in the ER-positive MCF7 cell line activation was restricted to less than 5-fold above vehicle control for both synthetic agonists (Figure 1a). We repeated GW3965 treatment in additional ER-positive (T47D) and ER-negative (MDA-MB-231) lines confirming our observation that ER-negative cells were significantly more responsive to LXR agonist than ER-positive cells in LXR-reporter assay (one-tailed students *t*-test: $p < 0.0001$ (Figure S2a)). GSK2033 suppressed basal LXR dependent transactivation similarly in both MCF7 and MDA-MB-468 cell cultures (Figure 1a). We then applied a panel of endogenous LXR ligands (7-KETO, 22-OHC, 24-OHC, 25-OHC, 26-OHC and 24,25-EC) and found LXR was activated in both cell lines by all ligands but to varying amounts. Similarly to the synthetic ligands, activation was more robust in MDA-MB-468 compared to MCF7 cells, across all ligands and all concentrations tested (Figure 1b). In the MDA-MB-468 reporter cells, 24,25-EC induced the greatest fold change in LXR dependent luciferase expression ($\times 40$ -fold increase), followed by 22-OHC ($\times 19$ -fold) and 24-OHC ($\times 18$ -fold). Induction by 26-OHC ($\times 9$ -fold), 25-OHC ($\times 6$ -fold) and 7-KETO ($\times 5$ -fold) were relatively attenuated (Figure 1b). In contrast, the maximum induction by any scOHC observed in MCF7 cells was < 5 -fold. As control experiments we first generated a stable luciferase reporter liver cell line HEPG2 and activation by agonists and repression by antagonists in HEPG2 was comparable to that observed in MDA-MB-468 cells (Figure S2b). In the absence of LXRA (following siRNA knockdown) basal luciferase activity was lowered and neither 26-OHC (Figure S2c) or 24,25-OHC (Figure S2d) treatment elicited any induction of luciferase activity, demonstrating the dependence on LXRA. As scOHC-LXR signalling is known to be anti-proliferative and pro-apoptotic in an array of cell lines, we applied MTT assays to test whether ER-negative MDA-MB-468 cells were

more sensitive to ligands than their ER-positive MCF7 counterparts in an alternative assay. MCF7 cells were significantly more resistant than MDA-MB-468 cells to treatment with 24-OHC (non-linear regression comparison of fits: non-converged for MCF7), 25-OHC ($p < 0.0001$) and 26-OHC ($p < 0.0001$) (Figure 1c).

To confirm the luciferase LXRA reporter was representative of regulation within a normal chromosomal context, we next examined expression at two endogenous canonical LXR target loci, *ABCA1* [35] and *APOE* [36]. Vehicle control, GW3965, 26-OHC (the most abundant scOHC in breast tumour tissue [7]) or 24,25-EC (the scOHC that elicited the greatest fold induction in reporter cells (Figure 1b)) were added to MDA-MB-468 or MCF7 cells for 4 or 16 h and changes to *ABCA1* and *APOE* expression determined. At 4 h *ABCA1* was induced in both cell lines by GW3965 and 24,25-EC but not by 26-OHC in MCF7 cells (Figure 2a). Induction was greater after treatment in MDA-MB-468 compared to MCF7 cells (multiple *t*-tests with FDR < 1% and Holm–Sidak correction: GW3965 $p = 0.0097$; 26-OHC $p = 0.0092$; 24,25-EC $p = 0.0086$; Figure 2a). GW3965, but not other agonists, induced *APOE* induction at 4 h in MDA-MB-468 cells (Figure 2b). At 16 h *ABCA1* was induced by all ligands in both cell lines, but again, to a significantly greater level in MDA-MB-468 cells (multiple *t*-tests with FDR < 1% and Holm–Sidak correction: GW3965 $p < 0.01$; 26-OHC $p < 0.01$; 24,25-EC $p < 0.01$; Figure 2c). At 16 h *APOE* was also induced by all ligands in MDA-MB-468 cells but interestingly, was repressed by 26-OHC and 24,25-EC (but not synthetic ligand) in MCF7 cells (compare columns 3 and 4 against vehicle; Figure 2d), and by 24,25-EC at 4 h (multiple *t*-tests with FDR < 1% and Holm–Sidak correction: $p = 0.003$). We repeated GW3965 treatment in second ER-positive (T47D) and ER-negative (MDA-MB-231) lines confirming our observations that *ABCA1* (two-way ANOVA: $p < 0.05$ (Figure S3a)) and *APOE* (two-way ANOVA: $p < 0.001$ (Figure S3b)), were significantly more induced in ER-negative cells compared to the ER-positive ones. Accumulation of *ABCA1* mRNA was LXR dependent, as the LXR inhibitor GSK2033 abrogated the scOHC response in both cell lines (Figure S4a) and knockdown of *LXRA* impaired *ABCA1* expression (Figure S4b). From these findings we concluded that at the transcriptional level, ER-negative cells are more responsive to LXR stimulation than their ER-positive counterparts.

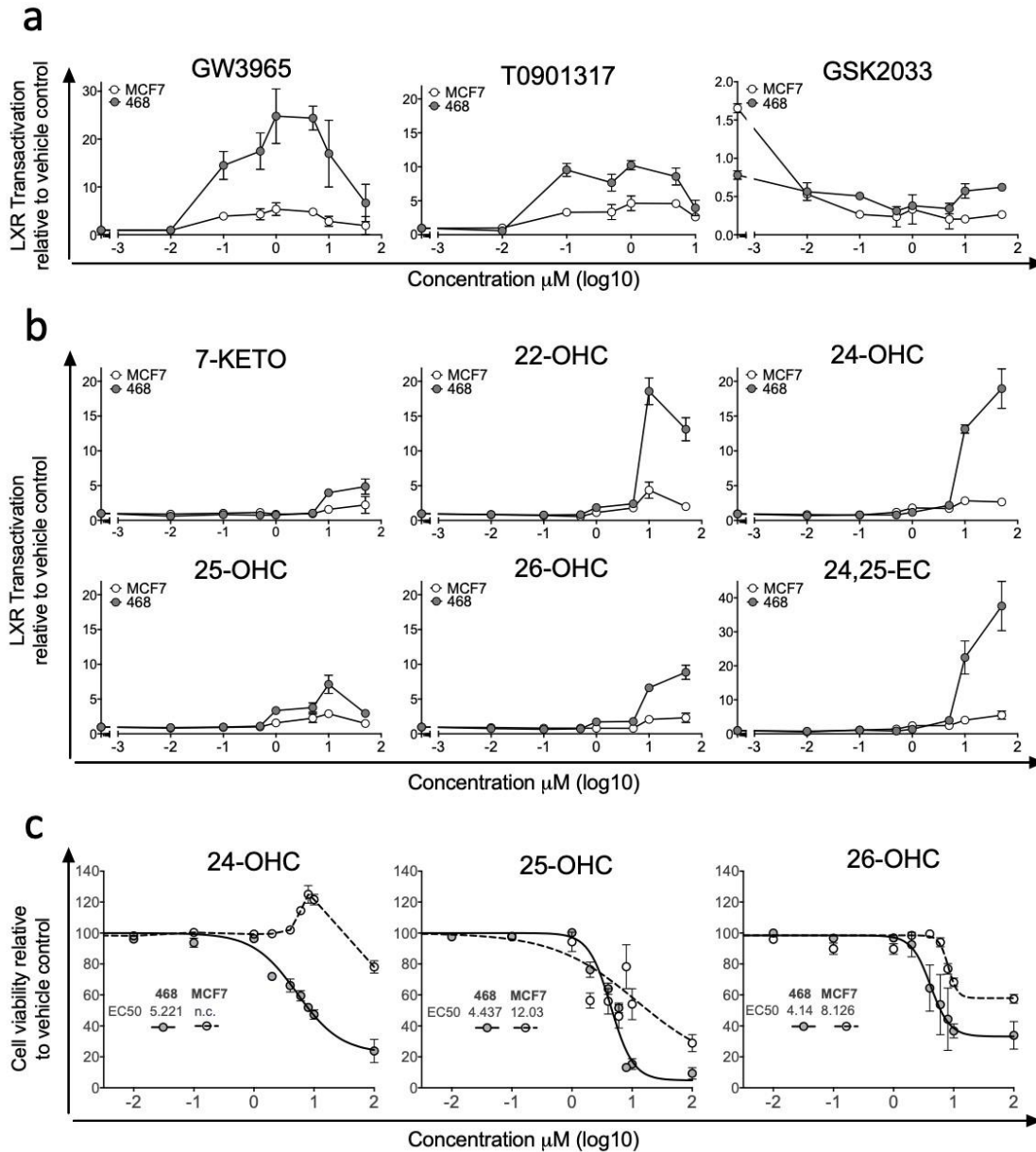


Figure 1. Synthetic ligands and side-chain hydroxycholesterols (scOHCs) activate Liver X Receptor- α (LXRA) dependent transcription in Oestrogen Receptor (ER)-negative but not ER-positive breast cancer cell culture. ER-negative (MDA-MB-468) and ER-positive (MCF7) cell lines were stably transfected with LXRA-Luciferase reporter constructs and treated with synthetic LXR agonists or the antagonist GSK2033 (a), or endogenous LXR ligands (b) at indicated concentrations. The anti-proliferative effects of scOHC over 48 h was assessed by MTT in MDA-MB-468 and MCF7 cells (c) with EC₅₀ given in μM . Data are presented as means of 2–4 independent replicates with SEM.

We next set out to establish if the enhanced LXR transcriptional activity observed in cell line models extended to primary tumours. To test this, we examined whether expression of *NR1H3/LXRA* or *NR1H2/LXRB* correlated with expression of canonical LXR target genes (*ABCA1* and *APOE*) in 81 ER-negative or 234 ER-positive primary breast tumours (obtained from TCGA dataset [24]). *ABCA1* correlated with *LXRA* (Pearson's correlation: $R = 0.502$; $p < 0.0001$) in ER-negative but not in ER-positive tumours (Figure 2e). *APOE* correlated with *LXRA* in both subtypes (Figure 2f), but the correlation

was much weaker in ER-positive than in ER-negative disease (Pearson correlation: ER-positive: $R = 0.27$, $p < 0.0001$; ER-negative: $R = 0.65$; $p < 0.0001$). Both *ABCA1* and *APOE* were assessed for correlation with *NR1H2/LXR* and whilst *APOE* weakly correlated with *NR1H2/LXR* in ER-positive tumours ($R = 0.25$) it was not correlated in ER-negative tumours; *ABCA1* was not correlated with *NR1H2/LXR* in either tumour type (Figure S5). From these observations we concluded that ER-status was inversely associated with the ability of LXR to induce canonical target gene expression.

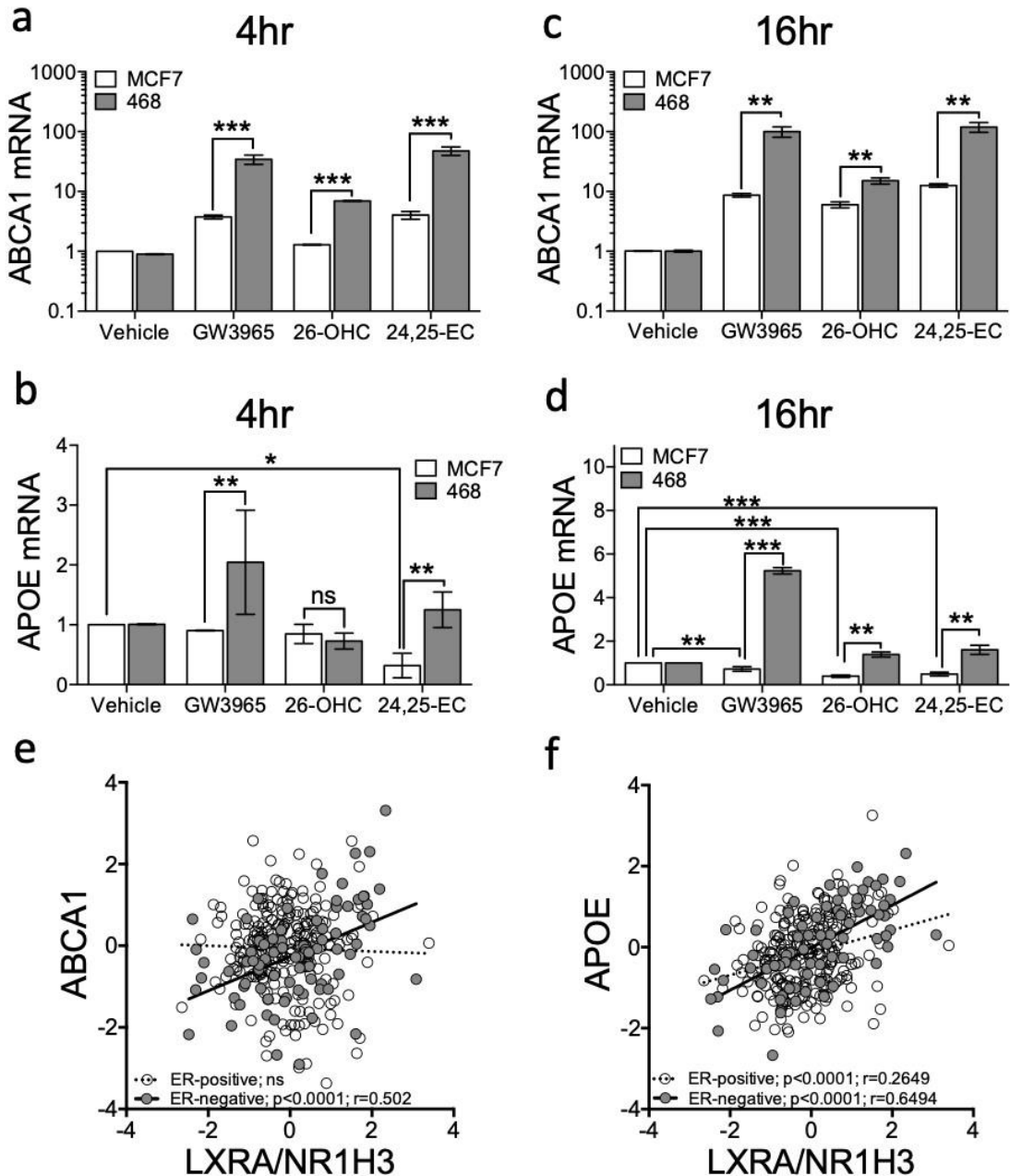


Figure 2. Ligand dependent transcriptional output of LXR target genes is enhanced in ER-negative relative to ER-positive breast cancer cell cultures. ER-negative (MDA-MB-468) and ER-positive (MCF7) cell lines were treated with a panel of ligands (Vehicle control, GW3965 (1 μ M), 26-OHC or 24,25-EC (both 10 μ M)) for 4 (a,b) and 16 h (c,d). Expression of the canonical LXR target genes *ABCA1* (a,c) and *APOE* (b,d) were assessed by qPCR using $\Delta\Delta$ Ct (normalised to HPRT1). Statistical analysis was

established using multiple *t*-tests and data are derived from three independent replicates with SEM. mRNA-Seq data from TCGA for 81 ER-negative and 234 Luminal A tumours was assessed using Pearson correlation between *NR1H3/LXRA* and *ABCA1* (e) or *APOE* (f). * $p < 0.05$, ** $p < 0.01$, *** $p < 0.001$. Lines represent linear regression.

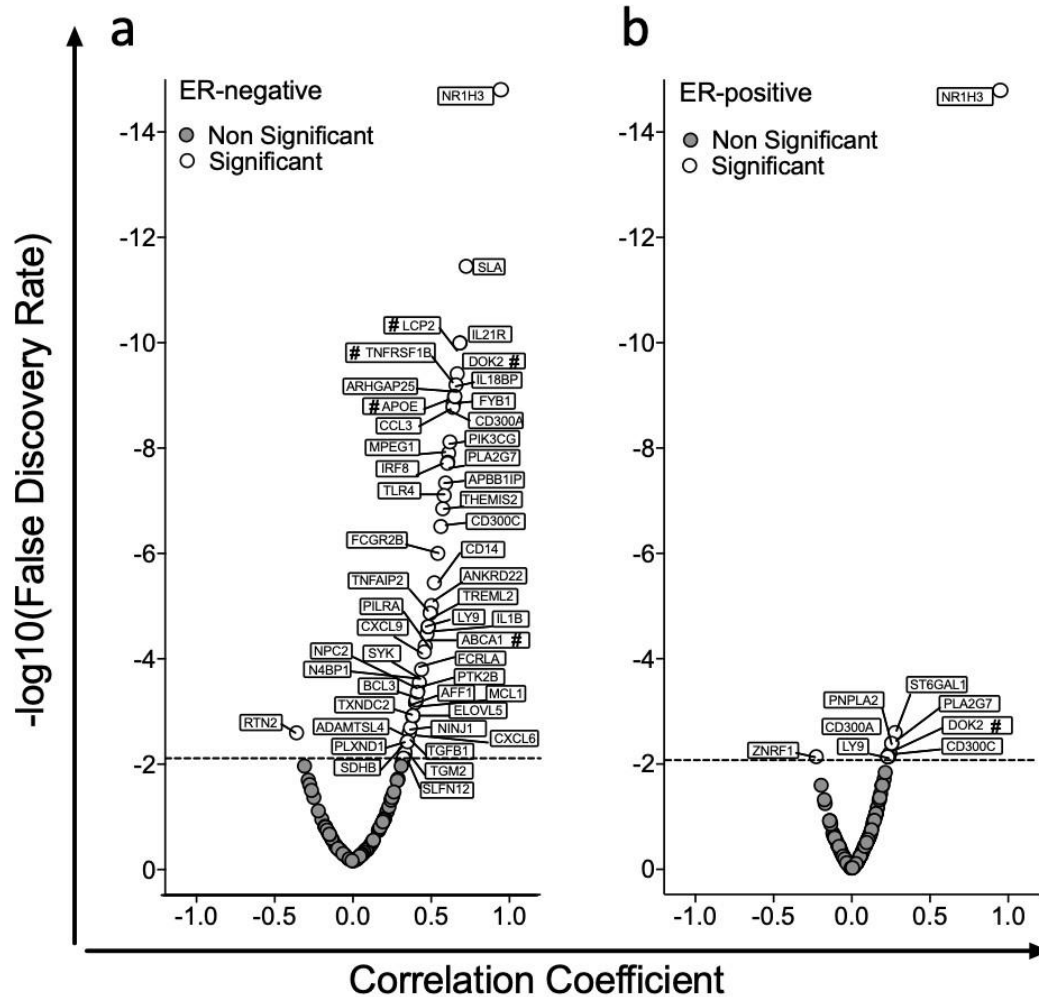
3.2. Expression of LXRA Correlates with Expression of Its Target Genes in Primary ER-Negative Tumours but not in ER-Positive Tumours

We then set out to test if expression of a wider and unbiased set of LXR target genes correlated with *NR1H3/LXRA* or *NR1H2/LXRB* expression in ER-positive or ER-negative tumours. A list of LXRA target genes was generated ‘agnostically’ by repeated interrogation of publicly available ChIP-Seq data sets as described above (full gene list in ST1 and example promoters shown in Figure S6 [29]) using cistrome.org [28]. Then, we assessed correlation of expression of each of these LXRA bound gene targets with *NR1H3/LXRA* and *NR1H2/LXRB* expression in publicly available RNA-Seq datasets from TCGA, as previously for *ABCA1* and *APOE*. In ER-negative tumours *NR1H3/LXRA* significantly correlated with 48/135 genes (Figure 3a), compared to 8/135 in ER-positive tumours (Figure 3b). This was a statistically significant difference in the number of correlating genes (Fisher’s exact test: $p < 0.0001$). Three genes that had not previously been validated as bona fide LXR target genes (*TNFRSF1B*, *LCP2* and *DOK2*) were selected from the top 10 strongest correlations, to test the in silico prediction that these genes should be inducible in MDA-MB-468 cells, but not (or less so) in MCF7 cells. qPCR analysis on cells exposed for 16 h to 1 μ M GW3965 revealed that all three genes were induced to significantly greater extent in the MDA-MB-468 cell line than in MCF7 (multiple *t*-tests with FDR < 1% and correction for multiple testing with Holm–Sidak: *TNFRSF1B* $p = 0.033$; *LCP2* $p = 0.006$; *DOK2* $p = 0.015$) (Figure 3c). We concluded that retention of LXRA’s transcriptional potential was associated with more stringent correlations between LXRA and its target genes in vivo, and more robust activation of target genes in vitro.

3.3. LXR Is Poised for Transcription in ER-Negative BCa but Repressed in ER-Positive BCa

The capacity for NRs to regulate their target genes depends on multiple factors, including receptor expression, ligand bioavailability and coactivator/corepressor expression. As we previously found no difference in ligand concentrations [7], we hypothesized that the balance of functional regulators of LXR would be different between ER-positive and ER-negative BCa. Expression of relevant genes was assessed in 234 ER-positive and 81 ER-negative human tumours from TCGA [24]. First, as a control, we show that as expected oestrogen receptor alpha (*ESR1*) and progesterone receptor (*PGR*) were significantly different between these groups, with median expression in ER-negative tumours dramatically lower than in ER-positive

tumours (Figure 4a). Next, more interestingly, *NR1H3/LXRA* was expressed at higher levels in ER-negative than in ER-positive tumours (two-tailed Mann–Whitney U test: $p < 0.01$ (Figure 4a)). *NR1H2/LXRB* was unchanged between subtypes. In the absence of agonist, LXRA but not LXRB, is primarily repressed by corepressors NCOR1 and NCOR2/SMRT [12] and previous reports demonstrate elevated corepressor expression helps prostate [9,10] and bladder [11] cancer cells to evade anti-proliferative actions of NRs through compromising the ligand response. Both NCOR1 and NCOR2/SMRT were expressed at significantly lower levels in ER-negative tumours compared to ER-positive tumours (two-tailed Mann–Whitney U test: $p < 0.001$ (Figure 4b)). Interestingly, expression of LCOR, a corepressor that is recruited to LXR upon agonist binding [37], was even more drastically reduced in primary ER-negative tumours (two-tailed Mann–Whitney U test: $p < 0.0001$, (Figure 4b)). We repeated these measurements in vitro and found the cell line models recapitulated these features of the primary tumours; MDA-MB-468 expressed significantly more LXRA but not LXRB (Figure 4c), and significantly less *NCOR1*, *NCOR2/SMRT* and *LCOR* transcript than the ER-positive cell line MCF7 (two-tailed student's *t*-test: $p < 0.0001$ for all corepressors (Figure 4d)). In a reanalysis of a previously published expression dataset of BCa cell lines [38], we found that *NCOR2/SMRT* and *LCOR* (but not *NCOR1*) were also expressed at significantly lower levels in ER-negative cell lines generally compared to ER-positive cell lines (Mann–Whitney-U test: $p < 0.05$ for NCOR2 and LCOR (Figure S7)).



c

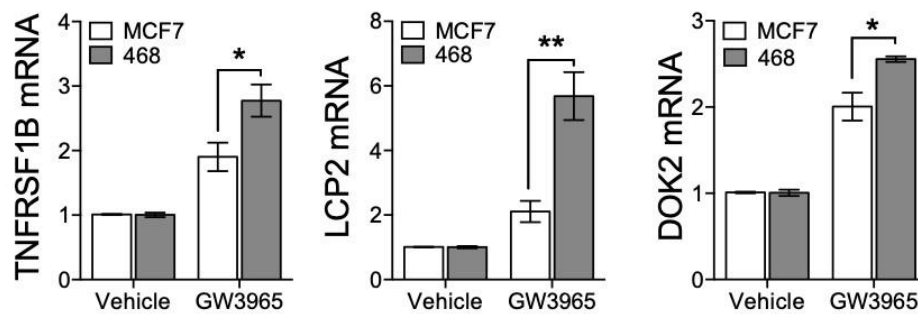


Figure 3. LXRA expression correlates with target genes in ER-negative tumours but not in ER-positive BCa. Genes with top LXRA occupancy scores from the seven NR1H3/LXRA ChIP-Seq datasets available at cistrome.org were identified along with 24 canonical LXR targets identified from the literature, and correlation with *LXRA/NR1H3* expression in 81 ER-negative and 234 Luminal A tumours from The Cancer Genome Atlas (TCGA) determined. Dotted line denotes false discovery rate corrected for multiple testing of expression of 135 genes. Data presented are correlation coefficients against correlation significance in ER-negative (a) and ER-positive (b) breast tumours. Genes marked with # were validated by qPCR analysis in (c) where ER-negative (MDA-MB-468) and ER-positive (MCF7) cell lines were treated with either Vehicle control or GW3965 (1 μ M) and expression of three highly significant genes (TNFRSF1B, LCP2 and DOK2) determined. Statistical significance was tested for using multiple *t*-tests (corrected with Holm–Sidak) and shows three independent replicates with SEM. * $p < 0.05$, ** $p < 0.01$.

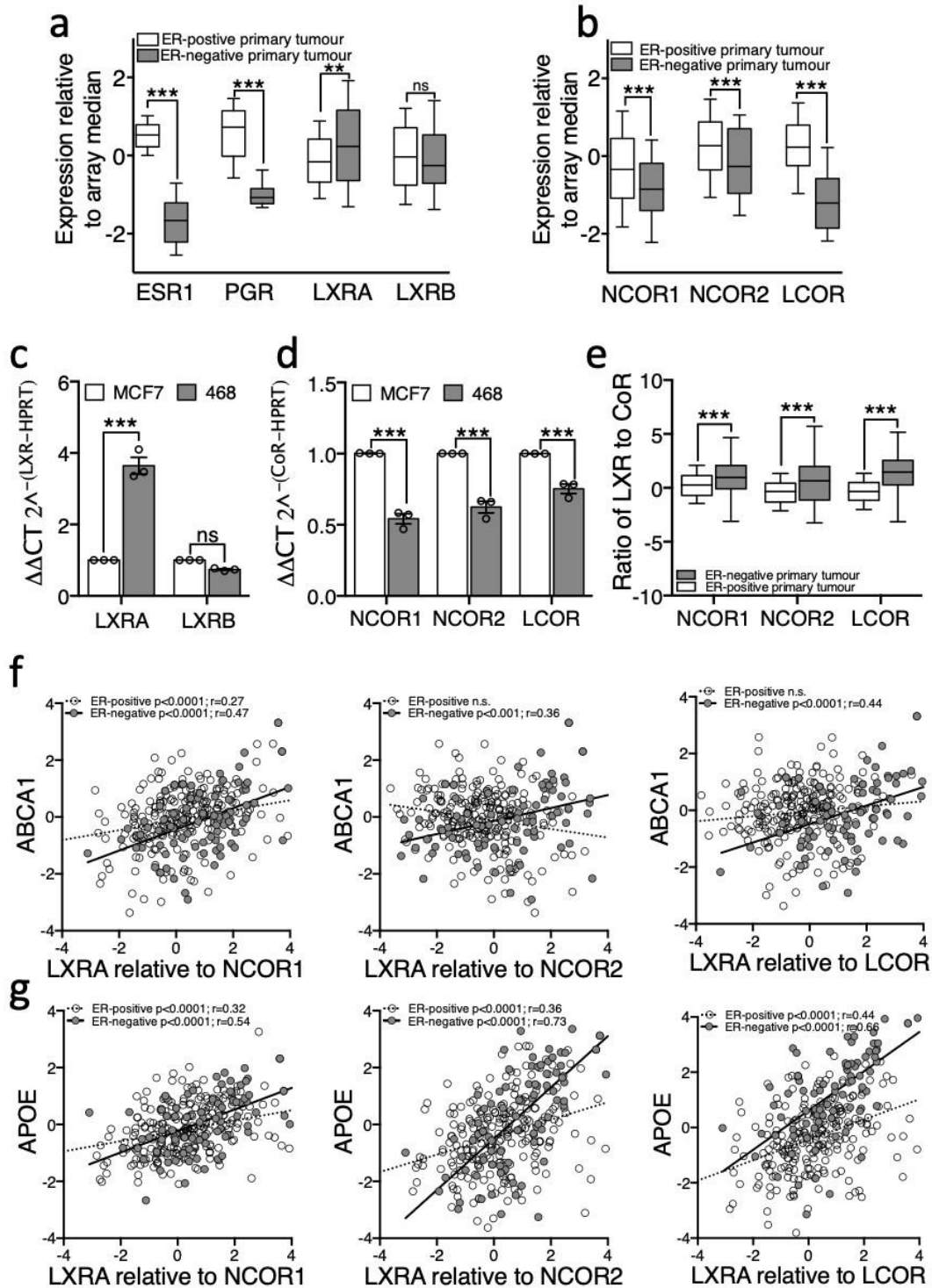


Figure 4. LXRA and its corepressors are differentially expressed between primary ER-negative and ER-positive breast cancers. RNA-Seq gene expression data (log transformed relative to array median) were obtained for 81 ER-negative and 234 Luminal A tumours from TCGA via cBioportal. NR (a) and CoR (b) expression was determined in from the TCGA database and in cell lines MDA-MB-468 and MCF7 (c,d). Expression of LXR relative to corepressor in the TCGA data is shown in (e). TCGA data are presented as log transformed and normalized to array-median with 10–90th centiles (a,c,e). Error bars represent SEM of 3–4 independent replicates for cell line analysis (c,d). Statistical analysis was performed using two-tailed Mann–Whitney U tests for (a,b), two-tailed student *t*-test (c,d), or Pearson’s correlation (f,g). ** $p < 0.01$, *** $p < 0.001$, ns = not significant.

Next, we hypothesised that if corepressors were responsible for the dampened response to ligand in ER-positive disease, then the ratio of LXR to corepressor should predict target gene expression. As expected, we found that the ratio of LXR to all three corepressors was significantly higher in ER-negative tumours compared to ER-positive (Figure 4e; two-way ANOVA: $p < 0.0001$) supporting the proposal that LXR is better able to activate its transcriptional targets in ER-negative disease. Furthermore, whilst there was no correlation between LXRA and ABCA1 in the ER-positive cohort (Figure 2e), when assessing a correlation between ABCA1 expression and the ratio of LXRA/NCOR1 we found a significant positive correlation (Pearson correlation: $R = 0.27$, $p < 0.0001$; Figure 4f). Although the expression of APOE was significantly correlated with LXRA alone (Figure 2f), when the corepressors were included in the analysis the strength of correlation increased (NCOR1 $r = 0.32$; NCOR2 $r = 0.36$; LCOR $r = 0.44$ (Figure 4g)). Surprisingly, the strength of correlation between target gene and LXR was not improved by the addition of CoR expression in ER-negative disease ratio analysis. As a control we performed the same analyses for LXR/NR1H2 and found no correlation with ABCA1 nor APOE in either subtype with any LXR/CoR ratio (data not shown). These analyses reveal that the ratio of LXR to CoR is strongly correlated with target gene expression in all breast cancers analysed. These data are consistent with the hypothesis that the relative expression of LXRA to corepressors is the determinant of target gene responsiveness to ligand and that differences in this ratio between BCa subtypes determines their ability to dynamically respond to changes in cholesterol metabolic flux.

3.4. Removal of Corepressors Equalizes the Response of ER-Negative and ER-Positive Cell Lines to Ligand

Since corepressor expression and LXR transcriptional response to ligand appeared to be associated, we tested if knock-down of the corepressors in ER-positive cells equalized the response to ligand between MCF7 and MDA-MB-468 cells. Furthermore, basal expression of target genes should become elevated in knock-down cells owing to derepression following loss of corepressor activity. To this end we impaired NCOR1/NCOR2 or LCOR expression in luciferase reporter MDA-MB-468 and MCF7 cells using silencing RNA (50%–80% knock-down was observed for all corepressors in both cell lines (Figure S8)), followed by treatment with 26-OHC or vehicle control. Under control conditions (siCON) LXR activation in response to 26-OHC was, as expected, significantly higher in MDA-MB-468 than MCF7 cells (two-tailed student's t -test: $p < 0.0001$ (Figure 5a)). Knock-down of NCOR or LCOR however, significantly enhanced the transcriptional response to ligand in both cell lines (two-way ANOVA: $p < 0.05$ (Figure 5a)) and led to equivalent transcriptional responses to 26-OHC in MCF7 and MDA-MB-468 cells (paired two-tailed t -test: siNCOR $p = 0.28$;

siLCOR $p = 0.29$ (Figure 5a)) suggesting corepressor expression was an important factor in determining the differential response of these two cell types to 26-OHC. This observation was recapitulated at the phenotype level, as corepressor knock-down led to a significantly enhanced attenuation of cell viability in response to 26-OHC treatment (non-linear regression comparison of fits: $p < 0.0001$ for both cell lines (Figure 5b)). When the basal expression of canonical LXR target genes were measured, we observed elevated expression of both ABCA1 and APOE with corepressor knock-down relative to control treated cells, again in both cell lines (two-way ANOVA: $p < 0.0001$ (Figure 5c)). In summary, these knock-down experiments support the hypothesis that corepressors are important determinants of the differential transcriptional activity of LXR between BCa subtypes.

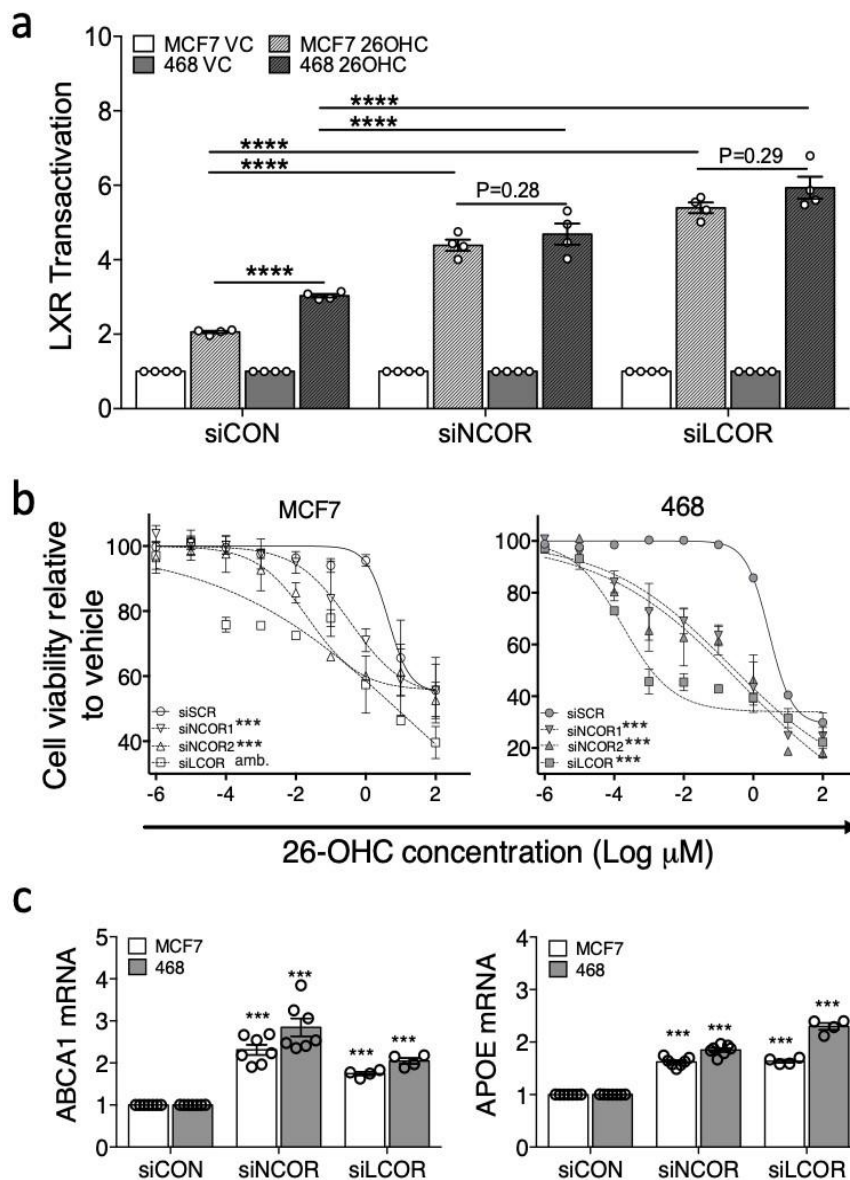


Figure 5. Corepressors determine differential response of cell lines to 26-OHC. NCOR or LCOR, were knocked-down in LXR-luciferase reporter MCF7 and MDA-MB-468 cells and treated with vehicle control (VC) or 26-OHC (10 μ M) for 16 h (a). Endogenous LXR activity was determined after knockdown for

ABCA1 (b) and APOE (c). Response to 26-OHC was assessed following corepressor knockdown by MTT (d). One-way ANOVA (a–c) and non-linear regression (d) were used to test for significant differences. *** $p < 0.001$, **** $p < 0.0001$, amb. = curve fit was ambiguous.

4. Discussion

The importance of cholesterol and cholesterol metabolism in breast and other cancers is increasingly appreciated. The purpose of this study was to clarify whether the activity of LXR was different between ER-positive and ER-negative BCa and identify factors that may be responsible for any difference. We established that expression of LXR's regulatory factors were skewed towards a transcriptionally poised state in ER-negative disease, but towards ligand insensitivity in ER-positive disease. Furthermore, LXRA expression positively correlated with that of its target genes in ER-negative tumours but not in ER-positive disease. Nuclear corepressor expression was elevated in primary ER-positive disease and experimental manipulation in vitro established they were critical in suppressing the response to ligand in ER-positive BCa. These data indicate that ER-negative tumours are particularly sensitive to elevated cholesterol and, given the increasing appreciation of the role of LXR signalling in BCa, potentially explain why ER-negative disease is more likely to be altered by cholesterol lowering interventions than ER-positive disease [39–41].

NR repression is a mechanism to overcome anti-proliferative actions in a range of cancer types including prostate [9,10] and bladder [11]. We observed anti-proliferative actions of the scOHC-LXR signalling axis, but it was surprising that a permissive anti-proliferative LXR signalling environment was retained in the more aggressive ER-negative BCa subtype. In our study we evaluated T47D, MCF7, MDA-MB-468 and MDA-MB-231 cells, all of which responded in vitro consistently with in vivo observations from primary breast tumours; the ER-positive models had a dampened transcriptional response to LXR ligands compared to ER-negative. A previous report indicated that ER-positive MCF7 and T47D cells were more sensitive to LXR induced G0/G1 arrest than ER-negative MDA-MB-231 cells [32], but at the same time indicated, like us, that LXR stimulation led to higher induction of *ABCA1* in ER-negative cells than in ER-positive ones. This discrepancy in sensitivity between cell cycle and direct transcriptional regulation, probably reflects the fact that the synthetic ligands used in the cell cycle arrest analysis are not oestrogenic, whereas in our study we observe the opposing actions of scOHCs on ER and LXR in ER-positive cells. As we demonstrate here, there are differences in NR biology between BCa subtypes beyond ER/PR expression, and responsiveness to LXR ligands is influenced by corepressor expression and indicates differential cholesterol metabolism between BCa subtypes.

Retention of LXR signalling in some tumour types suggests a selective advantage that compensates for the anti-proliferative actions of the scOHC-LXR axis [32]. The

oxysterol signalling axis is emerging as a route through which ER-negative BCa metastasis may occur [17]. It would be interesting to determine if the early tumour development requires repressed LXR activity so as to impair its anti-proliferative actions, and contrast with a return to LXR activation in later stage disease to support migration. Consistent with this is the observation that 25-OHC is elevated in the serum of breast cancer patients at relapse compared to those with primary disease [18].

The differences we observed in LXR activity between subtypes expand on previous observations that NR cofactors could usefully serve as therapeutic biomarkers, which are targetable through epigenetic drugs (e.g., HDAC inhibitors that impair their epigenetic transcription silencing targets and that are recruited by NCOR1 and NCOR2) aimed at reinstating pre-cancer gene expression patterns and responsiveness. NCOR1 expression, for example, was found to be an independent and favourable prognostic marker in a mixed BCa cohort [42]. This may in part be explained by Tamoxifen's dependence on NCOR1 recruitment to and repression of ER target genes in ER-positive BCa [43]. In therapy naïve ER-positive tumours our data suggest corepressor levels are high, perhaps to prevent LXR (and indeed other NRs such as VDR) from driving anti-proliferative transcriptional programs. The impact of high corepressor expression on scOHC dependent ER activity may also be important. Several scOHCs are oestrogenic and pro-proliferative when liganded with ER, indicating that elevated corepressor expression may serve to impede scOHC-ER dependent proliferation.

LCOR is also of therapeutic and prognostic interest as its recruitment to promoters by agonists can repress gene expression rather than activate [44]. It is tempting to link two of our observations; *LCOR* levels were significantly higher in ER-positive disease (and in MCF7 cells), and agonist treatment led to repression of *APOE* (Figure 2d) in MCF7 cells only. *LCOR* expression has previously been reported to be associated with better survival in BCa patients [37], particularly if nuclear localization is considered [45], which presumably reflects its inhibitory actions on oestrogen receptor signalling. Further research is required to understand if manipulation of *LCOR* expression can mediate the selective modulation of LXR ligand function, as our observations of *APOE* transcription could suggest. The methodology we employed to identify an unbiased panel of LXR target genes, which was then used to test if LXR was transcriptionally active or repressed in different tumour types, has potentially identified a large set of novel LXR target genes. Our analysis combined ChIP-Seq data from multiple cell types with validation of potential targets by assessing expression in primary BCa samples and induction analysis in vitro. This approach resulted in multiple apparently novel LXR target genes being identified, with three out of three validated by qPCR. The first of these *LCP2*, has been reported as differentially

expressed between primary and metastatic colorectal cancer [46] and is a prognostic biomarker for colorectal cancer patients [47]. *TNFRSF1B* expression has been linked to increased BCa risk [48,49] and to chemotherapy resistance via enhanced AKT signalling and PARP mediated DNA repair [50]. DOK2 has tumour suppression roles in several cancer types as it impairs MAPK activation and loss of its expression is associated with poor survival in lung adenocarcinoma [51], whilst in BCa greater DOK2 expression is associated with significantly longer disease free survival [52]. These possible LXR targets, as well as others in ST1 require further evaluation to ascertain the extent to which they, through aberrant cholesterol metabolism and LXR signalling, may influence tumour biology.

It is interesting to note that many of lifestyle factors reported by the World Cancer Research Fund's Continuous Update Project [53] that associate with BCa, are body composition metrics and nutritional parameters that are directly associated with LDL-C, a key precursor of scOHCs. LDL-C, Obesity, Waist-Hip-Ratio and Waist Circumference are associated with incidence and survival of BCa [54,55] and clinically recommended diets/lifestyle changes that lower LDL-C (e.g., high fish-oil and carotenoid intake, the Mediterranean Diet, reduced animal calorie intake), protect against BCa and relapse, particularly in the hormone receptor negative setting [41,53,56,57]. Pharmacological manipulation of LDL-C with lipophilic statins improves BCa survivorship [39], specifically reducing early (<4 years) relapse events [40], again, a feature typical of ER-negative disease. Our data are consistent with the hypothesis that ER-negative tumours are more sensitive to changes in systemic cholesterol flux; future work should clarify if dietary or pharmacological suppression of scOHC signalling could modify disease prognosis.

5. Conclusions

In this current study, scOHC were confirmed as natural LXR agonists in BCa cell lines, and we observed that their activity is regulated to a large extent by corepressors. This is the first demonstration that transcriptional activation of LXR target genes by scOHCs may be dependent on tumour-subtype specific expression of corepressors. A combination of mechanistic and clinical trial studies should help confirm the relevance of the data described here in people, and would allow further exploration of LXR as a potential therapeutic target that links dietary and lifestyle regulation of cholesterol metabolism with cancer progression and survival.

References

1. Janowski, B.A.; Willy, P.J.; Devi, T.R.; Falck, J.R.; Mangelsdorf, D.J. An oxysterol signalling pathway mediated by the nuclear receptor LXR alpha. *Nature* **1996**, *383*, 728–731. [[CrossRef](#)] [[PubMed](#)]
2. Lehmann, J.M.; Kliewer, S.A.; Moore, L.B.; Smith-Oliver, T.A.; Oliver, B.B.; Su, J.L.; Sundseth, S.S.; Winegar, D.A.; Blanchard, D.E.; Spencer, T.A.; et al. Activation of the nuclear receptor LXR by oxysterols defines a new hormone response pathway. *J. Biol. Chem.* **1997**, *272*, 3137–3140. [[CrossRef](#)] [[PubMed](#)]

3. Stiles, A.R.; Kozlitina, J.; Thompson, B.M.; McDonald, J.G.; King, K.S.; Russell, D.W. Genetic, anatomic, and clinical determinants of human serum sterol and vitamin D levels. *Proc. Natl. Acad. Sci. USA* **2014**, *111*, E4006–E4014. [[CrossRef](#)]
4. Wu, Q.; Ishikawa, T.; Sirianni, R.; Tang, H.; McDonald, J.G.; Yuhanna, I.S.; Thompson, B.; Girard, L.; Mineo, C.; Brekken, R.A.; et al. 27-Hydroxycholesterol Promotes Cell-Autonomous, ER-Positive Breast Cancer Growth. *Cell Rep.* **2013**, *5*, 637–645. [[CrossRef](#)] [[PubMed](#)]
5. Fakheri, R.J.; Javitt, N.B. 27-Hydroxycholesterol, does it exist? On the nomenclature and stereochemistry of 26-hydroxylated sterols. *Steroids* **2012**, *77*, 575–577. [[CrossRef](#)] [[PubMed](#)]
6. Janowski, B.A.; Grogan, M.J.; Jones, S.A.; Wisely, G.B.; Kliewer, S.A.; Corey, E.J.; Mangelsdorf, D.J. Structural requirements of ligands for the oxysterol liver X receptors LXRA and LXRβ. *Proc. Natl. Acad. Sci. USA* **1999**, *96*, 266–271. [[CrossRef](#)]
7. Solheim, S.; Hutchinson, S.A.; Lundanes, E.; Wilson, S.R.; Thorne, J.L.; Roberg-Larsen, H. Fast liquid chromatography-mass spectrometry reveals side chain oxysterol heterogeneity in breast cancer tumour samples. *J. Steroid Biochem. Mol. Biol.* **2019**, *192*, 105309. [[CrossRef](#)]
8. Thorne, J.L.; Campbell, M.J. Nuclear receptors and the Warburg effect in cancer. *Int. J. Cancer* **2015**, *137*, 1519–1527. [[CrossRef](#)]
9. Doig, C.L.; Singh, P.K.; Dhiman, V.K.; Thorne, J.L.; Battaglia, S.; Sobolewski, M.; Maguire, O.; O'Neill, L.P.; Turner, B.M.; McCabe, C.J.; et al. Recruitment of NCOR1 to VDR target genes is enhanced in prostate cancer cells and associates with altered DNA methylation patterns. *Carcinogenesis* **2012**, *34*, 248–256. [[CrossRef](#)]
10. Battaglia, S.; Maguire, O.; Thorne, J.L.; Hornung, L.B.; Doig, C.L.; Liu, S.; Sucheston, L.E.; Bianchi, A.; Khanim, F.L.; Gommersall, L.M.; et al. Elevated NCOR1 disrupts PPARα/γ signaling in prostate cancer and forms a targetable epigenetic lesion. *Carcinogenesis* **2010**, *31*, 1650–1660. [[CrossRef](#)]
11. Abedin, S.A.; Thorne, J.L.; Battaglia, S.; Maguire, O.; Hornung, L.B.; Doherty, A.P.; Mills, I.G.; Campbell, M.J. Elevated NCOR1 disrupts a network of dietary-sensing nuclear receptors in bladder cancer cells. *Carcinogenesis* **2009**, *30*, 449–456. [[CrossRef](#)] [[PubMed](#)]
12. Hu, X.; Li, S.; Wu, J.; Xia, C.; Lala, D.S. Liver X receptors interact with corepressors to regulate gene expression. *Mol. Endocrinol.* **2003**, *17*, 1019–1026. [[CrossRef](#)] [[PubMed](#)]
13. Long, M.D.; Thorne, J.L.; Russell, J.; Battaglia, S.; Singh, P.K.; Sucheston-Campbell, L.E.; Campbell, M.J. Cooperative behavior of the nuclear receptor superfamily and its deregulation in prostate cancer. *Carcinogenesis* **2014**, *35*, 262–271. [[CrossRef](#)]
14. Pencheva, N.; Buss, C.G.; Posada, J.; Merghoub, T.; Tavazoie, S.F. Broad-Spectrum Therapeutic Suppression of Metastatic Melanoma through Nuclear Hormone Receptor Activation. *Cell* **2014**, *156*, 986–1001. [[CrossRef](#)] [[PubMed](#)]
15. Wang, Q.; Sun, L.; Yang, X.; Ma, X.; Li, Q.; Chen, Y.; Liu, Y.; Zhang, D.; Li, X.; Xiang, R.; et al. Activation of liver X receptor inhibits the development of pulmonary carcinomas induced by 3-methylcholanthrene and butylated hydroxytoluene in BALB/c mice. *Sci. Rep.* **2016**, *6*, 27295. [[CrossRef](#)] [[PubMed](#)]
16. Nelson, E.R.; Wardell, S.E.; Jasper, J.S.; Park, S.; Suchindran, S.; Howe, M.K.; Carver, N.J.; Pillai, R.V.; Sullivan, P.M.; Sondhi, V.; et al. 27-Hydroxycholesterol links hypercholesterolemia and breast cancer pathophysiology. *Science* **2013**, *342*, 1094–1098. [[CrossRef](#)]
17. Baek, A.E.; Yu, Y.R.A.; He, S.S.; Wardell, S.E.; Chang, C.Y.; Kwon, S.; Pillai, R.V.; McDowell, H.B.; Thompson, J.W.; Dubois, L.G.; et al. The cholesterol metabolite 27 hydroxycholesterol facilitates breast cancer metastasis through its actions on immune cells. *Nat. Commun.* **2017**, *8*, 864. [[CrossRef](#)]
18. Dalenc, F.; Iuliano, L.; Filleron, T.; Zerbinati, C.; Voisin, M.; Arellano, C.; Chatelut, E.; Marquet, P.; Samadi, M.; Roche, H.; et al. Circulating oxysterol metabolites as potential new surrogate markers in patients with hormone receptor-positive breast cancer: Results of the OXYTAM study. *J. Steroid Biochem. Mol. Biol.* **2016**, *169*, 210–218. [[CrossRef](#)]
19. Hutchinson, S.A.; Lianto, P.; Moore, J.B.; Hughes, T.A.; Thorne, J.L. Phytosterols Inhibit Side-Chain Oxysterol Mediated Activation of LXR in Breast Cancer Cells. *Int. J. Mol. Sci.* **2019**, *20*, 3241. [[CrossRef](#)]
20. Kim, B.; Stephen, S.L.; Hanby, A.M.; Horgan, K.; Perry, S.L.; Richardson, J.; Roundhill, E.A.; Valleley, E.M.; Verghese, E.T.; Williams, B.J.; et al. Chemotherapy induces Notch1-dependent MRP1 up-regulation, inhibition of which sensitizes breast cancer cells to chemotherapy. *BMC Cancer* **2015**, *15*, 634. [[CrossRef](#)]

21. Thorne, J.L.; Battaglia, S.; Baxter, D.E.; Hayes, J.L.; Hutchinson, S.A.; Jana, S.; Millican-Slater, R.A.; Smith, L.; Teske, M.C.; Wastall, L.M.; et al. MiR-19b non-canonical binding is directed by HuR and confers chemosensitivity through regulation of P-glycoprotein in breast cancer. *Biochim. Biophys. Acta Gene Regul. Mech.* **2018**, *1861*, 996–1006. [[CrossRef](#)] [[PubMed](#)]
22. Broekema, M.F.; Hollman, D.A.A.; Koppen, A.; van den Ham, H.J.; Melchers, D.; Pijnenburg, D.; Ruijtenbeek, R.; van Mil, S.W.C.; Houtman, R.; Kalkhoven, E. Profiling of 3696 Nuclear Receptor-Coregulator Interactions: A Resource for Biological and Clinical Discovery. *Endocrinology* **2018**, *159*, 2397–2407. [[CrossRef](#)] [[PubMed](#)]
23. Cerami, E.; Gao, J.; Dogrusoz, U.; Gross, B.E.; Sumer, S.O.; Aksoy, B.A.; Jacobsen, A.; Byrne, C.J.; Heuer, M.L.; Larsson, E.; et al. The cBio cancer genomics portal: An open platform for exploring multidimensional cancer genomics data. *Cancer Discov.* **2012**, *2*, 401–404. [[CrossRef](#)] [[PubMed](#)]
24. Cancer Genome Atlas, N. Comprehensive molecular portraits of human breast tumours. *Nature* **2012**, *490*, 61–70. [[CrossRef](#)]
25. Gao, J.J.; Aksoy, B.A.; Dogrusoz, U.; Dresdner, G.; Gross, B.; Sumer, S.O.; Sun, Y.C.; Jacobsen, A.; Sinha, R.; Larsson, E.; et al. Integrative Analysis of Complex Cancer Genomics and Clinical Profiles Using the cBioPortal. *Sci. Signal.* **2013**, *6*, pl1. [[CrossRef](#)]
26. Long, M.D.; Campbell, M.J. Integrative genomic approaches to dissect clinically-significant relationships between the VDR cistrome and gene expression in primary colon cancer. *J. Steroid Biochem. Mol. Biol.* **2017**, *173*, 130–138. [[CrossRef](#)]
27. Gross, A.M.; Kreisberg, J.F.; Ideker, T. Analysis of Matched Tumor and Normal Profiles Reveals Common Transcriptional and Epigenetic Signals Shared across Cancer Types. *PLoS ONE* **2015**, *10*, e0142618. [[CrossRef](#)]
28. Liu, T.; Ortiz, J.A.; Taing, L.; Meyer, C.A.; Lee, B.; Zhang, Y.; Shin, H.; Wong, S.S.; Ma, J.; Lei, Y.; et al. Cistrome: An integrative platform for transcriptional regulation studies. *Genome Biol.* **2011**, *12*, R83. [[CrossRef](#)]
29. Oishi, Y.; Spann, N.J.; Link, V.M.; Muse, E.D.; Strid, T.; Edillor, C.; Kolar, M.J.; Matsuzaka, T.; Hayakawa, S.; Tao, J.; et al. SREBP1 Contributes to Resolution of Pro-inflammatory TLR4 Signaling by Reprogramming Fatty Acid Metabolism. *Cell Metab.* **2017**, *25*, 412–427. [[CrossRef](#)]
30. Savic, D.; Ramaker, R.C.; Roberts, B.S.; Dean, E.C.; Burwell, T.C.; Meadows, S.K.; Cooper, S.J.; Garabedian, M.J.; Gertz, J.; Myers, R.M. Distinct gene regulatory programs define the inhibitory effects of liver X receptors and PPARG on cancer cell proliferation. *Genome Med.* **2016**, *8*, 74. [[CrossRef](#)]
31. Galhardo, M.; Sinkkonen, L.; Berninger, P.; Lin, J.; Sauter, T.; Heinaniemi, M. Integrated analysis of transcript-level regulation of metabolism reveals disease-relevant nodes of the human metabolic network. *Nucleic Acids Res.* **2014**, *42*, 1474–1496. [[CrossRef](#)] [[PubMed](#)]
32. Vedin, L.L.; Lewandowski, S.A.; Parini, P.; Gustafsson, J.A.; Steffensen, K.R. The oxysterol receptor LXR inhibits proliferation of human breast cancer cells. *Carcinogenesis* **2009**, *30*, 575–579. [[CrossRef](#)] [[PubMed](#)]
33. Beltowski, J. Liver X Receptors (LXR) as Therapeutic Targets in Dyslipidemia. *Cardiovascular Therapeutics* **2008**, *26*, 297–316. [[CrossRef](#)] [[PubMed](#)]
34. Zuercher, W.J.; Buckholz, R.G.; Campobasso, N.; Collins, J.L.; Galardi, C.M.; Gampe, R.T.; Hyatt, S.M.; Merrihew, S.L.; Moore, J.T.; Oplinger, J.A.; et al. Discovery of Tertiary Sulfonamides as Potent Liver X Receptor Antagonists. *J. Med. Chem.* **2010**, *53*, 3412–3416. [[CrossRef](#)] [[PubMed](#)]
35. Wong, J.; Quinn, C.M.; Brown, A.J. SREBP-2 positively regulates transcription of the cholesterol efflux gene, ABCA1, by generating oxysterol ligands for LXR. *Biochem. J.* **2006**, *400*, 485–491. [[CrossRef](#)]
36. Laffitte, B.A.; Repa, J.J.; Joseph, S.B.; Wilpitz, D.C.; Kast, H.R.; Mangelsdorf, D.J.; Tontonoz, P. LXRs control lipid-inducible expression of the apolipoprotein E gene in macrophages and adipocytes. *Proc. Natl. Acad. Sci. USA* **2001**, *98*, 507–512. [[CrossRef](#)]
37. Jalaguier, S.; Teyssier, C.; Nait Achour, T.; Lucas, A.; Bonnet, S.; Rodriguez, C.; Elarouci, N.; Lapierre, M.; Cavailles, V. Complex regulation of LCoR signaling in breast cancer cells. *Oncogene* **2017**, *36*, 4790–4801. [[CrossRef](#)]

38. Heiser, L.M.; Sadanandam, A.; Kuo, W.L.; Benz, S.C.; Goldstein, T.C.; Ng, S.; Gibb, W.J.; Wang, N.J.; Ziyad, S.; Tong, F.; et al. Subtype and pathway specific responses to anticancer compounds in breast cancer. *Proc. Natl. Acad. Sci. USA* **2012**, *109*, 2724–2729. [[CrossRef](#)]
39. Manthravadi, S.; Shrestha, A.; Madhusudhana, S. Impact of statin use on cancer recurrence and mortality in breast cancer: A systematic review and meta-analysis. *Int. J. Cancer* **2016**, *139*, 1281–1288. [[CrossRef](#)]
40. Liu, B.; Yi, Z.; Guan, X.; Zeng, Y.X.; Ma, F. The relationship between statins and breast cancer prognosis varies by statin type and exposure time: A meta-analysis. *Breast Cancer Res. Treat.* **2017**, *164*, 1–11. [[CrossRef](#)]
41. Link, L.B.; Canchola, A.J.; Bernstein, L.; Clarke, C.A.; Stram, D.O.; Ursin, G.; Horn-Ross, P.L. Dietary patterns and breast cancer risk in the California Teachers Study cohort. *Am. J. Clin. Nutr.* **2013**, *98*, 1524–1532. [[CrossRef](#)] [[PubMed](#)]
42. Myers, E.; Hill, A.D.K.; Kelly, G.; McDermott, E.W.; O’Higgins, N.J.; Buggy, Y.; Young, L.S. Associations and interactions between Ets-1 and Ets-2 and coregulatory proteins, SRC-1, AIB1, and NCoR in breast cancer. *Clin. Cancer Res.* **2005**, *11*, 2111–2122. [[CrossRef](#)] [[PubMed](#)]
43. Lu, R.Q.; Hu, X.B.; Zhou, J.M.; Sun, J.J.; Zhu, A.Z.; Xu, X.F.; Zheng, H.; Gao, X.; Wang, X.; Jin, H.C.; et al. COPS5 amplification and overexpression confers tamoxifen-resistance in ER alpha-positive breast cancer by degradation of NCoR. *Nat. Commun.* **2016**, *7*, 12044. [[CrossRef](#)] [[PubMed](#)]
44. Asim, M.; Bin Hafeez, B.; Siddiqui, I.A.; Gerlach, C.; Patz, M.; Mukhtar, H.; Baniahmad, A. Ligand-dependent Corepressor Acts as a Novel Androgen Receptor Corepressor, Inhibits Prostate Cancer Growth, and Is Functionally Inactivated by the Src Protein Kinase. *J. Biol. Chem.* **2011**, *286*, 37108–37117. [[CrossRef](#)] [[PubMed](#)]
45. Sixou, S.; Muller, K.; Jalaguier, S.; Kuhn, C.; Harbeck, N.; Mayr, D.; Engel, J.; Jeschke, U.; Ditsch, N.; Cavailles, V. Importance of RIP140 and LCoR Sub-Cellular Localization for Their Association With Breast Cancer Aggressiveness and Patient Survival. *Transl. Oncol.* **2018**, *11*, 1090–1096. [[CrossRef](#)]
46. Chu, S.; Wang, H.; Yu, M. A putative molecular network associated with colon cancer metastasis constructed from microarray data. *World J. Surg. Oncol.* **2017**, *15*, 115. [[CrossRef](#)]
47. Jiang, H.; Dong, L.; Gong, F.; Gu, Y.; Zhang, H.; Fan, D.; Sun, Z. Inflammatory genes are novel prognostic biomarkers for colorectal cancer. *Int. J. Mol. Med.* **2018**, *42*, 368–380. [[CrossRef](#)]
48. Xu, F.; Zhou, G.; Han, S.; Yuan, W.; Chen, S.; Fu, Z.; Li, D.; Zhang, H.; Li, D.; Pang, D. Association of TNF-alpha, TNFRSF1A and TNFRSF1B gene polymorphisms with the risk of sporadic breast cancer in northeast Chinese Han women. *PLoS ONE* **2014**, *9*, e101138. [[CrossRef](#)]
49. Han, W.; Kang, S.Y.; Kang, D.; Park, S.K.; Lee, J.Y.; Kim, H.; Park, A.K.; Noh, D.Y. Multiplex genotyping of 1107 SNPs from 232 candidate genes identified an association between IL1A polymorphism and breast cancer risk. *Oncol. Rep.* **2010**, *23*, 763–769.
50. Yang, F.; Zhao, N.; Wu, N. TNFR2 promotes Adriamycin resistance in breast cancer cells by repairing DNA damage. *Mol. Med. Rep.* **2017**, *16*, 2962–2968. [[CrossRef](#)]
51. Chen, M.; Zhang, J.; Berger, A.H.; DiIombi, M.S.; Ng, C.; Fung, J.; Bronson, R.T.; Castillo-Martin, M.; Thin, T.H.; Cordon-Cardo, C.; et al. Compound haploinsufficiency of Dok2 and Dusp4 promotes lung tumorigenesis. *J. Clin. Investig.* **2019**, *129*, 215–222. [[CrossRef](#)] [[PubMed](#)]
52. Huang, J.; Peng, X.; Zhang, K.; Li, C.; Su, B.; Zhang, Y.; Yu, W. Co-expression and significance of Dok2 and Ras p21 protein activator 1 in breast cancer. *Oncol. Lett.* **2017**, *14*, 5386–5392. [[CrossRef](#)] [[PubMed](#)]
53. WCRF/AICR. *Continuous Update Project Report: Diet, Nutrition, Physical Activity and Cancer*; World Cancer Research Fund International/American Institute for Cancer Research: London UK, 2017.
54. Dos Santos, C.R.; Fonseca, I.; Dias, S.; de Almeida, J.C.M. Plasma level of LDL-cholesterol at diagnosis is a predictor factor of breast tumor progression. *BMC Cancer* **2014**, *14*, 132. [[CrossRef](#)]
55. Dos Santos, C.R.; Domingues, G.; Matias, I.; Matos, J.; Fonseca, I.; de Almeida, J.M.; Dias, S. LDL-cholesterol signaling induces breast cancer proliferation and invasion. *Lipids Health Dis.* **2014**, *13*, 16. [[CrossRef](#)]
56. Chlebowski, R.T.; Blackburn, G.L.; Thomson, C.A.; Nixon, D.W.; Shapiro, A.; Hoy, M.K.; Goodman, M.T.; Giuliano, A.E.; Karanja, N.; McAndrew, P.; et al. Dietary fat reduction and breast cancer outcome: Interim efficacy results from the Women’s Intervention Nutrition Study. *J. Natl. Cancer Inst.* **2006**, *98*, 1767–1776. [[CrossRef](#)]
57. Toledo, E.; Salas-Salvado, J.; Donat-Vargas, C.; Buil-Cosiales, P.; Estruch, R.; Ros, E.; Corella, D.; Fito, M.;

Hu, F.B.; Aros, F.; et al. Mediterranean Diet and Invasive Breast Cancer Risk Among Women at High Cardiovascular Risk in the PREDIMED Trial: A Randomized Clinical Trial. *JAMA Intern. Med.* **2015**, *175*, 1752–1760. [[CrossRef](#)]



© 2019 by the authors. Licensee MDPI, Basel, Switzerland. This article is an open access article distributed under the terms and conditions of the Creative Commons Attribution (CC BY) license (<http://creativecommons.org/licenses/by/4.0/>).

B.2 Phytosterols Inhibit Side-Chain Oxysterol Mediated Activation of LXR in Breast Cancer Cells



International Journal of
Molecular Sciences



Phytosterols Inhibit Side-Chain Oxysterol Mediated Activation of LXR in Breast Cancer Cells

Samantha A. Hutchinson ¹, Priscilia Lianto ¹, J. Bernadette Moore ¹, Thomas A. Hughes ² and James L. Thorne ^{1,*}

¹ School of Food Science & Nutrition, University of Leeds, Leeds LS9 7TF, UK

² School of Medicine, University of Leeds, Leeds LS9 7TF, UK

* Correspondence: j.l.thorne@leeds.ac.uk



Received: 13 June 2019; Accepted: 27 June 2019; Published: 2 July 2019

Abstract: Low fruit and vegetable consumption and high saturated fat consumption causes elevated circulating cholesterol and are breast cancer risk factors. During cholesterol metabolism, oxysterols form that bind and activate the liver X receptors (LXRs). Oxysterols halt breast cancer cell proliferation but enhance metastatic colonization, indicating tumour suppressing and promoting roles. Phytosterols and phytostanols in plants, like cholesterol in mammals, are essential components of the plasma membrane and biochemical precursors, and in human cells can alter LXR transcriptional activity. Here, a panel of breast cancer cell lines were treated with four dietary plant sterols and a stanol, alone or in combination with oxysterols. LXR activation and repression were measured by gene expression and LXR-luciferase reporter assays. Oxysterols activated LXR in all cell lines, but surprisingly phytosterols failed to modulate LXR activity. However, phytosterols significantly inhibited the ability of oxysterols to drive LXR transcription. These data support a role for phytosterols in modulating cancer cell behaviour via LXR, and therefore suggest

merit in accurate dietary recordings of these molecules in cancer patients during treatment and perhaps supplementation to benefit recovery.

Keywords: phytosterols; liver X receptor; transcription; breast cancer; cholesterol; oxysterols

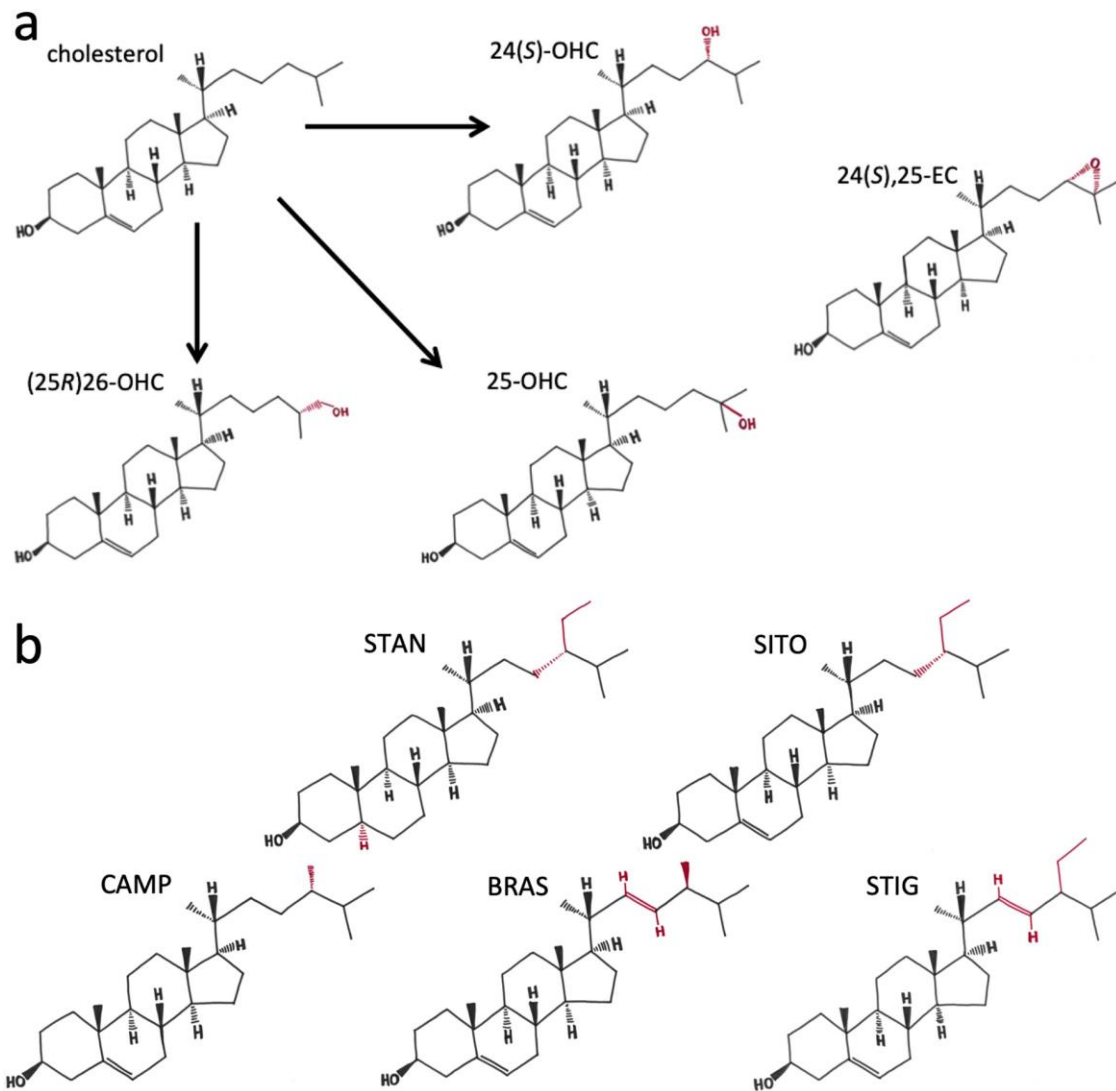


Figure 1. Chemical structure of cholesterol, side-chain oxysterols and plant sterols/stanols: (a) cholesterol differences from oxysterols 24(S)-OHC, 25-OHC, (25R)26-OHC and 24(S),25-EC are highlighted; (b) structures of phytostanol (sitostanol (STAN)) and phytosterols (β -sitosterol (SITO); campesterol (CAMP); brassicasterol (BRAS); stigmasterol (STIG) used in this study. Differences in structure with cholesterol are shown in red.

Plant sterols and stanols (PSSs) are analogous to cholesterol in that they are synthesized by plants to serve as structural components of plant cell membranes but are also functionally analogous to oxysterols as they are precursors in plant hormone synthesis. While cholesterol and ergosterol are ubiquitous as the 'bulk' sterols in mammalian and fungal cells respectively, plant cells contain a wide variety of sterols, with over 250 now known to exist [14]. The most abundant phytosterol in the human

diet is β -sitosterol (SITO) but several other plant sterol/stanols are commonly consumed, either in whole foods or added to common consumer products such as margarines and yoghurts, including sitostanol (STAN), campesterol (CAMP), brassicasterol (BRAS) and stigmasterol (STIG) [15]. The purpose of why plant cells require such an array of PSSs remains unclear, but the range of structural forms (Figure 1b), many of which mimic mammalian cholesterol modifications [16], provides an exploitable variety of biophysical properties [17] for use in prevention and treatment of cholesterol-related diseases in humans. The variety of properties, such as side chain branching, length and saturation, and the functions these different biophysical properties confer to PSSs in mammalian cell physiology remains far from fully understood.

Given the structural similarities of PSSs relative to mammalian cholesterol and oxysterol derivatives (Figure 1), it is not surprising that PSSs can modulate mammalian physiology if accumulated in sufficient concentrations. At the cellular level, PSSs integrate into the plasma membrane where they alter membrane fluidity, lateral pressure on protein complexes, and initiation of signalling cascades [17]. At the systemic level, PSSs have important effects on cholesterol metabolism: PSSs inhibit activity of key enzymes involved in cholesterol metabolism [18], impair cholesterol uptake from the diet [19], abrogate enzymatic conversion of cholesterol into oxysterols by competitive inhibition of members of the cytochrome P450 family [20], and are ligands of the LXRs [21]. LXRA and LXR_B are activated by PSS across the 20–100 nM range when assessed in cell-free coactivator recruitment assays [22]. In cell-based transcription assays, however, PSS treatment has been reported to be ineffective at altering transcription [18], or able to induce [21,22], and repress [20,23–25] LXR target gene expression. Selective modulation of LXRs by PSSs is therefore dependent on cell and tissue, and perhaps disease-specific factors.

Other than how PSSs can significantly lower circulating cholesterol levels, relatively little is known about their biological functions at the molecular level in normal and diseased tissues. In vitro and animal research suggests anti-cancer properties for PSSs, including inhibition of BCa growth and metastasis [26–28]. These data are supported by observational data from free-living individuals (i.e., not part of an intervention or trial) consuming diets rich in plant materials [29] and healthy dietary patterns associated with high PSSs intake, have lower cancer incidence and improved survival [30]. In addition, in clinically controlled intervention trials that have reduced saturated fat intake [5,31], lower rates of BCa and/or improved survival was observed

in the groups with highest PSS intakes. Improved understanding of the molecular pathways that underpin these clinical and epidemiological observations outlined above could help in the development and implementation of novel nutritive and lifestyle-based cancer prevention and treatment strategies. In this study, we have explored whether, at the transcriptional level, PSSs alter transcriptional programs exerted by oxysterols through LXR.

2. Results

2.1. PSSs Are Poor Transcriptional Activators of LXRA in Breast Cancer Cell Cultures

Given the structural similarities between oxysterols and phytosterols (Figure 1), and that previous reports that conflict as to whether PSSs activate or repress LXR, we wanted to establish if PSSs regulated the oxysterol-LXR signalling axis in breast cancer cells. We selected a range of PSSs with similar structures (with variations in branching and saturation) and that are commonly consumed in the diet (STAN, SITO, CAMP, BRAS, STIG). Biological activity of PSSs was confirmed by performing cell viability assays after 48 h of treatment. Aside from MCF7 cells being completely insensitive to BRAS, all PSSs lowered viability in all three cell lines at 100 μ M, and to varying extents at lower concentrations. MD-MB-468 were the most sensitive line to PSSs with viability significantly affected by STAN at 100 nM and above ($p < 0.05$ (Figure 2a)), by SITO, CAMP and BRAS at 1 μ M and above, and STIG at 10 μ M and above (Figure 2a). CAMP impaired MDA-MB-231 viability at 100 nM and above, while STIG was effective at 1 μ M and above, SITO and BRAS at 10 μ M and 100 μ M, and STAN at 100 μ M only (Figure 2b). MCF7 viability was impaired at 100 nM and above by both SITO and STIG, at 10 μ M by STAN and at 100 μ M by CAMP. MCF7 were insensitive to BRAS over the concentrations tested (Figure 2c).

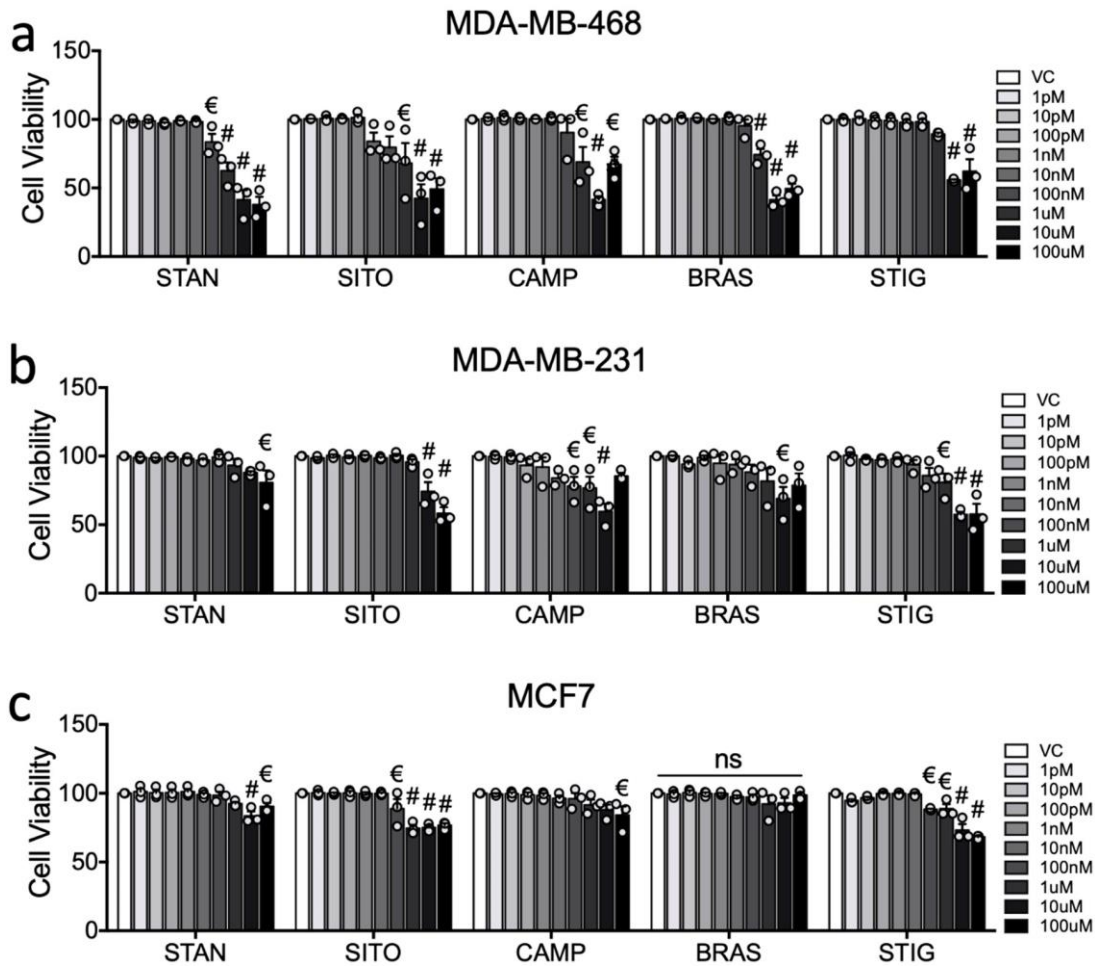


Figure 2. Phytosterols are anti-proliferative in breast cancer cell cultures. The anti-proliferative effects of STIG, SITO, CAMP, BRASS and STIG over 48 h was assessed by MTT in (a) MDA-MB-468, (b) MDA-MB-231, and (c) MCF7 cells. Cell viability relative to vehicle control was measured after treating with plant sterols and stanols (PSSs) at indicated concentrations. Data are presented as mean of three independent replicates (open circles) with SEM. For assessing changes between individual concentrations and vehicle, one-way ANOVA with Holm-Sidak correction for multiple testing and post-test for linear trend was performed. Significance levels are indicated by € = $p < 0.05$ and # = $p < 0.0001$. Linear trend was significant for all PSS in all cell lines except for BRAS in MCF7 (ns).

To determine the capacity of PSSs to drive LXRA specific transcription, a panel of stably transduced LXRA-luciferase reporter cell lines representing hormone receptor negative (MDA-MB-468, MDA-MB-231) and positive disease (MCF7) were treated with individual PSSs over a wide concentration range (from 1 pM to 100 μM) as described previously [32]. As a control we first treated cells with either the synthetic agonist (GW3965) or antagonist (GSK2033) and found LXR was induced in all cell lines by the agonist and repressed by the inhibitor (MDA-MB-468: 20-fold increase, 2-fold decrease (Figure 3a); MDA-MB-231 20-fold increase, 5-fold decrease (Figure 3b); MCF7 4-fold increase, 3-fold decrease (Figure 3c)). In contrast, treatment with PSSs led to far more modest responses. With increasing concentration, treatment with some PSSs induced linear trends towards repression (MDA-MB-468) or activation (MCF7). In MDA-MB-468 cells, increasing concentrations of STAN and SITO resulted in a

weak but significant linear trend towards repression (STAN: $p = 0.002$, $R^2 = 0.25$, Slope = -0.03 ; SITO: $p = 0.03$, $R^2 = 0.063$, Slope = -0.015 (Figure 3a)), but no single concentration led to a significant difference in LXRA activity when compared to vehicle control (Figure 3a). In MDA-MB-231 cells, there was a weak linear trend towards activation by SITO ($p = 0.038$, $R^2 = 0.09$, Slope = 0.017 (Figure 3b)). LXRA activity was increased by 1.4-fold with 100 nM STAN relative to vehicle control (two-way ANOVA with Holm-Sidak multiple correction: $p = 0.019$ (Figure 3b)), but not at any other concentrations nor by any other PSS. In MCF7 cells, increasing concentrations of BRAS and STIG were associated with significant linear trends towards weak LXRA activation (BRAS: $p = 0.0002$, $R^2 = 0.25$, Slope = -0.049 ; STIG: $p = 0.0049$, $R^2 = 0.15$, Slope = -0.023 ; (Figure 3c)). High concentrations of BRAS (50 μM $p < 0.0001$ (Figure 3c)) and multiple concentrations of STIG ($p < 0.05$ (Figure 3c)) resulted in statistically significant, but minor (<1.5) increases in LXRA activity compared to vehicle-treated control cells. From these reporter assays we concluded that across the typical physiological range, these PSSs had relatively little effect on LXRA activity in any cell type studied.

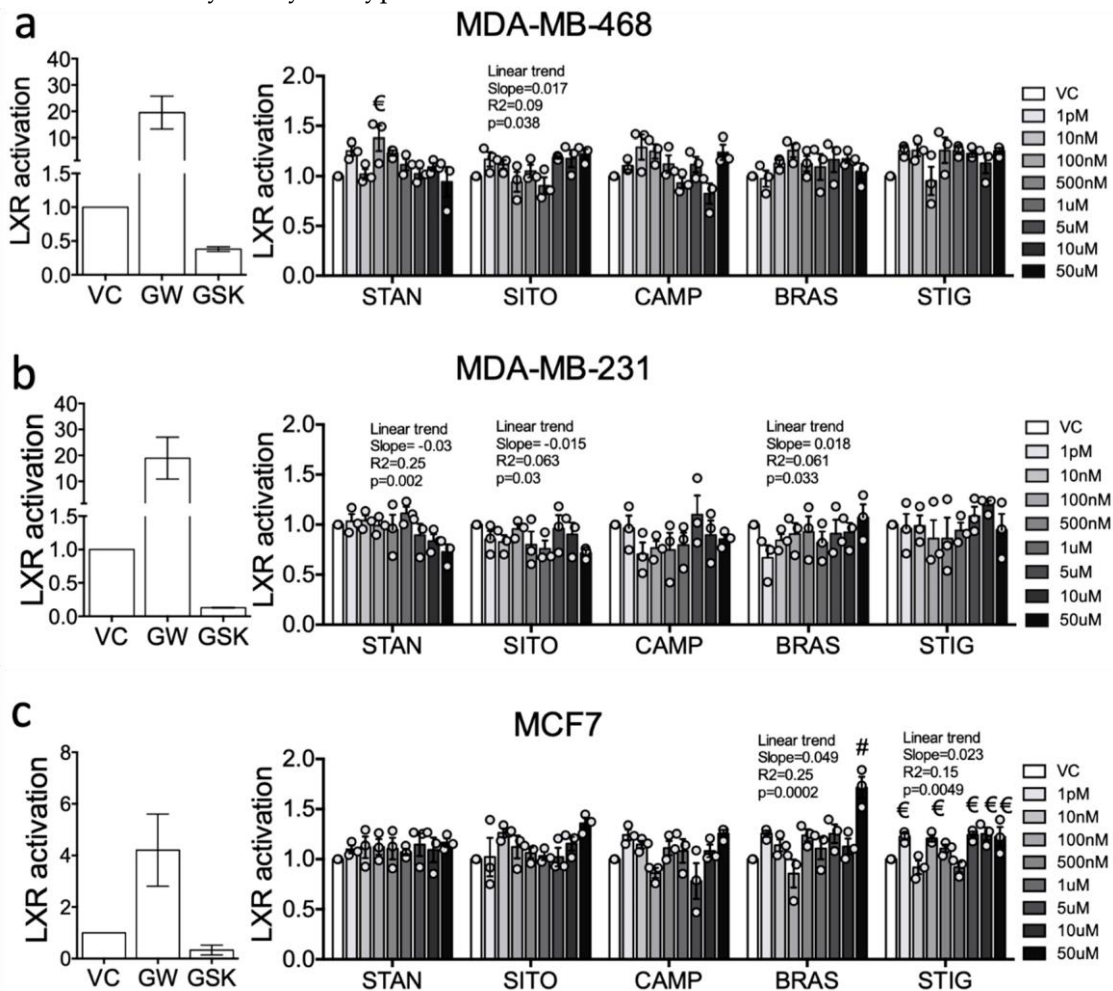


Figure 3. Liver X receptors (LXRs) is only weakly modulated by PSSs treatment in breast cancer cell lines. A luciferase reporter driven by an LXR alpha (LXRA) responsive promoter was stably transfected

into (a) MDA-MB-468, (b) MDA-MB-231, and (c) MCF7. Relative luciferase activity was measured after treating with synthetic ligands GW3965 (GW), GSK2033 (GSK), or PSSs at indicated concentrations for 16 h and is shown normalised to vehicle control (VC). Data are presented as mean of three independent replicates (open circles) with SEM. For assessing changes between individual concentrations and vehicle, one-way ANOVA with Holm-Sidak correction for multiple testing and post-test for linear trend was performed. Significance levels are indicated by $\epsilon = p < 0.05$ and $\# = p < 0.0001$, or for linear trend Slope, R2 and p value are indicated.

2.2. PSSs Impair Side-Chain Oxysterol Mediated Activation of LXRA

The effects of PSSs across all cell lines tested, combined with previous reports that PSSs are bona fide LXR ligands led us to hypothesize that in our cell lines at least, the role of PSSs could be to alter the response of LXR to other ligands rather than directly influence LXR. To test this, stable LXRA reporter cell lines were treated with individual oxysterols (24(s)-OHC, 25-OHC, (25*R*)26-OHC or 24(s),25-EC), at low (1 μ M) or high (10 μ M) concentrations alone, or paired with PSSs (STAN, SITO, CAMP, BRAS and STIG) at 10 μ M for 16 h.

The strong inducers of LXRA transcription being 24(s)-OHC and 24(s),25-EC (Figure 4) were in agreement with previous reports [9]. At low (1 μ M) dose, 24(s),25-EC driven activity was impaired equally by all PSSs, but to different magnitudes depending on the cell line. A 74–84% reduction in LXRA activity was observed in MDA-MB-468 cells ($p < 0.0001$ for all PSSs (Figure 4a)), 31–34% reduction in MDA-MB-231 cells ($p < 0.001$ for all PSSs (Figure 4b)) and 23–30% reduction in MCF7 cells ($p < 0.05$ for all PSSs except STAN where $p = 0.07$ (Figure 4c)). More variability was observed in the high (10 μ M) dose treatments. 10 μ M 24(s),25-EC elicited a stronger transcriptional response from LXRA compared to 1 μ M treatments, and differences in the abilities of the various PSSs to impair LXRA were now also evident. In MDA-MB-468 and MDA-MB-231 cell lines, SITO and STAN were more effective inhibitors than CAMP, BRAS and STIG (Figure 4a–c; Table S1). Interestingly, in MDA-MB-468 cells CAMP failed to repress 24-25-EC induced LXRA transcriptional activity ($p > 0.05$ (Figure 4a)), as did BRAS in MDA-MB-231 cells (Figure 4b). In MCF7 cells, repression of activation was similar irrespective of PSSs (Figure 4c).

At 1 μ M, 24(s)-OHC induced activity was similarly impaired by all PSSs (Figure 4). In MDA-MB-468 cells the PSSs suppressed by 62–68% ($p < 0.0001$ for all PSSs (Figure 4a)), by 24–48% in MDA-MB-231 cells ($p < 0.01$ for all PSSs except STAN where $p > 0.05$ (Figure 4b)), and by 30–42% in MCF7 cells ($p < 0.0001$ for all PSSs except SITO where $p > 0.05$ (Figure 4c)). Again, the higher dose, 10 μ M, elicited a stronger transcriptional response (3–4-fold stronger) LXRA compared to 1 μ M treatments. Differences in the ability of the PSSs to impair LXRA were again also evident at the higher dose

(10 μ M) experiment series. In both MDA-MB-468 and MDA-MB-231, SITO and STAN were more effective inhibitors (61–74%) than CAMP, BRASS or STIG (40–61%) which were statistically equivalent (Figure 4a–c; Table S1).

The weakest activators of LXRA were 25-OHC and (25*R*)26-OHC, eliciting maximum responses of 6- and 5-fold over vehicle control in the ER-negative lines respectively, and less than 2.5-fold activation in MCF7 cells. At the lower (1 μ M) dose 25-OHC, PSSs inhibited LXR by 54–83% in MDA-MB-468 ($p < 0.0001$ for all PSSs (Figure 4a), and by 40–48% in MDA-MB-231 ($p < 0.01$ for all PSSs (Figure 4b; Table S1)).

In MCF7 cells 25-OHC induced LXRA activity was only 1.8-fold above vehicle control, and this was almost entirely ablated by each PSS ($p < 0.01$ for all PSSs (Figure 4c)). Figure 4a shows that (25*R*)26-OHC failed to increase LXRA activity significantly in MCF7 cells. Unlike for the other oxysterols, 10 μ M 25-OHC did not increase LXRA activity relative to 1 μ M in MDA-MB-468 cells (Figure 4a) but did enhance LXRA activity in MDA-MB-231 (Figure 4b) and MCF7 (Figure 4c) cells. PSSs inhibited high dose 25-OHC driven LXR by 30–43% in MDA-MB-468 ($p < 0.001$ for all PSSs (Figure 4a; Table S1)). In MDA-MB-231 and MCF7 cells, SITO and STAN were stronger inhibitors (41–58%) than the other PSSs (0–36%) (Figure 4b,c; Table S1). (25*R*)26-OHC combined with the PSSs showed similar repression patterns as observed for 25-OHC. At the lower (1 μ M) dose in MDA-MB-468, all PSSs inhibited (25*R*)26-OHC induced activity ($p < 0.01$ for all PSSs (Figure 4a)), but SITO, CAMP BRAS and STIG failed to inhibit activation in either MDA-MB-231 or MCF7 cells (Figure 4b,c). SITO and STAN were highly effective at inhibiting high (10 μ M) dose (25*R*)26-OHC induced LXRA activity in MDA-MB-468 cells (Figure 4a), while in MDA-MB-231 cells inhibition was between 54–59% ($p < 0.0001$ for all PSSs (Figure 4b)) and in MCF7 with 10 μ M dose only BRAS and STIG failed to inhibit LXRA activity (Figure 4c).

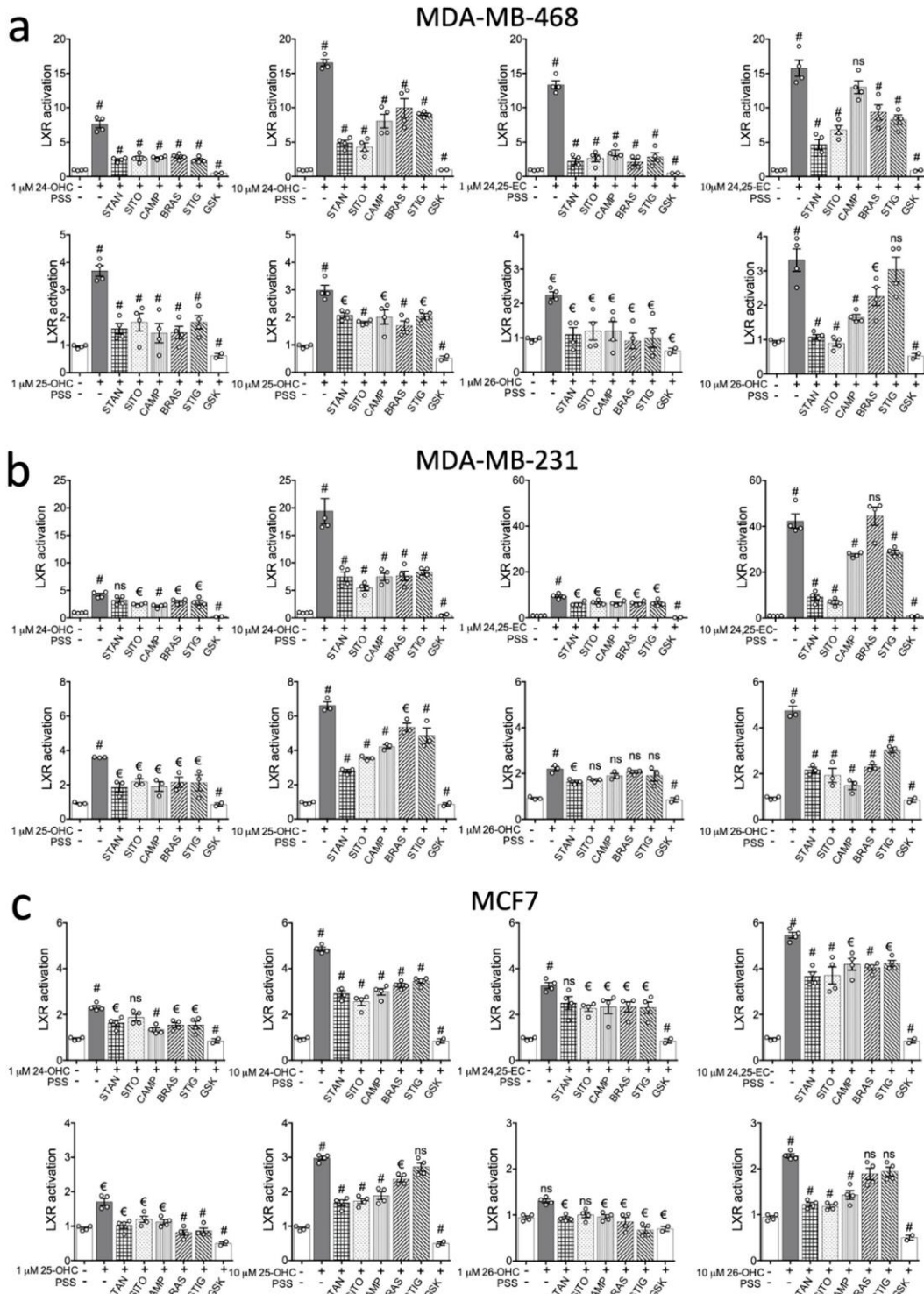


Figure 4. Phytosterols inhibit oxysterol driven LXR activation in breast cancer cells. Oxysterol-mediated LXR activity was measured in the presence of PSSs or synthetic LXR antagonist GSK2033. (a) MDA-MB-468 (b), MDA-MB-231 (c) and MCF7 LXR-luciferase reporter cell lines were treated with oxysterols alone or in combination with SITO, STAN, CAMP, BRASS, STIG (10 μ M) or GSK2033 (GSK; 1 μ M). Data show mean of four independent replicates (open circles) with SEM, except for GSK where mean and SEM of two independent replicates are shown. Significant induction by oxysterols relative to vehicle is indicated above the oxysterol columns. Significant repression of activation is indicated above the PSS columns. One-way ANOVA with Holm-Sidak correction for multiple testing was performed on for PSS co-treatments relative to oxysterol alone, or one-tailed *t*-test to compare GSK co-treatment with oxysterol alone. Significance levels are indicated by ϵ = p < 0.05 and # = p < 0.0001.

Interestingly, despite the PSSs having little to no effect alone (Figures 2 and 3), they significantly attenuated oxysterol mediated LXR activation. This was systematically observed across all three breast cancer cell lines for all the PSSs tested, but collectively our data indicated that SITO and STAN are more efficient inhibitors of oxysterol driven LXRA activity than the other PSSs assayed (Figure 5, Table S1). To formally assess this hypothesis, we established the percentage inhibitory activity (from 100% indicating the PSSs completely prevented oxysterol induced activity, to 0% where there was no significant difference in LXR activity between oxysterol and oxysterol plus PSSs treated cells) of each PSSs in combination with each oxysterol in each cell line. At low (1 μ M) dose oxysterol, there were no differences in the ability of the various PSSs to inhibit LXRA activation ($p > 0.05$ for all PSSs (Figure 5a; Table S1)), although, when considered together, PSSs were generally able to repress activation in MDA-MB-468 cells better than in MDA-MB-231 and MCF7 (Figure 5a). In the high (10 μ M) dose experiment series however, differences in the abilities of the PSSs to suppress oxysterol induced LXRA activity emerged. STAN and SITO emerged as the most potent inhibitors across all cell lines and all oxysterols (Figure 5b, Supplementary Table S1).

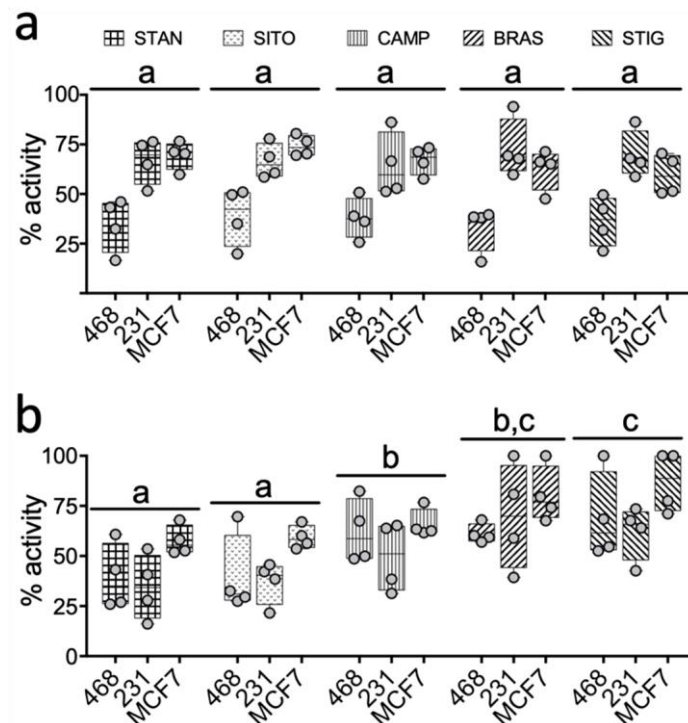


Figure 5. Inhibition of oxysterol induced LXR activity by PSS and cell lines. The percentage efficiency with which each PSS impairs activation of LXR by each oxysterol was calculated in each cell line for both low (1 μ M (a)) and high (10 μ M (b)) dose PSS treatment. Individual oxysterols are represented by circles with range and mean shown in box plots. Statistical differences in the abilities of different PSS to impair oxysterol mediated LXR activation are denoted by different letters (shared letters indicate no significant difference between PSS). Statistical significance was determined using two-way ANOVA.

2.3. STAN and SITO Inhibit Oxysterol Mediated Activation of the LXR Target Genes ABCA1 and APOE

Parental cell lines MDA-MB-468, MDA-MB-231 and MCF7 were treated with the endogenous agonists 24(*S*)-OHC or (25*R*)-26-OHC (10 μ M), or synthetic LXR ligand GW3965 (1 μ M) alone or in combination with SITO or STAN (10 μ M) for 16 h. As expected, ABCA1 was activated by both oxysterols and GW3965 in all three cell lines ($p < 0.0001$ in each cell line (Figure 6a–c)). In combination experiments, the induction of ABCA1 mRNA expression by both synthetic and the oxysterol ligands was impaired by SITO and STAN in MDA-MB-468, MDA-MB-231 and MCF7 cells ($p < 0.0001$ for all agonist:PSS pairings (Figure 6a–c)), with the exception of GW3965 in MCF7 ($p > 0.05$ (Figure 6c)).

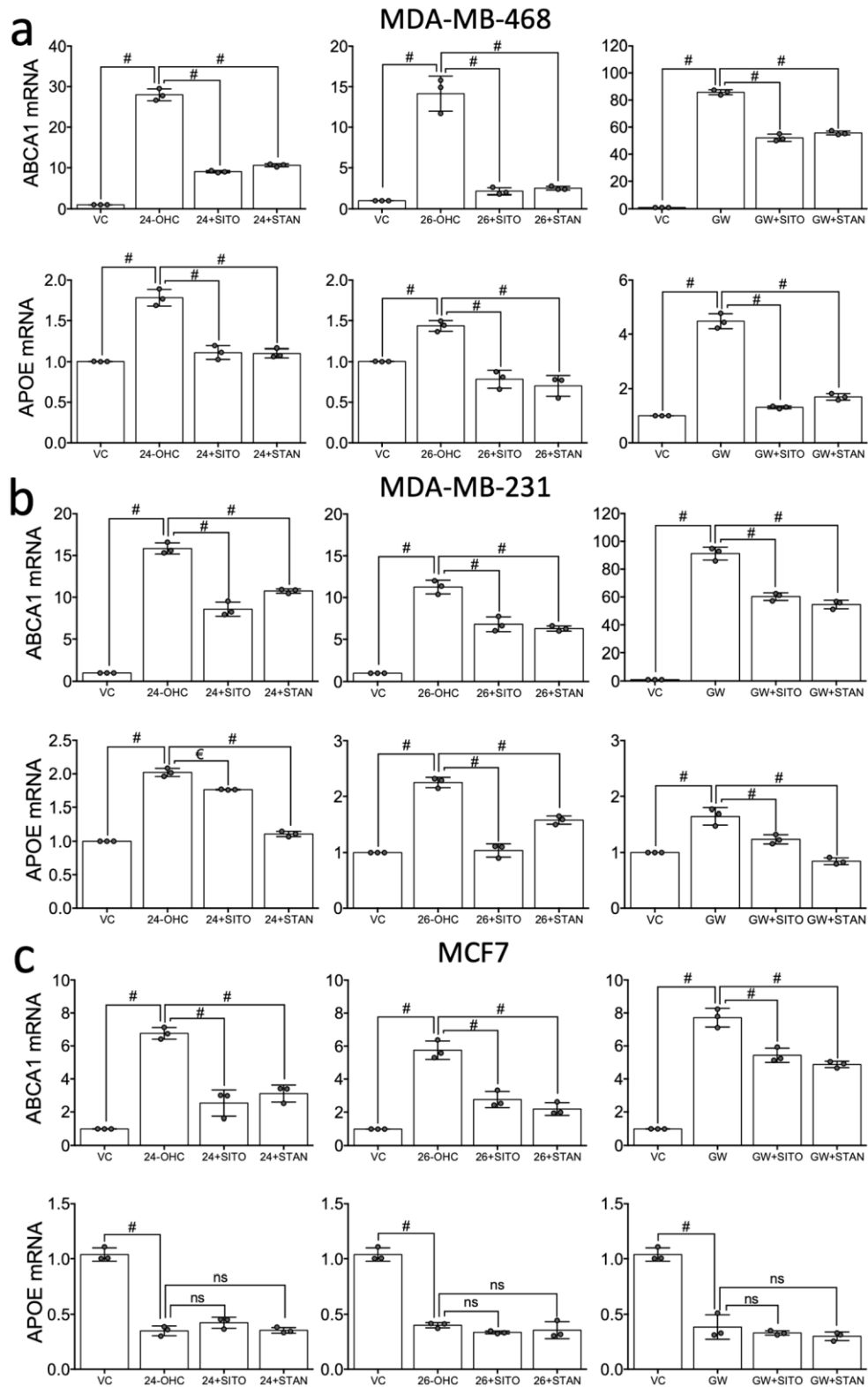


Figure 6. STAN and SITO suppress oxysterol mediated LXR expression of target genes. Hormone receptor negative (MDA-MB-468 (a) and MDA-MB-231 (b)) and positive (MCF7 (c)) cells were treated with LXR ligands (synthetic 1 μ M, oxysterol 10 μ M) for 16 h alone or in combination with SITO or STAN and expression of ABCA1 and APOE were assessed by Taqman assays ($\Delta\Delta$ Ct using HPRT and normalised to vehicle). Data shown are mean of three independent replicates (circles) with SEM. One-way ANOVA with Holm-Sidak correction for multiple testing was performed, significance is indicated by $\epsilon = p < 0.05$ and $\# = p < 0.0001$.

For APOE expression, results were similar to those observed for ABCA1 in MDA-MB-468 and MDA-MB-231, except the repression was more dramatic. For example, activation by any ligand in MDA-MB-468 cells was completely abrogated by either PSS (Figure 6a). In MDA-MB-231 cells this repression pattern was similar but not absolute (Figure 6b). In MCF7 cells, agonist-dependent inhibition of APOE expression was observed (as previously reported) and this was unaltered by co-treatment with either PSS (Figure 6c).

STAN and SITO alone did not elicit change in expression of either ABCA1 or APOE in MDA-MB-468 cells ($p > 0.05$ for all (Supplementary Figure S1a)). In MDA-MB-231 cells, however, both SITO and STAN induced ABCA1 and APOE ($p < 0.0001$ for all (Supplementary Figure S1b)). In MCF7 cells, ABCA1 was repressed by SITO ($p = 0.032$) but not by STAN, and APOE was significantly repressed by both PSSs ($p < 0.0001$ for both (Supplementary Figure S1c)). Collectively, these data suggest that small changes in LXR target genes are induced by PSS, but that there are cell line differences in responses. MDA-MB-468 are relatively resistant to PSSs mediated target gene changes, PSSs induce target gene expression in MDA-MB-231 and repress in MCF7.

3. Discussion

When humans consume PSSs, 0.04–5% is absorbed [19,33–35], but this depends on the chemistry of the specific PSS [19,35], the genetics of the individual, and any pathologies [19,34]. Although absorption efficiency is considered low when compared to dietary cholesterol, this belies the fact that PSSs circulate in concentrations far higher than many biologically active derivatives of cholesterol. Indeed, circulating concentrations of total PSSs may exceed 100 μM in some high intake individuals, and even in the general population, the mean concentration is likely to exceed 20 μM [36]. While this is some 50–200 times lower than cholesterol (4–5 mM), it is 5000–20,000 greater than typical 17 β -estradiol (1 nM), 20–100 times greater than Vitamin D (50 nM), and up to 1000-fold higher than most oxysterols. At physiological concentrations typical for high intake individuals and far below, we found PSSs have modest effects on LXR activity in BCa cell lines in culture. Although we did not measure levels of oxysterols or conversion of cholesterol to oxysterols in our cell culture systems, we note that there was little capacity for repression of basal LXR activity by PSS. In these breast cancer cell types however, LXR activity was strongly driven by oxysterols indicating a significant capacity for induction. It was only in this strongly ligand-activated state that PSSs could inhibit LXR mediated transcription. From our data, we concluded that classifying PSSs as LXR agonists or antagonists would be overly simplistic, and cell type and the presence of other ligands must be considered.

Instead, our data indicate phytosterols are, in regard to the BCa cell lines we evaluated and in the context of potent LXR agonists, competitive inhibitors. These data have implications for the development of novel LXR targeting drugs, as interaction with (a PSS rich) diet may alter the efficacy of LXR targeting. Controlling dietary intake and dietary recording during trials could help differentiate apparent responders and non-responders to LXR targeting compounds.

The extent to which PSSs inhibited oxysterol dependent LXR activity was dependent on the cell line and on the oxysterol with which they were co-incubated. The most efficient activators of LXR were 24(*s*),25-EC and 24(*s*)-OHC (in agreement with previous reports [9]), and SITO and STAN were the most efficient inhibitors of oxysterol-mediated LXR activation. SITO and STAN differ in molecular structure by just a single unsaturated bond in the B-ring (Figure 1b). As we observed such similar behaviour between SITO and STAN in terms of interfering with LXR transcription across all our assays and cell lines, saturation in the B-ring probably doesn't influence inhibition of LXR, and previous reports indicate that there is no difference between phytosterols and phytostanols in lowering circulating cholesterol [37]. Furthermore, STIG is identical to SITO except for an unsaturated bond between the 22nd and 23rd carbon in the side chain, and this difference appears sufficient to partially attenuate the ability of STIG to compete with oxysterols for LXR binding. An unsaturated bond such as this makes the side chain less flexible and allows for decreased rotational freedom but may also be more prone to oxidative or enzymatic attack. A series of synthetic STIG derivatives with modifications to either the 22nd or 23rd carbon led to several compounds able to selectively modulate LXR target genes; ABCA1 expression was strongly enhanced while other canonical targets such as FASN were unaltered [38]. In subsequent work addition of a hydroxyl group at C24 to stigmastane led to robust activation of ABCA1 and FASN [39]. Understanding selective modulation of LXR is a critical research gap as there are both disease-promoting and disease prevention components to the oxysterol-LXR signalling cascade.

PSSs are structurally and functionally related to oxysterols thus supporting at a biochemical and modelling level, the hypothesis they are selective LXR modulators rather than simple agonists or antagonists. Notably, Kaneko et al., demonstrated in a different cell type to those we assayed, HEK293 cells, that SITO, BRASS, CAMP and STIG at 10 μ M could activate LXR driven luciferase activity [21]. In contrast, SITO was unable to activate an LXR-luciferase reporter in CHO-7 cells [18]. The canonical LXR target gene ABCA1 was also shown to be increased by SITO, STAN and CAMP in Caco2 cell cultures [22], but Brauner et al., demonstrated in the same cell line that CAMP or SITO co-treatment attenuated cholesterol induced ABCA1 expression [20], supporting our conclusion that a biologically meaningful role for PSSs is most apparent

in fine-tuning or moderating LXR's response to ligand. Down-regulation of LXR target genes (NPC1L1, HMGCR, SR-BI and LDLR) occurs in HepG2 [23], and ABCG5/8 is reduced in Caco2 cells with 7-ketostigmasterol at 60 μ M [24]. In vivo, hamsters fed phytosterol diets show reduced expression of LXR targets ABCG5, microsomal triglyceride protein (MTP) and the esterification enzyme ACAT [25]. Mice fed high doses of STIG, which reached 7 mM in the lumen, had unaltered LXR transcription [40].

In silico docking of polyphenols to LXR has recently been reported [41], and the interactions described here would benefit from similar computational modelling, especially by assessing additional PSSs with more diverse biophysical properties (e.g., side chain branching, saturation and length) to yield information about the structural requirements of PSSs that allow them to inhibit LXR. At the physiological level, dietary PSS intervention in BCa patients with a time-resolved sampling of normal and tumour breast tissue would allow assessment of the molecular and cell biology changes initiated by PSSs. Longer term follow-ups of patients would help indicate if antagonism of LXR altered risk of disease relapse or whether ER-dependent tumour growth could be inhibited by chronic low-dose dietary changes or acute pharmacological intake of PSS.

The data on PSSs we report here indicate that dietary sterols may have differential effects on breast cancer pathophysiology. The stringent activation of LXR by oxysterols is inhibited by PSS, but whether this translates into a possible dietary suppression of human LXR-oxysterol signalling in tumour prone tissues such as the breast, or metastatic sites such as the bone, remains to be determined. This is a clinically important question as ER-negative disease remains more challenging to successfully treat than ER-positive disease and a role for oxysterol signalling in breast cancer progression is now apparent, despite no clear difference in oxysterol concentrations between subtypes [42]. Our data provide a potential molecular explanation as to why diets, lifestyles, and chronic pharmacological treatments, which are associated with cholesterol suppression, are also associated with improved outcomes. In our model, PSSs could limit the ability of oxysterols to drive LXR signalling, which is an important observation given (25R)26-OHC promotes ER-negative breast cancer metastasis in mouse models [11]. Further work that directly addresses how dietary PSSs accumulate in tumour prone tissues and metastatic sites, and their ability to enter and regulate immune cells is warranted following our observations.

4. Materials and Methods

4.1. Cell Culture and Cell Lines

MDA-MB-468, MDA-MB-231 (models of triple negative breast cancer), and MCF7 (model of luminal A breast cancer) cell lines were originally obtained from ATCC. All cells were routinely maintained at 37 °C with 5% CO₂ in a humidified incubator and cultured in Dulbecco's Modified Eagle Medium (DMEM, Thermo Fisher, Altrincham, UK, Cat: 31966047) supplemented with 10% fetal calf serum (FCS) (Thermo Fisher, Cat: 11560636). Routine passaging of cells was completed every 3–4 days and seeded at 1×10^6 live cells per T75 tissue culture treated flask (Nunc, Thermo Fisher, Cat:

10364131) to maintain confluence between 20% and 80%.

4.2. Drugs and Reagents

Drugs stocks were stored at –20 °C as follows: GSK2033 was provided by C. Cummins (University of Toronto, Canada) and then later purchase from ToCris (Bristol, UK, Cat: 5694) and stored at 20 mM diluted in ETOH, T0901317 (Cayman, Ann Arbor, USA, Cat: 71810) at 100 mM diluted in DMSO. Oxysterols were sourced from Avanti Polar Lipids: 24(s)-OHC (Cat: 700071), 25-OHC (Cat: 700019), (25*R*)26-OHC (Cat: 700021) and 24(s),25-EC (Cat: 700037). Stocks of 10 mM were prepared in nitrogen flushed ethanol to prevent auto-oxidation. The following phytosterols were provided by E. Trautwein (Unilever, Vlaardingen, The Netherlands) or later purchased from Avanti and stored in NFE at 5 or 20 mM stocks at –20 °C: β -sitosterol (Cat: 700095) (SITO), β -sitostanol (Cat: 700121) (STAN), campesterol (Cat: 700126) (CAMP), brassicasterol (Cat: 700122) (BRAS) or stigmasterol (Cat: 700062)

(STIG). Puromycin Hydrochloride (Santa Cruz, Cat: sc-108071) stocks diluted in water and stored as 25 mg/mL aliquots.

4.3. MTT Assays

Cells were seeded in 96 well plates at 2.5×10^4 cells/well and incubated for 16 h. Vehicle (ethanol) or PSSs with the range of concentration between 1 pM to 100 μ M was added for 48 h, media was removed, and cells were washed with PBS. Phenol red free DMEM with 10% FBS was added to each well along with MTT reagent (final concentration 0.5 mg/mL). After 4 h incubation at 37 °C, media was removed and replaced with 100 μ L of DMSO/well. Absorbance at 540 nm was read using a CLARIOstar.

4.4. Reporter Cell Lines and Luciferase Assays

This method has been published previously [32]. Briefly, 3×10^4 cells were plated in each well of a

24-well plate and incubated overnight. Signal Lentiviral particles (LXR α) were purchased from Qiagen (Manchester, UK, Cat: CLS-7041L) and transduced into the cells using 8 μ g/mL SureEntry transduction reagent at MOI at manufacturers recommendations. After 18h the particles were removed and fresh DMEM supplemented with 0.1 mM Non-Essential Amino Acids (Thermo Fisher, Cat: 12084947) and

100 U/mL penicillin and 100 μ g/mL streptomycin (Thermo Fisher, Cat: 10378016) were added to the cells. Cells were passaged and puromycin used to select successfully transduced cells. Reporter cell line insertion and response were validated previously [32]. For luciferase quantitation, 30,000 transfected cells/well were seeded into 24-well plates and allowed to attach under normal culture conditions for 8 h. Cultures were treated with ligands, inhibitors or vehicle control as indicated in figure legends for 16 h. Luciferase assays were carried out by transferring cell lysates to white-walled 96-well plates and luminescence was assessed using the Tecan Spark using autoinjectors.

4.5. mRNA Isolation, Reverse Transcription and qPCR

Cells were plated in 6 well plates (2.5×10^5 cells/well) and incubated overnight before treatment with vehicle (ethanol) or LXR ligands. mRNA analysis was performed as described previously [43,44]. Briefly, Promega ReliaprepTM RNA Cell Miniprep System was used for the RNA extraction (Promega, Southampton, UK, Cat: #Z6012), and product guidelines were followed using approximately 5×10^5 cells (allowing for doubling time). On column DNase 1 digestion was performed and RNA was eluted in 30 μ L water. Purified RNA was stored at -80 °C. The GoScriptTM Reverse Transcription kit (Promega, Cat: A5003) was used for the cDNA synthesis, and product guidelines followed using 500 ng total RNA/reaction and x random primers. The resulting cDNA was then diluted 1 in 5 in water and stored at -20 °C. Taqman Fast Advanced Mastermix (Thermo Fisher, Paisley, UK, Cat: 4444557) was used with Taqman assays (Thermo Fisher, Paisley, UK, Cat: 4331182) on a QuantStudio Flex 7 (Applied Biosystems Life Tech, Thermo Scientific) for gene expression experiments. Taqman assays (Hs02800695_m1-HPRT1, Hs01059137_m1-ABCA1, Hs00171168_m1-APOE) and Mastermix were stored at -20 °C. Gene expression was analysed using the $\Delta\Delta C_t$ method and normalised to the housekeeping gene HPRT1.

4.6. Statistical Analysis

All statistics and graph preparation were performed in Graph pad Prism version 6. One-way ANOVA with Holm-Sidak correction for multiple testing was used to determine differences between vehicle and individual concentrations of PSS in MTT

cell viability and LXR-Luciferase activation assays. A post-test was applied to test for a linear trend with increasing PSS concentration and Slope, R² and p value reported. For analysis of PSS repression of oxysterol induced LXR activity one-way ANOVA with Holm-Sidak correction for multiple testing was used and to compare effects of PSS across all cells and oxysterols two-way ANOVA was applied. For gene expression analysis one-way ANOVA was applied.

References

1. Bonsang-Kitzis, H.; Chaltier, L.; Belin, L.; Savignoni, A.; Rouzier, R.; Sablin, M.P.; Lerebours, F.; Bidard, F.C.; Cottu, P.; Sastre-Garau, X.; et al. Beyond Axillary Lymph Node Metastasis, BMI and Menopausal Status Are Prognostic Determinants for Triple-Negative Breast Cancer Treated by Neoadjuvant Chemotherapy. *PLoS ONE* **2015**, *10*, e0144359. [[CrossRef](#)]
2. Crispo, A.; Grimaldi, M.; D'Aiuto, M.; Rinaldo, M.; Capasso, I.; Amore, A.; D'Aiuto, G.; Giudice, A.; Ciliberto, G.; Montella, M. BMI and breast cancer prognosis benefit: Mammography screening reveals differences between normal weight and overweight women. *Breast* **2015**, *24*, 86–89. [[CrossRef](#)]
3. Dos Santos, C.R.; Fonseca, I.; Dias, S.; de Almeida, J.C.M. Plasma level of LDL-cholesterol at diagnosis is a predictor factor of breast tumor progression. *BMC Cancer* **2014**, *14*, 132.
4. Brennan, S.F.; Woodside, J.V.; Lunny, P.M.; Cardwell, C.R.; Cantwell, M.M. Dietary fat and breast cancer mortality: A systematic review and meta-analysis. *Crit. Rev. Food Sci. Nutr.* **2017**, *57*, 1999–2008. [[CrossRef](#)]
5. Chlebowski, R.T.; Blackburn, G.L.; Thomson, C.A.; Nixon, D.W.; Shapiro, A.; Hoy, M.K.; Goodman, M.T.; Giuliano, A.E.; Karanja, N.; McAndrew, P.; et al. Dietary fat reduction and breast cancer outcome: Interim efficacy results from the Women's Intervention Nutrition Study. *J. Natl. Cancer Inst.* **2006**, *98*, 1767–1776. [[CrossRef](#)]
6. Manthravadi, S.; Shrestha, A.; Madhusudhana, S. Impact of statin use on cancer recurrence and mortality in breast cancer: A systematic review and meta-analysis. *Int. J. Cancer* **2016**, *139*, 1281–1288. [[CrossRef](#)]
7. Liu, B.; Yi, Z.; Guan, X.; Zeng, Y.X.; Ma, F. The relationship between statins and breast cancer prognosis varies by statin type and exposure time: A meta-analysis. *Breast Cancer Res. Treat.* **2017**, *164*, 1–11. [[CrossRef](#)]
8. Janowski, B.A.; Willy, P.J.; Devi, T.R.; Falck, J.R.; Mangelsdorf, D.J. An oxysterol signalling pathway mediated by the nuclear receptor LXR alpha. *Nature* **1996**, *383*, 728–731. [[CrossRef](#)]
9. Janowski, B.A.; Grogan, M.J.; Jones, S.A.; Wisely, G.B.; Kliewer, S.A.; Corey, E.J.; Mangelsdorf, D.J. Structural requirements of ligands for the oxysterol liver X receptors LXRalpha and LXRbeta. *Proc. Natl. Acad. Sci. USA* **1999**, *96*, 266–271. [[CrossRef](#)]
10. Nelson, E.R.; Wardell, S.E.; Jasper, J.S.; Park, S.; Suchindran, S.; Howe, M.K.; Carver, N.J.; Pillai, R.V.; Sullivan, P.M.; Sondhi, V.; et al. 27-Hydroxycholesterol links hypercholesterolemia and breast cancer pathophysiology. *Science* **2013**, *342*, 1094–1098. [[CrossRef](#)]
11. Baek, A.E.; Yu, Y.R.A.; He, S.S.; Wardell, S.E.; Chang, C.Y.; Kwon, S.; Pillai, R.V.; McDowell, H.B.; Thompson, J.W.; Dubois, L.G.; et al. The cholesterol metabolite 27 hydroxycholesterol facilitates breast cancer metastasis through its actions on immune cells. *Nat. Commun.* **2017**, *8*, 864. [[CrossRef](#)]
12. Wu, Q.; Ishikawa, T.; Sirianni, R.; Tang, H.; McDonald, J.G.; Yuhanna, I.S.; Thompson, B.; Girard, L.; Mineo, C.; Brekken, R.A.; et al. 27-Hydroxycholesterol Promotes Cell-Autonomous, ER-Positive Breast Cancer Growth. *Cell Rep.* **2013**, *5*, 637–645. [[CrossRef](#)]
13. Dalenc, F.; Iuliano, L.; Filleron, T.; Zerbinati, C.; Voisin, M.; Arellano, C.; Chatelut, E.; Marquet, P.; Samadi, M.; Roche, H.; et al. Circulating oxysterol metabolites as potential new surrogate markers in patients with hormone receptor-positive breast cancer: Results of the OXYTAM study. *J. Steroid Biochem. Mol. Biol.* **2016**, *169*, 210–218. [[CrossRef](#)]

14. Moreau, R.A.; Nystrom, L.; Whitaker, B.D.; Winkler-Moser, J.K.; Baer, D.J.; Gebauer, S.K.; Hicks, K.B. Phytosterols and their derivatives: Structural diversity, distribution, metabolism, analysis, and health-promoting uses. *Prog. Lipid Res.* **2018**, *70*, 35–61. [[CrossRef](#)]
15. Pollak, O.J.; Kritchevsky, D. Sitosterol. *Monogr. Atheroscl.* **1981**, *10*, 1–219.
16. Olkkonen, V.M.; Gylling, H.; Ikonen, E. Plant sterols, cholesterol precursors and oxysterols: Minute concentrations-Major physiological effects. *J. Steroid Biochem. Mol. Biol.* **2017**, *169*, 4–9. [[CrossRef](#)]
17. Fakih, O.; Sanver, D.; Kane, D.; Thorne, J.L. Exploring the biophysical properties of phytosterols in the plasma membrane for novel cancer prevention strategies. *Biochimie* **2018**, *153*, 150–161. [[CrossRef](#)]
18. Yang, C.; Yu, L.; Li, W.; Xu, F.; Cohen, J.C.; Hobbs, H.H. Disruption of cholesterol homeostasis by plant sterols. *J. Clin. Investig.* **2004**, *114*, 813–822. [[CrossRef](#)]
19. Lutjohann, D.; Bjorkhem, I.; Beil, U.F.; von Bergmann, K. Sterol absorption and sterol balance in phytosterolemia evaluated by deuterium-labeled sterols: Effect of sitostanol treatment. *J. Lipid Res.* **1995**, *36*, 1763–1773.
20. Brauner, R.; Johannes, C.; Ploessl, F.; Bracher, F.; Lorenz, R.L. Phytosterols reduce cholesterol absorption by inhibition of 27-hydroxycholesterol generation, liver X receptor alpha activation, and expression of the basolateral sterol exporter ATP-binding cassette A1 in Caco-2 enterocytes. *J. Nutr.* **2012**, *142*, 981–989. [[CrossRef](#)]
21. Kaneko, E.; Matsuda, M.; Yamada, Y.; Tachibana, Y.; Shimomura, I.; Makishima, M. Induction of intestinal ATP-binding cassette transporters by a phytosterol-derived liver X receptor agonist. *J. Biol. Chem.* **2003**, *278*, 36091–36098. [[CrossRef](#)]
22. Plat, J.; Nichols, J.A.; Mensink, R.P. Plant sterols and stanols: Effects on mixed micellar composition and LXR (target gene) activation. *J. Lipid Res.* **2005**, *46*, 2468–2476. [[CrossRef](#)]
23. Park, Y.; Carr, T.P. Unsaturated fatty acids and phytosterols regulate cholesterol transporter genes in Caco-2 and HepG2 cell lines. *Nutr. Res.* **2013**, *33*, 154–161. [[CrossRef](#)]
24. Alemany, L.; Laparra, J.M.; Barbera, R.; Alegria, A. Relative expression of cholesterol transport-related proteins and inflammation markers through the induction of 7-ketosterol-mediated stress in Caco-2 cells. *Food Chem. Toxicol.* **2013**, *56*, 247–253. [[CrossRef](#)]
25. Liang, Y.T.; Wong, W.T.; Guan, L.; Tian, X.Y.; Ma, K.Y.; Huang, Y.; Chen, Z.Y. Effect of phytosterols and their oxidation products on lipoprotein profiles and vascular function in hamster fed a high cholesterol diet. *Atherosclerosis* **2011**, *219*, 124–133. [[CrossRef](#)]
26. Awad, A.B.; Williams, H.; Fink, C.S. Effect of phytosterols on cholesterol metabolism and MAP kinase in MDA-MB-231 human breast cancer cells. *J. Nutr. Biochem.* **2003**, *14*, 111–119. [[CrossRef](#)]
27. Awad, A.B.; Williams, H.; Fink, C.S. Phytosterols reduce in vitro metastatic ability of MDA-MB-231 human breast cancer cells. *Nutr. Cancer* **2001**, *40*, 157–164. [[CrossRef](#)]
28. Awad, A.B.; Fink, C.S.; Williams, H.; Kim, U. In vitro and in vivo (SCID mice) effects of phytosterols on the growth and dissemination of human prostate cancer PC-3 cells. *Eur. J. Cancer Prev.* **2001**, *10*, 507–513. [[CrossRef](#)]
29. Link, L.B.; Canchola, A.J.; Bernstein, L.; Clarke, C.A.; Stram, D.O.; Ursin, G.; Horn-Ross, P.L. Dietary patterns and breast cancer risk in the California Teachers Study cohort. *Am. J. Clin. Nutr.* **2013**, *98*, 1524–1532. [[CrossRef](#)]
30. Weigl, J.; Hauner, H.; Hauner, D. Can Nutrition Lower the Risk of Recurrence in Breast Cancer? *Breast Care* **2018**, *13*, 86–91.
31. Blackburn, G.L.; Wang, K.A. Dietary fat reduction and breast cancer outcome: Results from the Women's Intervention Nutrition Study (WINS). *Am. J. Clin. Nutr.* **2007**, *86*, s878–s881. [[CrossRef](#)]
32. Hutchinson, S.; Thorne, J.L. *Lipid-Activated Nuclear Receptors*, 1st ed.; Springer: New York, NY, USA, 2019.
33. Salen, G.; Ahrens, E.H., Jr.; Grundy, S.M. Metabolism of beta-sitosterol in man. *J. Clin. Investig.* **1970**, *49*, 952–967. [[CrossRef](#)]
34. Salen, G.; Tint, G.S.; Shefer, S.; Shore, V.; Nguyen, L. Increased sitosterol absorption is offset by rapid elimination to prevent accumulation in heterozygotes with sitosterolemia. *Arterioscl. Thromb.* **1992**, *12*, 563–568. [[CrossRef](#)]
35. Shahzad, N.; Khan, W.; Md, S.; Ali, A.; Saluja, S.S.; Sharma, S.; Al-Allaf, F.A.; Abduljaleel, Z.; Ibrahim, I.A.A.;

- Abdel-Wahab, A.F.; et al. Phytosterols as a natural anticancer agent: Current status and future perspective. *Biomed. Pharmacother.* **2017**, *88*, 786–794. [[CrossRef](#)]
36. Stiles, A.R.; Kozlitina, J.; Thompson, B.M.; McDonald, J.G.; King, K.S.; Russell, D.W. Genetic, anatomic, and clinical determinants of human serum sterol and vitamin D levels. *Proc. Natl. Acad. Sci. USA* **2014**, *111*, E4006–E4014. [[CrossRef](#)]
 37. Ras, R.T.; Geleijnse, J.M.; Trautwein, E.A. LDL-cholesterol-lowering effect of plant sterols and stanols across different dose ranges: A meta-analysis of randomised controlled studies. *Br. J. Nutr.* **2014**, *112*, 214–219. [[CrossRef](#)]
 38. Marinozzi, M.; Castro Navas, F.F.; Maggioni, D.; Carosati, E.; Bocci, G.; Carloncelli, M.; Giorgi, G.; Cruciani, G.; Fontana, R.; Russo, V. Side-Chain Modified Ergosterol and Stigmasterol Derivatives as Liver X Receptor Agonists. *J. Med. Chem.* **2017**, *60*, 6548–6562. [[CrossRef](#)]
 39. Navas, F.F.C.; Giorgi, G.; Maggioni, D.; Pacciarini, M.; Russo, V.; Marinozzi, M. C24-hydroxylated stigmasterol derivatives as Liver X Receptor agonists. *Chem. Phys. Lipids* **2018**, *212*, 44–50. [[CrossRef](#)]
 40. Lifsey, H.C. The Impact of Bioactive Phytosterol, Stigmasterol, on Cholesterol Elimination Pathways in Mice. Master's Thesis, University of Kentucky, Lexington, Kentucky, 2018.
 41. Fouache, A.; Zabaïou, N.; De Jousineau, C.; Morel, L.; Silvente-Poirot, S.; Namsi, A.; Lizard, G.; Poirot, M.; Makishima, M.; Baron, S.; et al. Flavonoids differentially modulate liver X receptor activity-Structure-function relationship analysis. *J. Steroid Biochem. Mol. Biol.* **2019**, *190*, 173–182. [[CrossRef](#)]
 42. Solheim, S.; Hutchinson, S.A.; Lundanes, E.; Wilson, S.R.; Thorne, J.L.; Roberg-Larsen, H. Fast liquid chromatography-mass spectrometry reveals side chain oxysterol heterogeneity in breast cancer tumour samples. *J. Steroid Biochem. Mol. Biol.* **2019**. [[CrossRef](#)]
 43. Thorne, J.L.; Battaglia, S.; Baxter, D.E.; Hayes, J.L.; Hutchinson, S.A.; Jana, S.; Millican-Slater, R.A.; Smith, L.; Teske, M.C.; Wastall, L.M.; et al. MiR-19b non-canonical binding is directed by HuR and confers chemosensitivity through regulation of P-glycoprotein in breast cancer. *Biochim. Biophys. Acta* **2018**, *1861*, 996–1006. [[CrossRef](#)]
 44. Kim, B.; Stephen, S.; Hanby, A.; Horgan, K.; Perry, S.; Richardson, J.; Roundhill, E.; Valleley, E.; Verghese, E.; Williams, B.; et al. Chemotherapy induces Notch1-dependent MRP1 up-regulation, inhibition of which sensitizes breast cancer cells to chemotherapy. *BMC Cancer* **2015**, *15*, 634. [[CrossRef](#)]



© 2019 by the authors. Licensee MDPI, Basel, Switzerland. This article is an open access article distributed under the terms and conditions of the Creative Commons Attribution (CC BY) license (<http://creativecommons.org/licenses/by/4.0/>).

List of References

1. Organization., W.H. *Breast Cancer: prevention and control*. 2017; Available from: <http://www.who.int/cancer/detection/breastcancer/en/index2.html>.
2. Siegel, R.L., K.D. Miller, and A. Jemal, *Cancer statistics, 2015*. CA Cancer J Clin, 2015. **65**(1): p. 5-29.
3. Bonsang-Kitzis, H., et al., *Beyond Axillary Lymph Node Metastasis, BMI and Menopausal Status Are Prognostic Determinants for Triple-Negative Breast Cancer Treated by Neoadjuvant Chemotherapy*. PLoS One, 2015. **10**(12): p. e0144359.
4. Crispo, A., et al., *BMI and breast cancer prognosis benefit: mammography screening reveals differences between normal weight and overweight women*. Breast, 2015. **24**(1): p. 86-9.
5. dos Santos, C.R., et al., *Plasma level of LDL-cholesterol at diagnosis is a predictor factor of breast tumor progression*. BMC Cancer, 2014. **14**.
6. Brennan, S.F., et al., *Dietary fat and breast cancer mortality: A systematic review and meta-analysis*. Crit Rev Food Sci Nutr, 2017. **57**(10): p. 1999-2008.
7. Jemal, A., et al., *Cancer statistics, 2009*. CA Cancer J Clin, 2009. **59**(4): p. 225-49.
8. La Vecchia, C., et al., *Cancer mortality in Europe, 2000-2004, and an overview of trends since 1975*. Ann Oncol, 2010. **21**(6): p. 1323-60.
9. Miller, K.D., et al., *Cancer treatment and survivorship statistics, 2016*. CA Cancer J Clin, 2016. **66**(4): p. 271-89.
10. American College of Surgeons, C.o.C., *National Cancer Database, 2013 Data Submission*. 2015, Chicago, IL: American College of Surgeons.
11. Pusztai, L., et al., *Molecular classification of breast cancer: limitations and potential*. Oncologist, 2006. **11**(8): p. 868-77.
12. Herschkowitz, J.I., et al., *Identification of conserved gene expression features between murine mammary carcinoma models and human breast tumors*. Genome Biol, 2007. **8**(5): p. R76.
13. Prat, A., et al., *Phenotypic and molecular characterization of the claudin-low intrinsic subtype of breast cancer*. Breast Cancer Res, 2010. **12**(5): p. R68.
14. Deroo, B.J. and K.S. Korach, *Estrogen receptors and human disease*. J Clin Invest, 2006. **116**(3): p. 561-70.
15. Voduc, K.D., et al., *Breast cancer subtypes and the risk of local and regional relapse*. J Clin Oncol, 2010. **28**(10): p. 1684-91.
16. Timmerman, L.A., et al., *Glutamine sensitivity analysis identifies the xCT antiporter as a common triple-negative breast tumor therapeutic target*. Cancer Cell, 2013. **24**(4): p. 450-65.
17. Kaplan, H.G. and J.A. Malmgren, *Impact of triple negative phenotype on breast cancer prognosis*. Breast J, 2008. **14**(5): p. 456-63.
18. Albergaria, A., et al., *Nottingham Prognostic Index in triple-negative breast cancer: a reliable prognostic tool?* BMC Cancer, 2011. **11**: p. 299.
19. Howlander, N., et al., *US incidence of breast cancer subtypes defined by joint hormone receptor and HER2 status*. J Natl Cancer Inst, 2014. **106**(5).
20. Liedtke, C., et al., *Response to neoadjuvant therapy and long-term survival in patients with triple-negative breast cancer*. J Clin Oncol, 2008. **26**(8): p. 1275-81.
21. Baek, A.E., et al., *The cholesterol metabolite 27 hydroxycholesterol facilitates breast cancer metastasis through its actions on immune cells*. Nat Commun, 2017. **8**(1): p. 864.

22. Jordan, V.C., *Tamoxifen for breast cancer prevention*. Proc Soc Exp Biol Med, 1995. **208**(2): p. 144-9.
23. Chen, P., et al., *Tamoxifen-induced endometrial cancer*. Eur J Gynaecol Oncol, 2003. **24**(2): p. 135-7.
24. Klijn, J.G., et al., *Combined tamoxifen and luteinizing hormone-releasing hormone (LHRH) agonist versus LHRH agonist alone in premenopausal advanced breast cancer: a meta-analysis of four randomized trials*. J Clin Oncol, 2001. **19**(2): p. 343-53.
25. Curigliano, G., et al., *Cardiovascular toxicity induced by chemotherapy, targeted agents and radiotherapy: ESMO Clinical Practice Guidelines*. Ann Oncol, 2012. **23 Suppl 7**: p. vii155-66.
26. Network, N.C.I., *Chemotherapy, Radiotherapy and Surgical Tumour Resections in England: 2013-2014 (V2)*
- C.R. UK, Editor. 2018, Public Health England: <http://www.ncin.org.uk/publications/reports/>.
27. Cancer Genome Atlas, N., *Comprehensive molecular portraits of human breast tumours*. Nature, 2012. **490**(7418): p. 61-70.
28. Eccles, S.A., et al., *Critical research gaps and translational priorities for the successful prevention and treatment of breast cancer*. Breast Cancer Res, 2013. **15**(5): p. R92.
29. Borugian, M.J., et al., *Waist-to-hip ratio and breast cancer mortality*. Am J Epidemiol, 2003. **158**(10): p. 963-8.
30. Anderson, G.L., et al., *Implementation of the Women's Health Initiative study design*. Ann Epidemiol, 2003. **13**(9 Suppl): p. S5-17.
31. Bianchini, F., R. Kaaks, and H. Vainio, *Overweight, obesity, and cancer risk*. Lancet Oncol, 2002. **3**(9): p. 565-74.
32. Cowey, S. and R.W. Hardy, *The metabolic syndrome: A high-risk state for cancer?* Am J Pathol, 2006. **169**(5): p. 1505-22.
33. Llaverias, G., et al., *Role of cholesterol in the development and progression of breast cancer*. Am J Pathol, 2011. **178**(1): p. 402-12.
34. McMillan, D.C., N. Sattar, and C.S. McArdle, *ABC of obesity. Obesity and cancer*. BMJ, 2006. **333**(7578): p. 1109-11.
35. Lee, I.M., *Physical activity and cancer prevention--data from epidemiologic studies*. Med Sci Sports Exerc, 2003. **35**(11): p. 1823-7.
36. Polyak, K., *Pregnancy and breast cancer: the other side of the coin*. Cancer Cell, 2006. **9**(3): p. 151-3.
37. Research, W.C.R.F.I.A.I.f.C. *Continuous Update Project Report: Diet, Nutrition, Physical Activity and Cancer*. 2017; Available from: wcrf.org/breast-cancer-2017.
38. Boyd, N.F., et al., *Mammographic densities as a marker of human breast cancer risk and their use in chemoprevention*. Curr Oncol Rep, 2001. **3**(4): p. 314-21.
39. Greendale, G.A., et al., *Postmenopausal hormone therapy and change in mammographic density*. J Natl Cancer Inst, 2003. **95**(1): p. 30-7.
40. Stuedal, A., et al., *Postmenopausal hormone therapy with estradiol and norethisterone acetate and mammographic density: findings from a cross-sectional study among Norwegian women*. Climacteric, 2009. **12**(3): p. 248-58.
41. Cuzick, J., et al., *Tamoxifen-induced reduction in mammographic density and breast cancer risk reduction: a nested case-control study*. J Natl Cancer Inst, 2011. **103**(9): p. 744-52.
42. Barbone, F., et al., *Socioeconomic status, migration and the risk of breast cancer in Italy*. Int J Epidemiol, 1996. **25**(3): p. 479-87.
43. Buell, P., *Changing incidence of breast cancer in Japanese-American women*. J Natl Cancer Inst, 1973. **51**(5): p. 1479-83.

44. McPherson, K., C.M. Steel, and J.M. Dixon, *ABC of breast diseases. Breast cancer-epidemiology, risk factors, and genetics*. *BMJ*, 2000. **321**(7261): p. 624-8.
45. Stellman, S.D. and Q.S. Wang, *Cancer mortality in Chinese immigrants to New York City. Comparison with Chinese in Tianjin and with United States-born whites*. *Cancer*, 1994. **73**(4): p. 1270-5.
46. Liu, B., et al., *The relationship between statins and breast cancer prognosis varies by statin type and exposure time: a meta-analysis*. *Breast Cancer Res Treat*, 2017. **164**(1): p. 1-11.
47. Manthravadi, S., A. Shrestha, and S. Madhusudhana, *Impact of statin use on cancer recurrence and mortality in breast cancer: A systematic review and meta-analysis*. *Int J Cancer*, 2016. **139**(6): p. 1281-8.
48. Chlebowski, R.T., et al., *Dietary fat reduction and breast cancer outcome: interim efficacy results from the Women's Intervention Nutrition Study*. *J Natl Cancer Inst*, 2006. **98**(24): p. 1767-76.
49. Nindrea, R.D., T. Aryandono, and L. Lazuardi, *Breast Cancer Risk From Modifiable and Non-Modifiable Risk Factors among Women in Southeast Asia: A Meta-Analysis*. *Asian Pac J Cancer Prev*, 2017. **18**(12): p. 3201-3206.
50. Organisation, W.H., *Diet, nutrition and the prevention of chronic diseases*. *World Health Organ Tech Rep Ser*, 2003. **916**: p. i-viii, 1-149, backcover.
51. Gallagher, E.J., et al., *Elevated tumor LDLR expression accelerates LDL cholesterol-mediated breast cancer growth in mouse models of hyperlipidemia*. *Oncogene*, 2017. **36**(46): p. 6462-6471.
52. Eccles, S.A. and L. Paon, *Breast cancer metastasis: when, where, how?* *Lancet*, 2005. **365**(9464): p. 1006-7.
53. Ovcaricek, T., et al., *Triple negative breast cancer - prognostic factors and survival*. *Radiol Oncol*, 2011. **45**(1): p. 46-52.
54. Kauvar, L.M., et al., *Glutathione based approaches to improving cancer treatment*. *Chem Biol Interact*, 1998. **111-112**: p. 225-38.
55. Riddick, D.S., et al., *Cancer chemotherapy and drug metabolism*. *Drug Metab Dispos*, 2005. **33**(8): p. 1083-96.
56. Guchelaar, H.J., et al., *Apoptosis: molecular mechanisms and implications for cancer chemotherapy*. *Pharm World Sci*, 1997. **19**(3): p. 119-25.
57. Pogoda, K., et al., *Analysis of pattern, time and risk factors influencing recurrence in triple-negative breast cancer patients*. *Med Oncol*, 2013. **30**(1): p. 388.
58. Parise, C.A. and V. Caggiano, *Breast Cancer Survival Defined by the ER/PR/HER2 Subtypes and a Surrogate Classification according to Tumor Grade and Immunohistochemical Biomarkers*. *J Cancer Epidemiol*, 2014. **2014**: p. 469251.
59. Pal, S., et al., *The treatment and survival of patients with triple negative breast cancer in a London population*. Springerplus, 2014. **3**: p. 553.
60. Housman, G., et al., *Drug resistance in cancer: an overview*. *Cancers (Basel)*, 2014. **6**(3): p. 1769-92.
61. Chang, A., *Chemotherapy, chemoresistance and the changing treatment landscape for NSCLC*. *Lung Cancer*, 2011. **71**(1): p. 3-10.
62. Martinez-Outschoorn, U.E., et al., *Ketones and lactate increase cancer cell "stemness," driving recurrence, metastasis and poor clinical outcome in breast cancer: achieving personalized medicine via Metabolo-Genomics*. *Cell Cycle*, 2011. **10**(8): p. 1271-86.
63. Pontiggia, O., et al., *The tumor microenvironment modulates tamoxifen resistance in breast cancer: a role for soluble stromal factors and fibronectin through beta1 integrin*. *Breast Cancer Res Treat*, 2012. **133**(2): p. 459-71.
64. Strouse, J.J., et al., *Fluorescent substrates for flow cytometric evaluation of efflux inhibition in ABCB1, ABCC1, and ABCG2 transporters*. *Anal Biochem*, 2013. **437**(1): p. 77-87.

65. Tamehiro, N., et al., *Riccardin C: a natural product that functions as a liver X receptor (LXR)alpha agonist and an LXRBeta antagonist*. FEBS Lett, 2005. **579**(24): p. 5299-304.
66. Kaneko, E., et al., *Induction of intestinal ATP-binding cassette transporters by a phytosterol-derived liver X receptor agonist*. J Biol Chem, 2003. **278**(38): p. 36091-8.
67. Torra, I.P., et al., *Phosphorylation of liver X receptor alpha selectively regulates target gene expression in macrophages*. Mol Cell Biol, 2008. **28**(8): p. 2626-36.
68. Long, M.D., et al., *Cooperative behavior of the nuclear receptor superfamily and its deregulation in prostate cancer*. Carcinogenesis, 2014. **35**(2): p. 262-71.
69. Janowski, B.A., et al., *An oxysterol signalling pathway mediated by the nuclear receptor LXR alpha*. Nature, 1996. **383**(6602): p. 728-31.
70. Apfel, R., et al., *A novel orphan receptor specific for a subset of thyroid hormone-responsive elements and its interaction with the retinoid/thyroid hormone receptor subfamily*. Mol Cell Biol, 1994. **14**(10): p. 7025-35.
71. Shinar, D.M., et al., *NER, a new member of the gene family encoding the human steroid hormone nuclear receptor*. Gene, 1994. **147**(2): p. 273-6.
72. Song, C., et al., *Ubiquitous receptor: a receptor that modulates gene activation by retinoic acid and thyroid hormone receptors*. Proc Natl Acad Sci U S A, 1994. **91**(23): p. 10809-13.
73. Willy, P.J., et al., *LXR, a nuclear receptor that defines a distinct retinoid response pathway*. Genes Dev, 1995. **9**(9): p. 1033-45.
74. Annalora, A.J., C.B. Marcus, and P.L. Iversen, *Alternative Splicing in the Nuclear Receptor Superfamily Expands Gene Function to Refine Endo-Xenobiotic Metabolism*. Drug Metab Dispos, 2020. **48**(4): p. 272-287.
75. Fan, X., et al., *Expression of liver X receptor beta is essential for formation of superficial cortical layers and migration of later-born neurons*. Proc Natl Acad Sci U S A, 2008. **105**(36): p. 13445-50.
76. Chen, M., S. Beaven, and P. Tontonoz, *Identification and characterization of two alternatively spliced transcript variants of human liver X receptor alpha*. J Lipid Res, 2005. **46**(12): p. 2570-9.
77. Fradera, X., et al., *X-ray structures of the LXRAalpha LBD in its homodimeric form and implications for heterodimer signaling*. J Mol Biol, 2010. **399**(1): p. 120-32.
78. Farnegardh, M., et al., *The three-dimensional structure of the liver X receptor beta reveals a flexible ligand-binding pocket that can accommodate fundamentally different ligands*. J Biol Chem, 2003. **278**(40): p. 38821-8.
79. Thorne, J.L. and M.J. Campbell, *Nuclear receptors and the Warburg effect in cancer*. Int J Cancer, 2015. **137**(7): p. 1519-27.
80. Komati, R., et al., *Ligands of Therapeutic Utility for the Liver X Receptors*. Molecules, 2017. **22**(1).
81. Wu, C., et al., *Modulation of Macrophage Gene Expression via Liver X Receptor alpha Serine 198 Phosphorylation*. Mol Cell Biol, 2015. **35**(11): p. 2024-34.
82. Horlein, A.J., et al., *Ligand-independent repression by the thyroid hormone receptor mediated by a nuclear receptor co-repressor*. Nature, 1995. **377**(6548): p. 397-404.
83. Chen, J.D. and R.M. Evans, *A transcriptional co-repressor that interacts with nuclear hormone receptors*. Nature, 1995. **377**(6548): p. 454-7.
84. Fernandes, I., et al., *Ligand-dependent nuclear receptor corepressor LCoR functions by histone deacetylase-dependent and -independent mechanisms*. Mol Cell, 2003. **11**(1): p. 139-50.
85. Lazar, M.A., *Nuclear receptor corepressors*. Nucl Recept Signal, 2003. **1**: p. e001.

86. Wurtz, J.M., et al., *A canonical structure for the ligand-binding domain of nuclear receptors*. Nat Struct Biol, 1996. **3**(2): p. 206.
87. Zhang, J., X. Hu, and M.A. Lazar, *A novel role for helix 12 of retinoid X receptor in regulating repression*. Mol Cell Biol, 1999. **19**(9): p. 6448-57.
88. Schulman, I.G., et al., *The phantom ligand effect: allosteric control of transcription by the retinoid X receptor*. Genes Dev, 1997. **11**(3): p. 299-308.
89. Gurnell, M., et al., *A dominant-negative peroxisome proliferator-activated receptor gamma (PPARgamma) mutant is a constitutive repressor and inhibits PPARgamma-mediated adipogenesis*. J Biol Chem, 2000. **275**(8): p. 5754-9.
90. Wagner, M., et al., *NCOA3 is a selective co-activator of estrogen receptor α -mediated transactivation of PLAC1 in MCF-7 breast cancer cells*. BMC Cancer, 2013. **13**: p. 570.
91. Qin, L., et al., *The steroid receptor coactivator-1 regulates twist expression and promotes breast cancer metastasis*. Cancer Res, 2009. **69**(9): p. 3819-27.
92. Qin, L., et al., *Steroid receptor coactivator-1 upregulates integrin alpha(5) expression to promote breast cancer cell adhesion and migration*. Cancer Res, 2011. **71**(5): p. 1742-51.
93. Motamed, M., et al., *Steroid receptor coactivator 1 is an integrator of glucose and NAD⁺/NADH homeostasis*. Mol Endocrinol, 2014. **28**(3): p. 395-405.
94. Battaglia, S., et al., *Elevated NCOR1 disrupts PPARalpha/gamma signaling in prostate cancer and forms a targetable epigenetic lesion*. Carcinogenesis, 2010. **31**(9): p. 1650-60.
95. Doig, C.L., et al., *Recruitment of NCOR1 to VDR target genes is enhanced in prostate cancer cells and associates with altered DNA methylation patterns*. Carcinogenesis, 2013. **34**(2): p. 248-56.
96. Stephens, P.J., et al., *The landscape of cancer genes and mutational processes in breast cancer*. Nature, 2012. **486**(7403): p. 400-4.
97. Olsen, B.N., et al., *Side-chain oxysterols: from cells to membranes to molecules*. Biochim Biophys Acta, 2012. **1818**(2): p. 330-6.
98. Horton, J.D., J.L. Goldstein, and M.S. Brown, *SREBPs: activators of the complete program of cholesterol and fatty acid synthesis in the liver*. J Clin Invest, 2002. **109**(9): p. 1125-31.
99. Ory, D.S., *The niemann-pick disease genes; regulators of cellular cholesterol homeostasis*. Trends Cardiovasc Med, 2004. **14**(2): p. 66-72.
100. van Meer, G., D.R. Voelker, and G.W. Feigenson, *Membrane lipids: where they are and how they behave*. Nat Rev Mol Cell Biol, 2008. **9**(2): p. 112-24.
101. Bovenga, F., C. Sabba, and A. Moschetta, *Uncoupling nuclear receptor LXR and cholesterol metabolism in cancer*. Cell Metab, 2015. **21**(4): p. 517-26.
102. Simons, K. and E. Ikonen, *Functional rafts in cell membranes*. Nature, 1997. **387**(6633): p. 569-72.
103. Crane, J.M. and L.K. Tamm, *Role of cholesterol in the formation and nature of lipid rafts in planar and spherical model membranes*. Biophys J, 2004. **86**(5): p. 2965-79.
104. Sabol, S.L., H.B. Brewer, and S. Santamarina-Fojo, *The human ABCG1 gene: identification of LXR response elements that modulate expression in macrophages and liver*. Journal of Lipid Research, 2005. **46**(10): p. 2151-2167.
105. Nelson, E.R., et al., *27-Hydroxycholesterol links hypercholesterolemia and breast cancer pathophysiology*. Science, 2013. **342**(6162): p. 1094-8.
106. El Roz, A., et al., *LXR agonists and ABCG1-dependent cholesterol efflux in MCF-7 breast cancer cells: relation to proliferation and apoptosis*. Anticancer Res, 2012. **32**(7): p. 3007-13.

107. Edwards, P.A., M.A. Kennedy, and P.A. Mak, *LXRs; oxysterol-activated nuclear receptors that regulate genes controlling lipid homeostasis*. *Vascul Pharmacol*, 2002. **38**(4): p. 249-56.
108. Forman, B.M., et al., *The orphan nuclear receptor LXRalpha is positively and negatively regulated by distinct products of mevalonate metabolism*. *Proc Natl Acad Sci U S A*, 1997. **94**(20): p. 10588-93.
109. Park, Y. and T.P. Carr, *Unsaturated fatty acids and phytosterols regulate cholesterol transporter genes in Caco-2 and HepG2 cell lines*. *Nutr Res*, 2013. **33**(2): p. 154-61.
110. Wu, Q., et al., *27-Hydroxycholesterol promotes cell-autonomous, ER-positive breast cancer growth*. *Cell Rep*, 2013. **5**(3): p. 637-45.
111. Janowski, B.A., et al., *An oxysterol signalling pathway mediated by the nuclear receptor LXR alpha*. *Nature*, 1996. **383**(6602): p. 728-731.
112. Lehmann, J.M., et al., *Activation of the nuclear receptor LXR by oxysterols defines a new hormone response pathway*. *J Biol Chem*, 1997. **272**(6): p. 3137-40.
113. Seidell, J.C., *The epidemiology of obesity*. *International Textbook of Obesity*., ed. E. Björntorp P. 2001, Chichester: : John Wiley & Sons Ltd.
114. Flegal, K.M., et al., *Overweight and obesity in the United States: prevalence and trends, 1960-1994*. *Int J Obes Relat Metab Disord*, 1998. **22**(1): p. 39-47.
115. Monteiro, C.A., et al., *Shifting obesity trends in Brazil*. *Eur J Clin Nutr*, 2000. **54**(4): p. 342-6.
116. Danilo, C. and P.G. Frank, *Cholesterol and breast cancer development*. *Curr Opin Pharmacol*, 2012. **12**(6): p. 677-82.
117. Hu, J., et al., *Dietary cholesterol intake and cancer*. *Ann Oncol*, 2012. **23**(2): p. 491-500.
118. Karp, I., et al., *Statins and cancer risk*. *Am J Med*, 2008. **121**(4): p. 302-9.
119. Kozar, K., et al., *Cerivastatin demonstrates enhanced antitumor activity against human breast cancer cell lines when used in combination with doxorubicin or cisplatin*. *Int J Oncol*, 2004. **24**(5): p. 1149-57.
120. Muck, A.O., H. Seeger, and D. Wallwiener, *Inhibitory effect of statins on the proliferation of human breast cancer cells*. *Int J Clin Pharmacol Ther*, 2004. **42**(12): p. 695-700.
121. Cholesterol Treatment Trialists, C., et al., *Efficacy and safety of more intensive lowering of LDL cholesterol: a meta-analysis of data from 170,000 participants in 26 randomised trials*. *Lancet*, 2010. **376**(9753): p. 1670-81.
122. Kumar, A.S., et al., *Estrogen receptor-negative breast cancer is less likely to arise among lipophilic statin users*. *Cancer Epidemiol Biomarkers Prev*, 2008. **17**(5): p. 1028-33.
123. Boudreau, D.M., et al., *The association between 3-hydroxy-3-methylglutaryl coenzyme A inhibitor use and breast carcinoma risk among postmenopausal women: a case-control study*. *Cancer*, 2004. **100**(11): p. 2308-16.
124. Pocobelli, G., et al., *Statin use and risk of breast cancer*. *Cancer*, 2008. **112**(1): p. 27-33.
125. Garwood, E.R., et al., *Fluvastatin reduces proliferation and increases apoptosis in women with high grade breast cancer*. *Breast Cancer Res Treat*, 2010. **119**(1): p. 137-44.
126. Ahern, T.P., et al., *Statins and breast cancer prognosis: evidence and opportunities*. *Lancet Oncol*, 2014. **15**(10): p. e461-8.
127. Campbell, M.J., et al., *Breast cancer growth prevention by statins*. *Cancer Res*, 2006. **66**(17): p. 8707-14.
128. Kotamraju, S., et al., *Statin-induced breast cancer cell death: role of inducible nitric oxide and arginase-dependent pathways*. *Cancer Res*, 2007. **67**(15): p. 7386-94.

129. Koyuturk, M., M. Ersoz, and N. Altıok, *Simvastatin induces apoptosis in human breast cancer cells: p53 and estrogen receptor independent pathway requiring signalling through JNK*. *Cancer Lett*, 2007. **250**(2): p. 220-8.
130. Solheim, S., et al., *Fast liquid chromatography-mass spectrometry reveals side chain oxysterol heterogeneity in breast cancer tumour samples*. *J Steroid Biochem Mol Biol*, 2019.
131. Hutchinson, S.A., et al., *Phytosterols Inhibit Side-Chain Oxysterol Mediated Activation of LXR in Breast Cancer Cells*. *Int J Mol Sci*, 2019. **20**(13).
132. Forman, B.M., et al., *The orphan nuclear receptor LXR alpha is positively and negatively regulated by distinct products of mevalonate metabolism*. *Proceedings of the National Academy of Sciences of the United States of America*, 1997. **94**(20): p. 10588-10593.
133. Sabol, S.L., H.B. Brewer, Jr., and S. Santamarina-Fojo, *The human ABCG1 gene: identification of LXR response elements that modulate expression in macrophages and liver*. *J Lipid Res*, 2005. **46**(10): p. 2151-67.
134. Vedin, L.L., et al., *The oxysterol receptor LXR inhibits proliferation of human breast cancer cells*. *Carcinogenesis*, 2009. **30**(4): p. 575-9.
135. Torres, C.G., et al., *27-hydroxycholesterol induces the transition of MCF7 cells into a mesenchymal phenotype*. *Oncol Rep*, 2011. **26**(2): p. 389-97.
136. Dalenc, F., et al., *Circulating oxysterol metabolites as potential new surrogate markers in patients with hormone receptor-positive breast cancer: Results of the OXYTAM study*. *J Steroid Biochem Mol Biol*, 2017. **169**: p. 210-218.
137. Thuwajit, C., et al., *The metabolic cross-talk between epithelial cancer cells and stromal fibroblasts in ovarian cancer progression: Autophagy plays a role*. *Med Res Rev*, 2018. **38**(4): p. 1235-1254.
138. Kogure, A., N. Kosaka, and T. Ochiya, *Cross-talk between cancer cells and their neighbors via miRNA in extracellular vesicles: an emerging player in cancer metastasis*. *J Biomed Sci*, 2019. **26**(1): p. 7.
139. Tsuyada, A., et al., *CCL2 mediates cross-talk between cancer cells and stromal fibroblasts that regulates breast cancer stem cells*. *Cancer Res*, 2012. **72**(11): p. 2768-79.
140. Albini, A. and M.B. Sporn, *The tumour microenvironment as a target for chemoprevention*. *Nat Rev Cancer*, 2007. **7**(2): p. 139-47.
141. Gouirand, V., F. Guillaumond, and S. Vasseur, *Influence of the Tumor Microenvironment on Cancer Cells Metabolic Reprogramming*. *Front Oncol*, 2018. **8**: p. 117.
142. Babiker, A., et al., *Elimination of cholesterol in macrophages and endothelial cells by the sterol 27-hydroxylase mechanism. Comparison with high density lipoprotein-mediated reverse cholesterol transport*. *J Biol Chem*, 1997. **272**(42): p. 26253-61.
143. Dirat, B., et al., *Cancer-associated adipocytes exhibit an activated phenotype and contribute to breast cancer invasion*. *Cancer Res*, 2011. **71**(7): p. 2455-65.
144. Hasebe, T., et al., *Proliferative activity of intratumoral fibroblasts is closely correlated with lymph node and distant organ metastases of invasive ductal carcinoma of the breast*. *Am J Pathol*, 2000. **156**(5): p. 1701-10.
145. Mahmoud, S.M., et al., *Tumour-infiltrating macrophages and clinical outcome in breast cancer*. *J Clin Pathol*, 2012. **65**(2): p. 159-63.
146. Axelson, M. and O. Larsson, *Low density lipoprotein (LDL) cholesterol is converted to 27-hydroxycholesterol in human fibroblasts. Evidence that 27-hydroxycholesterol can be an important intracellular mediator between LDL and the suppression of cholesterol production*. *J Biol Chem*, 1995. **270**(25): p. 15102-10.
147. Zhang, J., O. Larsson, and J. Sjövall, *7 alpha-Hydroxylation of 25-hydroxycholesterol and 27-hydroxycholesterol in human fibroblasts*. *Biochim Biophys Acta*, 1995. **1256**(3): p. 353-9.

148. Saucier, S.E., et al., *Identification of regulatory oxysterols, 24(S),25-epoxycholesterol and 25-hydroxycholesterol, in cultured fibroblasts*. J Biol Chem, 1985. **260**(27): p. 14571-9.
149. Quail, D.F. and J.A. Joyce, *Microenvironmental regulation of tumor progression and metastasis*. Nat Med, 2013. **19**(11): p. 1423-37.
150. de Kruijf, E.M., et al., *Tumor-stroma ratio in the primary tumor is a prognostic factor in early breast cancer patients, especially in triple-negative carcinoma patients*. Breast Cancer Res Treat, 2011. **125**(3): p. 687-96.
151. Li, Q., et al., *MiR-21/Smad 7 signaling determines TGF- β 1-induced CAF formation*. Sci Rep, 2013. **3**: p. 2038.
152. Kunita, A., et al., *MicroRNA-21 in cancer-associated fibroblasts supports lung adenocarcinoma progression*. Sci Rep, 2018. **8**(1): p. 8838.
153. Liao, D., et al., *Cancer associated fibroblasts promote tumor growth and metastasis by modulating the tumor immune microenvironment in a 4T1 murine breast cancer model*. PLoS One, 2009. **4**(11): p. e7965.
154. Singer, C.F., et al., *Differential gene expression profile in breast cancer-derived stromal fibroblasts*. Breast Cancer Res Treat, 2008. **110**(2): p. 273-81.
155. Varol, C., A. Mildner, and S. Jung, *Macrophages: development and tissue specialization*. Annu Rev Immunol, 2015. **33**: p. 643-75.
156. Williams, C.B., E.S. Yeh, and A.C. Soloff, *Tumor-associated macrophages: unwitting accomplices in breast cancer malignancy*. NPJ Breast Cancer, 2016. **2**.
157. Mantovani, A., et al., *Macrophage polarization: tumor-associated macrophages as a paradigm for polarized M2 mononuclear phagocytes*. Trends Immunol, 2002. **23**(11): p. 549-55.
158. Mantovani, A., et al., *The chemokine system in diverse forms of macrophage activation and polarization*. Trends Immunol, 2004. **25**(12): p. 677-86.
159. Gentek, R., K. Molawi, and M.H. Sieweke, *Tissue macrophage identity and self-renewal*. Immunol Rev, 2014. **262**(1): p. 56-73.
160. Yamashiro, S., et al., *Tumor-derived monocyte chemoattractant protein-1 induces intratumoral infiltration of monocyte-derived macrophage subpopulation in transplanted rat tumors*. Am J Pathol, 1994. **145**(4): p. 856-67.
161. Azenshtein, E., et al., *The CC chemokine RANTES in breast carcinoma progression: regulation of expression and potential mechanisms of promalignant activity*. Cancer Res, 2002. **62**(4): p. 1093-102.
162. Shibata, N. and C.K. Glass, *Macrophages, oxysterols and atherosclerosis*. Circ J, 2010. **74**(10): p. 2045-51.
163. Hansson, M., et al., *Marked induction of sterol 27-hydroxylase activity and mRNA levels during differentiation of human cultured monocytes into macrophages*. Biochim Biophys Acta, 2003. **1593**(2-3): p. 283-9.
164. Kimura, T., et al., *Polarization of M2 macrophages requires Lamtor1 that integrates cytokine and amino-acid signals*. Nat Commun, 2016. **7**: p. 13130.
165. Rowe, A.H., et al., *Enhanced synthesis of the oxysterol 24(S),25-epoxycholesterol in macrophages by inhibitors of 2,3-oxidosqualene:lanosterol cyclase: a novel mechanism for the attenuation of foam cell formation*. Circ Res, 2003. **93**(8): p. 717-25.
166. Li, J., et al., *De novo synthesis of steroids and oxysterols in adipocytes*. J Biol Chem, 2014. **289**(2): p. 747-64.
167. Guo, L., et al., *Intramuscular preadipocytes impede differentiation and promote lipid deposition of muscle satellite cells in chickens*. BMC Genomics, 2018. **19**(1): p. 838.
168. Franck, N., et al., *Identification of adipocyte genes regulated by caloric intake*. J Clin Endocrinol Metab, 2011. **96**(2): p. E413-8.

169. Ory, D.S., *Nuclear receptor signaling in the control of cholesterol homeostasis: have the orphans found a home?* *Circ Res*, 2004. **95**(7): p. 660-70.
170. Shimizu, H., et al., *Cancers of the prostate and breast among Japanese and white immigrants in Los Angeles County.* *Br J Cancer*, 1991. **63**(6): p. 963-6.
171. Mitro, N., et al., *The nuclear receptor LXR is a glucose sensor.* *Nature*, 2007. **445**(7124): p. 219-23.
172. Yang, C., et al., *Disruption of cholesterol homeostasis by plant sterols.* *J Clin Invest*, 2004. **114**(6): p. 813-22.
173. Robertson, T.B. and T.C. Burnett, *THE INFLUENCE OF LECITHIN AND CHOLESTERIN UPON THE GROWTH OF TUMORS.* *J Exp Med*, 1913. **17**(3): p. 344-52.
174. Kolanjiappan, K., C.R. Ramachandran, and S. Manoharan, *Biochemical changes in tumor tissues of oral cancer patients.* *Clin Biochem*, 2003. **36**(1): p. 61-5.
175. Dessì, S., et al., *Cholesterol content in tumor tissues is inversely associated with high-density lipoprotein cholesterol in serum in patients with gastrointestinal cancer.* *Cancer*, 1994. **73**(2): p. 253-8.
176. Yoshioka, Y., et al., *Quantitation by (1)H-NMR of dolichol, cholesterol and choline-containing lipids in extracts of normal and pathological thyroid tissue.* *NMR Biomed*, 2000. **13**(7): p. 377-83.
177. Zhang, X., et al., *Lipid levels in serum and cancerous tissues of colorectal cancer patients.* *World J Gastroenterol*, 2014. **20**(26): p. 8646-52.
178. Kitahara, C.M., et al., *Total cholesterol and cancer risk in a large prospective study in Korea.* *J Clin Oncol*, 2011. **29**(12): p. 1592-8.
179. Benn, M., et al., *Low-density lipoprotein cholesterol and the risk of cancer: a mendelian randomization study.* *J Natl Cancer Inst*, 2011. **103**(6): p. 508-19.
180. Strasak, A.M., et al., *Time-dependent association of total serum cholesterol and cancer incidence in a cohort of 172,210 men and women: a prospective 19-year follow-up study.* *Ann Oncol*, 2009. **20**(6): p. 1113-20.
181. Notarnicola, M., et al., *Up-regulation of 3-hydroxy-3-methylglutaryl coenzyme A reductase activity in left-sided human colon cancer.* *Anticancer Res*, 2004. **24**(6): p. 3837-42.
182. Hentosh, P., et al., *Sterol-independent regulation of 3-hydroxy-3-methylglutaryl coenzyme A reductase in tumor cells.* *Mol Carcinog*, 2001. **32**(3): p. 154-66.
183. Graziani, S.R., et al., *Uptake of a cholesterol-rich emulsion by breast cancer.* *Gynecol Oncol*, 2002. **85**(3): p. 493-7.
184. Schimanski, S., et al., *Expression of the lipid transporters ABCA3 and ABCA1 is diminished in human breast cancer tissue.* *Horm Metab Res*, 2010. **42**(2): p. 102-9.
185. Ki, D.H., et al., *Whole genome analysis for liver metastasis gene signatures in colorectal cancer.* *Int J Cancer*, 2007. **121**(9): p. 2005-12.
186. Kloudova, A., Guengerich, F.P., and Soucek, P., *The Role of Oxysterols in Human Cancer.* *Trends in Endocrinology & Metabolism*, 2017. **28**(7): p. 485-496.
187. Lee, D., *High androgen receptor levels are predictive of decreased survival in prostate cancer.* *Clin Prostate Cancer*, 2003. **2**(1): p. 13-4.
188. Fukuchi, J., et al., *Antiproliferative effect of liver X receptor agonists on LNCaP human prostate cancer cells.* *Cancer Res*, 2004. **64**(21): p. 7686-9.
189. de Bousac, H., et al., *LXR, prostate cancer and cholesterol: the Good, the Bad and the Ugly.* *Am J Cancer Res*, 2013. **3**(1): p. 58-69.
190. Chuu, C.P., et al., *Inhibition of tumor growth and progression of LNCaP prostate cancer cells in athymic mice by androgen and liver X receptor agonist.* *Cancer Res*, 2006. **66**(13): p. 6482-6.

191. Chuu, C.P. and H.P. Lin, *Antiproliferative effect of LXR agonists T0901317 and 22(R)-hydroxycholesterol on multiple human cancer cell lines*. *Anticancer Res*, 2010. **30**(9): p. 3643-8.
192. Bahl, M., et al., *Serum lipids and outcome of early-stage breast cancer: results of a prospective cohort study*. *Breast Cancer Res Treat*, 2005. **94**(2): p. 135-44.
193. Pollak, O.J. and D. Kritchevsky, *Sitosterol*. *Monogr Atheroscler*, 1981. **10**: p. 1-219.
194. Bean, G.A., *Phytosterols*. *Adv Lipid Res*, 1973. **11**: p. 193-218.
195. Moreau, R.A., B.D. Whitaker, and K.B. Hicks, *Phytosterols, phytostanols, and their conjugates in foods: structural diversity, quantitative analysis, and health-promoting uses*. *Prog Lipid Res*, 2002. **41**(6): p. 457-500.
196. Moreau, R.A., et al., *Phytosterols and their derivatives: Structural diversity, distribution, metabolism, analysis, and health-promoting uses*. *Prog Lipid Res*, 2018. **70**: p. 35-61.
197. Grundy, S.M., *Absorption and metabolism of dietary cholesterol*. *Annu Rev Nutr*, 1983. **3**: p. 71-96.
198. Carr, T.P., et al., *Stearate-enriched plant sterol esters lower serum LDL cholesterol concentration in normo- and hypercholesterolemic adults*. *J Nutr*, 2009. **139**(8): p. 1445-50.
199. Miettinen, T.A., et al., *Reduction of serum cholesterol with sitostanol-ester margarine in a mildly hypercholesterolemic population*. *N Engl J Med*, 1995. **333**(20): p. 1308-12.
200. Plösch, T., et al., *Reduction of cholesterol absorption by dietary plant sterols and stanols in mice is independent of the Abcg5/8 transporter*. *J Nutr*, 2006. **136**(8): p. 2135-40.
201. Katan, M.B., et al., *Efficacy and safety of plant stanols and sterols in the management of blood cholesterol levels*. *Mayo Clin Proc*, 2003. **78**(8): p. 965-78.
202. Carr, T.P. and E.D. Jesch, *Food components that reduce cholesterol absorption*. *Adv Food Nutr Res*, 2006. **51**: p. 165-204.
203. BEST, M.M., et al., *Lowering of serum cholesterol by the administration of a plant sterol*. *Circulation*, 1954. **10**(2): p. 201-6.
204. Stiles, A.R., et al., *Genetic, anatomic, and clinical determinants of human serum sterol and vitamin D levels*. *Proc Natl Acad Sci U S A*, 2014. **111**(38): p. E4006-14.
205. Miettinen, T.A., et al., *Serum, biliary, and fecal cholesterol and plant sterols in colectomized patients before and during consumption of stanol ester margarine*. *Am J Clin Nutr*, 2000. **71**(5): p. 1095-102.
206. Carter, B.A., et al., *Stigmasterol, a soy lipid-derived phytosterol, is an antagonist of the bile acid nuclear receptor FXR*. *Pediatr Res*, 2007. **62**(3): p. 301-6.
207. Manna, S. and M.K. Holz, *Tamoxifen Action in ER-Negative Breast Cancer*. *Sign Transduct Insights*, 2016. **5**: p. 1-7.
208. Olkkonen, V.M., H. Gylling, and E. Ikonen, *Plant sterols, cholesterol precursors and oxysterols: Minute concentrations-Major physiological effects*. *J Steroid Biochem Mol Biol*, 2017. **169**: p. 4-9.
209. Fakhri, O., et al., *Exploring the biophysical properties of phytosterols in the plasma membrane for novel cancer prevention strategies*. *Biochimie*, 2018. **153**: p. 150-161.
210. Lütjohann, D., et al., *Sterol absorption and sterol balance in phytosterolemia evaluated by deuterium-labeled sterols: effect of sitostanol treatment*. *J Lipid Res*, 1995. **36**(8): p. 1763-73.
211. Brauner, R., et al., *Phytosterols reduce cholesterol absorption by inhibition of 27-hydroxycholesterol generation, liver X receptor α activation, and*

- expression of the basolateral sterol exporter ATP-binding cassette A1 in Caco-2 enterocytes. *J Nutr*, 2012. **142**(6): p. 981-9.
212. Plat, J., J.A. Nichols, and R.P. Mensink, *Plant sterols and stanols: effects on mixed micellar composition and LXR (target gene) activation*. *J Lipid Res*, 2005. **46**(11): p. 2468-76.
213. Liang, Y.T., et al., *Effect of phytosterols and their oxidation products on lipoprotein profiles and vascular function in hamster fed a high cholesterol diet*. *Atherosclerosis*, 2011. **219**(1): p. 124-33.
214. Alemany, L., et al., *Relative expression of cholesterol transport-related proteins and inflammation markers through the induction of 7-ketosterol-mediated stress in Caco-2 cells*. *Food Chem Toxicol*, 2013. **56**: p. 247-53.
215. Sabeva, N.S., et al., *Phytosterols differentially influence ABC transporter expression, cholesterol efflux and inflammatory cytokine secretion in macrophage foam cells*. *J Nutr Biochem*, 2011. **22**(8): p. 777-83.
216. O'Callaghan, Y., F.O. McCarthy, and N.M. O'Brien, *Recent advances in Phytosterol Oxidation Products*. *Biochem Biophys Res Commun*, 2014. **446**(3): p. 786-91.
217. Institute, N.C. *Cancer control and population science*. 2006 04/08/2019]; Available from: <https://cancercontrol.cancer.gov/bb/docs/NCI-DCCPS-Overview-and-Highlights-2006.pdf>.
218. Surh, Y.J., *Cancer chemoprevention with dietary phytochemicals*. *Nat Rev Cancer*, 2003. **3**(10): p. 768-80.
219. Weigl, J., H. Hauner, and D. Hauner, *Can Nutrition Lower the Risk of Recurrence in Breast Cancer?* *Breast Care (Basel)*, 2018. **13**(2): p. 86-91.
220. Link, L.B., et al., *Dietary patterns and breast cancer risk in the California Teachers Study cohort*. *Am J Clin Nutr*, 2013. **98**(6): p. 1524-32.
221. Blackburn, G.L. and K.A. Wang, *Dietary fat reduction and breast cancer outcome: results from the Women's Intervention Nutrition Study (WINS)*. *Am J Clin Nutr*, 2007. **86**(3): p. s878-81.
222. Mihaylova, B., et al., *The effects of lowering LDL cholesterol with statin therapy in people at low risk of vascular disease: meta-analysis of individual data from 27 randomised trials*. *Lancet*, 2012. **380**(9841): p. 581-90.
223. Nanayakkara, A.K., et al., *Targeted inhibitors of P-glycoprotein increase chemotherapeutic-induced mortality of multidrug resistant tumor cells*. *Sci Rep*, 2018. **8**(1): p. 967.
224. Cavaco, M.C., et al., *Evading P-glycoprotein mediated-efflux chemoresistance using Solid Lipid Nanoparticles*. *Eur J Pharm Biopharm*, 2017. **110**: p. 76-84.
225. Zhang, L., et al., *Highly Prevalent Multidrug-Resistant*. *Front Microbiol*, 2018. **9**: p. 2104.
226. Noguchi, K., K. Katayama, and Y. Sugimoto, *Human ABC transporter ABCG2/BCRP expression in chemoresistance: basic and clinical perspectives for molecular cancer therapeutics*. *Pharmgenomics Pers Med*, 2014. **7**: p. 53-64.
227. Saint-Pol, J., et al., *Oxysterols decrease apical-to-basolateral transport of Aβ peptides via an ABCB1-mediated process in an in vitro Blood-brain barrier model constituted of bovine brain capillary endothelial cells*. *Brain Res*, 2013. **1517**: p. 1-15.
228. Saint-Pol, J., et al., *Oxysterols decrease apical-to-basolateral transport of Aβ peptides via an ABCB1-mediated process in an in vitro Blood-brain barrier model constituted of bovine brain capillary endothelial cells*. *Brain Res*, 2013. **1517**: p. 1-15.
229. Cerami, E., et al., *The cBio cancer genomics portal: an open platform for exploring multidimensional cancer genomics data*. *Cancer Discov*, 2012. **2**(5): p. 401-4.

230. Koboldt, D.C., et al., *Comprehensive molecular portraits of human breast tumours*. Nature, 2012. **490**(7418): p. 61-70.
231. Liu, T., et al., *Cistrome: an integrative platform for transcriptional regulation studies*. Genome Biol, 2011. **12**(8): p. R83.
232. Griffiths, W.J., et al., *Discovering oxysterols in plasma: a window on the metabolome*. J Proteome Res, 2008. **7**(8): p. 3602-12.
233. Roberg-Larsen, H., et al., *Highly automated nano-LC/MS-based approach for thousand cell-scale quantification of side chain-hydroxylated oxysterols*. J Lipid Res, 2014. **55**(7): p. 1531-6.
234. Hutchinson, S.A., et al., *ER-Negative Breast Cancer Is Highly Responsive to Cholesterol Metabolite Signalling*. Nutrients, 2019. **11**(11).
235. Li, T. and J.Y. Chiang, *Regulation of bile acid and cholesterol metabolism by PPARs*. PPAR Res, 2009. **2009**: p. 501739.
236. Bjorkhem, I., *Do oxysterols control cholesterol homeostasis?* J Clin Invest, 2002. **110**(6): p. 725-30.
237. Abankwa, D., et al., *Ski-interacting protein (SKIP) interacts with androgen receptor in the nucleus and modulates androgen-dependent transcription*. BMC Biochem, 2013. **14**: p. 10.
238. Htun, H., et al., *Visualization of glucocorticoid receptor translocation and intranuclear organization in living cells with a green fluorescent protein chimera*. Proc Natl Acad Sci U S A, 1996. **93**(10): p. 4845-50.
239. Leung, Y.K., et al., *Estrogen receptor (ER)-beta isoforms: a key to understanding ER-beta signaling*. Proc Natl Acad Sci U S A, 2006. **103**(35): p. 13162-7.
240. Courtney, R. and G.E. Landreth, *LXR Regulation of Brain Cholesterol: From Development to Disease*. Trends Endocrinol Metab, 2016. **27**(6): p. 404-414.
241. Janowski, B.A., et al., *Structural requirements of ligands for the oxysterol liver X receptors LXRalpha and LXRBeta*. Proc Natl Acad Sci U S A, 1999. **96**(1): p. 266-71.
242. Abedin, S.A., et al., *Elevated NCOR1 disrupts a network of dietary-sensing nuclear receptors in bladder cancer cells*. Carcinogenesis, 2009. **30**(3): p. 449-56.
243. Hu, X., et al., *Liver X receptors interact with corepressors to regulate gene expression*. Mol Endocrinol, 2003. **17**(6): p. 1019-26.
244. Osborne, C.K., et al., *Role of the estrogen receptor coactivator AIB1 (SRC-3) and HER-2/neu in tamoxifen resistance in breast cancer*. J Natl Cancer Inst, 2003. **95**(5): p. 353-61.
245. Debes, J.D., et al., *p300 in prostate cancer proliferation and progression*. Cancer Res, 2003. **63**(22): p. 7638-40.
246. Zhou, H.J., et al., *SRC-3 is required for prostate cancer cell proliferation and survival*. Cancer Res, 2005. **65**(17): p. 7976-83.
247. Henke, R.T., et al., *Overexpression of the nuclear receptor coactivator AIB1 (SRC-3) during progression of pancreatic adenocarcinoma*. Clin Cancer Res, 2004. **10**(18 Pt 1): p. 6134-42.
248. Chen, W., et al., *Enzymatic reduction of oxysterols impairs LXR signaling in cultured cells and the livers of mice*. Cell Metab, 2007. **5**(1): p. 73-9.
249. Wang, Q., et al., *Activation of liver X receptor inhibits the development of pulmonary carcinomas induced by 3-methylcholanthrene and butylated hydroxytoluene in BALB/c mice*. Sci Rep, 2016. **6**: p. 27295.
250. Pencheva, N., et al., *Broad-spectrum therapeutic suppression of metastatic melanoma through nuclear hormone receptor activation*. Cell, 2014. **156**(5): p. 986-1001.
251. Broekema, M.F., et al., *Profiling of 3696 Nuclear Receptor-Coregulator Interactions: A Resource for Biological and Clinical Discovery*. Endocrinology, 2018. **159**(6): p. 2397-2407.

252. Laffitte, B.A., et al., *LXRs control lipid-inducible expression of the apolipoprotein E gene in macrophages and adipocytes*. Proc Natl Acad Sci U S A, 2001. **98**(2): p. 507-12.
253. Nelson, J.K., et al., *EEPD1 Is a Novel LXR Target Gene in Macrophages Which Regulates ABCA1 Abundance and Cholesterol Efflux*. Arterioscler Thromb Vasc Biol, 2017. **37**(3): p. 423-432.
254. Venkateswaran, A., et al., *Control of cellular cholesterol efflux by the nuclear oxysterol receptor LXR alpha*. Proc Natl Acad Sci U S A, 2000. **97**(22): p. 12097-102.
255. Galhardo, M., et al., *Integrated analysis of transcript-level regulation of metabolism reveals disease-relevant nodes of the human metabolic network*. Nucleic Acids Res, 2014. **42**(3): p. 1474-96.
256. Oishi, Y., et al., *SREBP1 Contributes to Resolution of Pro-inflammatory TLR4 Signaling by Reprogramming Fatty Acid Metabolism*. Cell Metab, 2017. **25**(2): p. 412-427.
257. Savic, D., et al., *Distinct gene regulatory programs define the inhibitory effects of liver X receptors and PPARG on cancer cell proliferation*. Genome Med, 2016. **8**(1): p. 74.
258. Research., W.C.R.F.I.A.I.f.C., *Continuous Update Project Report: Diet, Nutrition, Physical Activity and Breast Cancer*. 2017.
259. Myers, E., et al., *Associations and interactions between Ets-1 and Ets-2 and coregulatory proteins, SRC-1, AIB1, and NCoR in breast cancer*. Clin Cancer Res, 2005. **11**(6): p. 2111-22.
260. Lu, R., et al., *COPS5 amplification and overexpression confers tamoxifen-resistance in ERalpha-positive breast cancer by degradation of NCoR*. Nat Commun, 2016. **7**: p. 12044.
261. Asim, M., et al., *Ligand-dependent corepressor acts as a novel androgen receptor corepressor, inhibits prostate cancer growth, and is functionally inactivated by the Src protein kinase*. J Biol Chem, 2011. **286**(43): p. 37108-17.
262. Jalaguier, S., et al., *Complex regulation of LCoR signaling in breast cancer cells*. Oncogene, 2017. **36**(33): p. 4790-4801.
263. Gramajo, A.L., et al., *Mitochondrial DNA damage induced by 7-ketocholesterol in human retinal pigment epithelial cells in vitro*. Invest Ophthalmol Vis Sci, 2010. **51**(2): p. 1164-70.
264. Appukuttan, A., et al., *Oxysterol-induced apoptosis of smooth muscle cells is under the control of a soluble adenylyl cyclase*. Cardiovasc Res, 2013. **99**(4): p. 734-42.
265. Kang, K.A., et al., *Cytotoxic effect of 7beta-hydroxycholesterol on human NCI-H460 lung cancer cells*. Biol Pharm Bull, 2005. **28**(8): p. 1377-80.
266. Lee, T. and L. Chau, *Fas/Fas ligand-mediated death pathway is involved in oxLDL-induced apoptosis in vascular smooth muscle cells*. Am J Physiol Cell Physiol, 2001. **280**(3): p. C709-18.
267. Baxter, D.E., et al., *Neoadjuvant Endocrine Therapy in Breast Cancer Upregulates the Cytotoxic Drug Pump ABCG2/BCRP, and May Lead to Resistance to Subsequent Chemotherapy*. Clin Breast Cancer, 2018. **18**(6): p. 481-488.
268. Thorne, J.L., et al., *MiR-19b non-canonical binding is directed by HuR and confers chemosensitivity through regulation of P-glycoprotein in breast cancer*. Biochim Biophys Acta Gene Regul Mech, 2018. **1861**(11): p. 996-1006.
269. Kim, B., et al., *Chemotherapy induces Notch1-dependent MRP1 up-regulation, inhibition of which sensitizes breast cancer cells to chemotherapy*. BMC Cancer, 2015. **15**: p. 634.

270. Kim, B., et al., *Neoadjuvant chemotherapy induces expression levels of breast cancer resistance protein that predict disease-free survival in breast cancer*. PLoS One, 2013. **8**(5): p. e62766.
271. Bao, L., et al., *Increased expression of P-glycoprotein and doxorubicin chemoresistance of metastatic breast cancer is regulated by miR-298*. Am J Pathol, 2012. **180**(6): p. 2490-503.
272. Ozols, R.F., et al., *Verapamil and adriamycin in the treatment of drug-resistant ovarian cancer patients*. J Clin Oncol, 1987. **5**(4): p. 641-7.
273. Amin, M.L., *P-glycoprotein Inhibition for Optimal Drug Delivery*. Drug Target Insights, 2013. **7**: p. 27-34.
274. Chung, F.S., et al., *Disrupting P-glycoprotein function in clinical settings: what can we learn from the fundamental aspects of this transporter?* Am J Cancer Res, 2016. **6**(8): p. 1583-98.
275. Bougaret, L., et al., *Adipocyte/breast cancer cell crosstalk in obesity interferes with the anti-proliferative efficacy of tamoxifen*. PLoS One, 2018. **13**(2): p. e0191571.
276. Kalluri, R., *Basement membranes: structure, assembly and role in tumour angiogenesis*. Nat Rev Cancer, 2003. **3**(6): p. 422-33.
277. Parsonage, G., et al., *A stromal address code defined by fibroblasts*. Trends Immunol, 2005. **26**(3): p. 150-6.
278. Tomasek, J.J., et al., *Myofibroblasts and mechano-regulation of connective tissue remodelling*. Nat Rev Mol Cell Biol, 2002. **3**(5): p. 349-63.
279. Rodemann, H.P. and G.A. Muller, *Characterization of human renal fibroblasts in health and disease: II. In vitro growth, differentiation, and collagen synthesis of fibroblasts from kidneys with interstitial fibrosis*. Am J Kidney Dis, 1991. **17**(6): p. 684-6.
280. Elenbaas, B. and R.A. Weinberg, *Heterotypic signaling between epithelial tumor cells and fibroblasts in carcinoma formation*. Exp Cell Res, 2001. **264**(1): p. 169-84.
281. Tlsty, T.D. and P.W. Hein, *Know thy neighbor: stromal cells can contribute oncogenic signals*. Curr Opin Genet Dev, 2001. **11**(1): p. 54-9.
282. Mueller, M.M. and N.E. Fusenig, *Friends or foes - bipolar effects of the tumour stroma in cancer*. Nat Rev Cancer, 2004. **4**(11): p. 839-49.
283. Frolov, A., et al., *NPC1 and NPC2 regulate cellular cholesterol homeostasis through generation of low density lipoprotein cholesterol-derived oxysterols*. J Biol Chem, 2003. **278**(28): p. 25517-25.
284. Lange, Y., et al., *Regulation of fibroblast mitochondrial 27-hydroxycholesterol production by active plasma membrane cholesterol*. J Lipid Res, 2009. **50**(9): p. 1881-8.
285. Shi, S.Z., et al., *Recruitment of monocytes and epigenetic silencing of intratumoral CYP7B1 primarily contribute to the accumulation of 27-hydroxycholesterol in breast cancer*. Am J Cancer Res, 2019. **9**(10): p. 2194-2208.
286. Hong, W., et al., *Hydroxysteroid sulfotransferase 2B1 affects gastric epithelial function and carcinogenesis induced by a carcinogenic agent*. Lipids Health Dis, 2019. **18**(1): p. 203.
287. Camp, J.T., et al., *Interactions with fibroblasts are distinct in Basal-like and luminal breast cancers*. Mol Cancer Res, 2011. **9**(1): p. 3-13.
288. Kalluri, R. and M. Zeisberg, *Fibroblasts in cancer*. Nat Rev Cancer, 2006. **6**(5): p. 392-401.
289. Orimo, A., et al., *Stromal fibroblasts present in invasive human breast carcinomas promote tumor growth and angiogenesis through elevated SDF-1/CXCL12 secretion*. Cell, 2005. **121**(3): p. 335-48.
290. Ronnov-Jessen, L., O.W. Petersen, and M.J. Bissell, *Cellular changes involved in conversion of normal to malignant breast: importance of the stromal reaction*. Physiol Rev, 1996. **76**(1): p. 69-125.

291. Smith, L., et al., *Down-Regulation of miR-92 in Breast Epithelial Cells and in Normal but Not Tumour Fibroblasts Contributes to Breast Carcinogenesis*. PLoS One, 2015. **10**(10): p. e0139698.
292. Awad, A.B., et al., *In vitro and in vivo (SCID mice) effects of phytosterols on the growth and dissemination of human prostate cancer PC-3 cells*. Eur J Cancer Prev, 2001. **10**(6): p. 507-13.
293. Awad, A.B., H. Williams, and C.S. Fink, *Phytosterols reduce in vitro metastatic ability of MDA-MB-231 human breast cancer cells*. Nutr Cancer, 2001. **40**(2): p. 157-64.
294. Awad, A.B., H. Williams, and C.S. Fink, *Effect of phytosterols on cholesterol metabolism and MAP kinase in MDA-MB-231 human breast cancer cells*. J Nutr Biochem, 2003. **14**(2): p. 111-9.
295. Jiang, L., et al., *The Protective Effect of Dietary Phytosterols on Cancer Risk: A Systematic Meta-Analysis*. J Oncol, 2019. **2019**: p. 7479518.
296. Choi, Y.H., et al., *Induction of Bax and activation of caspases during beta-sitosterol-mediated apoptosis in human colon cancer cells*. Int J Oncol, 2003. **23**(6): p. 1657-62.
297. Kim, Y.S., et al., *Stigmasterol isolated from marine microalgae Navicula incerta induces apoptosis in human hepatoma HepG2 cells*. BMB Rep, 2014. **47**(8): p. 433-8.
298. Al-Sheddi, E., Al-Oqail, M.M., El-Shaibany, A.S., and Farshori, N. , *Phytochemicals and their anti-proliferative activity of Aloe perryi flowers extract against various human cancer cell lines*. . Planta Medica, 2015. **81**.
299. von Holtz, R.L., C.S. Fink, and A.B. Awad, *beta-Sitosterol activates the sphingomyelin cycle and induces apoptosis in LNCaP human prostate cancer cells*. Nutr Cancer, 1998. **32**(1): p. 8-12.
300. Awad, A.B., et al., *beta-Sitosterol enhances tamoxifen effectiveness on breast cancer cells by affecting ceramide metabolism*. Mol Nutr Food Res, 2008. **52**(4): p. 419-26.
301. Sharmila, R. and G. Sindhu, *Modulation of Angiogenesis, Proliferative Response and Apoptosis by beta-Sitosterol in Rat Model of Renal Carcinogenesis*. Indian J Clin Biochem, 2017. **32**(2): p. 142-152.
302. Awad, A.B., A.C. Downie, and C.S. Fink, *Inhibition of growth and stimulation of apoptosis by beta-sitosterol treatment of MDA-MB-231 human breast cancer cells in culture*. Int J Mol Med, 2000. **5**(5): p. 541-5.
303. Awad, A.B., M.D. Garcia, and C.S. Fink, *Effect of dietary phytosterols on rat tissue lipids*. Nutr Cancer, 1997. **29**(3): p. 212-6.
304. Janezic, S.A. and A.V. Rao, *Dose-dependent effects of dietary phytosterol on epithelial cell proliferation of the murine colon*. Food Chem Toxicol, 1992. **30**(7): p. 611-6.
305. Raicht, R.F., et al., *Protective effect of plant sterols against chemically induced colon tumors in rats*. Cancer Res, 1980. **40**(2): p. 403-5.
306. Park, C., et al., *Beta-sitosterol induces anti-proliferation and apoptosis in human leukemic U937 cells through activation of caspase-3 and induction of Bax/Bcl-2 ratio*. Biol Pharm Bull, 2007. **30**(7): p. 1317-23.
307. Katan, M.B., et al., *Efficacy and safety of plant stanols and sterols in the management of blood cholesterol levels*. Mayo Clin Proc, 2003. **78**(8): p. 965-78.
308. Li, X., et al., *Ergosterol peroxide activates Foxo3-mediated cell death signaling by inhibiting AKT and c-Myc in human hepatocellular carcinoma cells*. Oncotarget, 2016. **7**(23): p. 33948-59.
309. Ramprasath, V.R. and A.B. Awad, *Role of Phytosterols in Cancer Prevention and Treatment*. J AOAC Int, 2015. **98**(3): p. 735-738.
310. Salen, G., E.H. Ahrens, Jr., and S.M. Grundy, *Metabolism of beta-sitosterol in man*. J Clin Invest, 1970. **49**(5): p. 952-67.

311. Salen, G., et al., *Increased sitosterol absorption is offset by rapid elimination to prevent accumulation in heterozygotes with sitosterolemia*. *Arterioscler Thromb*, 1992. **12**(5): p. 563-8.
312. Shahzad, N., et al., *Phytosterols as a natural anticancer agent: Current status and future perspective*. *Biomed Pharmacother*, 2017. **88**: p. 786-794.
313. Charlton-Menys, V. and P.N. Durrington, *Human cholesterol metabolism and therapeutic molecules*. *Exp Physiol*, 2008. **93**(1): p. 27-42.
314. Stiles, A.R., et al., *Genetic, anatomic, and clinical determinants of human serum sterol and vitamin D levels*. *Proceedings of the National Academy of Sciences of the United States of America*, 2014. **111**(38): p. E4006-E4014.
315. Ras, R.T., J.M. Geleijnse, and E.A. Trautwein, *LDL-cholesterol-lowering effect of plant sterols and stanols across different dose ranges: a meta-analysis of randomised controlled studies*. *Br J Nutr*, 2014. **112**(2): p. 214-9.
316. Hac-Wydro, K., *The replacement of cholesterol by phytosterols and the increase of total sterol content in model erythrocyte membranes*. *Chem Phys Lipids*, 2010. **163**(7): p. 689-97.
317. Marinozzi, M., et al., *Side-Chain Modified Ergosterol and Stigmasterol Derivatives as Liver X Receptor Agonists*. *J Med Chem*, 2017. **60**(15): p. 6548-6562.
318. Castro Navas, F.F., et al., *C24-hydroxylated stigmastane derivatives as Liver X Receptor agonists*. *Chem Phys Lipids*, 2018. **212**: p. 44-50.
319. Yang, C., et al., *Sterol intermediates from cholesterol biosynthetic pathway as liver X receptor ligands*. *J Biol Chem*, 2006. **281**(38): p. 27816-26.
320. Campbell, M.J., et al., *Proliferating macrophages associated with high grade, hormone receptor negative breast cancer and poor clinical outcome*. *Breast Cancer Res Treat*, 2011. **128**(3): p. 703-711.
321. Bauman, D.R., et al., *25-Hydroxycholesterol secreted by macrophages in response to Toll-like receptor activation suppresses immunoglobulin A production*. *Proc Natl Acad Sci U S A*, 2009. **106**(39): p. 16764-9.
322. Tangirala, R.K., et al., *Identification of macrophage liver X receptors as inhibitors of atherosclerosis*. *Proc Natl Acad Sci U S A*, 2002. **99**(18): p. 11896-901.
323. Megias-Vericat, J.E., et al., *Pharmacogenetics of Metabolic Genes of Anthracyclines in Acute Myeloid Leukemia*. *Curr Drug Metab*, 2018. **19**(1): p. 55-74.
324. Roundhill, E.A., S. Jabri, and S.A. Burchill, *ABCG1 and Pgp identify drug resistant, self-renewing osteosarcoma cells*. *Cancer Lett*, 2019. **453**: p. 142-157.
325. Gyorffy, B., et al., *Gene expression profiling of 30 cancer cell lines predicts resistance towards 11 anticancer drugs at clinically achieved concentrations*. *Int J Cancer*, 2006. **118**(7): p. 1699-712.
326. Arumugam, T., et al., *S100P promotes pancreatic cancer growth, survival, and invasion*. *Clin Cancer Res*, 2005. **11**(15): p. 5356-64.
327. Gagnon, V., et al., *AKT involvement in cisplatin chemoresistance of human uterine cancer cells*. *Gynecol Oncol*, 2004. **94**(3): p. 785-95.
328. Tan, L., et al., *Trichostatin A restores Apaf-1 function in chemoresistant ovarian cancer cells*. *Cancer*, 2011. **117**(4): p. 784-94.
329. Law, E.K., et al., *The DNA cytosine deaminase APOBEC3B promotes tamoxifen resistance in ER-positive breast cancer*. *Sci Adv*, 2016. **2**(10): p. e1601737.
330. Brasseur, K., N. Gevry, and E. Asselin, *Chemoresistance and targeted therapies in ovarian and endometrial cancers*. *Oncotarget*, 2017. **8**(3): p. 4008-4042.
331. Inoue, Y., et al., *Association of ATP7A expression and in vitro sensitivity to cisplatin in non-small cell lung cancer*. *Oncol Lett*, 2010. **1**(5): p. 837-840.

332. Mangala, L.S., et al., *Therapeutic Targeting of ATP7B in Ovarian Carcinoma*. Clin Cancer Res, 2009. **15**(11): p. 3770-80.
333. Wang, D., et al., *BIRC3 is a novel driver of therapeutic resistance in Glioblastoma*. Sci Rep, 2016. **6**: p. 21710.
334. Banerjee Mustafi, S., et al., *MDR1 mediated chemoresistance: BMI1 and TIP60 in action*. Biochim Biophys Acta, 2016. **1859**(8): p. 983-93.
335. Taron, M., et al., *BRCA1 mRNA expression levels as an indicator of chemoresistance in lung cancer*. Hum Mol Genet, 2004. **13**(20): p. 2443-9.
336. Wang, Z., et al., *Caveolin-1, a stress-related oncotarget, in drug resistance*. Oncotarget, 2015. **6**(35): p. 37135-50.
337. Yin, F., et al., *Tumor suppressor genes associated with drug resistance in ovarian cancer (review)*. Oncol Rep, 2013. **30**(1): p. 3-10.
338. Zhao, J., *Cancer stem cells and chemoresistance: The smartest survives the raid*. Pharmacol Ther, 2016. **160**: p. 145-58.
339. Song, Y., et al., *Activated hepatic stellate cells play pivotal roles in hepatocellular carcinoma cell chemoresistance and migration in multicellular tumor spheroids*. Sci Rep, 2016. **6**: p. 36750.
340. Zhao, L., et al., *Glutathione selectively modulates the binding of platinum drugs to human copper chaperone Cox17*. Biochem J, 2015. **472**(2): p. 217-23.
341. Singh, S., et al., *CXCL12-CXCR4 signalling axis confers gemcitabine resistance to pancreatic cancer cells: a novel target for therapy*. Br J Cancer, 2010. **103**(11): p. 1671-9.
342. Wang, C., et al., *CXCL5 promotes mitomycin C resistance in non-muscle invasive bladder cancer by activating EMT and NF-kappaB pathway*. Biochem Biophys Res Commun, 2018. **498**(4): p. 862-868.
343. Du, F., et al., *DDIT4 promotes gastric cancer proliferation and tumorigenesis through the p53 and MAPK pathways*. Cancer Commun (Lond), 2018. **38**(1): p. 45.
344. Yun, C.H., et al., *The T790M mutation in EGFR kinase causes drug resistance by increasing the affinity for ATP*. Proc Natl Acad Sci U S A, 2008. **105**(6): p. 2070-5.
345. Tan, M. and D. Yu, *Molecular mechanisms of erbB2-mediated breast cancer chemoresistance*. Adv Exp Med Biol, 2007. **608**: p. 119-29.
346. Liu, X., et al., *Development of Effective Therapeutics Targeting HER3 for Cancer Treatment*. Biol Proced Online, 2019. **21**: p. 5.
347. Li, W. and D.W. Melton, *Cisplatin regulates the MAPK kinase pathway to induce increased expression of DNA repair gene ERCC1 and increase melanoma chemoresistance*. Oncogene, 2012. **31**(19): p. 2412-22.
348. Weaver, D.A., et al., *ABCC5, ERCC2, XPA and XRCC1 transcript abundance levels correlate with cisplatin chemoresistance in non-small cell lung cancer cell lines*. Mol Cancer, 2005. **4**(1): p. 18.
349. Feng, X., et al., *miR-4521-FAM129A axial regulation on ccRCC progression through TIMP-1/MMP2/MMP9 and MDM2/p53/Bcl2/Bax pathways*. Cell Death Discov, 2019. **5**: p. 89.
350. Dai, C.H., et al., *RNA interferences targeting the Fanconi anemia/BRCA pathway upstream genes reverse cisplatin resistance in drug-resistant lung cancer cells*. J Biomed Sci, 2015. **22**: p. 77.
351. Vera-Ramirez, L., et al., *Transcriptional shift identifies a set of genes driving breast cancer chemoresistance*. PLoS One, 2013. **8**(1): p. e53983.
352. Marin, J.J., et al., *The role of reduced intracellular concentrations of active drugs in the lack of response to anticancer chemotherapy*. Acta Pharmacol Sin, 2014. **35**(1): p. 1-10.
353. Kikutake, C., et al., *Intratumor heterogeneity of HMCN1 mutant alleles associated with poor prognosis in patients with breast cancer*. Oncotarget, 2018. **9**(70): p. 33337-33347.

354. Liu, T., X. Wang, and L. Zhang, [*The correlation between the up-regulation of Hsp90 and drug resistance to cisplatin in lung cancer cell line*]. Zhongguo Fei Ai Za Zhi, 2011. **14**(6): p. 472-7.
355. Yuan, Z.Q., et al., *AKT2 inhibition of cisplatin-induced JNK/p38 and Bax activation by phosphorylation of ASK1: implication of AKT2 in chemoresistance*. J Biol Chem, 2003. **278**(26): p. 23432-40.
356. Tao, S., et al., *Oncogenic KRAS confers chemoresistance by upregulating NRF2*. Cancer Res, 2014. **74**(24): p. 7430-41.
357. Mutlu, P., A.U. Ural, and U. Gunduz, *Differential gene expression analysis related to extracellular matrix components in drug-resistant RPMI-8226 cell line*. Biomed Pharmacother, 2012. **66**(3): p. 228-31.
358. Tripathi, S.C., et al., *MCAM Mediates Chemoresistance in Small-Cell Lung Cancer via the PI3K/AKT/SOX2 Signaling Pathway*. Cancer Res, 2017. **77**(16): p. 4414-4425.
359. Li, R.M., et al., *Down-expression of GOLM1 enhances the chemo-sensitivity of cervical cancer to methotrexate through modulation of the MMP13/EMT axis*. Am J Cancer Res, 2018. **8**(6): p. 964-980.
360. Li, Q.Q., et al., *Involvement of CD147 in regulation of multidrug resistance to P-gp substrate drugs and in vitro invasion in breast cancer cells*. Cancer Sci, 2007. **98**(7): p. 1064-9.
361. Pellicani, R., et al., *Multimerin-2 maintains vascular stability and permeability*. Matrix Biol, 2019.
362. Meng, X., K.W. Thiel, and K.K. Leslie, *Drug resistance mediated by AEG-1/MTDH/LYRIC*. Adv Cancer Res, 2013. **120**: p. 135-57.
363. Grossi, V., et al., *p38alpha MAPK pathway: a key factor in colorectal cancer therapy and chemoresistance*. World J Gastroenterol, 2014. **20**(29): p. 9744-58.
364. Godwin, P., et al., *Targeting nuclear factor-kappa B to overcome resistance to chemotherapy*. Front Oncol, 2013. **3**: p. 120.
365. Korber, M.I., et al., *NFkappaB-Associated Pathways in Progression of Chemoresistance to 5-Fluorouracil in an In Vitro Model of Colonic Carcinoma*. Anticancer Res, 2016. **36**(4): p. 1631-9.
366. Mao, H., et al., *RhoBTB2 (DBC2) functions as tumor suppressor via inhibiting proliferation, preventing colony formation and inducing apoptosis in breast cancer cells*. Gene, 2011. **486**(1-2): p. 74-80.
367. Nagai, M.A., et al., *Down-regulation of the candidate tumor suppressor gene PAR-4 is associated with poor prognosis in breast cancer*. Int J Oncol, 2010. **37**(1): p. 41-9.
368. Yang, H., et al., *MicroRNA expression profiling in human ovarian cancer: miR-214 induces cell survival and cisplatin resistance by targeting PTEN*. Cancer Res, 2008. **68**(2): p. 425-33.
369. Huang, F. and A.V. Mazin, *A small molecule inhibitor of human RAD51 potentiates breast cancer cell killing by therapeutic agents in mouse xenografts*. PLoS One, 2014. **9**(6): p. e100993.
370. Alavi, A.S., et al., *Chemoresistance of endothelial cells induced by basic fibroblast growth factor depends on Raf-1-mediated inhibition of the proapoptotic kinase, ASK1*. Cancer Res, 2007. **67**(6): p. 2766-72.
371. Chen, Z., et al., *Overcoming tumor cell chemoresistance using nanoparticles: lysosomes are beneficial for (stearoyl) gemcitabine-incorporated solid lipid nanoparticles*. Int J Nanomedicine, 2018. **13**: p. 319-336.
372. Dai, S., et al., *SCD1 Confers Temozolomide Resistance to Human Glioma Cells via the Akt/GSK3beta/beta-Catenin Signaling Axis*. Front Pharmacol, 2017. **8**: p. 960.
373. Yang, Q., et al., *Acquisition of epithelial-mesenchymal transition is associated with Skp2 expression in paclitaxel-resistant breast cancer cells*. Br J Cancer, 2014. **110**(8): p. 1958-67.

374. Naka, A., et al., *Organic cation transporter 2 for predicting cisplatin-based neoadjuvant chemotherapy response in gastric cancer*. *Am J Cancer Res*, 2015. **5**(7): p. 2285-93.
375. Li, Q. and Y. Shu, *Role of solute carriers in response to anticancer drugs*. *Mol Cell Ther*, 2014. **2**: p. 15.
376. Bogsted, M., et al., *Proof of the concept to use a malignant B cell line drug screen strategy for identification and weight of melphalan resistance genes in multiple myeloma*. *PLoS One*, 2013. **8**(12): p. e83252.
377. de Morree, E.S., et al., *Loss of SLCO1B3 drives taxane resistance in prostate cancer*. *Br J Cancer*, 2016. **115**(6): p. 674-81.
378. Wilson, C., et al., *Overcoming EMT-associated resistance to anti-cancer drugs via Src/FAK pathway inhibition*. *Oncotarget*, 2014. **5**(17): p. 7328-41.
379. Moreira, M.P., et al., *STAT3 as a promising chemoresistance biomarker associated with the CD44(+high)/CD24(-low)/ALDH(+) BCSCs-like subset of the triple-negative breast cancer (TNBC) cell line*. *Exp Cell Res*, 2018. **363**(2): p. 283-290.
380. Carden, C.P., et al., *The association of PI3 kinase signaling and chemoresistance in advanced ovarian cancer*. *Mol Cancer Ther*, 2012. **11**(7): p. 1609-17.
381. Liu, S., et al., *NANOG regulates epithelial-mesenchymal transition and chemoresistance through activation of the STAT3 pathway in epithelial ovarian cancer*. *Tumour Biol*, 2016. **37**(7): p. 9671-80.
382. Han, C.H., et al., *Polymorphisms in the SULF1 gene are associated with early age of onset and survival of ovarian cancer*. *J Exp Clin Cancer Res*, 2011. **30**: p. 5.
383. Lu, F., et al., *TFPI-2 downregulates multidrug resistance protein in 5-FU-resistant human hepatocellular carcinoma BEL-7402/5-FU cells*. *Anat Rec (Hoboken)*, 2013. **296**(1): p. 56-63.
384. Liu, C.C., et al., *Sigma-2 receptor/TMEM97 agonist PB221 as an alternative drug for brain tumor*. *BMC Cancer*, 2019. **19**(1): p. 473.
385. Ferguson, S.D., et al., *Ependymomas overexpress chemoresistance and DNA repair-related proteins*. *Oncotarget*, 2018. **9**(8): p. 7822-7831.
386. Mirski, S.E., et al., *A truncated cytoplasmic topoisomerase IIalpha in a drug-resistant lung cancer cell line is encoded by a TOP2A allele with a partial deletion of exon 34*. *Int J Cancer*, 2000. **85**(4): p. 534-9.
387. Lonning, P.E. and S. Knappskog, *Mapping genetic alterations causing chemoresistance in cancer: identifying the roads by tracking the drivers*. *Oncogene*, 2013. **32**(46): p. 5315-30.
388. Yin, H., et al., *GPER promotes tamoxifen-resistance in ER+ breast cancer cells by reduced Bim proteins through MAPK/Erk-TRIM2 signaling axis*. *Int J Oncol*, 2017. **51**(4): p. 1191-1198.